24-hour Probable Maximum Precipitation Updating Study

GEO Report No. 314

AECOM Asia Company Limited & B. Lin

Geotechnical Engineering Office
Civil Engineering and Development Department
The Government of the Hong Kong
Special Administrative Region

24-hour Probable Maximum Precipitation Updating Study

GEO Report No. 314

AECOM Asia Company Limited & B. Lin

First published, September 2015

Prepared by:

Geotechnical Engineering Office,
Civil Engineering and Development Department,
Civil Engineering and Development Building,
101 Princess Margaret Road,
Homantin, Kowloon,
Hong Kong.

Preface

In keeping with our policy of releasing information which may be of general interest to the geotechnical profession and the public, we make available selected internal reports in a series of publications termed the GEO Report series. The GEO Reports can be downloaded from the website of the Civil Engineering and Development Department (http://www.cedd.gov.hk) on the Internet. Printed copies are also available for some GEO Reports. For printed copies, a charge is made to cover the cost of printing.

The Geotechnical Engineering Office also produces documents specifically for publication in print. These include guidance documents and results of comprehensive reviews. They can also be downloaded from the above website.

The publications and the printed GEO Reports may be obtained from the Government's Information Services Department. Information on how to purchase these documents is given on the second last page of this report.

H.N. Wong
Head, Geotechnical Engineering Office
September 2015

Foreword

The Probable Maximum Precipitation (PMP) scoping study of Geotechnical Engineering Office (GEO), which was completed in 2011, has identified areas for improvement in the estimation of PMP in Hong Kong. In response to the scoping study, a Phase 2 PMP updating study has been undertaken.

In this updating study, the international best practice for the estimation of 24-hour PMP in Hong Kong was adopted by using an improved PMP estimation technique. Storm separation technique based on the Step Duration Orographic Intensification Factor (SDOIF) Method was applied to separate orographic effect from rainfall data for non-local storms. The convergence component was combined with local orographic factors, together with moisture maximization and storm transposition methods, to estimate a new 24-hour PMP. Moreover, verification of the new 24-hour PMP was conducted based on comprehensive comparison of findings from Depth-Area-Duration (DAD) analysis and Statistical approach as well as worldwide rainfall records and PMP estimates in China.

Professor Lin Bingzhang of Applied Hydrometeorological Research Institute of Nanjing University of Information Science & Technology prepared this report with the technical support of Dr Benjamin S.L. Yeung and Dr Axel K.L. Ng of AECOM Asia Company Ltd. Messrs Chris S.C. Tang and C.F. Yam of the GEO provided the technical assistance in the study. The study was also reviewed by a Working Group comprising Mr Ken K.S. Ho initially and Mr Herman Y.K. Shiu later of the GEO as the chairman, and Mr Alan C.W. Wong initially and Dr H.W. Sun later and Dr Dominic O.K. Lo of the GEO, Dr T.C. Lee of Hong Kong Observatory, Ms K.M. Lin initially and Mr Wilson Y.M. Chung later of Drainage Services Department, Mr K.K. Tse initially and Mr Martin W.M. Tong of Water Supplies Department, Professor Y.K. Tung of the Hong Kong University of Science and Technology, Dr J. Chen of the University of Hong Kong and Dr C.F. Wan of the Hong Kong Institution of Engineers as the members. All contributions are gratefully acknowledged.

Mr Patrick Chao
Project Director
AECOM Asia Company Ltd.

Contents

Page No.

Page No.

List of Tables

List of Figures

1 Introduction

1.1 Background

Probable Maximum Precipitation (PMP) is defined as the greatest depth of precipitation for a given duration meteorologically possible for a design watershed or a given storm area at a particular location at a particular time of year, with no allowance made for long-term climate trends (WMO, 2009).

PMP is primarily considered to be the precipitation resulting from a storm induced by the optimal dynamic factor (usually the precipitation efficiency) and the maximum moisture factor simultaneously. There are generally two types of approaches to the estimation of PMP. The first is a hydrometeorological or a causal approach in which the PMP for different durations over an area is mainly determined by transposition and/or maximization of major historical rainstorms. The second is a statistical approach where the estimation of PMP is derived from a modified frequency analysis (or called quasi-frequency analysis) of the annual maximum rainfall series for different durations.

The Manual on Estimation of PMP published by the World Meteorological Organization (WMO) presents six methods currently in use (WMO, 2009):

(a) The local method (local storm maximization or local model);

(b) The transposition method (storm transposition or transposition model);

(c) The combination method (temporal and spatial maximization of storm or storm combination or combination model);

(d) The inferential method (theoretical model or ratiocination model);

(e) The generalized method (generalized estimation); and

(f) The statistical method (statistical estimation).

Methods (a) to (e) can be categorized as a hydrometeorological or a causal approach. Method (f) is a statistical approach. Among them, methods (a) and (b) are the basic methods used in PMP estimation, i.e. maximization and transposition; method (c) is applied to large watershed; method (e) is adopted for large area including two or more regions while method (d) is a theoretical-like model which is less used in practice of PMP estimation due to lack of data to calibrate and validate.

In 2011, the Geotechnical Engineering Office (GEO) completed a PMP scoping study which recommended that a Phase 2 PMP updating study should be carried out. Subsequently, AECOM was commissioned by the GEO of Civil Engineering and Development Department to undertake the “PMP Updating Study - Stage 1” in September 2011, under Agreement No. CE 9/2009 (GE), Study of Landslides Occurring in Hong Kong

Island and Outlying Islands in 2010 and 2011 - Feasibility Study, and the "PMP Updating Study - Stage 2" in September 2012, under Agreement No. CE 13/2011 (GE), Study of Landslides Occurring in Kowloon and Outlying Islands in 2012 and 2013 - Feasibility Study. Professor Lin Bingzhang (Prof. B. Lin) of Applied Hydrometeorological Research Institute (AHMRI) of Nanjing University of Information Science & Technology (NUIST) is engaged as a sub-consultant to undertake both stages of the updating study.

The objectives of this updating study are to update the existing 24-hour PMP estimate in Hong Kong using the international best practice and explore how the PMP estimates could be further adjusted with due account of possible effects of climate change. The study covers storm areas ranging from 10 km^2 to about 2,600 km^2 with storm transposition and orographic adjustments in addition to the storm maximization approach. Moreover, a statistical approach is also adopted to obtain a quick estimation of 24-hour PMP for benchmarking the corresponding value using the storm transposition approach. The collected rainfall data are further used for investigating the use of storm transposition approach in estimation of 4-hour PMP.

1.2 Scope of the Study

To facilitate the study, the following tasks were set out and undertaken in stages:

(a) Submit an inception report to briefly describe the study approach and data requirements for both study stages;

(b) Liaise with the relevant authorities to collect all required information and meteorological data;

(c) Set the storm selection criteria for both local and non-local storms for use in PMP updating;

(d) Carry out transposition analysis for the selected non-local storms using the storm separation technique (based on the Step Duration Orographic Intensification Factor (SDOIF) Method);

(e) Obtain a quick estimation of point PMP using the statistical approach of extreme rainfall data series;

(f) Depth-Area-Duration (DAD) analyses for selected local storms and non-local storms for producing the updated 24-hour PMP estimates;

(g) Assess possible effects of climate change on PMP estimation;

(h) Review possible change in the amount of precipitable water in moisture maximization as a result of increase of sea surface temperature for the source areas of inflow moisture jet; and

(i) Justify the level of consistency for the PMP estimates through a comprehensive comparison with rainfall records and PMP estimates in other comparable areas.

1.3 Approach and Methodology

1.3.1 Statistical Approach

1.3.1.1 Principle of Statistical Approach

Statistical estimation is one of the methods recommended in WMO's Manual on Estimation of PMP (WMO, 2009) for international practice in PMP estimation. Details of the method are also given in 林炳章 (1981) and Lin & Vogel (1993). This method is based on frequency analysis, but different from the traditional frequency analysis (China Water & Power Press, 1995) in such a way that the number of standard deviation, K_m, to be added (to multiply actually) to the mean to get the PMP in the frequency equation is to be calculated in a way that the maximum observed value from the historical series is omitted in the computation (see the following computation equation for K_m). As a result of this modification, K_m represents essentially a pseudo amplification ratio of the deviation of the maximum observed rainfall from the incomplete mean to the incomplete standard deviation, in which the maximum observed value is omitted. Then, this pseudo amplification ratio is used to mimic the future maximum. In order to ensure the maximization of the mimic, the pseudo amplification ratio is determined based not only on a local single raingauge, but also raingauges in a wide area. The advantage of this determination is that it reduces the sampling error which comes from using rainfall data just at only one station. Therefore, the process of enveloping, or regionalization in other word, is applied here. In addition, the C_{vn} and $\overline{X}_n$ (see definition below) are also to be regionalized to ensure the maximization for a relative small region. Thus, the essence of the method is storm transposition, but instead of transposing the specific rainfall amount of one storm, an abstracted or enveloping statistic K_m is transposed. This statistical estimation is particularly useful for making quick estimates of PMP. Obviously, the longer data series is welcomed and appreciated for the method.

The results of the PMP estimates from the statistical approach are used for comparing the results obtained from the traditional storm transposing approach which is the core of this updating study.

Point statistical PMP estimate, X_{PMP}, is computed using the following equation:

$$X_{PMP} = \overline{X}_n + K_m \times S_n = (1 + K_m \times C_{vn}) \times \overline{X}_n \quad \text{..... (1.1)}$$

where $\overline{X}_n$ and S_n are the mean and the standard deviation of the n maxima, and C_{vn} is the coefficient of variation of the sample with n values. K_m is the number of standard deviation to be added to $\overline{X}_n$ to get X_{PMP}, as follows:

$$K_m = \frac{(X_m - \overline{X}_{n-1})}{S_{n-1}} \quad \text{..... (1.2)}$$

where X_{n-1} and S_{n-1} are the mean and standard deviation of the rainfall series from which the maximum record rainfall is omitted. X_m is the maximum observed value.

1.3.1.2 Data Screening Criteria and Probable Adjustment of Mean

Two criteria have been introduced to the method, N_m as the minimum data length and N_s as the stable data length for estimation at a relative error of 10% in K_m.

(1) The criterion of minimum data size, N_m:

$$N_m = \phi_m^2 + 2 \quad \text{..... (1.3)}$$

where ϕ_m is the maximum deviation from mean (i.e. the variation coefficient) and is directly computed from the following equation:

$$\phi_m = \frac{(X_m - \overline{X}_n)}{S_n} \quad \text{..... (1.4)}$$

(2) As suggested by Lin & Vogel (1993), the criterion of the stable size, N_s:

$$N_s \geq 5.76 \times (\phi_m^2 + 2) \quad \text{..... (1.5)}$$

A chart showing the relationship between the N_s and ϕ_m is given in Figure 1.1.

(3) Probable maximum adjustment of sample mean at 99.7% confidence level is given below:

$$\overline{X}'_n = \overline{X}_n + 3 \times \sigma_{\overline{X}_n} \approx (1 + \frac{3 \times C_{vn}}{\sqrt{n}}) \times \overline{X}_n \quad \text{..... (1.6)}$$

where $\sigma_{\overline{X}_n}$ is the standard deviation of the mean $\overline{X}_n$.

1.3.1.3 Computation of PMP Estimate

Hence, the PMP estimate for 24-hour can be obtained using the following equation:

$$X_{PMP,24} = \overline{X}_{n,24} + K_{m,24} \times S_{n,24} = (1 + K_{m,24} \times C_{vn,24}) \times \overline{X}_{n,24} \quad \text{..... (1.7)}$$

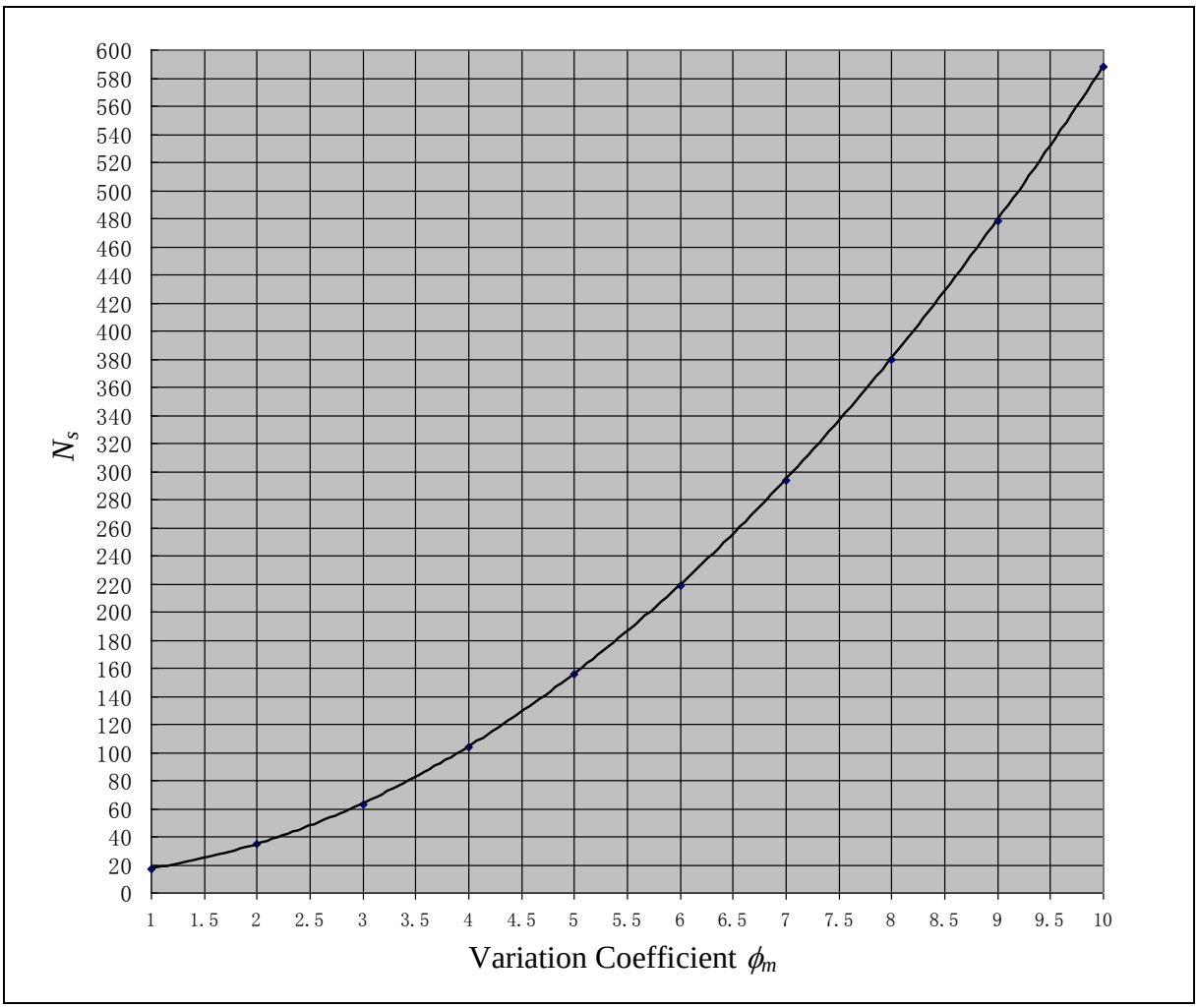

Figure 1.1 Relationship of Variation Coefficient ϕ_m with N_s

1.3.2 Storm Transposition Approach Using the Step Duration Orographic Intensification Factor (SDOIF) Method

The storm transposition used to be restricted to regions that are meteorologically and topographically homogeneous where storms that have been observed are considered to be equally likely to occur, allowing adjustment only for moisture differences. The difference in topography between target area and the design area is a major obstacle which confines an outstanding storm being transposed in a relatively small area. This is because there is no other reasonable way, such as meteorological model quantitatively, that considers the effects of topography on rainfall storms. The storm separation technique now allows a non-orographic (i.e. convergence) component to be transposed in a wider area. This liberal transposition has benefited by the recent development of storm separation technique such as the SDOIF method developed by Prof. B. Lin during the PMP Estimation of Daguangba Project (林炳章, 1987 & 1988), on Hainan Island of China funded by the World Bank in 1987 - 1988. The SDOIF method was recommended by WMO in its Third Version of Manual on Estimation of PMP (WMO, 2009) for PMP estimation in mountainous regions. The storm separation technique separates mountainous storm rainfall into components caused by atmospheric forcing and those caused by terrain forcing. It is a combined engineering

hydrologic-meteorological approach based on long-term rainfall statistics, synoptic analysis of storms and topographic features in a gridded design area. Thus, it may be assumed that one can transpose the atmospheric force (referred to as convergence or non-orographic) component within a mountainous region in a larger area. Then, the transposed convergence component can be merged with the designed local terrain force (referred as orographic) component to make a PMP estimate for the designed mountainous areas. The concepts of storm transposition and the storm separation technique of SDOIF are considered to be applicable to the PMP estimation for Hong Kong.

Unlike consideration of a general weather analysis or synoptic analysis for a given region that may require going over different synoptic patterns, the major concern for a PMP study is the rainfall intensity at a given duration for a given location or for a design area with its temporal and spatial pattern no matter what the synoptic type is. The selection of a target storm for transposition in PMP study is mainly based on the severity (i.e. rainfall intensity for 24-hour and other short durations such as 1-hour and/or 6-hour) and spatial coverage to distinguish local convective storms and other types of storms with respect to PMP estimation for this updating study.

1.3.2.1 Procedures of Storm Transposition

A flow chart of the storm transposition by using the SDOIF method is given in Figure 1.2.

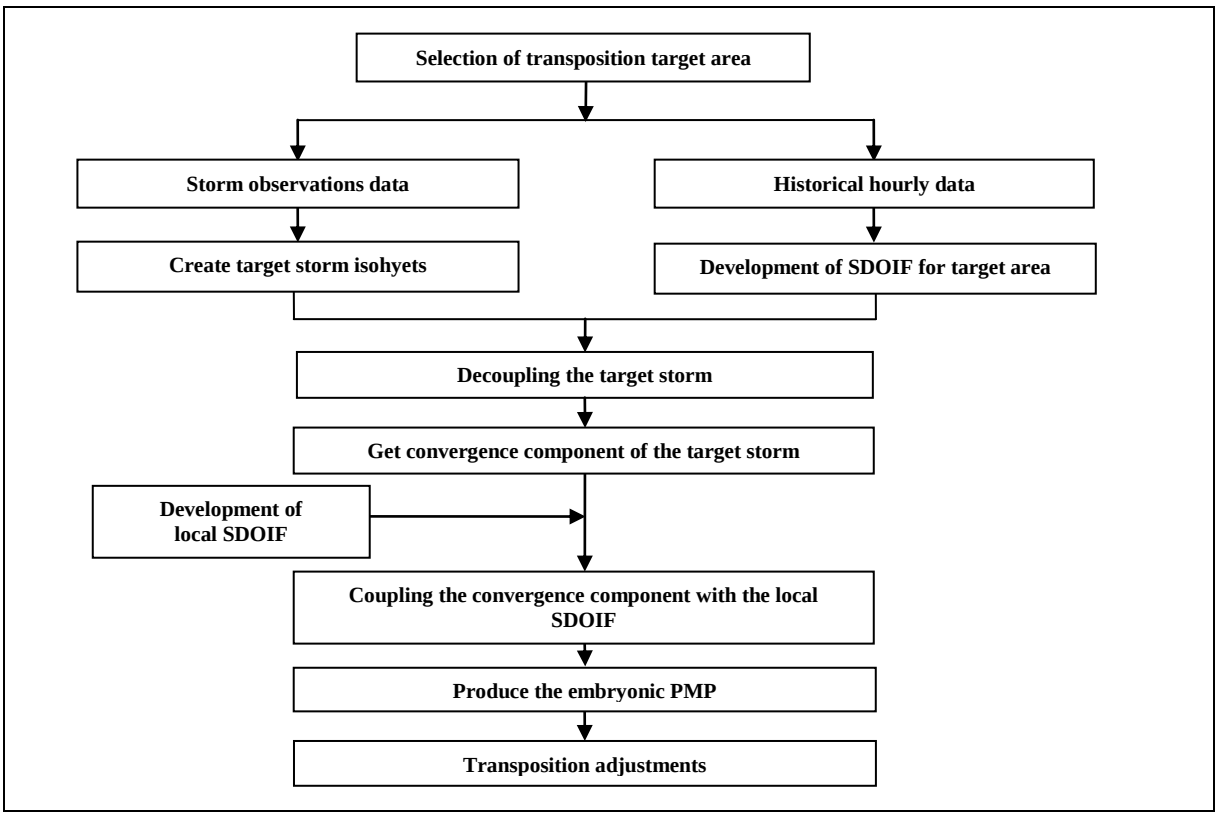

Figure 1.2 Flowchart of the Storm Transposition via SDOIF Method

1.3.2.2 Principle of SDOIF Method

(1) *In Theory*

For a rainstorm, the rainfall intensity at a given point (place) $P(x,y)$ within a catchment at any time can be defined by:

$$I(x,y,t) = I_0(x,y,t) \times f(x,y,t) \quad \text{..... (1.8)}$$

where $I_0(x,y,t)$ is the convergence component and $f(x,y,t)$ is the orographic intensification factor. Both are considered in nature as the random variables.

The average rainfall intensity during an interval of $\triangle t$ is given below:

$$I_{\Delta t}(x,y) = I_{0,\Delta t}(x,y) \times f_{\Delta t}(x,y) \quad \text{..... (1.9)}$$

where $I_{0,\triangle t}(x,y)$ and $f_{\triangle t}(x,y)$ are the average values over $\triangle t$ corresponding to the convergence component and the orographic intensification respectively. Thus, the rainfall amount $r_{\triangle t}(x,y)$ for a given point in $\triangle t$ can be obtained by:

$$r_{\Delta t}(x,y) = \int_{\Delta t} I(x,y,t)dt \approx I_{\Delta t}(x,y) \times \Delta t = I_{0,\Delta t}(x,y) \times f_{\Delta t}(x,y) \times \Delta t = r_{0,\Delta t}(x,y) \times f_{\Delta t}(x,y) \quad \text{..... (1.10)}$$

where the $r_{0,\triangle t}(x,y)$ is the convergence rainfall without orographic influence for the given point (place) in $\triangle t$.

Hence, the area-averaged rainfall R for the whole catchment of A during the period of $\triangle t$ is given below:

$$\overline{R}_{\Delta t,A} = \frac{\iint_A r_{\Delta t}(x,y)dxdy}{\iint_A dxdy} = \frac{\iint_A r_{0,\Delta t}(x,y) \times f_{\Delta t}(x,y)dxdy}{\iint_A dxdy} \approx \frac{\sum_i^m \sum_j^n r_{0,\Delta t}(x_i,y_j) \times f_{\Delta t}(x_i,y_j)\Delta x_i \Delta y_j}{\sum_i^m \sum_j^n \Delta x_i \Delta y_j}$$

..... (1.11)

Furthermore, if taking $\Delta x_1 = \Delta x_2 = ... = \Delta x_m$, $\Delta y_1 = \Delta y_2 = ... = \Delta y_n$, the above formula can be reduced as:

$$\overline{R}_{\Delta t,A} = \frac{1}{m \times n}\left[\sum_i^m \sum_j^n r_{0,\Delta t}(x_i,y_j) \times f_{\Delta t}(x_i,y_j)\right] \quad \text{..... (1.12)}$$

where $r_{0,\triangle t}(x_i,y_j)$ and $f_{\triangle t}(x_i,y_j)$ represent the convergence rainfall and the orographic intensification factor for the square of $\triangle x_i \times \triangle y_j$ during the period of $\triangle t$ while m and n are the numbers of $\triangle x_i$ and $\triangle y_j$ respectively.

(2) *In Practice*

The averaged orographic intensification factor over $\triangle t$ for a given point (x,y) can be written as:

$$f_{\Delta t}(x,y) = \frac{r_{\Delta t}(x,y)}{r_{0,\Delta t}(x,y)} \quad \text{..... (1.13)}$$

where $r_{\triangle t}(x,y)$ is the total rainfall containing the orographic influence while the $r_{0,\triangle t}(x,y)$ is the rainfall without the orographic influence during $\triangle t$ for the same point (x,y).

(3) *Major Assumptions*

The method is based on the following assumptions:

(a) The mechanism of a heavy rainstorm approaches the mechanism of a PMP-level storm. So, there is a possibility to estimate the $f_{\triangle t}(x,y)$ for a particular duration based on the annual extreme rainfall series, mean of annual maximum rainfall, for the corresponding duration.

(b) The rainfall recorded on flatlands and/or the nearby coastal areas in the storm moisture inflow jet route is not influenced by the topography in terms of the intensification. Therefore, the rainfall data of stations located in these areas can be chosen to estimate the value of $r_{0,\triangle t}(x,y)$. For a single point, the $f_{\triangle t}(x,y)$ may not have significant implication of effect of topography on rainfall. However, a number of $f_{\triangle t}(x,y)$ from a number of locations with different elevations in the terrain area may jointly reflect the effect of the topography on rainfall in this mountainous area.

(c) To determine the denominator, $r_{0,\triangle t}(x,y)$ in Equation 1.13, raingauge stations are selected as base stations. To reduce the sampling error, the average of the means of annual maxima for a given duration over the base stations is taken. The mean of 24-hour annual maximum rainfall of each station located in different elevations within the study area serves as the numerator of Equation 1.13, $r_{0,\triangle t}(x,y)$, when calculating the individual orographic intensification $f_{\triangle t}(x_i,y_j)$.

1.3.2.3 Storm Transposition

When the generalized isohyetal pattern as representative convergence component for target area is transposed to the design areas, it is coupled with the local SDOIF pattern or orographic component to generate a PMP embryo by superposing the generalized convergence component pattern onto the local SDOIF. The word "embryo" used here means

it is a preliminary PMP estimate.

1.3.2.4 Transposition Adjustment and Moisture Maximization

The embryonic PMP is further adjusted to produce the PMP estimate. The adjustments include transposition adjustments taking into account the orientation to the prevailing moisture inflow jet during the invasion of typhoon storm to the design area and moisture maximization.

2 Storm Survey and Rainfall Data

2.1 Overview

The reliability of a PMP estimate depends on the availability and quality of hydrological and meteorological data as well as the depth and appropriateness of the analysis. For storm transposition in PMP estimation, storm survey and investigation in a wider region with meteorological similarity are required. In this regard, the storm survey and selection in the Southeast China including Zhejiang, Fujian, Guangdong, Guangxi, Hainan, and Taiwan, is considered as an important step to the PMP estimation for Hong Kong.

2.2 Approach and Methodology

2.2.1 Approach to Storm Survey

A literature review on published reports and technical papers was undertaken to identify severe storms. Preliminary rainfall data for the identified storms were examined through a data screening process. As a result of the screening process, the identified storms were ranked according to their 24-hour rainfalls. The top ranked storms were further investigated to determine whether they should be included in this study. Apart from the literature review, the outstanding convective local storms and other types of local storm such as troughs or tropical depressions were also identified by searching through raw data.

2.2.2 Criteria for Storm Selection

The selection of an outstanding storm is based on the criteria listed below:

(a) the initial screening of the storm in history in the investigated area (province or region), in terms of its severity i.e. rainfall intensity for 24-hour, other short durations such as 6-hour if 24-hour data unavailable and its spatial coverage; and

(b) the availability of rainfall data for the life span of the storm.

2.2.3 Determination of T-hour Maximum Rainfall

During further investigation of a storm, T-hour maximum rainfall such as 24-hour was determined from raw data by going through the following process:

(a) Moving window with fixed T-hour was used to determine the T-hour maximum rainfall over hourly observations.

(b) The starting and ending hours of the storm centre were fixed to determine the T-hour area-average rainfall. This is to ensure that the rainfall observations encompassed by isohyets to make averaging are concurrent.

(c) Assumption of continuity of rainfall over time and space was applied to data quality control wherever observations were unavailable, such as those in sea portion, when developing DAD curves.

(d) In QC for data from Mainland China and Taiwan, any suspicious data including missing data were called for an original observation check. As long as an anomalous-like datum such as outlier has been confirmed to be a real observation, it was used no matter how different (large) from others. The original rainfall records are kept by the owners due to restrictions imposed in Mainland China; however they are accessible for checking of suspicious data upon request. In case the verification was not successful or missing data could not be recovered, for example, due to raingauge malfunction as a result of power outage or flooding, simple interpolation temporally such as between hours or a more reliable technique such as the inverse distance square method spatially were applied. For example, there were 6 individual hours with no observations for two raingauges in Alishan area during Typhoon Morakot storm. Then, simple interpolation was adopted to fill the missing data by using observations in neighbouring hours after the data owner confirmed that there was no way to recover them.

2.3 Results of Survey for Local Storms

2.3.1 Rainfall Data between 1984 and 2010

Local storms affecting Hong Kong, including tropical cyclones and other synoptic types such as trough of low pressure have been investigated. References were made to historical hourly rainfall data from GEO's Factual Reports on Hong Kong Rainfall and Landslides (published between 2000 and 2010) that contain maximum rainfall observations at Hong Kong Observatory's (HKO) and GEO's raingauges. 5-min raw data from raingauge

stations of GEO and HKO for the period between 1984 and 2010 were also studied. Based on those data, the top ten storms for 24-hour rainfall have been surveyed and listed in Table 2.1.

The top 10 local storms have been used for updating local DAD curves together with the DAD curves based on the South Guangdong (SGD) data. In addition, the top 10 local storms together with their corresponding time series at local raingauge stations are the major storms for statistical estimation of PMP.

Table 2.1 Top 10 Outstanding Local Storms in 24-hour Rainfall Intensity (1984 - 2010)

No.	Date	24-hr Rainfall (mm)	Storm Type (Name)
1	21-25 July 1994	956	Trough of low pressure
2	1-4 July 1997	799	Trough of low pressure
3	4-5 Nov 1993	742	Severe Typhoon (IRA)
4	6-9 Jun 2008	622	Trough of low pressure
5	16-21 Aug 2005	570	Trough of low pressure
6	20-21 May 1989	566	Typhoon (BRENDA)
7	22-26 Aug 1999	565	Typhoon (SAM)
8	8-9 Jun 1998	562	Trough of low pressure
9	5-6 May 2003	505	Trough of low pressure
10	11-15 Aug 1995	468	Severe Tropical Storm (HELEN)

2.3.2 Rainfall Data between 1966 and 1983

Referring to the technical report “Supplement to Meteorological Results 1966 - the Severe Rainstorms in Hong Kong During June 1966” (Chen, 1969), the June 1966 storm caused considerable damage that the continuous violent thunderstorms and heavy rainfalls resulted in extensive landslides and flooding. The June 1966 storm was not identified and covered in the 1999 PMP Study (HKO, 1999).

An investigation has been carried out in this study using rainfall data between years 1966 and 1983 which were collected from HKO to identify outstanding storms in this time period. Hourly rainfall data for raingauge stations at HKO headquarter (“HKO”), Kai Tak

("AMO"), Cheung Chau ("CCH") and Chek Lap Kok ("CLK") were analysed. Top 10 storms are identified and tabulated in Table 2.2. They are also included for updating local DAD curves in this study.

Table 2.2 Top 10 Outstanding Local Storms in 24-hour Rainfall Intensity (1966 - 1983)

No.	Date	24-hr Rainfall (mm)	Storm Type (Name)
1	8-16 Jun 1966	557	Trough of low pressure
2	24-26 Aug 1976	548	Tropical Storm (HELEN)
3	15-16 Jun 1972	466	Trough of low pressure
4	16-18 Jun 1983	453	Typhoon (VERA)
5	10-12 May 1972	374	Trough of low pressure
6	13-23 Aug 1971	374	Super Typhoon (ROSE)
7	17-19 Jun 1972	341	Trough of low pressure
8	11-19 May 1970	316	Trough of low pressure
9	28-30 Sep 1981	237	Trough of low pressure
10	20-22 Aug 1973	225	Tropical Storm (JOAN)

2.4 Results of Survey for Non-local Storms

As a result of the preliminary storm screening, 20 severe storms including 16 from the Southeast Mainland China and 4 from Taiwan covering a variety of synoptic types such as typhoon, trough of low pressure and tropical depression etc., were selected for storm survey in the earlier time of the survey (referring to Table 2.3). Detailed description of major non-local storms is shown in Appendix A.

Having considered unavailability and difficulty in procurement of rainfall data, 10 out of the 20 severe storms as tabulated in Table 2.4 were further identified as outstanding storms for further investigation in transposition analysis. Rainfall data for the 10 outstanding storms including 6 from Guangdong and 4 from Taiwan were procured from relevant authorities from Mainland China and Taiwan for developing storm isohyets.

Table 2.3 20 Severe Storms in the Southeast China Surveyed

No.	Province/ Region	Storm Name	Storm Type	Location	24-hr Rainfall (mm)	Period of data
1	Zhejiang	#0414	Typhoon	Leqing Foutou	874	12-14 Aug 2004
2	Fujian			Jinjiang Yinglin	632.5	22-24 Sep 1989
3	Guangdong	#5508	Tropical Low	Taishan Zhenhai	850.6	11-13 Jul 1955
4	Guangdong		Trough	Dianbai Lidong	858	18-20 May 1959
5	Guangdong		Front	Luffeng Baishimen	884	30-31 May 1977
6	Guangdong		Jet	Yangjiang Maodong Reservoir	738	12-14 May 1979
7	Guangdong		Front	Chenghai Dongxikou	756.1	10-12 Jun 1979
8	Guangdong	#8607	Typhoon	Fengshun Gaojiping	786.2	11-13 Jul 1986
9	Guangdong		Front	Lufeng Shuangpei	915.6	21-23 May 1987
10	Guangdong			Qingyuan Yuantan	939.3	8-10 May 1997
11	Guangdong	#0707, #0708	Typhoon	Leizhou Peninsula Xingfu Farm	1188.2	9-11 Aug 2007
12	Guangdong	Fanapi	Typhoon	Shangmaoping	839.5	20-22 Sep 2010
13	Guangxi		Wind shear	Yongshui Zailao	779.1	15-17 Jul 1996
14	Hainan	#8303 Vera	Typhoon	Ledong Tianchi	962.2	17-19 Jul 1983
15	Hainan	#0010	Tropical Cyclone	Tunchang Dalupo	N/A*	11-13 Oct 2000
16	Hainan	#1010	Tropical Low	Qionghai	881.8	5-7 Oct 2010
17	Taiwan	Herb	Typhoon	Ahlishan	1748.5	31-2 Jul 1996
18	Taiwan	Aere	Typhoon	Madala	1154	24-26 Aug 2004
19	Taiwan	Haitang	Typhoon	Weiliaoshan	1254.5	18-20 Jul 2005
20	Taiwan	Morakot	Typhoon	Ahlishan	1623.5	8-10 Aug 2009

Note: * The No. 15 of Tunchang Dalupo (屯昌大陸坡) in Hainan with 818 mm/6-hr was verified and double-checked later as incorrect. The figure "818 mm/6-h" was a misprint in a published literature. Having confirmed from the original source, it should be written as "818 mm/6-day".

Table of Contents
Table of Contents
Table of Contents
Table of Contents

Table 2.4 10 Outstanding Storms Considered for Transposition Study

No.	Province/ Region	Storm Name	Storm Type	Location	24-hr Rainfall (mm)	Period of Data Reviewed	
						From	To
1	Guangdong	--	Front (SW Jet)	Lufeng Baishimen (陸豐 白石門)	884	29 May 77	31 May 77
2	Guangdong	--	Jet	Yangjiang Reservoir Maodong (陽江 茅洞水庫)	738	11 May 79	17 May 79
3	Guangdong	--	Front	Lufeng Shuangpei (陸豐 雙沛)	915.6	20 May 87	22 May 87
4	Guangdong	--	Front	Qingyuan Yuantang (清遠 源潭)	939.3 (20-hr)	7 May 97	9 May 97
5	Guangdong	Pabuk, Wutip	Typhoon	Leizhou Peninsula Farm Happy (雷州半島 幸福農場)	1188.2	8 Aug 07	12 Aug 07
6	Guangdong	Fanapi	Typhoon	West Guangdong Shangmao- ping (上茂坪)	839.5	21 Sep 10	23 Sep 10
7	Taiwan	Herb	Typhoon	Ahlishan (阿里山)	1376*	31 Jul 96	2 Aug 96
8	Taiwan	Aere	Typhoon	Madala (馬達拉)	1003.5*	23 Aug 04	26 Aug 04
9	Taiwan	Haitang	Typhoon	Weiliaoshan (尾寮山)	1473*	16 Jul 05	20 Jul 05
10	Taiwan	Morakot	Typhoon	Ahlishan (阿里山)	1583.5*	6 Aug 09	10 Aug 09

Note: * These figures were revised according to procured data. In particular, there were some missing data in the CWB's records of Herb and Haitang and many "big numbers" for hourly data, which were deemed to be suspicious. These suspicious records were not used in the subsequent analysis.

2.5 Historical Annual Maximum Rainfall Data

Historical rainfall data, Annual Maximum Series (AMS), have been used in the statistical analysis and also the transposition analysis together with storm data to obtain the PMP estimate.

2.5.1 Data Adopted for Statistical Analysis

Hong Kong

The historical rainfall data provided by GEO were obtained from a total of 116 raingauge stations. However, only 43 stations (42 from GEO and 1 from HKO) have data with the length of time period of 27 years or more. These raingauge stations were selected for statistical estimate in order to fulfil the selection criteria as given in Section 1.3.1.2. The geographic locations of these 43 stations are shown in Figure 2.1. These stations are located in Hong Kong, Kowloon and part of the New Territories. No station is located on Lantau Island. The details (e.g. period of observation and type of data) are given in Appendix B.

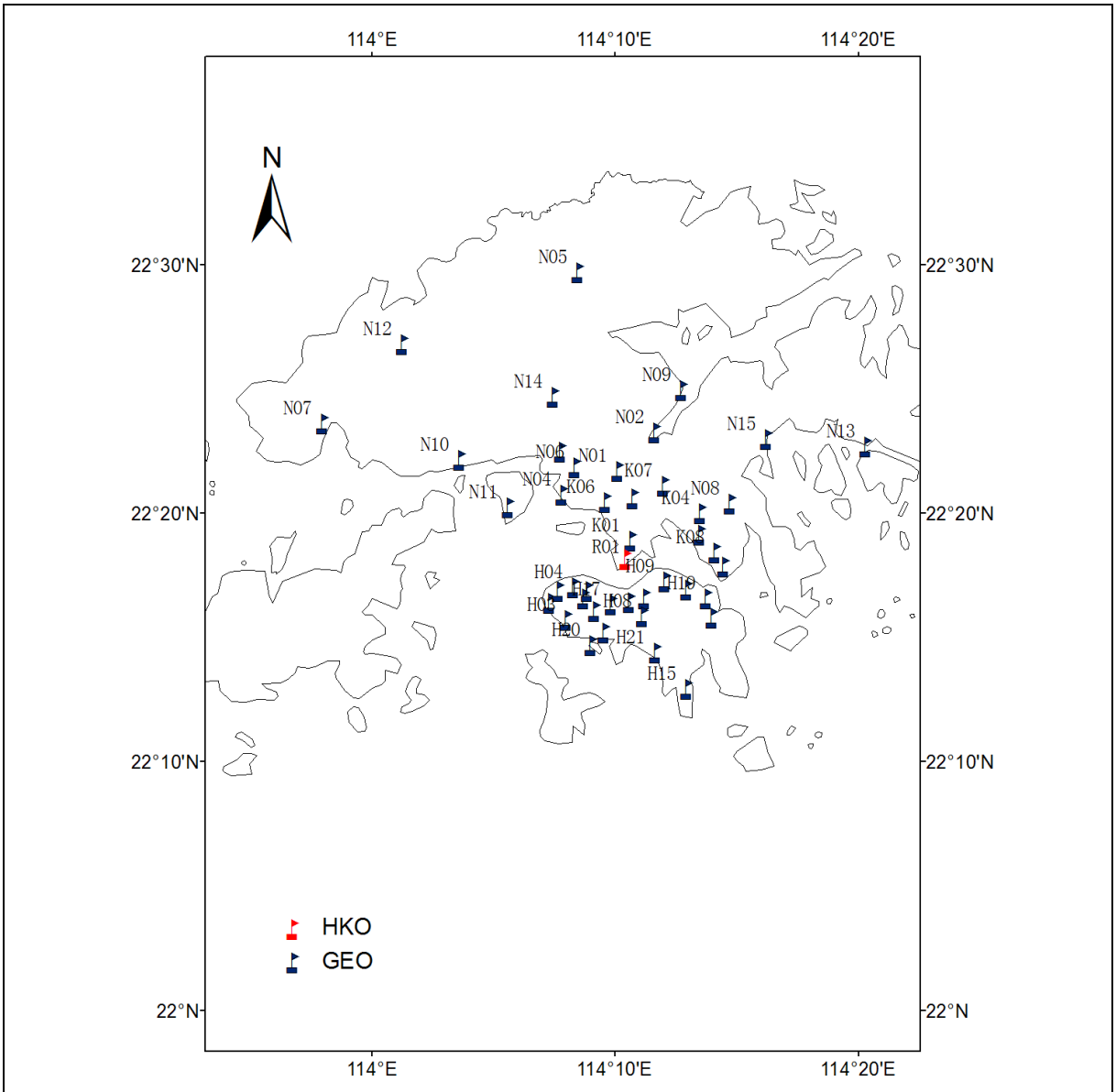

Note: Some station IDs are not shown for better presentation.

Figure 2.1 Locations of 43 Raingauges in Hong Kong

South Guangdong

The historical rainfall data of 12 stations located in the South of Guangdong Province were purchased from Guangdong Hydrological Bureau (GD HB). The geographic locations of the stations are given in Figure 2.2. The details of the time period and type of the data are given in Appendix B. The details of historical hourly maxima of the 12 South Guangdong stations are given in Appendix C. The locations of the 43 Hong Kong stations and the 12 South Guangdong stations are given in Figure 2.3.

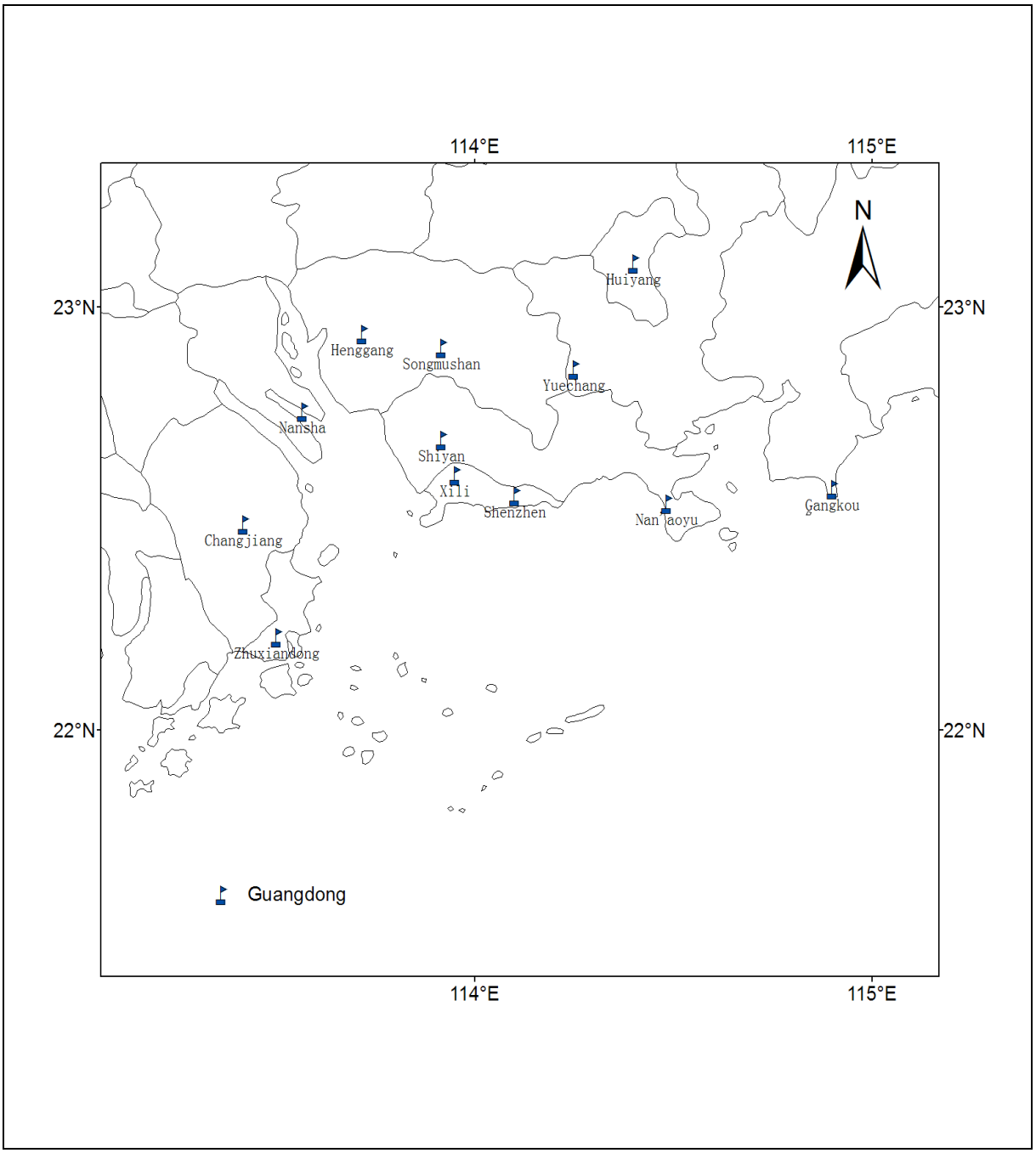

Figure 2.2 Locations of South Guangdong Stations

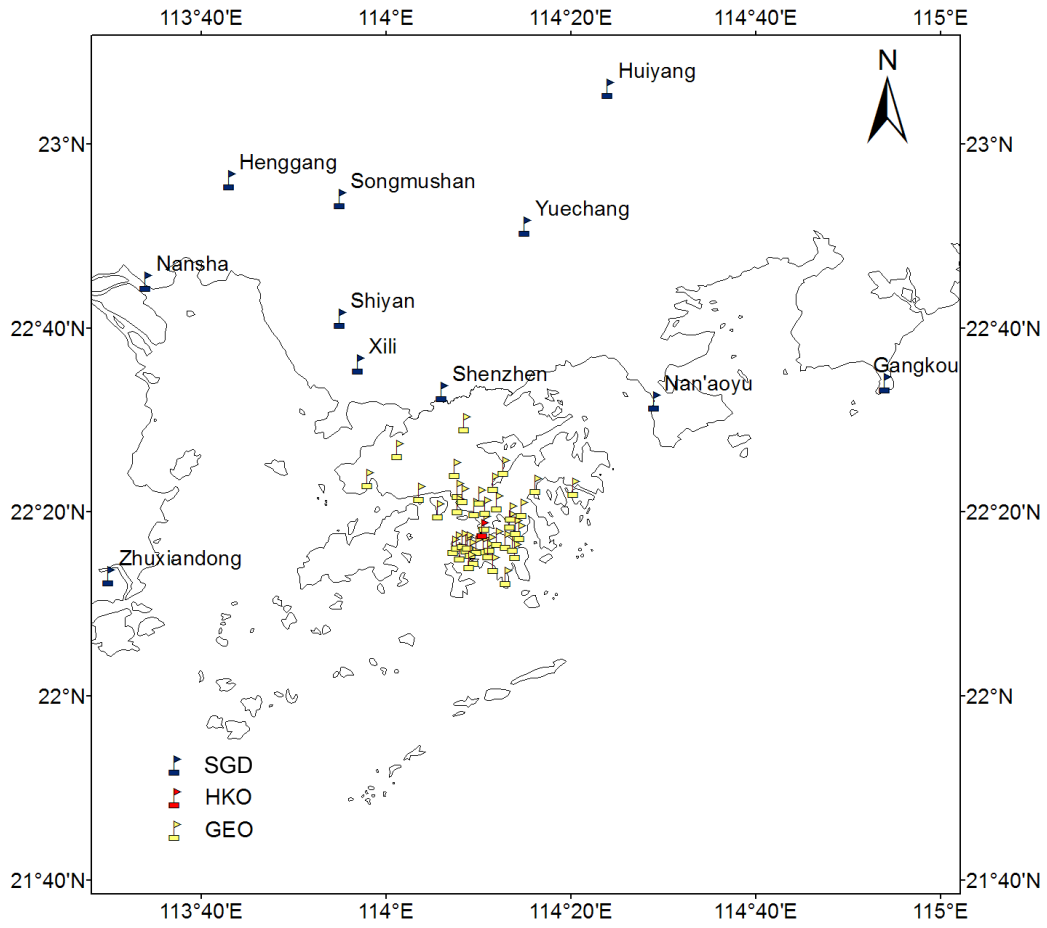

Note: Station Changjiang 長江 is located out of the range of this figure.

Figure 2.3 Locations of 43 Hong Kong Stations and 12 South Guangdong Stations

2.5.2 Processing of Historical Data

Hong Kong Data

Invalid data and missing data are replaced by '0'. Data showing "trace", referring to rainfall less than 0.05 mm, are replaced by '0.05'. The maximum hourly values were picked up by an n-hour moving window. The "n" here stands for 1, 2, 4, 6, 12 and 24 for different durations. Since the station "HKO" and the automatic raingauge "R01" are located at the headquarters of Hong Kong Observatory, data from these 2 stations are combined with the name "HKO" unchanged to give the longest observation period of rainfall data in Hong Kong. The combined station covers data for 116 years from 1885 to 2010 with data missing between 1940 and 1946 due to the World War II.

South Guangdong Data

The annual maximum hourly data for durations of 1-, 3-, 6-, 12- and 24-hour are

available for the 12 stations in South Guangdong that were purchased from the GD HB. There were a couple of years of data missing for some stations. (Details are given in the Table B2 in Appendix B).

2.5.3 Data Adopted for Transposition Analysis

Taiwan

A total of 55 Water Resources Agency (WRA) stations and 11 Central Weather Bureau (CWB) stations of Taiwan with historical hourly data that were acquired from Taiwan have been used in the computation of SDOIFs. Table 2.5 summarizes the 24-hour mean of annual maximum rainfall data at the 66 Taiwan stations and Figure 2.4 shows the geographic locations of the stations. The mean of 24-hour annual maximum rainfalls for each station in Table 2.5 are developed with observation periods longer than 18 years.

Table 2.5 24-hour Mean of Annual Maximum Rainfalls in Taiwan (Sheet 1 of 2)

	No	ID	Name	Long	Lat	Elev.	N-yr	24-hr Mean of Annual Maximum Rainfall
WRA	1	00F390	雙崎 Shuangqi(2)	120.91	24.29	543	46	308.38
	2	00H540	龍神橋 Longshenqiao	120.87	23.78	322	47	250.76
	3	00H710	集集 Jiji(2)	120.78	23.83	9	56	255.58
	4	00J810	北港 Beigang(2)	120.30	23.58	215	54	215.26
	5	00P470	旗山 Qishan(4)	120.48	22.88	64	50	268.73
	6	00Q070	屏東 Pingdong(5)	120.47	22.65	25	60	285.35
	7	00S120	鹿鳴橋 Lumingqiao	121.09	22.90	190	49	300.18
	8	01A160	林口 Linkou(1)	121.38	25.08	250	35	190.22
	9	01A200	火燒寮 Huoshaoliao	121.75	24.98	380	55	342.66
	10	01A430	福山 Fushan(3)	121.50	24.78	500	32	430.21
	11	01D100	太閣南 Taigenan	121.15	24.63	940	45	282.52
	12	01E030	橫龍山 Henglongshan	120.97	24.47	550	38	375.44
	13	01E330	大坪頂 Dapingding	120.73	24.43	190	30	227.97
	14	01F100	八仙山 baxianshan(1)	121.00	24.13	1600	20	374.39
	15	01F350	雪嶺 Xueling	121.03	24.28	2575	38	417.12
	16	01F680	頭汴坑 Toubiankeng	120.81	24.12	480	42	277.04
	17	01G240	萬興 Wanxing(2)	120.42	23.96	11	43	197.47
	18	01H310	翠峰 Cuifeng	121.20	24.11	2303	45	268.33
	19	01H390	望鄉 Wangxiang	120.93	23.62	2200	49	319.85
	20	01H440	卡奈托灣 Kanaituowan(2)	121.09	23.75	1390	41	243.16
	21	01H470	西巒 Xiluan	120.92	23.71	1666	49	276.47
	22	01H590	六分寮 Liufengliao	120.64	23.93	427	43	234.34
	23	01H680	北山 Beishan(2)	120.89	23.99	339	42	249.20
	24	01J100	西螺 Xiluo(2)	120.47	23.80	30	48	215.70
	25	01J930	林內 Linnei(1)	120.61	23.76	82	49	215.46
	26	01J960	大埔 Dapu	120.62	23.63	205	51	248.54

Table 2.5 24-hour Mean of Annual Maximum Rainfalls in Taiwan (Sheet 2 of 2)

	No	ID	Name	Long	Lat	Elev.	N-yr	24-hr Mean of Annual Maximum Rainfall
	27	01K060	褒忠 Baozhong(2)	120.31	23.70	13	49	204.86
	28	01L390	大湖山 Dahushan	120.62	23.48	725	53	469.95
	29	01L480	樟腦寮 Zhangnaoliao(2)	120.60	23.53	545	48	391.82
	30	01L910	中坑 Zhongkeng(3)	120.52	23.57	95	48	249.89
	31	01O070	關子嶺 Guanziling(2)	120.51	23.33	350	52	371.66
	32	01P190	木柵 Mushan	120.47	22.98	78	52	302.36
	33	01P500	阿蓮 Ahlian(2)	120.33	22.88	21	50	262.67
	34	01P660	甲仙 Jiaxian(2)	120.59	23.08	355	56	354.63
	35	01Q160	新豐 Xinfeng	120.65	22.88	166	55	323.44
	36	01Q250	泰武 Taiwu(1)	120.70	22.61	950	56	647.66
	37	01Q360	南和 Nanhe	120.64	22.43	140	46	339.95
	38	01Q910	阿禮 Ahli	120.76	22.73	1158	43	588.07
	39	01Q930	三地門 Sandimen	120.65	22.71	150	42	393.45
	40	01S210	知本 Zhiben(5)	121.00	22.69	100	31	291.32
WRA	41	01S360	紹家 Shaojia	120.86	22.38	520	55	299.38
	42	01S430	霧鹿 Wulu	121.04	23.17	910	56	277.23
	43	01S440	新武 Xinwu(3)	121.13	23.13	420	39	322.84
	44	01S470	向陽 Xiangyang(2)	120.99	23.25	2400	38	370.97
	45	01T220	卓麓 zhuolu(4)	121.27	23.30	210	36	321.40
	46	01T230	立山 lishan	121.31	23.43	180	49	333.68
	47	01T560	西林 Xilin	121.43	23.82	200	37	380.22
	48	01T640	哇拉鼻 Walabi	121.19	23.35	960	29	337.83
	49	01T660	馬太安 Mataian	121.37	23.67	1000	30	456.00
	50	01U080	南山 Nanshan	121.38	24.44	1050	46	258.37
	51	01U230	大濁水 Dazhuoshui	121.74	24.33	48	31	341.05
	52	01U470	武塔 Wuta	121.78	24.45	32	31	325.25
	53	01V050	藤枝 Tengzi(2)	120.76	23.07	1640	30	460.95
	54	01V070	天池 Tianchi	120.92	23.28	2230	32	431.27
	55	01V080	民族 Mingzhu	120.70	23.22	530	33	419.45
	56	467420	永康 Yongkang*	120.22	23.04	8.1	30	273.54
	57	467440	高雄 Gaoxiong*	120.30	22.57	2.3	30	286.35
	58	467550	玉山 Yushan	120.95	23.49	3845	30	334.78
	59	467530	阿里山 Ahlishan	120.80	23.51	2413	30	587.34
	60	466990	花蓮 Hualian	121.60	23.98	16	30	289.21
CWB	61	467080	宜蘭 Yilan	121.73	24.77	7.2	30	241.55
	62	467590	恆春 Hengchun	120.73	22.01	22.1	30	288.23
	63	467660	臺東 Taidong	121.13	22.75	9	30	275.56
	64	C1M510	樸子 Puzi*	120.23	23.47	8	19	244.84
	65	C1X070	北門 Beimeng*	120.10	23.27	14	19	230.13
	66	C1X060	下營 Xiaying*	120.27	23.24	5	19	258.79

Note: * Stations were selected as the base stations for development of SDOIF, referring to Section 1.3.2.2 (3) (c).

Table of Contents
Table of Contents
Table of Contents
Table of Contents

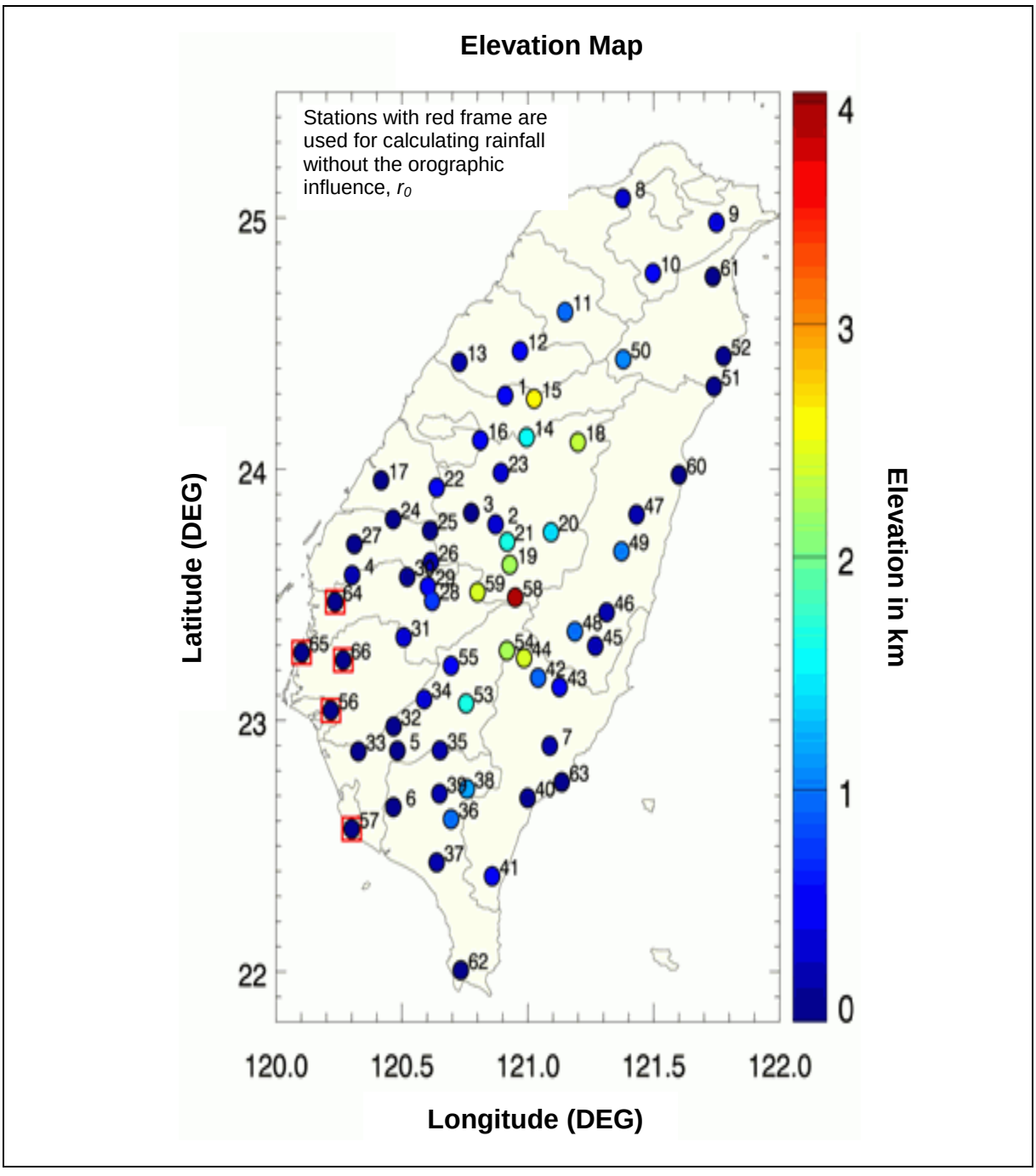

Figure 2.4 Locations of 66 Stations for Historical Hourly Data in Taiwan

Hong Kong and South Guangdong

In total, 65 Hong Kong stations with observation periods longer than 17 year have been used in the computation of the local SDOIFs. The cut-off of 17 year used here was adopted with a view to maximizing the use of the data while assuring the quality of statistical analysis in application of SDOIF method. Table 2.6 summarizes the 24-hour mean of the annual maximum rainfall data for the 65 stations in Hong Kong and Figure 2.5 shows their locations.

Table of Contents
Table of Contents
Table of Contents
Table of Contents

Figure 2.5 Locations of 65 Raingauges in Hong Kong with Hourly Rainfall Data Observation Periods Longer than 17 years

Table 2.6 24-hour Mean of Annual Maximum Rainfalls in Hong Kong (Sheet 1 of 2)

No	ID	Long	Lat	Elev	N-yr	Time Period of Available Data	24 hour Mean of Annual Maximum Rainfall
1	H01	114.12	22.27	107	27	1984 - 2010	223.41
2	H02	114.13	22.28	95	27	1984 - 2010	240.26
3	H03	114.13	22.26	132	27	1984 - 2010	216.76
4	H04	114.14	22.28	123	27	1984 - 2010	256.22
5	H05	114.16	22.25	103	27	1984 - 2010	229.35
6	H06	114.18	22.27	88	27	1984 - 2010	246.96
7	H07	114.19	22.28	94	27	1984 - 2010	239.41
8	H08	114.19	22.26	129	27	1984 - 2010	247.48
9	H09	114.20	22.29	160	27	1984 - 2010	256.85
10	H10	114.15	22.28	530	27	1984 - 2010	253.59
11	H12	114.15	22.28	188	27	1984 - 2010	256.85
12	H14	114.23	22.26	141	27	1984 - 2010	216.85
13	H15	114.22	22.22	50	27	1984 - 2010	216.52
14	H16	114.15	22.27	439	27	1984 - 2010	249.17
15	H17	114.16	22.27	200	27	1984 - 2010	251.19
16	H18	114.22	22.28	77	27	1984 - 2010	238.54
17	H19	114.23	22.28	53	27	1984 - 2010	233.54
18	H20	114.15	22.24	104	27	1984 - 2010	210.72
19	H21	114.19	22.24	139	27	1984 - 2010	211.54
20	K01	114.18	22.31	91	27	1984 - 2010	239.04
21	K02	114.18	22.34	92	27	1984 - 2010	258.26
22	K03	114.23	22.32	91	27	1984 - 2010	234.91
23	K04	114.23	22.33	178	27	1984 - 2010	247.33
24	K05	114.24	22.30	117	27	1984 - 2010	234.78
25	K06	114.16	22.34	35	27	1984 - 2010	245.22
26	K07	114.20	22.35	197	27	1984 - 2010	254.44
27	K08	114.24	22.31	77	27	1984 - 2010	230.22
28	N01	114.17	22.36	38	27	1984 - 2010	267.96
29	N02	114.19	22.39	73	27	1984 - 2010	253.07
30	N03	114.13	22.37	113	27	1984 - 2010	247.11
31	N04	114.13	22.35	96	27	1984 - 2010	237.20
32	N05	114.14	22.49	111	27	1984 - 2010	219.17
33	N06	114.14	22.36	106	27	1984 - 2010	261.33
34	N07	113.97	22.39	41	27	1984 - 2010	211.52
35	N08	114.25	22.34	256	27	1984 - 2010	245.13
36	N09	114.21	22.42	6	27	1984 - 2010	257.78
37	N10	114.06	22.37	35	26	1984 - 2010	242.98
38	N11	114.09	22.34	40	26	1984 - 2010	228.63
39	N12	114.02	22.45	79	27	1984 - 2010	212.69
40	N13	114.34	22.38	87	27	1984 - 2010	243.74
41	N14	114.12	22.41	944	27	1984 - 2010	327.07
42	N15	114.27	22.38	41	26	1984 - 2010	234.58
43	N16	114.27	22.32	114	26	1986 - 2010	233.19

Table 2.6 24-hour Mean of Annual Maximum Rainfalls in Hong Kong (Sheet 2 of 2)

No	ID	Long	Lat	Elev	N-yr	Time Period of Available Data	24 hour Mean of Annual Maximum Rainfall
44	N17	113.94	22.28	17	19	1992 - 2010	296.18
45	N18	114.00	22.27	69	19	1992 - 2010	257.13
46	R01	114.17	22.30	32	24	1885 - 2010	233.75
47	R11	113.91	22.26	478	24	1987 - 2010	270.58
48	R12	114.01	22.29	106	24	1987 - 2010	219.38
49	R13	114.12	22.22	32	24	1987 - 2010	182.69
50	R14	114.26	22.21	45	24	1987 - 2010	211.71
51	R17	114.11	22.29	90	24	1987 - 2010	205.17
52	R18	114.29	22.31	122	24	1987 - 2010	192.90
53	R19	114.21	22.29	7	18	1993 - 2010	233.81
54	R21	113.92	22.38	28	24	1987 - 2010	225.81
55	R22 *	114.01	22.49	8	24	1987 - 2010	195.79
56	R23	114.17	22.45	23	24	1987 - 2010	239.67
57	R24	114.21	22.54	39	24	1987 - 2010	230.17
58	R25	114.33	22.41	106	24	1987 - 2010	211.75
59	R26	114.09	22.44	20	24	1987 - 2010	248.52
60	R27	114.00	22.42	102	24	1987 - 2010	225.19
61	R28	114.05	22.45	3	24	1987 - 2010	217.94
62	R29	114.08	22.51	67	24	1987 - 2010	190.23
63	R31	114.24	22.48	10	24	1987 - 2010	191.19
64	R32	114.35	22.35	24	24	1987 - 2010	217.56
65	R30 *	114.30	22.54	13	21	1987 - 2008	199.95

Note: * base stations for development of SDOIF referring to Section 1.3.2.2 (3) (c).

South Guangdong

Data of the 12 South Guangdong stations were studied in detail. Of these 12 stations, only three stations are located relatively close to Hong Kong and were considered relevant in developing the Hong Kong Orographic Intensification Factor (OIF) pattern. Historical hourly data for the three stations are summarized in Table 2.7. Their locations are shown in Figures 2.2 and 2.3.

Table 2.7 24-hour Mean of Annual Maximum Rainfalls in Guangdong

No	ID	Long	Lat	Elev	N-yr	Time Period of Available Data	24 hour Mean of Annual Maximum Rainfall
1	Xili	113.95	22.59	35	36	1975 - 2010	166.90
2	Shiyan	113.92	22.68	38	37	1974 - 2010	172.40
3	Shenzhen*	114.10	22.55	27	29	1981 - 1989 1991 - 2010	204.45

Note: * base stations for development of SDOIF referring to Section 1.3.2.2 (3) (c).

Table of Contents
Table of Contents
Table of Contents
Table of Contents

3 Statistical Estimate of 24-hour PMP

3.1 Application of the Method to 24-hour PMP for Hong Kong

Criteria and procedures applied to screening of data for regionalization (referring to Section 1.3.1.2) of the computation are described in items (a) to (e) below.

(a) Sort the station data in descending order based on the maximum value, X_m.

(b) Take the top 10 stations into the computation process for the study area.

(c) Check the required stable size N_s and then take some stations out when $N_s > 3.5\ n$ as it may cause 50% in error in terms of K_m by taking the stable sample size $N_s = 220$ as an example. By considering the stable sample size $N_s = 220$ and the actual data size $n = 60$ available, the corresponding values of ϕ_m are 6 and 3 respectively. Hence the difference is 50% (i.e. 3/6), referring to the chart of N_s and ϕ_m in Figure 1.1.

(d) Pick up the highest values of $\overline{X}_n'$, K_m and C_{vn} of Equation 1.7 over the eligible stations in the concerned region.

(e) Following criteria in (c) above, two stations of N09 and N15 for 24-hour were taken out of the computation; the data of the other stations are eligible for computation as described in Section 1.3.1.2.

The details of the computation are shown in Appendix D.

3.2 Recommended Statistical PMP Estimates

The regionalized 24-hour PMP estimates based on Hong Kong data and South Guangdong data are 1,650 mm and 1,453 mm respectively. This suggests that the 24-hour PMP for Hong Kong would fall between 1,453 mm and 1,650 mm.

4 Storm Separation

4.1 Study Area

Further to the preliminary screening as discussed in Section 2.4, four major storms in Taiwan have been selected and further studied for transposition in PMP study to the Southeast (SE) China typhoon-prone area. The 6 Guangdong storms were not selected as target storms for transposition as they were less severe and due to limitation in data availability. Based on the severity of the storm and the outcome of the storm disaster, the 2009 Morakot storm has

been selected as the major target storm together with other three storms for storm separation analysis. The SDOIF method is applied as a storm separation technique to decouple the Morakot rainfall into two components, the convergence component and the orographic component. Also, the SDOIF method is applied to decouple the other three storms. The four convergence components are joined together to form a generalized pattern of the convergence component to be transposed to Hong Kong. The shape of the generalized pattern of the isohyets is formed based on the four convergence components and its intensity is determined by the value of the Morakot's convergence component which is expressed in isohyets.

4.2 Storm Separation of Four Major Storms Affecting Taiwan

4.2.1 Development of the SDOIF for the Target Area

A group of 5 stations were selected as the base stations without orographic influence for development of SDOIF referring to Section 1.3.2.2 (3) (c). The 5 CWB stations are 永康(56), 高雄(57), 樸子(64), 北門(65) and 下營(66) at elevations less than 20 m above MSL in the southwest coastal area of Taiwan.

A gridded calculation frame covering the whole land area of Taiwan was adopted. Figure 4.1 shows the spatial distribution of the 24-hour SDOIF at a resolution of (5 km x 5 km) for Taiwan that is in accord with the pattern of the distribution of the 24-hour average annual maximum rainfall for Taiwan (Figure 4.2). The number in each grid (cell) indicates the OIF value for that grid.

4.2.2 Development of Convergence Rainfall Isohyets for the Four Major Storms Affecting Taiwan

The 24-hour convergence component isohyets have been generated by applying the 24-hour SDOIF (see Figure 4.1) to decouple the corresponding 24-hour isohyets based on Equation 1.13 for the four major storms in Taiwan below. The results are given in Figures 4.3 to 4.6.

(a) Typhoon Herb of 31 July to 2 August 1996;

(b) Typhoon Aere of 24 August to 26 August 2004;

(c) Typhoon Haitang of 18 July to 20 July 2005 (A detailed comparison of CWB and WRA data is given in Appendix E); and

(d) Typhoon Morakot of 8 August to10 August 2009.

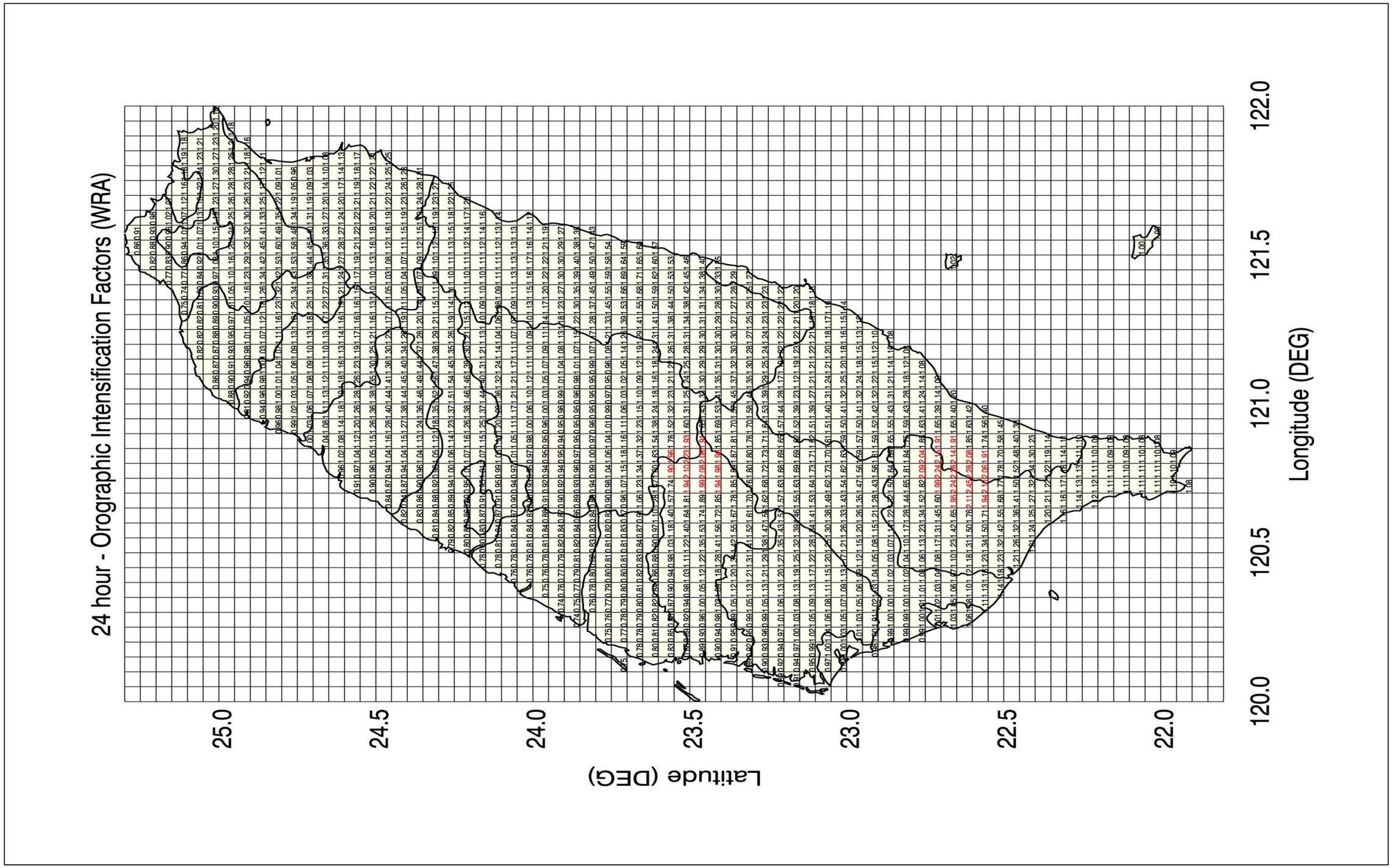

Figure 4.1 24-hour SDOIF for Taiwan at a Resolution of 5 km x 5 km

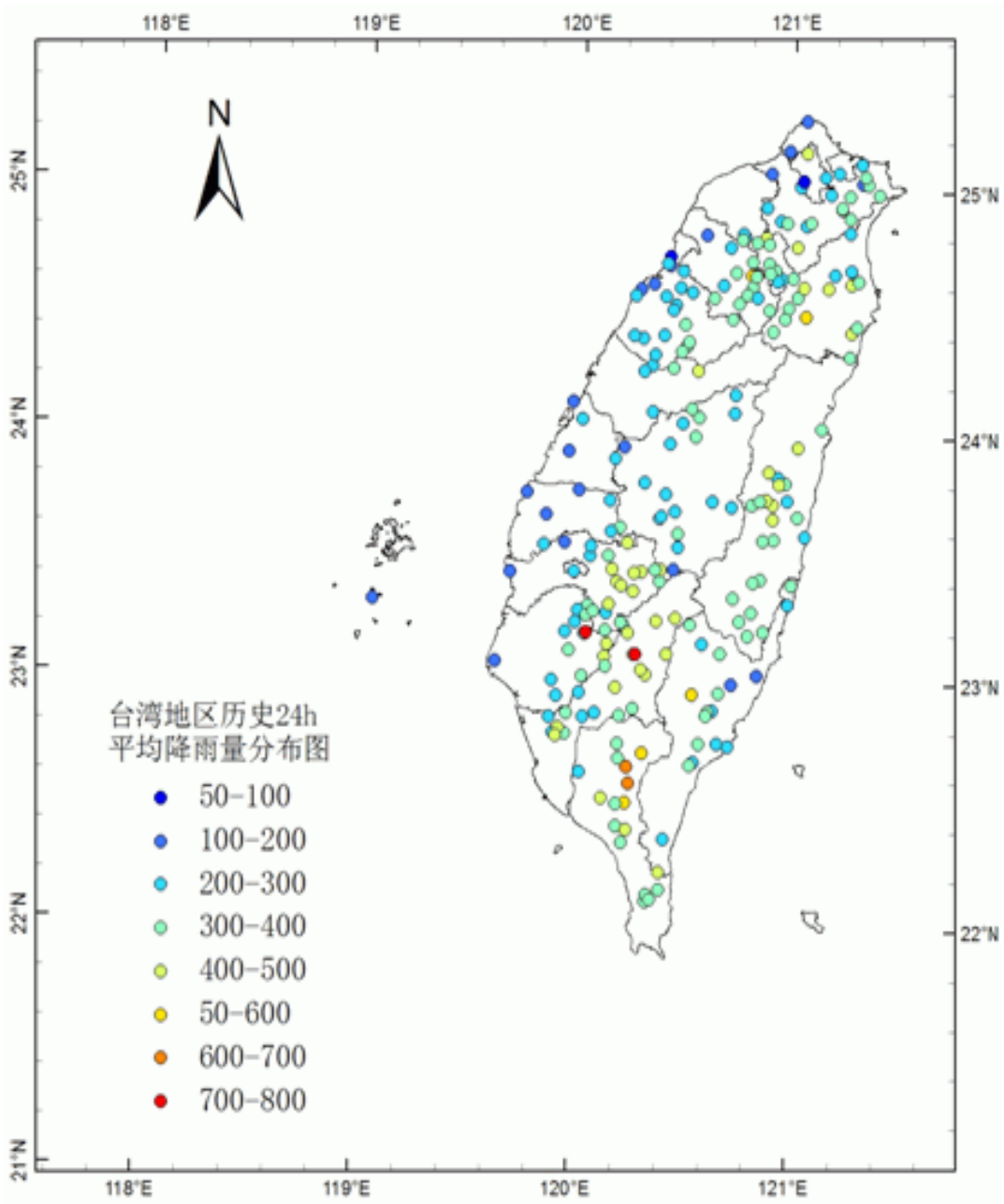

Note: Courtesy by Sinotech's data via AHMRI.

Figure 4.2 24-hour Average Annual Maximum Rainfall in Taiwan

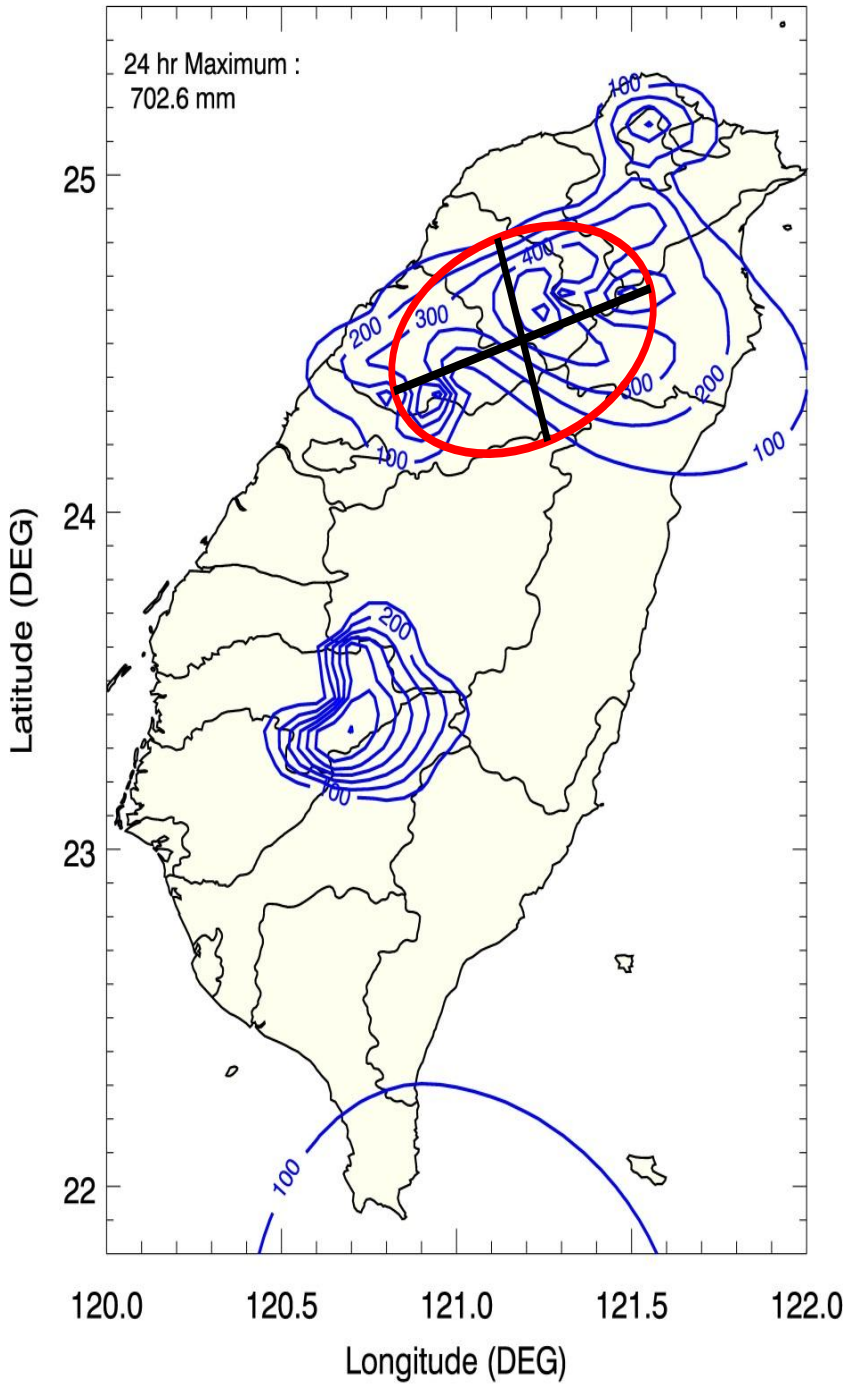

Note: r = major radius/minor radius = 3.5/2.1 = 1.67 (based on the shape of 300 mm isohyets; the same below).

Figure 4.3 The Shape of the Generalized Convergence Component Pattern of Storm Herb

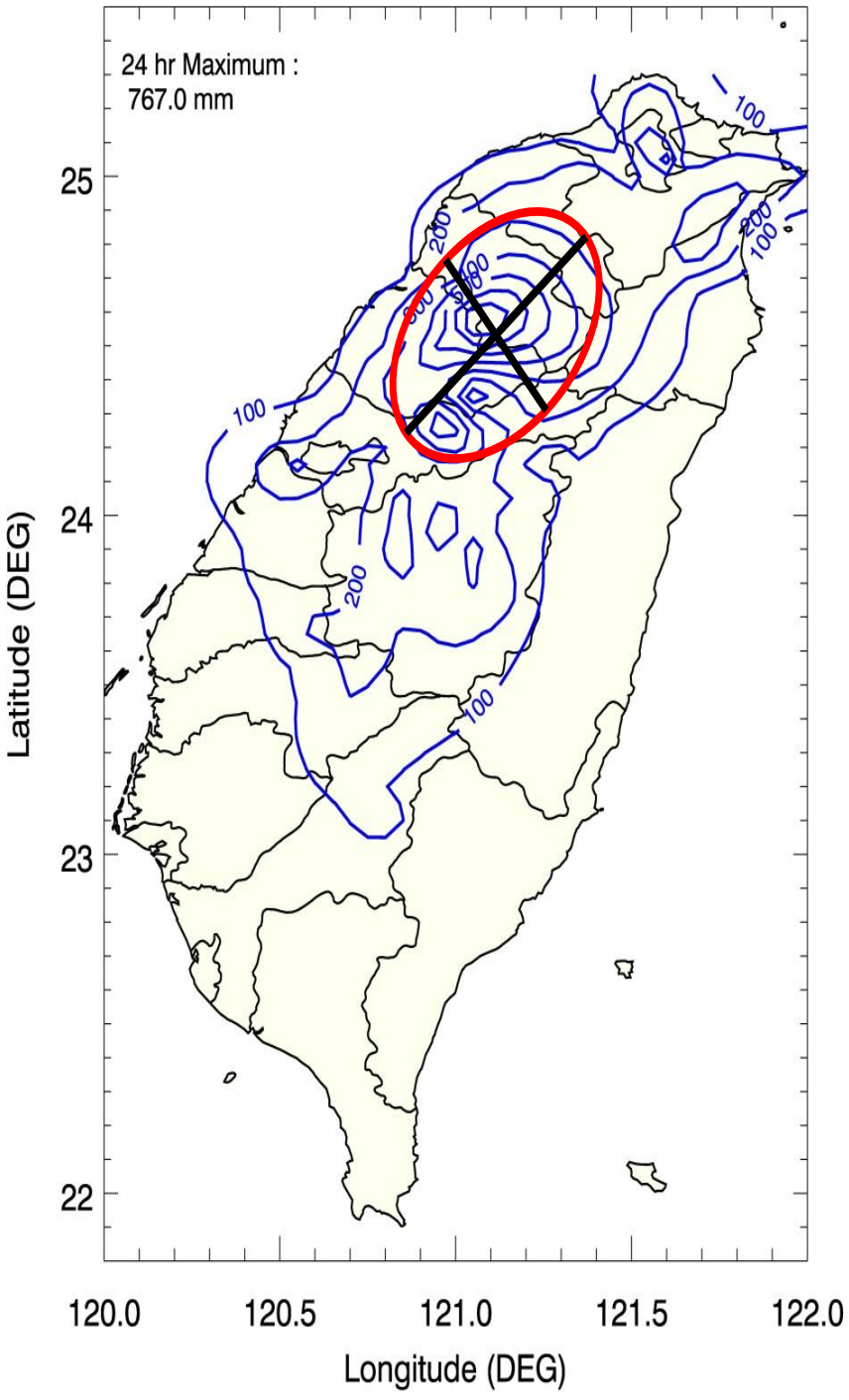

Note: r = major radius/minor radius = 3.1/2.0 = 1.55.

Figure 4.4 The Shape of the Generalized Convergence Component Pattern of Storm Aere

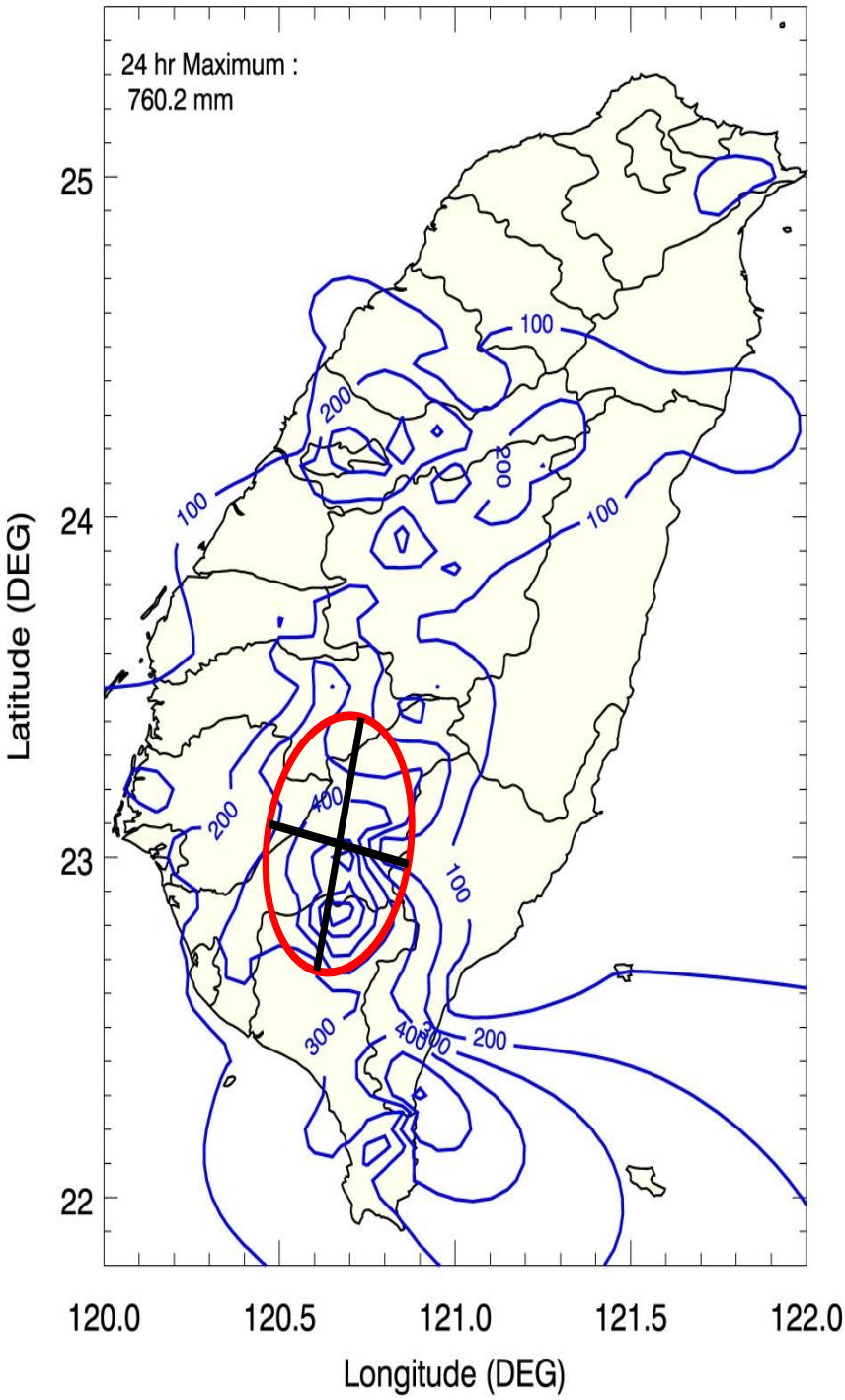

Note: r = major radius/minor radius = 2.7/1.8 = 1.5.

Figure 4.5 The Shape of the Generalized Convergence Component Pattern of Storm Haitang

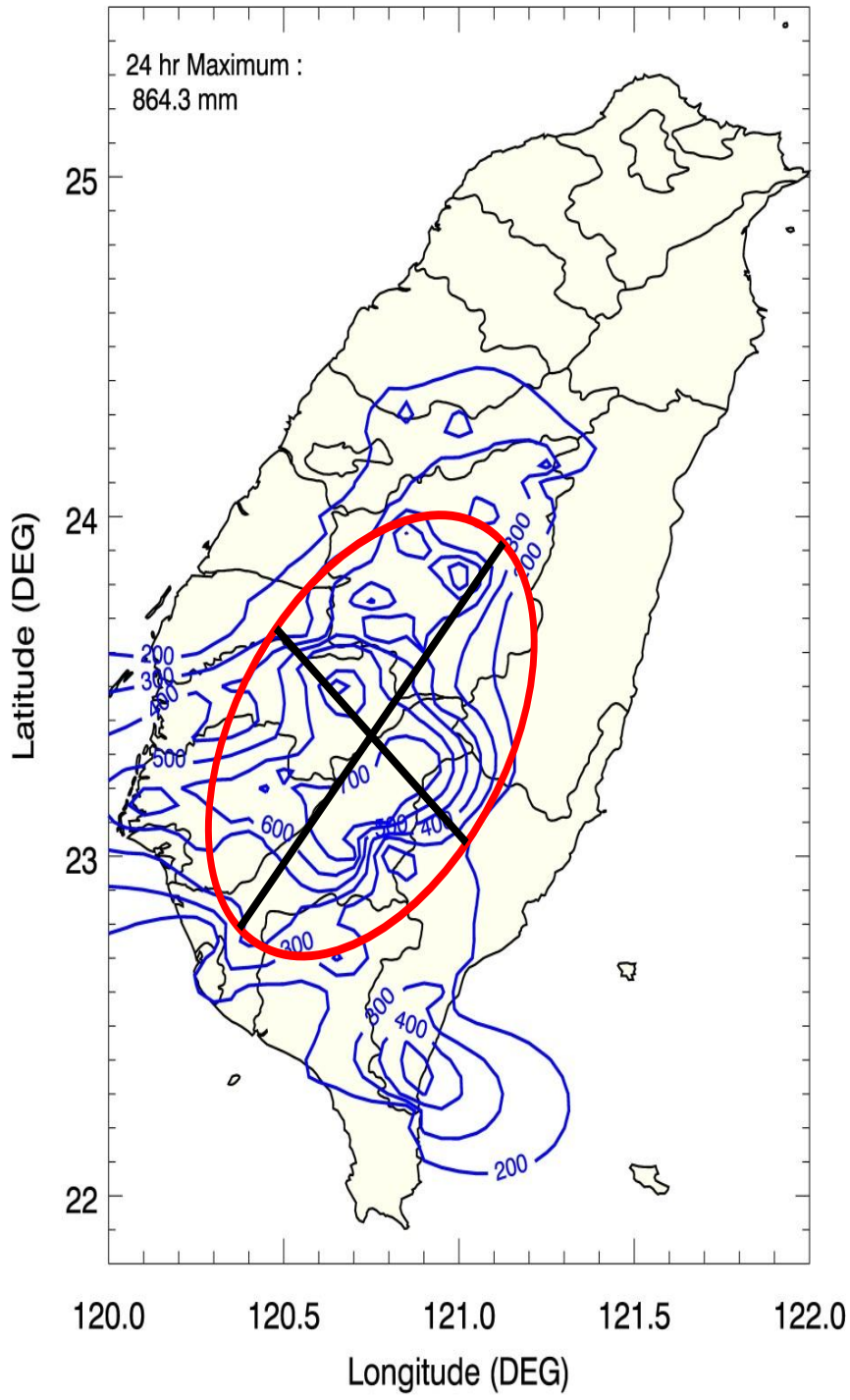

Note: r = major radius/minor radius = 5.2/3.3 = 1.58.

Figure 4.6 The Shape of the Generalized Convergence Component Pattern of Storm Morakot

4.2.3 Development of the Relation of Area Average Rainfall with Area Size for Taiwan

The relation between the area average 24-hour convergence rainfall and the area size for the four major storms affecting Taiwan have been developed as shown in Table 4.1.

Table 4.1 Relation of Area Average 24-hour Convergence Rainfall with Area Size in Taiwan

Isohyets (mm)	Area (km^2)				
	Herb	Aere	Haitang	Morakot	Generalised Convergence Component Pattern
0 - 50	26206	28181	13220	14690	14690
50 - 100	6075	3157	6436	5757	5757
100 - 150	4053	2257	4647	5061	5061
150 - 200	1266	2418	6134	5371	5371
200 - 250	1149	2116	4230	2128	2128
250 - 300	946	1478	2510	1677	1677
300 - 350	613	759	1853	1230	1230
350 - 4 00	395	340	1036	1131	1131
400 - 450	289	225	590	1133	1133
450 - 500	236	166	385	720	720
500 - 550	113	124	286	576	576
550 - 600	68	72	82	476	476
600 - 650	39	55	40	554	554
650 - 700	0	45		449	449
700 - 750		33		401	401
750 - 800		22		81	81
800 - 900				10	10

4.3 Construction of Generalized Convergence Component Pattern of Transposed Storm in the Target Area, Taiwan

4.3.1 Basics

The generalized convergence component pattern of transposed storm consists of the values of isohyets and shape of the isohyets. The values are determined by the convergence

component of Morakot storm while the shape is a pattern generalized over the four outstanding storms Morakot, Herb, Aere and Haitang.

4.3.2 Construction of the Generalized Convergence Component Pattern

The generalized convergence component pattern is obtained by undertaking the following procedures:

(a) Development of the Depth-Area relation of the generalized convergence component.

(i) Convergence rainfall isohyets of the 4 major storms in Taiwan are drawn as shown in Figures 4.3 to 4.6.

(ii) According to the convergence rainfall isohyets, tables summarizing the Depth-Area of the convergence pattern for the 4 major storms were developed as shown in Table 4.1 for 24-hour duration.

(iii) 24-hour convergence of Morakot pattern was used for storm transposition.

(b) Determination of the shape of the generalized component pattern.

For the purpose of engineering design studies, a generalized pattern of the convergence component with reasonable shape and quantitative parameters is needed. The pattern of the isohyets over the four major storms has been examined. The isohyets of 300 mm were used as the representative for studying the shape of the generalized convergence component pattern. A working ellipse was drawn to match or rotate around the 300 mm isohyets as better as possible for each of the storms. The aspect ratios (i.e. the ratio of the major radius to the minor radius) for Aere, Haitang, Herb, and Morakot were estimated to be 1.55, 1.5, 1.67 and 1.58 respectively (See Figures 4.3 to 4.6). As a result, an elliptical shape of the generalized pattern with an aspect ratio of 1.6 was suggested.

(c) Construction of the generalized convergence component pattern.

The generalized convergence component pattern of Taiwan storms was constructed with a size to cover the design area of Hong Kong at the same scale as shown in Figure 4.7. This is a conventional way to take a fix increment between isohyets for a general pattern such as 50 mm for 24-hour pattern. This makes the general isohyets pattern more flexible to use for different applications. They look uneven for ellipses that have major-radius and minor-radius because a storm may not pour rainfall evenly in space in the real world.

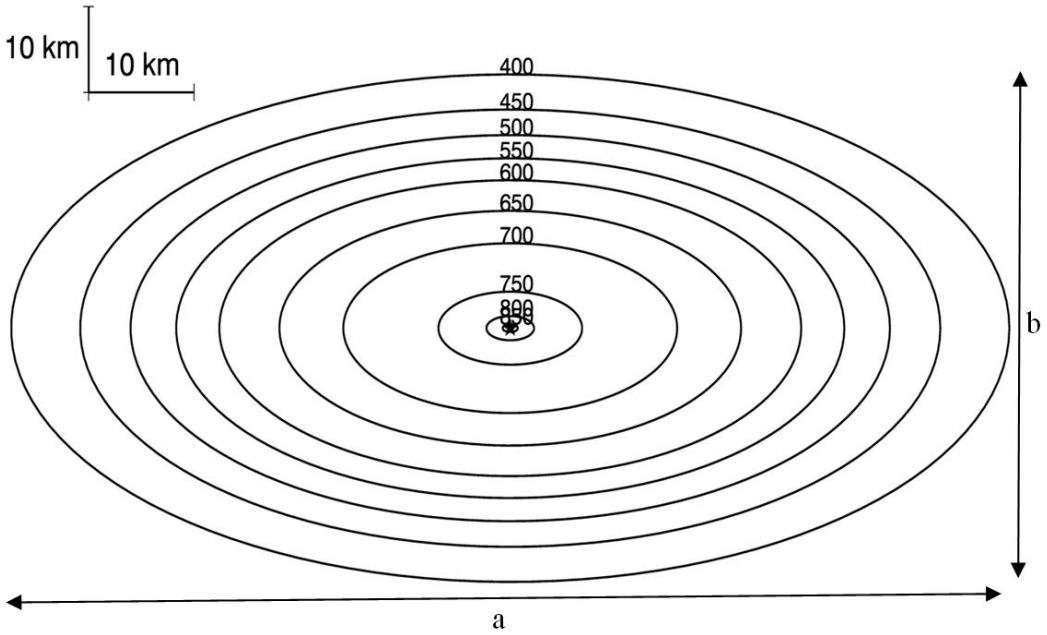

Note: a:b = 1.6:1.

Figure 4.7 24-hour Generalized Convergence Component Pattern of Taiwan Storms

4.4 Development of SDOIF for Hong Kong

A group of three stations were selected as the base stations without orographic influence referring to Section 1.3.2.2 (3) (c). They are Shenzhen (深圳) of Guangdong and R22 and R30 of Hong Kong as shown in Figures 2.3 and 2.5 for their locations.

A gridded calculation frame was set up so that it would well cover the whole Hong Kong. Figure 4.8 shows the spatial distribution of the 24-hour SDOIF for Hong Kong at a resolution of (5 km x 5 km).

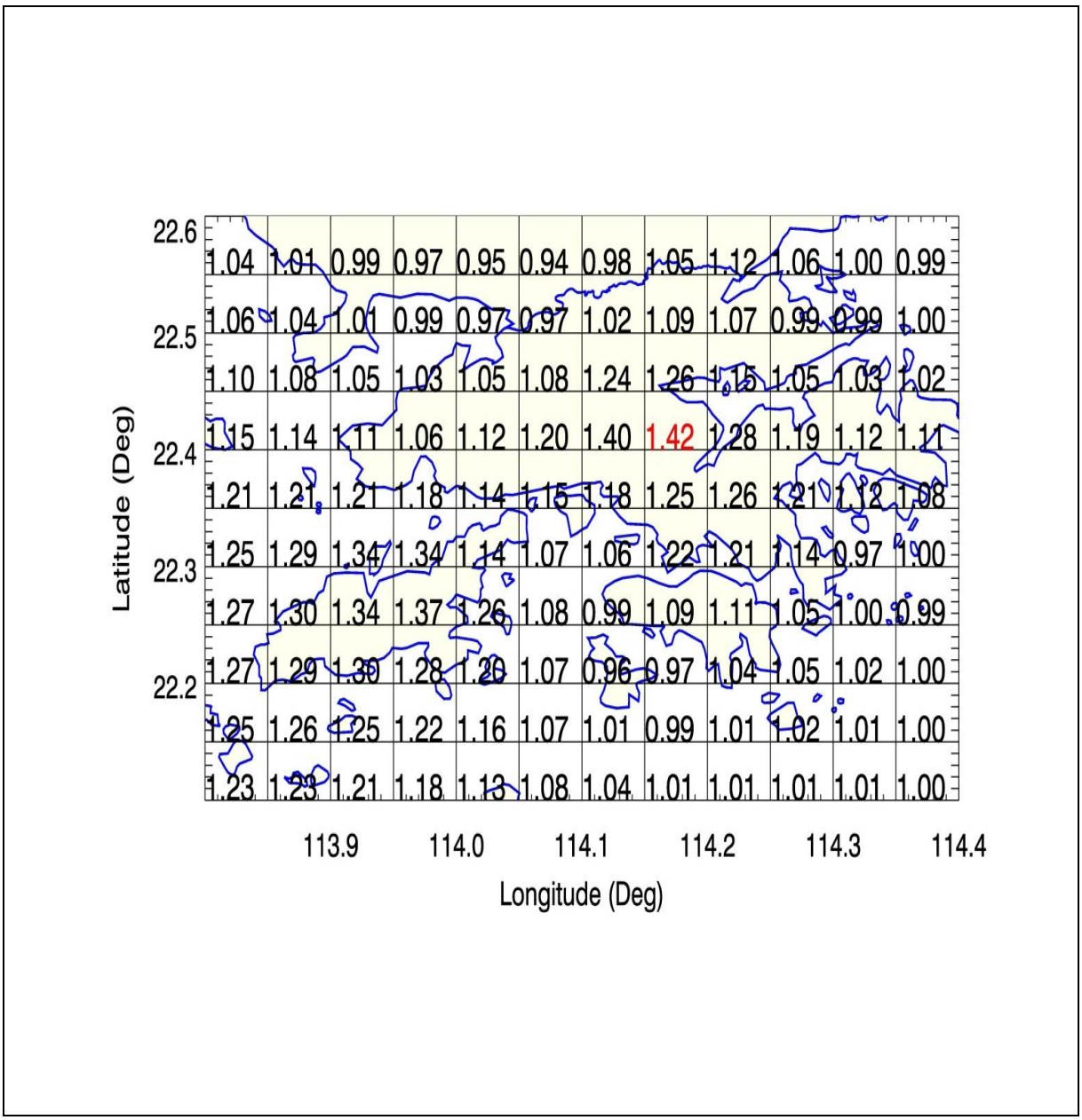

Figure 4.8 24-hour SDOIF for Hong Kong at a Resolution of 5 km x 5 km

5 Storm Transposition and Orientation Adjustment

The generalized convergence component pattern of Taiwan storms was coupled with the local SDOIF pattern or orographic component to generate a PMP embryo by superposing the generalized convergence component pattern onto the local SDOIF. The word "embryo" used here means it is a preliminary PMP estimate. It is required to further adjust this embryonic PMP by transposition adjustments to take into account the orientations to the prevailing moisture inflow jet during the invasion of typhoon storm to Hong Kong.

5.1 Storm Transposition

The generalized convergence component pattern of Taiwan storms as shown in Figure 4.7 was superposed on the local OIF grids to calculate the PMP fraction or portion at each grid. As an example, the centre of the generalized convergence pattern superposed on the OIF grid cell for Tai Mo Shan is illustrated in Figure 5.1.

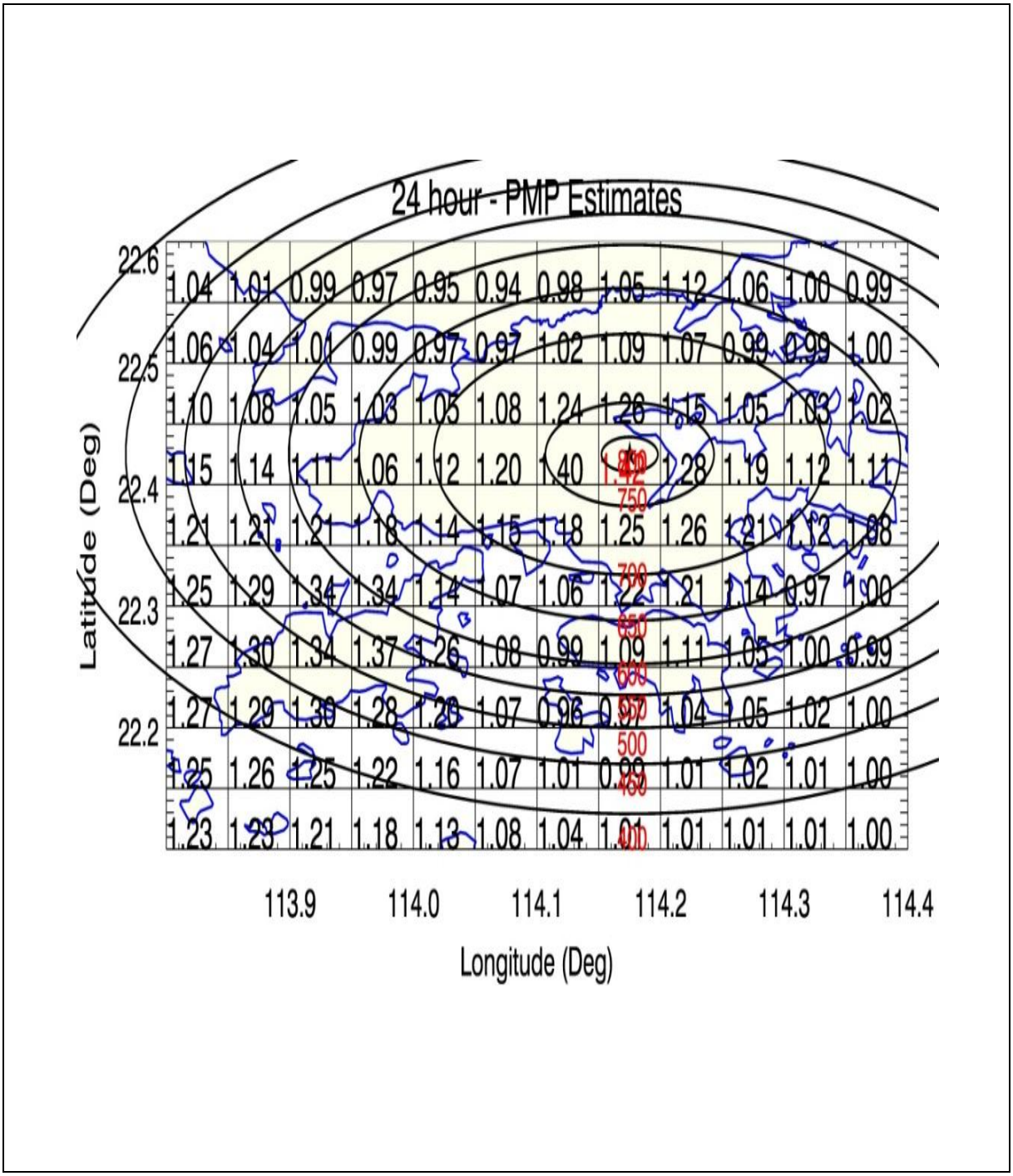

Figure 5.1 Generalized Convergence Component Pattern Superposed on OIF Grid for Tai Mo Shan

5.2 Orientation Adjustment

The orientation of a potential PMP-level storm in the future is random. The worst scenario should be prepared. Therefore, more orientations for the major ellipse axis of the generalized convergence pattern from 22.5° to 180° at increment of 22.5° (in anticlockwise direction) have been studied. They are 22.5°, 45°, 67.5°, 90°, 112.5°, 135°, 157.5° and 180°. The orientation of 85° was actually used for 90° due to technical difficulties encountered in programming. The orientation of 180° is the same as at 0°. An example showing the rotated generalized convergence pattern superposing the local OIF grids is given in Figure 5.2. A complete set of orientation of convergence pattern centred at Tai Mo Shan, Lantau and Hong Kong Island is given in Appendix F.

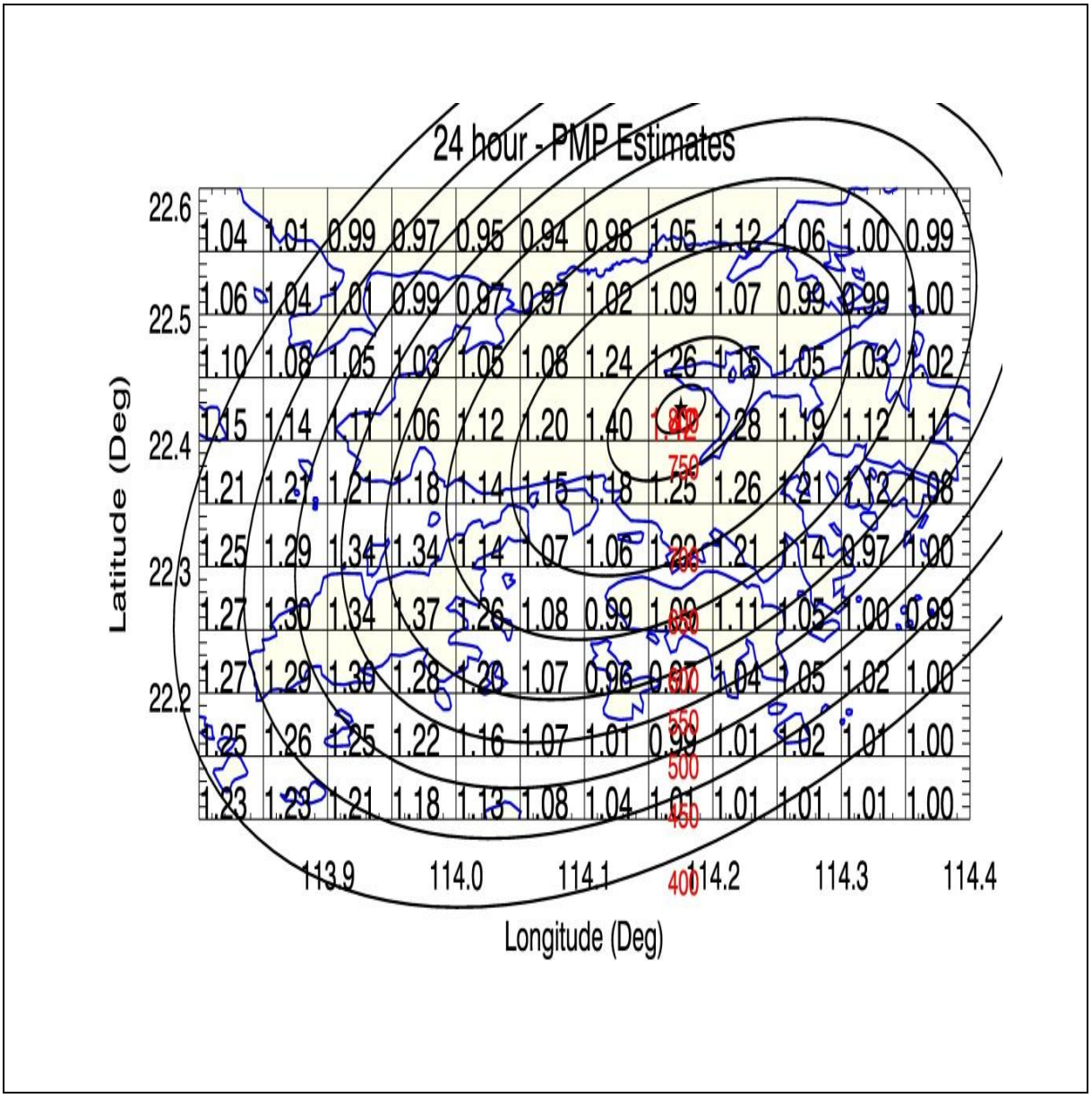

Figure 5.2 Generalized Convergence Component Pattern Superposed on OIF Grid for Tai Mo Shan with 45° Orientation Adjustment

5.3 Embryonic PMP

After the orientation adjustment of the convergence pattern has been applied to the gridded PMP fractions (OIF), embryonic PMP can be obtained for the 8 selected orientation adjustment directions. Embryonic PMP in isohyets and grids are presented in Appendices G to I for the generalized convergence pattern centred at Tai Mo Shan, Lantau and Hong Kong Island respectively. An example of the embryonic PMP centred at Tai Mo Shan with 22.5° orientation adjustment is given in Figure 5.3.

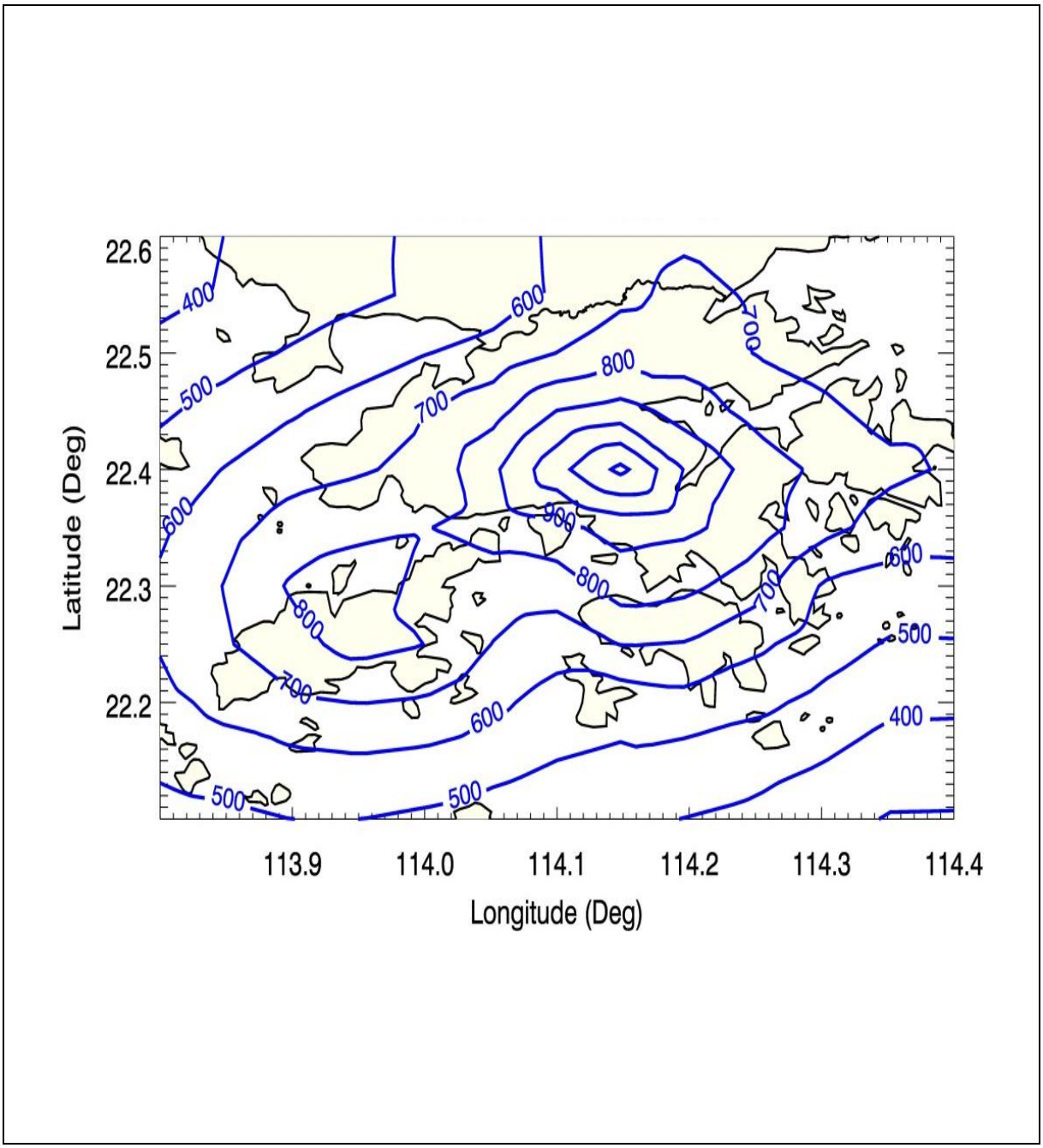

Figure 5.3 Isohyets of Embryonic 24-hour PMP Centred at Tai Mo Shan with Orientation Adjustment of 22.5°

5.4 The Centre Point Value of the Embryonic PMP

No matter what orientation is, the centre point value of the embryonic PMP is the same. The centre point values of the embryonic PMP estimates were derived as follows:

Centre point value of 24-hour embryonic PMP = the highest grid value of OIF map × the highest centre value of the 24-hour convergence component of Morakot

= 1.42 × 864 = 1227 mm
(*centred at Tai Mo Shan area* (*the highest OIF cell for whole Hong Kong*))

Centre point value if convergence component superposed on other grid cells *(For reference)*

= 1.37 × 864 = 1184 mm
(*centred at the highest OIF cell at Lantau*); or

= 1.113 × 864 = 962 mm
(*centred at the highest OIF cell at Hong Kong Island*)

5.5 Table of the Depth-Area Relation for the Embryonic PMP

Four scenarios for orientation: (1) the East-West orientation specified as E-W; (2) the NE-SW or 45°; (3) the ENE-WSW or 22.5°; and (4) the NNE-SSW or 67.5° for the major ellipse axis of the convergence pattern are given in Table 5.1, when they are superposed on Hong Kong (i.e. centred at Tai Mo Shan). The dimensions of the superposition area are given below:

Hong Kong area:

	Lower Bound (°)	Upper Bound (°)	Range (°)
Longitude	113.8	114.4	0.6
Latitude	22.1	22.6	0.5

Notes: *(1) 1° ~ 100 km.*
(2) Area ~ 3000 km^2 (including the ocean area).

Table 5.1 Relation of Depth-Area of the Embryonic 24-hour PMP for Hong Kong

Area (km^2)	Orientation of Major Storm Axis			
	E-W 0°	NE-SW 45°	ENE-WSW 22.5°	NNE-SSW 67.5°
	Depth (mm)	Depth (mm)	Depth (mm)	Depth (mm)
0	1227	1227	**1227**	1227
10	1167	1180	**1181**	1179
20	1133	1147	**1149**	1146
50	1072	1093	**1096**	1092
100	1009	1036	**1039**	1035
150	968	997	**1002**	998
200	940	972	**976**	973
300	898	934	**937**	932
400	873	905	**909**	903
500	847	885	**887**	882
600	833	867	**870**	861
700	821	850	**853**	845
800	809	838	**841**	832
900	796	826	**829**	820
1000	785	814	**817**	807
1500	744	767	**770**	761
2000	704	728	**731**	721
3000	599	642	**649**	638

Note: The embryonic PMP with orientation adjustment of 90°, 112.5°, 135° and 157.5° are less critical and not shown here for clarity.

6 Moisture Maximization for Transposed Storm

The embryonic PMP with orientation adjustment was further adjusted by the moisture maximization ratio.

6.1 Basics

In storm transposition, the moisture adjustment is the transposed storm rainfall amounts of the target area, i.e. Taiwan, multiplied by the ratio of precipitable water for the enveloping, or historical maximum dew point in the design location (W_2), i.e. Hong Kong, to the precipitable water for the representative storm dew point (W_1) in the target area, which is given below:

Table of Contents
Table of Contents
Table of Contents
Table of Contents

$$R_2 = R_1(\frac{W_2}{W_1}) \quad \text{..... (6.1)}$$

where R_1 is the transposed storm rainfall for a particular duration and areal coverage and R_2 is the storm rainfall adjusted for transposition to the design area. In maximizing for moisture, the maximum dew point used is for the same location as that of the representative storm dew point. The historical maximum persisting 12-hour dew points based on 6-hour interval dew point observations are commonly used for moisture maximization if the available dew point data series is longer than 50 years. Alternatively, frequency analysis for 100-year return period events is adopted as the representative of the maximum atmospheric moisture if the annual dew point record series is appreciably shorter than approximately 50 years. Dew points selected at locations between the rainfall area and the moisture source tend to be more representative of the atmospheric moisture content, or precipitable water, supplying moisture to the storm than dew points within the rainfall area. To minimize sampling errors, an average over the dew point locations (sites) in the between-area is recommended if the data are available after taking a synoptic analysis of the storm in question.

6.2 Representative 12-hour Persisting Dew Point in the Target Area

Dew points observations during Morakot storm at 4 stations, including Yongkang (永康 #56), Gaoxiong (高雄 #57), Hualian (花蓮 #60) and Yilan (宜蘭 #61) were collected as shown in Figure 2.4 for locations.

Two of the 4 stations in the SW moisture inflow direction during Morakot storm, Yongkang (永康 #56) and Gaoxiong (高雄 #57), were selected to be the representative stations. The representative maximum 12-hour persisting dew points are 23.3℃ for Yongkang (永康 #56) and 24.6℃ for Gaoxiong (高雄 #57) with an average dew point of 24℃. For details of data processing of the raw dew point observations, see Appendix J.

6.3 Historical Maximum 12-hour Persisting Dew Point in the Design Area

6.3.1 Data Selection

The HKO station which is the only station in Hong Kong having historical dew point data of more than 50 years (data available between 1947 and April 2013) is chosen for calculation of the historical 12-hour maximum persisting dew point, which is then converted to the corresponding 1,000 hPa dew point. However, dew point data between 1947 and 1960 were recorded in whole integer of °F, conversion to ℃ would introduce certain degrees of error. Therefore, dew point between 1947 and 1960 is not further considered. Details of the data screening process are listed as follows:

(a) Pick out each single observation greater than the preset threshold (25℃).

(b) Use a 12-hour window to pick up the maximum persisting 12-hour dew point between year 1961 and year 2010 to form an Annual Maximum Series for dew point.

(c) Check and make sure that the 12-hour persisting dew point comes from a period of 24-hour prior to the onset of the corresponding major intensified rainfall.

(d) As a result of (c) above, obtain a dew point series of 50-year for the period between 1961 and 2010 for frequency analysis and the rest two years of dew point data at HKO were ignored since there were no rainfall data for the period of 2011 - 2013 at HKO to be used for checking the onset of the corresponding major intensified rainfall.

6.3.2 Frequency Analysis

The 100-year return period of the historical 12-hour maximum persisting dew point at HKO, which is calculated based on Generalized Extreme Value (GEV) distribution which is the best fitting by using the L-moments Method (Lin et al, 2006), is 27.04℃. The converted 1,000 hPa dew point is 27.17℃ corresponding to precipitable water of 96.48 mm under the assumption of pseudo adiabatic atmosphere. If the Regional L-moments Approach (RLA) is used for frequency analysis of dew point, the quantile estimate of a 100-year return period event employing the 50 years (1961 - 2010) of data will not be appreciably different from that employing the 64 years (1947 - 2010) of data because the dew point data series does not exhibit large dispersion and heavy skewness in comparison with the AMS of rainfall data in terms of statistical characteristics.

In essence, there is no big difference between the two methods, historical maximum or 100-year, for determining the maximum persisting 12-hour dew point when the available dew point data series is quite long. However, in practice the 100-year return period estimate is recommended even the dew point observation series is longer than 50 years.

Gumbel distribution has been widely used in combination of use of Conventional Moments Method (CMM) as a parameter estimation technique to fit the dew point data series for obtaining the 100-year return period estimate. However, for this study, a more advanced technique of L-Moments Method (LMM) as parameter estimation in combination of goodness-of-fit over five plausible 3-parameter probability distributions (GLO, GEV, GNO, GPA, PE3) was used. The advantages of LMM over CMM are of unbiasedness in terms of parameter estimation and robustness to outlier (Lin et al, 2006).

A GEV distribution was selected to best fit the dew point series by 3 tests or criteria:

Test 1: The Monte Carlo Simulation test to test and compare the deviates from the averaging point of simulated data series over all stations to the selected distribution in L-Kurtosis scale over the five plausible distributions at a L-Kurtosis vs L-Skewness diagram.

Test 2: Root Mean Square Error of the sample L-moments to test and count all deviates from each of the stations to the selected distribution in L-Kurtosis scale over the

five plausible distributions at a L-Kurtosis vs L-Skewness diagram.

Test 3: Real-data-check test to test the significance of the difference between the empirical frequencies of data and the theoretical probabilities from 2-year to 50-year quantiles over the five plausible distributions.

The three tests are described in details in Section "Goodness-of-fit" of Lin et al (2006). All these three tests pointed to the GEV as the best fitting distribution to the data, with quantile of 27.04 for 100-year indicated. The computer output from these three tests is given in Appendix K for reference.

Trough and Cyclonic are the major types of storms associated with heavy rainfalls in Hong Kong based on the investigation of the top 10 local storms. Therefore, the monthly maximum persisting dew point series in June to October was employed for the frequency analysis, referring to the Southeast (SE) China Sea Surface Temperature (SST) isolines in Appendix L. It is clear that the SE China SST reached their highest values of about 26 to 28℃ in the period of June to October, in which the Trough and Cyclonic of the major types of storms associated with heavy rainfalls in Hong Kong appeared to be most active. Hence the monthly maximum persisting 12-hour dew points are picked from June to October ignoring other months to obtain the yearly maximum persisting 12-hour dew point. On the other hand, referring to data selection in Section 6.3.1, a direct way to pick up the yearly maximum persisting 12-hour dew point via a 12-hour window over the entire year was used as long as data available. It turned out that most of the 12-hour dew points came from the period of June to October. Finally, the annual maximum persisting 12-hour dew point series was adopted in the frequency analysis.

6.4 Ratio of Moisture Maximization

The storm rainfall adjusted for transposition (R_2) (see Section 6.1) is given as follows:

$$R_2 = R_1 \times (\frac{W_2}{W_1}) = R_1 \times (\frac{W_{27.17}}{W_{24.0}}) = R_1 \times (\frac{96.48}{74.0}) \quad \text{.....(6.2)}$$

Ratio of moisture maximization for transposition is estimated as follow:

$$r = W_2 / W_1 = W_{27.17} / W_{24} = 96.48 / 74.0 = 1.304$$

in which, W_2 is the precipitable water for the historical maximum 12-hour persisting dew point for the design area of Hong Kong, which is 27.17℃, while the W_1 is the precipitable water for the representative dew point, 24.0℃, for the Morakot storm. Under the assumption of pseudo adiabatic atmosphere, the 1,000 hPa dew point of 27.17℃ and 24.0℃ are corresponding to precipitable water of 96.48 mm and 74.0 mm respectively (see Annex I of WMO, 2009).

6.5 Estimated PMP for Hong Kong

The PMP value at the centre of the design PMP pattern (i.e. centred at Tai Mo Shan) is as below:

24-hour: 1,227 mm × 1.304 = 1,600 mm

Isohyets in Appendices G to I are multiplied by the ratio 1.304 and presented in Appendix M. The corresponding rainfall in the Table of Depth-Area (Table 5.1) is increased correspondingly by multiplying by the same ratio for moisture maximization (Table 6.1).

Table 6.1 Relation of Depth-Area of the Updated 24-hour PMP for Hong Kong

Area (km^2)	Orientation of Major Storm Axis			
	E-W 0°	NE-SW 45°	ENE-WSW 22.5°	NNE-SSW 67.5°
	Depth (mm)	Depth (mm)	Depth (mm)	Depth (mm)
0	1600	1600	**1600**	1600
10	1522	1539	**1540**	1537
20	1477	1496	**1498**	1494
50	1398	1425	**1429**	1424
100	1316	1351	**1355**	1350
150	1262	1300	**1307**	1301
200	1226	1267	**1273**	1269
300	1171	1218	**1222**	1215
400	1138	1180	**1185**	1178
500	1104	1154	**1157**	1150
600	1086	1131	**1134**	1123
700	1071	1108	**1112**	1102
800	1055	1093	**1097**	1085
900	1038	1077	**1081**	1069
1000	1024	1061	**1065**	1052
1500	970	1000	**1004**	992
2000	918	949	**953**	940
3000	781	837	**846**	832

Note: The centre of the PMP storm is at Tai Mo Shan.

Table of Contents
Table of Contents
Table of Contents
Table of Contents

The isohyets of the PMP (centred at Tai Mo Shan with orientation 22.5°) representing the critical case are shown in Figure 6.1.

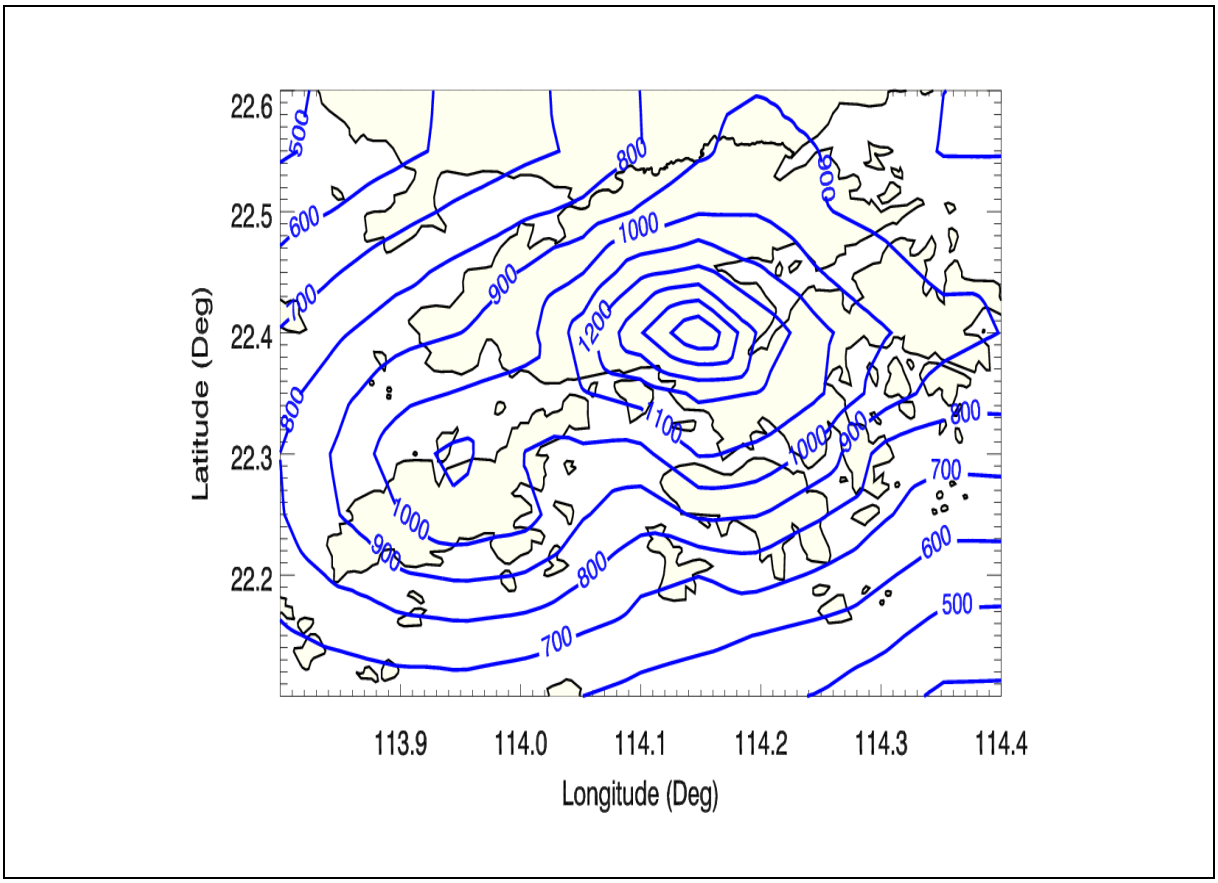

Figure 6.1 Isohyets of 24-hour PMP Centred at Tai Mo Shan with Orientation Adjustment of 22.5°

7 Application of PMP to Landslide Risk Assessment

7.1 Approach

Theoretically, the generalised convergence component from the target area (Taiwan) can be superimposed with each OIF grid cell for the design area (Hong Kong) to generate an individual PMP estimate for each cell. In view of the uncertainties (see Section 11.1) involved in the estimation and the relatively small size of the territory of Hong Kong, the worst scenario involving all possible locations and orientations should be adopted in application such as landslide risk assessment.

7.2 PMP Value with Centre Point at Lantau

If the embryonic PMP is placed at Lantau, the centre point value is:

$$1{,}184 \text{ mm} \times 1.304 = 1{,}543 \text{ mm}$$

The above centre point value is slightly less than that centred at Tai Mo Shan (see Section 6.5). The isohyets of the PMP if centred at Lantau are shown in Figure 7.1.

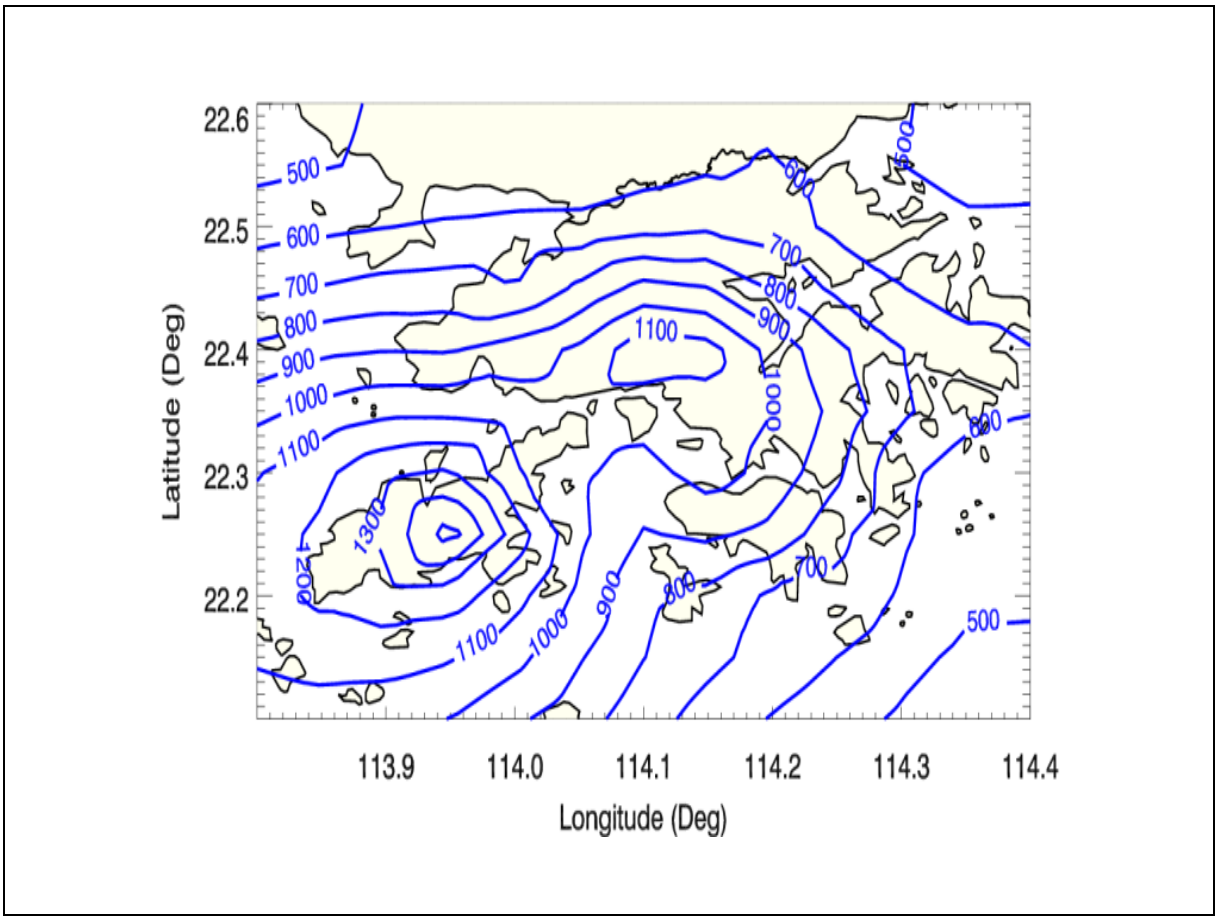

Figure 7.1 Isohyets of 24-hour PMP Centred at Lantau with Orientation Adjustment of 22.5°

7.3 Application

The DAD curves of PMP estimates with centre point placed at Tai Mo Shan and Lantau (simply denoted as Tai Mo Shan PMP and Lantau PMP) are shown in Figure 7.2. As shown, Tai Mo Shan PMP is more critical for area less than 100 km^2 or larger than 1,700 km^2 while Lantau PMP is more critical for area between 100 km^2 and 1,700 km^2. In application, from the points of view of design study it is recommended that the average of the two DAD curves as shown in Figure 7.2 should be used to represent the worst scenario for landslide risk assessment. The relation of depth-area of the average is shown in Table 7.1.

The average of the theoretical centre point values of the Tai Mo Shan PMP and Lantau PMP is 1,570 mm. For application in landslide risk management, the minimum area concerned is assumed to be 10 km^2. Hence, in practice, it is recommended to adopt the value corresponding to 10 km^2 as the updated PMP which is equal to **1,510 mm**.

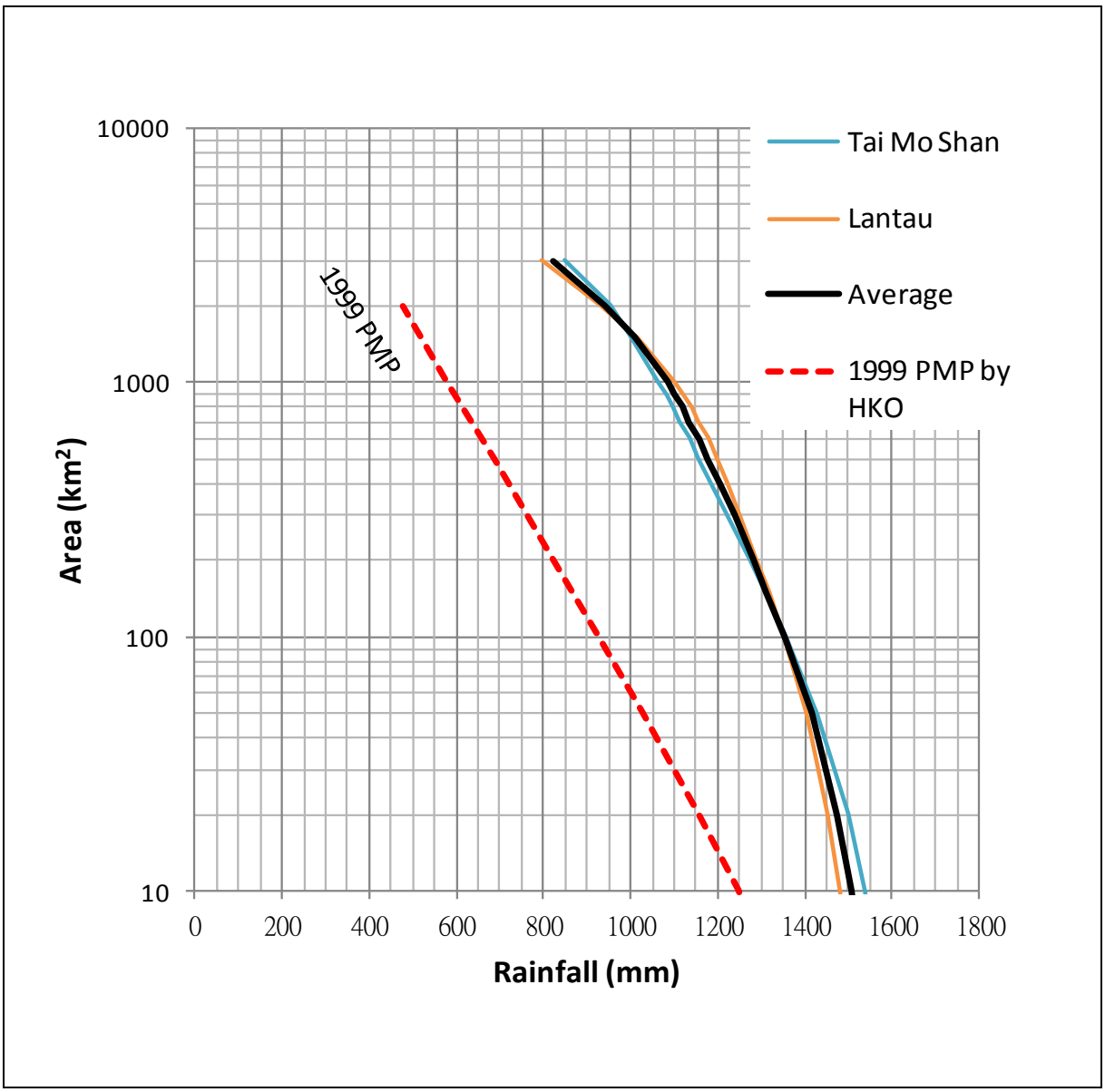

Figure 7.2 DAD Curves of Updated 24-hour PMP for Application

For reference, the DAD curve of the last update of PMP estimates in 1999 (HKO, 1999) is plotted in Figure 7.2. It is noted that apart from the significant increase in 24-hour rainfall from 1,250 mm to 1,510 mm for a rainfall area of 10 km^2, the greatest increase of 24-hour rainfall (from 580 mm to 1,085 mm) is corresponding to an area of 1,000 km^2.

For landslide risk assessment, PMP isohyets will be applied to study areas to assess the landslide responses. For this purpose, the Tai Mo Shan PMP and Lantau PMP should be further generalized and combined to generate a set of PMP isohyets which maintains the same DAD relationship of the average of the two PMP. It is recommended that elliptical-shaped isohyets with an aspect ratio of 1.6 which is similar to the generalized convergence component pattern should be adopted. The dimensions of the PMP isohyets are shown in Table 7.2.

Table 7.1 Relation of Depth-Area of the Updated 24-hour PMP for Application

Area (km^2)	Depth (mm)
10	1510
20	1476
50	1417
100	1353
150	1312
200	1282
300	1237
400	1205
500	1177
600	1156
700	1135
800	1118
900	1102
1000	1085
1500	1010
2000	942
3000	822

Table 7.2 24-hour PMP Isohyets for Landslide Risk Assessment

Isohyet (mm)	Minor Axis (km)	Major Axis (km)	Area (km^2)
1500	2.1	3.4	5.8
1400	4.0	6.4	20
1300	7.5	11.9	70
1200	10.9	17.5	150
1100	17.8	28.5	400
1000	22.4	35.8	630
900	28.2	45.1	1000
800	35.7	57.1	1600
700	40.9	65.4	2100
600	44.2	70.6	2450
500	47.2	75.5	2800

Note: Area of ellipse = π(major axis x minor axis)/4.

8 DAD Analysis

8.1 Overview

DAD analysis is one of the well-known international practices for interpreting PMP estimation. DAD curves are developed from areal mean rainfalls for different durations over several major storms in the study area including local storms and storms in the vicinity. The quality and value of DAD curves greatly depends upon the samples of major storm that have been surveyed and investigated. Sometimes storm moisture maximization is incorporated with DAD analysis in PMP estimation to make up the local estimates for the worst situation in accordance with the concept of PMP for the study area.

In the study, a total of 22 storms have been surveyed and investigated, including 20 local storms and two major storms from the neighbouring Guangdong Province. The Kriging method, which requires a denser network of raingauges, was used for spatial interpolation when areal mean rainfall to a certain area for the local storms after 1984 as well as for two Guangdong storms was generated. The inverse distance method was used for local storms before 1984 as rainfall data from fewer stations are available. Since Hong Kong is a coastal area, the sea-portion of area was counted together with its land-portion to form a complete storm rainfall area within and/or between isohyets in order to represent the real world of Depth-Area as meaningful as possible based on the availability of the data.

8.2 Top 10 Local Storms between 1984 and 2010

Top 10 Hong Kong storms between 1984 and 2010, based on 5-min running window and using Kriging method, for 24-hour duration refer to Table 2.1. The corresponding DAD curves are shown in Figure O1 in Appendix O.

8.3 Top 10 Local Storms between 1966 and 1983

Top 10 Hong Kong storms, based on 1-hour running window, inverse distance method for sparser network or Kriging method for denser network, for 24-hour duration are given in Table 2.2. The corresponding DAD curves are shown in Figure O2 in Appendix O.

8.4 Two Representative Guangdong Storms

Two representative Guangdong storms (based on 1-hour running window and Kriging method) are tabulated in Table 8.1. DAD curves for the two representative Guangdong storms are shown in Figure O3 in Appendix O.

Table 8.1 Top Two Outstanding Storms for Guangdong

No.	Date	Max 24-hr Rainfall (mm)	No. of Raingauge Stations	Storm Type (Name)
1	9-12 August 2007	1188.2	42	Typhoon (Pabuk)
2	21-23 September 2010	839.5	171	Typhoon (Fanapi)

8.5 Moisture Maximization Ratios for Local Storms

A complete set of moisture maximization ratios for the top 20 Hong Kong storms are given in the Table 8.2. Steps for calculation of moisture maximization ratios are detailed in Appendix N.

Table 8.2 Moisture Maximization Ratios for Top 20 Hong Kong Storms

Storm	Moisture Maximization Ratio	Storm	Moisture Maximization Ratio
1993	**1.65 ***	1966	1.32
1994	**1.21 ***	1970	1.20
2008	**1.36 ***	1971	1.27
1995	1.07	1972-3	1.27
2003	1.33	1972-2	1.13
1998	1.49	1972-1	1.42
1999	1.30	1973	1.16
1989	1.45	1976	**1.29 ***
2005	1.18	1983	1.22
1997	1.11	1981	1.30

Note: * the ratios are used for development of the master DAD with moisture maximization.

8.6 Master DAD

8.6.1 Master DAD Developed Based on Hong Kong and Guangdong Storms without Moisture Maximization

A generalized or the master DAD curves without moisture maximization based on 20 local storms, which are the top 10 between 1966 and 1983 and the top 10 between 1984 and 2010 for 24-hour rainfalls, and two major Guangdong storms (Typhoons Pabuk and Fanapi) is shown in Figure O4 in Appendix O. Table O1 in Appendix O gives the detail of the DAD relation corresponding to the DAD curves.

8.6.2 Master DAD Developed Based on Hong Kong and Guangdong Storms with Moisture Maximization

The master DAD curve with moisture maximization for 24-hour rainfall based on the top 20 Hong Kong storms is shown in Figure 8.1. For comparison purpose, the two outstanding Guangdong storms were merged into the above master DAD curve. The points based on Typhoon Pabuk became the controlling points in the DAD after merging. The above results are also shown in Figure 8.1. The details of the above DAD relation are tabulated in Tables 8.3 and 8.4. The master DAD curves for other rainfall durations are also shown in Appendix O.

The storm transposition and DAD analysis are two different approaches and there is no common ground to compare the results of the two methods in details. Nevertheless, the DAD curve based on transposition of Taiwan storms (i.e. the average of the PMP estimate with centres at Tai Mo Shan and Lantau) is also plotted in Figure 8.1. It is shown that the results based on storm transposition are generally higher than those based on local DAD analysis. In practice, the results based on storm transposition could be adopted in landslide risk assessment.

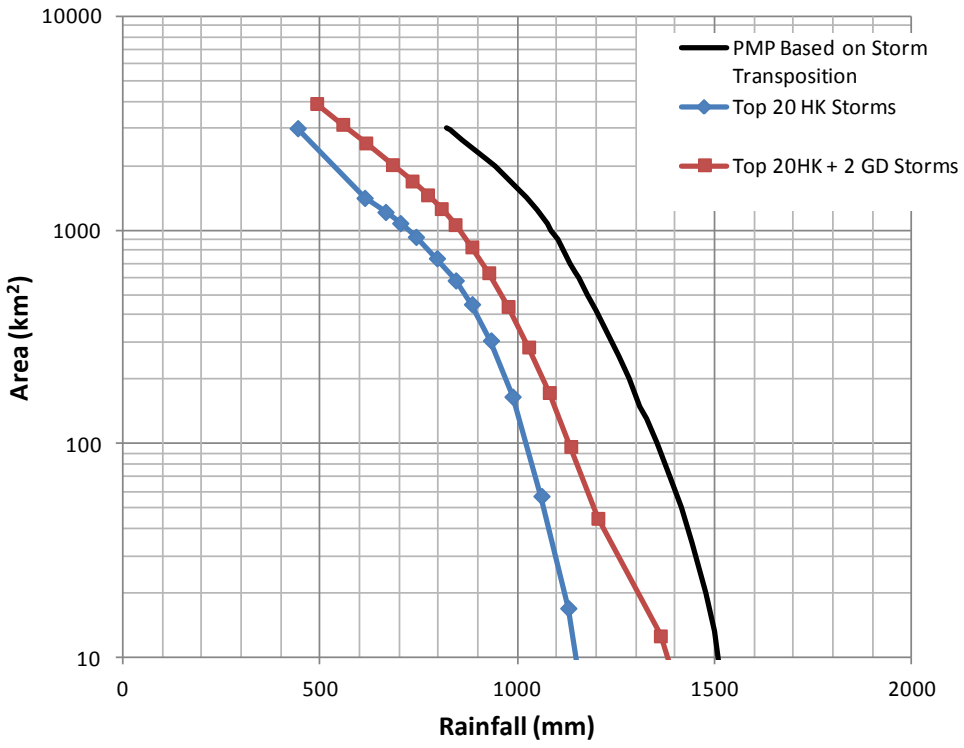

Note: "PMP based on storm transposition" above means the average of the DAD curves of the PMP estimates centred at Tai Mo Shan and Lantau.

Figure 8.1 Master DAD Curve with Moisture Maximization for 24-hour Rainfall

Table of Contents
Table of Contents
Table of Contents
Table of Contents

Table 8.3 Master DAD Based on Top 20 Hong Kong and Two Guangdong Storms for 24-hour Rainfall with Moisture Maximization

Area (km^2)	Depth (mm)
1	1549
13	1362
45	1203
97	1135
174	1080
284	1028
440	976
633	927
835	884
1062	841
1262	806
1464	771
1699	732
2027	682
2560	615
3127	557
3915	491

Note: The controlling points are based on the Guangdong 2007 storm (i.e. Typhoon Pabuk). Moisture maximization ratio of 1.304 is assumed.

Table 8.4 Master DAD Based on Top 20 Hong Kong for 24-hour Rainfall with Moisture Maximization

Area (km^2)	Depth (mm)
3	1192 [1]
17	1128 [1]
57	1060 [1]
167	987 [1]
305	932 [1]
451	884 [1]
582	843 [1]
740	795 [1]
931	742 [1]
1079	702 [1]
1217	665 [1]
1416	612 [2]
3000	442 [2]

Notes: (1) [1] 1993 Hong Kong storm (moisture maximization ratio r = 1.65).
(2) [2] 1976 Hong Kong storm (r = 1.29).

Table of Contents
Table of Contents
Table of Contents
Table of Contents

9 Climate Change Impact on PMP

9.1 Review of Existing Research Findings

An attempt has been made to review the literatures on the long term effects of climate change on PMP estimation. The relevant literatures are summarized as follows:

A study by National Oceanic and Atmospheric Administration (NOAA) on probable maximum precipitation and climate change (Kunkel et al, 2013) concluded that "***the most scientifically sound projection is that PMP values will increase in the future due to higher levels of atmospheric moisture content and consequent higher levels of moisture transport into storms***", which was drawn by means of climate model simulation. Kunkel et al (2013) suggested that PMP would increase by 20 to 30% in US by Year 2100 based on results from GCM simulations. This rise is mainly due to the increase in atmospheric moisture content while the effects of other factors are too small to offset the increase.

Nevertheless, a study for PMP for Australia (Bureau of Meteorology, 2009) concluded that "***So far we cannot confirm that PMP estimates will definitely increase under a changing climate***." This study focuses on the Australia region where decreasing rainfall was projected for a number of areas in Australia.

Actually, in the definition of PMP, there is "no allowance made for long-term climate trends" (WMO, 2009). However, in the context of PMP, two issues may be taken into account practically:

(a) Effect on the selection of the transposed storms because more extreme storms would occur due to global warming and hence more potential candidates would be used for storm transposition.

(b) Effect on the precipitable water: If the SST increases, for example, by 1℃ from 24° to 25°, in a particular sea waters (such as East Sea of China) as a result of global warming, the precipitable water used for moisture maximization in the design area (such as Henan Province in the central China) where the prevailing moisture inflow comes from this particular sea waters will increase roughly by 9% according to a standard precipitable water table (Table A.1.3, P.218, WMO (2009)). The increase is based on the assumption that the maximum moisture availability is derived from the 12-hour persisting dew points in a pseudo adiabatic saturated atmosphere. Also according to the Clausius-Clapeyron relation (a thermodynamic relationship) for each 1℃ increase in global mean temperature, the precipitable water increases by about 7%.

Regarding point (a) above, according to the study on trend and shift statistics on annual maximum precipitation in Ohio River Basin (Lin & Julian, 2001), it is found that 229 or 55% of 417 tested stations with records of 80 years or longer in the Ohio River Basin of the US

exhibited a significant shift in the variance of the extreme precipitation time series for the recent four decades (1959 - 1998) in comparison with the earlier four to six decades (1919 or earlier - 1958). More than 90% of the shift in variance was upward resulting in a regional average increase of 23% in the standard deviation of the time series. This implies that more and more extreme hydro-meteorological events, outstanding storms or severe droughts may be observed in the next few decades if the pattern of the shift in variance continues.

According to the Fifth Assessment Report (AR5) of Intergovernmental Panel on Climate Change, IPCC (2013), it is likely that anthropogenic influences have affected the global water cycle since 1960. There are likely more land regions where the number of heavy precipitation events has increased than where it has decreased. The frequency or intensity of heavy precipitation events has likely increased in North America and Europe. There is medium confidence that anthropogenic influences have contributed to observed increases in atmospheric moisture content in the atmosphere, to global-scale changes in precipitation patterns over land, to intensification of heavy precipitation over land regions where data are sufficient. IPCC AR5 also suggested that, depending on the future greenhouse gas emission scenario, the global mean temperatures (land and ocean) averaged in the period 2081 - 2100 are projected to likely exceed 1.5℃ to 2℃ above preindustrial conditions with high confidence. With respect to the long-term changes in the water cycle, changes in the global water cycle in response to the warming over the 21st century will not be uniform. As global mean surface temperature increases, extreme precipitation events over most of the mid-latitude land masses and over wet tropical regions will very likely become more intense and more frequent by the end of this century. This observation has been discussed by O'Gorman (2012). His estimate suggested a sensitivity of the 99.9th percentile of daily tropical precipitation to climate change at 10% per ℃ of surface warming, with a 90% confidence interval of 6 to 14% per ℃. This tropical sensitivity is higher than expectations for the extratropics of about 5% per ℃.

Locally, the HKO undertook a trend analysis on climate parameters for Hong Kong using time-dependent GEV distribution for determining the long term trends of variation of probability of occurrence of extreme weather events (Wong et al, 2011). An increasing trend in the frequency of occurrence of heavy rain days in Hong Kong since 1885 was observed. The study also showed that the frequency of occurrence of extreme hourly, 2-hourly and 3-hourly rainfall amounts at the HKO Headquarters increased significantly. On the other hand, the trends in the extreme 4- to 24-hourly rainfall are not statistically significant. The HKO also conducted a study on the extreme rainfall projections for Hong Kong using the higher temporal resolution model data IPCC AR4 (Lee et al, 2011). The projection suggested that, in the 21st century, the number of rain days in Hong Kong is expected to decrease while the daily rainfall intensity and the number of extreme rainfall days (daily rainfall greater than or equal to 100 mm) will increase. However, inter-model differences are still rather large with a divergence in the projections for the future precipitation changes. This, to a certain extent, reflects that climate projection, especially in regional scale, is still subject to various uncertainties in the model simulation of the future climate.

Ying et al (2012) reviewed the recent studies on the relationship between projected 21st century climate change and tropical cyclone activity in the western North Pacific basin. They summarized that most studies reviewed project an increase in the tropical cyclone intensity and all six studies reviewed project increase in tropical cyclone precipitation rates.

Regarding the point (b) above, analysis of past trend of relevant climate parameters were conducted in this study and detailed in the following section.

9.2 Changes in Sea Surface Temperature (SST) and Dew Point

9.2.1 NOAA Global Gridded (2° × 2°) Monthly Extended Reconstructed SST Data

The investigation area for the SST shown in Figure 9.1 is a rectangle of about [113.75°E - 115.6°E] and [21.0°N - 22.6°N] which was selected as the transposition of the convergence component of a typhoon storm comes from the east with prevailing typhoon track of southeast in the north Pacific. While the prevailing wind direction of Hong Kong in summer is mainly from the southwest, during a typhoon invasion of Hong Kong, the prevailing moisture inflow mainly comes northeasterly and/or northerly with a typhoon approaching from the east and/or southeast, so that the selection of this investigation area for the SST is justified in accordance with the transposition of the convergence component from the Typhoon Morakot.

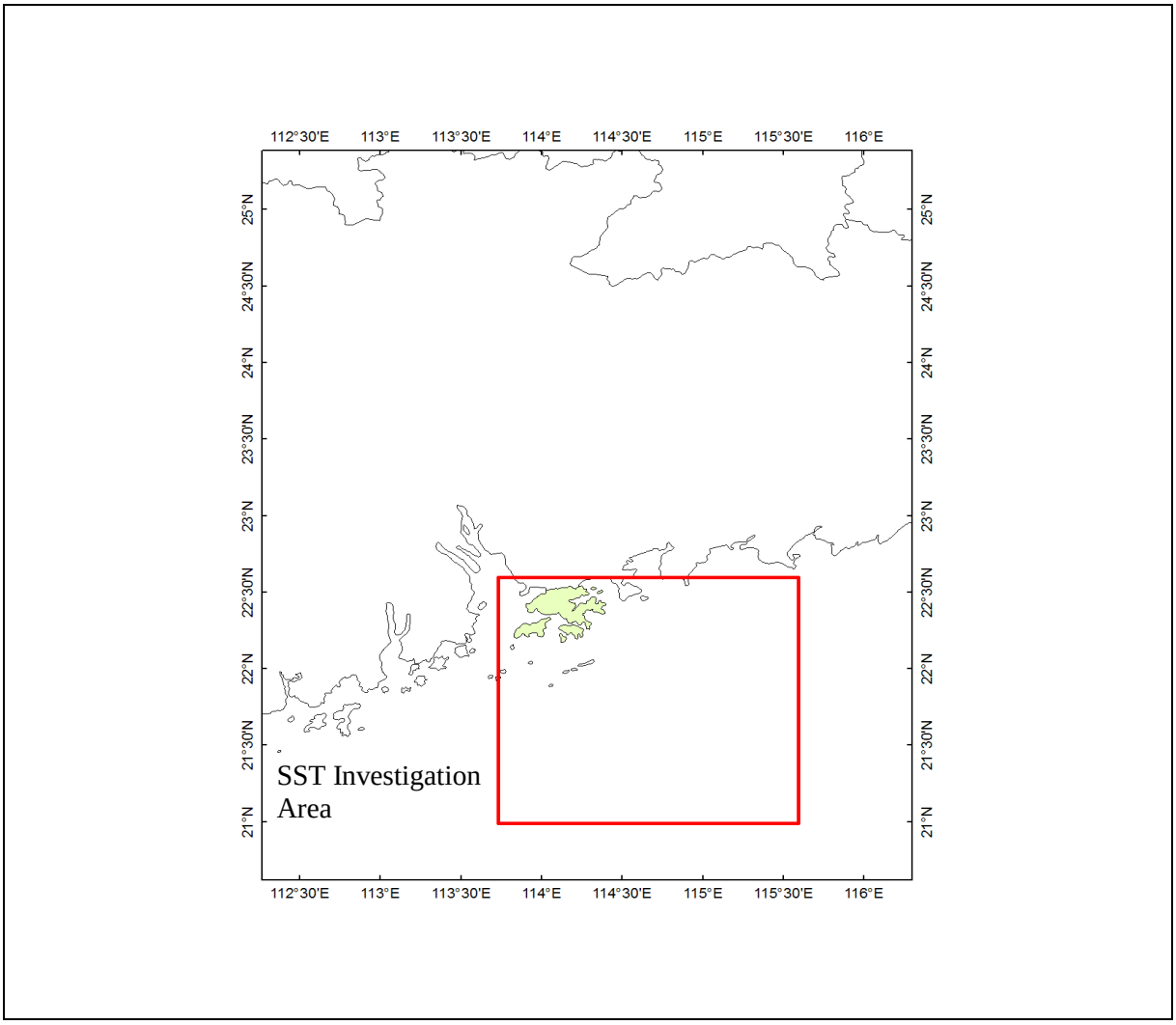

Figure 9.1 Investigation Area for Statistical Test of SST

9.2.2 Hourly Dew Point Temperature Data for Hong Kong

Based on data for the period of 1961 to 2010 at HKO, the average monthly SST series for the study area and the maximum persisting 12-hour dew point series in Hong Kong are tabulated in Table 9.1

Table 9.1 Time Series of SST and Dew Point

year	averaged SST in July and August(℃)	annual maximum persisting Td(℃)	year	averaged SST in July and August(℃)	annual maximum persisting Td(℃)
1961	28.82716	25.9	1986	28.59311	25.9
1962	28.34933	26.9	1987	28.93054	25.6
1963	28.29973	25.6	1988	29.21041	26.2
1964	28.37135	26.3	1989	28.69811	26
1965	28.04203	26.7	1990	28.74662	26
1966	29.2073	25.6	1991	28.42432	26.1
1967	28.67027	26.6	1992	28.72906	26.1
1968	28.50986	26.5	1993	29.03216	26.2
1969	28.6123	25.9	1994	28.70689	26.2
1970	28.79595	26.3	1995	28.525	25.6
1971	28.59608	25.6	1996	29.17014	26.2
1972	28.12851	26.4	1997	28.62378	25.8
1973	28.89662	26.5	1998	29.25838	26.3
1974	28.27567	26.4	1999	28.87716	26.2
1975	28.82959	25.6	2000	29.16879	25.9
1976	28.22257	25.8	2001	29.2827	26
1977	28.80122	26.5	2002	29.09203	26.1
1978	28.95932	26.2	2003	29.68419	26.1
1979	28.92176	26	2004	29.30635	26.8
1980	28.82243	26.5	2005	28.66243	25.9
1981	28.81433	26	2006	29.09473	26.5
1982	28.34311	25.9	2007	29.30351	25.9
1983	28.97311	26.2	2008	28.79608	25.8
1984	28.3154	26.1	2009	28.74703	26.8
1985	28.06716	26.6	2010	28.96419	26.6

Note: *Td* = dew point.

9.2.3 T-test for Testing the Linear Trend of Dew Point and SST

A time series of annual maximum hydrometeorological event (item) like other time series data sometimes exhibits a tendency to grow or to decrease gradually over a long period of time. This pattern is identified as trend. Graphically, a linear trend in a data set means that the data set depicts a linear regression trend either upward or downward. Assume that P_t , t = 1, 2, ..., n, is a time series and n is the sample size. A simple linear regression between P and t can be written as

$$P_t = a + b\,t \quad (t = 1, 2, ..., n) \quad \text{..... (9.1)}$$

where a is the intercept and b is the slope of the linear regression model. There is a linear trend in the time series of P_t if b is significantly different from zero. The hypothesis that b is significantly different from zero is accepted, or the null hypothesis is rejected, if

$$t = \left| \frac{r\sqrt{n-2}}{\sqrt{1-r^2}} \right| > t_{\alpha/2,\nu} \quad \text{..... (9.2)}$$

in which t follows Student's t distribution, where r is the correlation coefficient, 1 - α is the confidence level and $\nu = n - 2$ degree of freedom. In the study, the sample size of the annual maximum persisting 12-hour dew point temperature and averaged SST in July and August around Hong Kong is 50, so $\nu = 48$. The term $t_{\alpha/2,\nu}$ is the $\alpha/2$ quantile of the t distribution. (Maidment, 1992).

Creation of Maximum Persisting 12-hour Dew Point Temperature

The maximum persisting 12-hour dew point temperature for each year from 1961 to 2010 has been processed using the following steps:

(a) Pick out each single observation greater than a threshold, which is 25℃ in this case, to reduce the effort required in screening the dew point observations for study;

(b) Use a 12-hour window to pick up the maximum persisting 12-hour dew point between year 1961 and year 2010 to form an Annual Maximum Series of dew point;

(c) Check and make sure that the 12-hour persisting dew point comes from a period of 24-hour prior to the onset of the corresponding major intensified rainfall; and

(d) As a result of (c) above, obtain a dew point series of 50-year for the period between 1961 and 2010 for trend analysis.

A time series of the dew point temperature at HKO is shown in Table 9.1 above.

Linear Tendency of the Annual Maximum Persisting 12-hour Dew Point Temperature at HKO

Figure 9.2 shows time series of the annual maximum persisting 12-hour dew point temperature at HKO. It is clear that the maximum persisting 12-hour dew point of 26.9℃ occurred in 1962, while the minimum value 25.6℃ occurred in years of 1963, 1966, 1971, 1975, 1987 and 1995. There is no significant linear trend in the time series of the annual maximum persisting 12-hour dew point temperature at HKO over the period of 1961 to 2010.

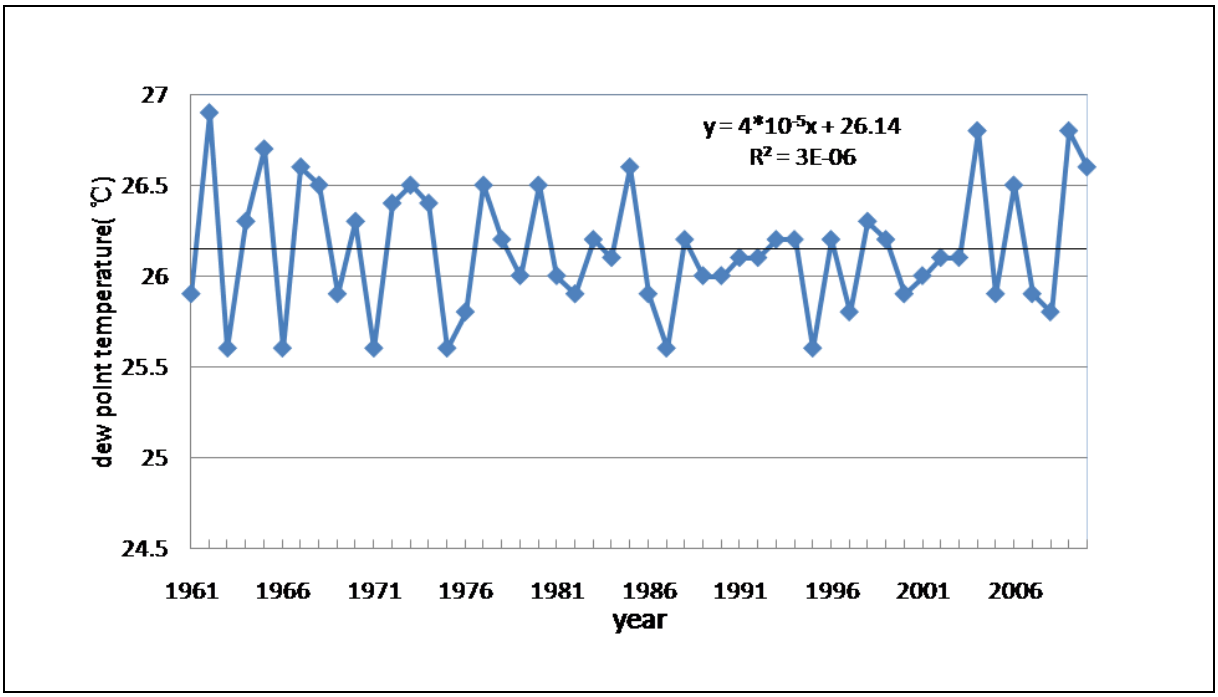

Figure 9.2 Regression Chart of Linear Tendency of the Annual Maximum Persisting 12-hour Dew Point Temperature at HKO Station from 1961 to 2010

Linear Tendency of Averaged SST in July and August around Hong Kong Sea Waters

Statistics in Table 9.2 below shows that the annual maximum persisting 12-hour dew point temperature from 1961 to 2010 mostly occurs in July and August, with the percent of 36% and 40%, respectively.

Table 9.2 Number of Occurrence-month of Annual Maximum Persisting 12-hour Dew Point Temperature at Hong Kong Observatory (1961 to 2010)

Month	May	June	July	August	September
Times	3	7	18	20	2
Percentage (%)	6	14	36	40	4

In accordance with the characteristics of the dew point at HKO, a time series of averaged monthly SST within the rectangular study area in red of [113.75°E - 115.6°E] and [21.0°N - 22.6°N] shown in Figure 9.1 has been processed and given in Table 9.1.

The regression chart of the SST time series is given in Figure 9.3.

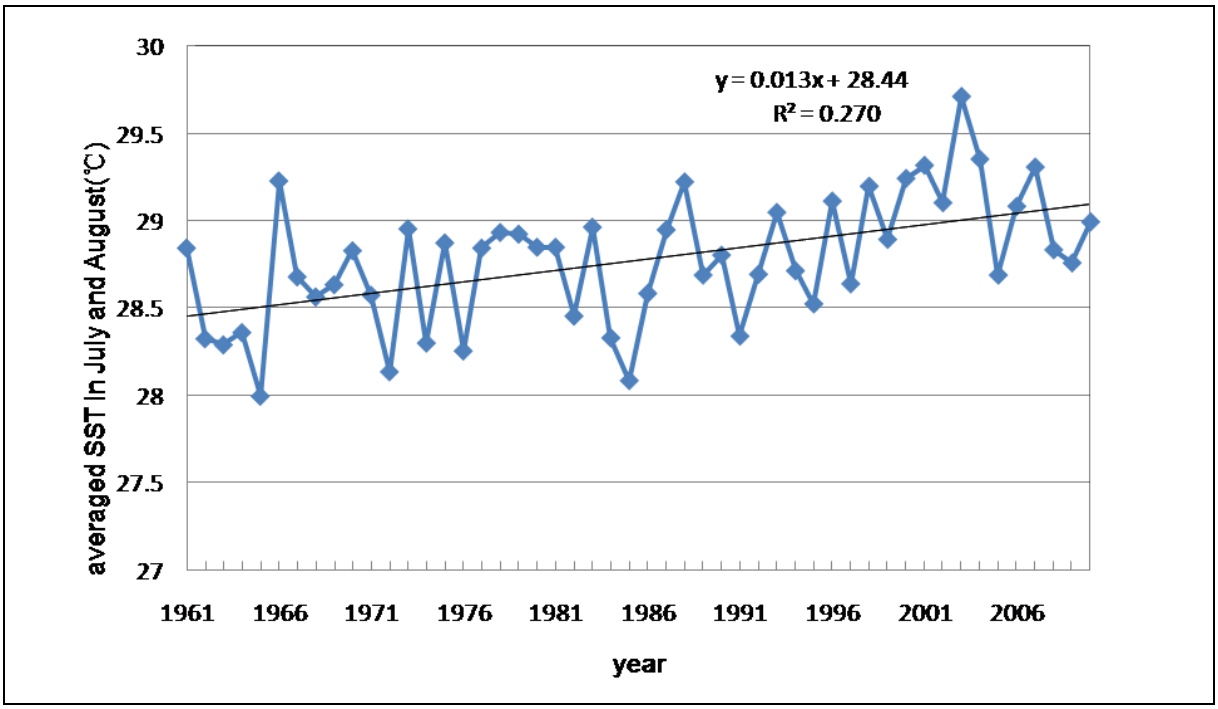

Figure 9.3 Regression Chart of Linear Tendency of the Monthly Averaged SST in July and August in the Study Area from 1961 to 2010

Figure 9.3 shows time series of the monthly averaged SST over July and August in the study area. According to Figure 9.3, the linear tendency is 0.131℃/10 yr, and the correlation coefficient between the time in year and the averaged SST in July and August is 0.5198, which passed the significance *T* test (t = 4.21) as illustrated in equation below:

$$t = \left| \frac{r\sqrt{n-2}}{1-r^2} \right| = \left| \frac{0.5198\sqrt{50-2}}{1-0.270} \right| = 4.933 > t_{2.5\%,48} = 4.21$$

This means that the SST time series for the period of 1961 to 2010 exhibits an upward linear trend at confidence level of 95%.

Correlation Analysis between the Annual Maximum Persisting 12-hour Dew Point Temperature and the Averaged SST in July and August around Hong Kong

The correlation coefficient between the annual maximum persisting 12-hour dew point temperature at HKO and the averaged SST in July and August around Hong Kong is r = -0.0864, which did not pass the significance *T* test (t = -0.60082). This infers that the

annual maximum persisting 12-hour dew point temperature at HKO at HKO and the averaged SST in July and August in the Hong Kong near sea waters has no statistically significant correlation.

9.2.4 Findings of Trend Analysis

Findings from the trend analysis are summarized as follows:

(a) The annual maximum 12-hour persisting dew point time series at HKO for the period of 1961 - 2010 does not have a significant linear trend.

(b) The averaged SST over July and August in the Hong Kong offshore sea waters shows a significant increasing trend for the past half-century (1961 - 2010), at a rate of 0.131℃/10 yr.

(c) The annual maximum persisting 12-hour dew point temperature at HKO has little correlation with the SST in the Hong Kong offshore sea waters. This may be due to: (i) the SST in the moisture source of inflow jet is considered as the upper limit to dew point when the air layers in an air column are fully saturated, but the air column during rainfalls in the past has in fact never been fully saturated; and (ii) the single HKO station may not represent well the Hong Kong area in terms of dew point.

(d) The dew point and SST time series exhibit less skewed properties, so the T-test, which requires normality of the tested variable, was applied.

9.3 Potential Impact on PMP Estimates

There are high uncertainties in projection of extreme rainfalls, frequency and intensity of tropical cyclones, potential changes in precipitable water as well as the relationship between extreme rainfalls and PMP. It is difficult to quantify the impact of climate change on the future change of PMP in Hong Kong at this stage.

The PMP in fact is considered as the upper limit of quantiles from statistical points of view. However, the current studies have not been able to point out whether the quantiles are bounded or not. This is a major fundamental issue relating to the basics of PMP. Results from a series of recent studies on precipitation frequency analysis (Lin et al, 2006; 林炳章等, 2012) showed that the quantiles do not vary normally as having assumed in current textbooks and/or papers that leads to a divergent upper tail of probability distribution but asymmetrically from positively skewed to negatively skewed when quantile moves from small to large and approach an unknown upper limit via an asymptote. This was the first time of finding an indication that the upper tail of the probability distribution will be convergent to a value as upper limit via the asymptote. Therefore, the topic of climate change impact on PMP

becomes an issue about how this upper limit is estimated and how stable this upper limit is from the viewpoints of statistical analysis. This important finding opens a new window for PMP investigators though there is no simple answer to the issue. This gives a new angle on climate change impact on PMP.

10 Evaluation of PMP Estimates

10.1 General

As what Mr. Marshall E. Hansen, an American meteorologist and prominent PMP investigator, pointed out that it is not possible to know what the correct answer is for PMP, only that the estimates presented represent the best answer that current knowledge and data will support (Hansen, 1987).

To verify the rationality and reliability of Hong Kong PMP estimates, the Hong Kong PMP updates are compared with the PMP estimates of existing local projects and the extreme rainfall records of Hong Kong, the Southeast China region including Zhejiang, Fujian, Guangdong, Guangxi, Hainan and Taiwan, and the world as well.

10.2 Comparison with Extreme Rainfall Records for Hong Kong, Southeast China Region and the World

The 24-hour PMP update of Hong Kong, with storm transposition method and moisture maximization adjustment centred at Tai Mo Shan is 1,600 mm. Comparisons between the PMP estimate and the records mentioned above are illustrated in Figure 10.1. The figure shows that the PMP update is higher than the extreme rainfall records of Hong Kong to some noticeable extent and higher than the rainfall records in Southeast China (王國安, 1999; 王家祁, 2002) and is approaching to the records in Taiwan (Kung, 2010). However, the 24-hour PMP estimate is slightly lower than the world records (王國安, 1999; 王家祁, 2002) by about 17%. Tables 10.1 to 10.4 give the rainfall records that are leading to Figure 10.1.

Table 10.1 Maximum Rainfall Records for Hong Kong

No.	Duration	Rainfall (mm)	Date	Location	Storm Type
1	1-hr	211.5	22 July 1994	Tai Mo Shan	Trough of low pressure
2	4-hr	384.0	June 2008	Lantau	Trough of low pressure
3	6-hr	457.5	22 July 1994	Tai Mo Shan	Trough of low pressure
4	8-hr	558.0	22 July 1994	Tai Mo Shan	Trough of low pressure
5	12-hr	793.5	22 July 1994	Tai Mo Shan	Trough of low pressure
6	24-hr	956.0	21-22 July 1994	Tai Mo Shan	Trough of low pressure

Table 10.2 Maximum Rainfall Records for Taiwan

No.	Duration	Rainfall (mm)	Date	Location	Storm Type
1	1-hr	123.0	8 August 2009	Alishan 阿里山	Morakot
2	2-hr	226.0	8 August 2009	Alishan 阿里山	Morakot
3	3-hr	325.0	8 August 2009	Alishan 阿里山	Morakot
4	6-hr	616.5	31 July 1996	Alishan 阿里山	Herb
5	12-hr	1157.5	31 July 1996	Alishan 阿里山	Herb
6	18-hr	1272.5	8 August 2009	Alishan 阿里山	Morakot
7	24-hr	1623.5	8 August 2009	Alishan 阿里山	Morakot
8	2-day	2361.0	8-9 August 2009	Alishan 阿里山	Morakot
9	3-day	2748.0	8-10 August 2009	Alishan 阿里山	Morakot

Table 10.3 Maximum Rainfall Records for Zhejiang, Fujian, Guangdong, Guangxi and Hainan

No.	Duration	Rainfall (mm)	Date	Location	Storm Type
1	10-min	84.8	24 August 1985	Jinkeng, Zengcheng, Guangdong 金坑、增城、廣東	Front
2	15-min	117.0	4 July 1992	Bengshan, Guangze, Fujian 崩山、光澤、福建	Front
3	30-min	148.4	10 June 1979	Dongxikou, Chenghai, Guangdong 東溪口、澄海、廣東	Front
4	40-min	182.4	10 June 1979	Dongxikou, Chenghai, Guangdong 東溪口、澄海、廣東	Front
5	1-hr	245.1	10 June 1979	Dongxikou, Chenghai, Guangdong 東溪口、澄海、廣東	Front
6	1.5-hr	347.1	10 June 1979	Dongxikou, Chenghai, Guangdong 東溪口、澄海、廣東	Front
7	2-hr	380.9	10 June 1979	Dongxikou, Chenghai, Guangdong 東溪口、澄海、廣東	Front
8	4-hr	416.5	2010	Guangdong 廣東	
9	6-hr	818.0	11 October 2000	Dalupo, Tunchang, Hainan 大陸坡、屯昌、海南	Tropical cyclone
10	24-hr	1188.2	9 August 2007	Happy Farm, Leizhou Peninsula, Guangdong 幸福農場、雷州半島、廣東	Tropical cyclone
11	3-day	1396.0	29 September 1965	Kangtong, Enping, Guangdong 康垌、恩平、廣東	Tropical cyclone
12	3.4-day	1471.0	29 September 1965	Kangtong, Enping, Guangdong 康垌、恩平、廣東	Tropical cyclone
13	6-day	1483.0	30 May 1977	Baishimen, Lufeng, Guangdong 白石門、陸豐、廣東	Jet stream
14	7-day	1689.4	15 July 1996	Zailao, Rongshui, Guangxi 再老、融水、廣西	Shear

Table of Contents
Table of Contents
Table of Contents
Table of Contents

Table 10.4 World Rainfall Records

Duration	Rainfall (mm)	Start Date	Location
9-hr	1087	28 February 1964	Belouve, La Réunion
18-hr	1589	7 January 1966	Foc-Foc, La Réunion
18.5-hr	1689	28 February 1964	Belouve, La Réunion
20-hr	1697	7 January 1966	Foc-Foc, La Réunion
22-hr	1780	7 January 1966	Foc-Foc, La Réunion
24-hr	1870	15 March 1952	Cilaos, La Réunion
2-day	2500	15 March 1952	Cilaos, La Réunion
3-day	3929	24 February 2007	Commerson, La Réunion
4-day	4869	24 February 2007	Commerson, La Réunion
5-day	4979	24 February 2007	Commerson, La Réunion
6-day	5075	24 February 2007	Commerson, La Réunion
7-day	5400	24 February 2007	Commerson, La Réunion
8-day	5510	24 February 2007	Commerson, La Réunion
9-day	5512	24 February 2007	Commerson, La Réunion
10-day	5678	18 January 1980	Commerson, La Réunion
11-day	5949	17 January 1980	Commerson, La Réunion
12-day	5949	16 January 1980	Commerson, La Réunion
13-day	6072	15 January 1980	Commerson, La Réunion
14-day	6082	15 January 1980	Commerson, La Réunion
15-day	6083	14 January 1980	Commerson, La Réunion

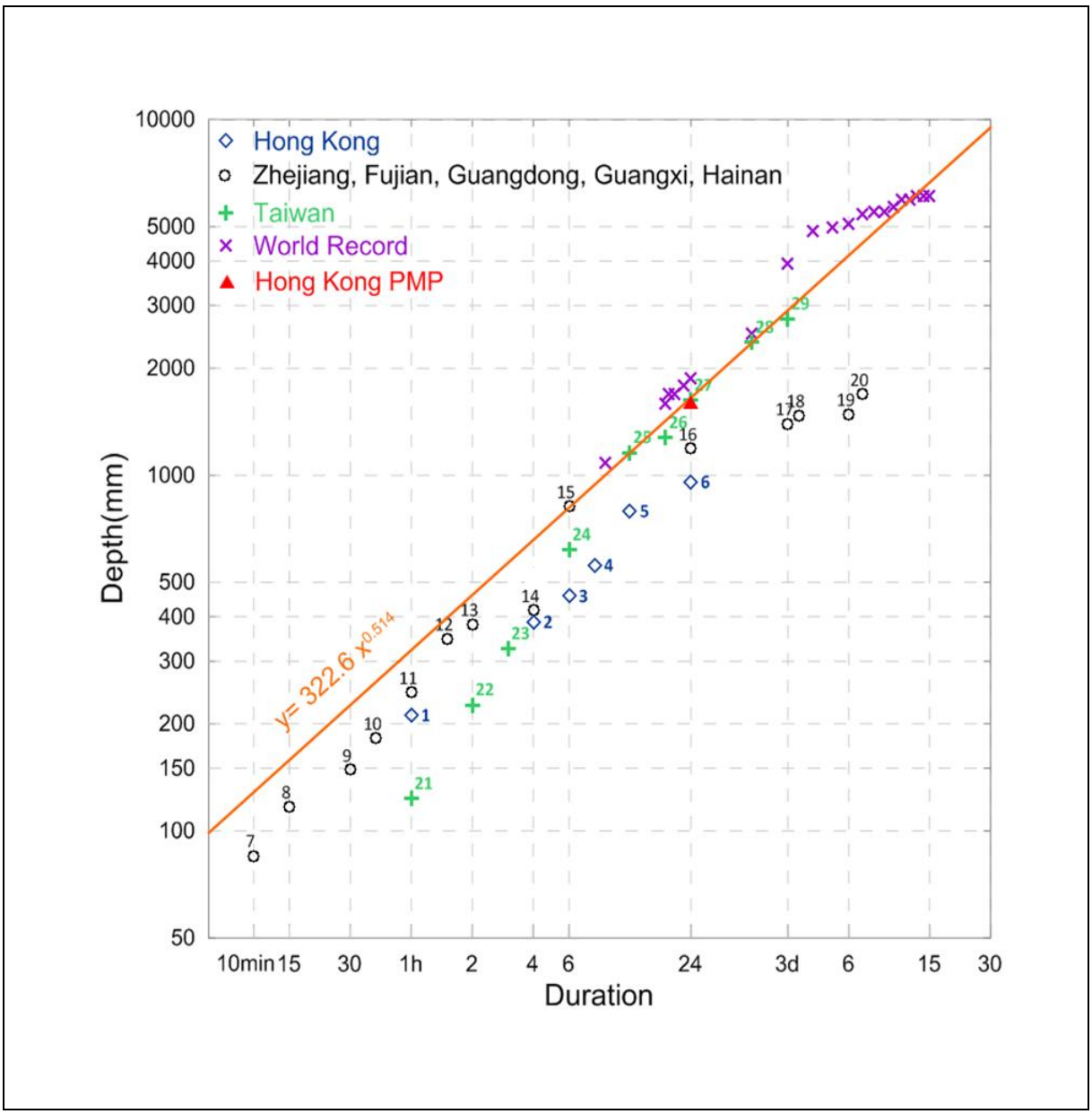

Figure 10.1 Comparison of Hong Kong PMP Updates with Extreme Rainfall Records in Hong Kong, Southeast China including Taiwan As Well As the World Records, with Envelopment Line Suggested

10.3 Comparison with PMP Estimates for Hong Kong and PMP Estimates for China

The Hong Kong PMP estimates via storm transposition with moisture maximization being centred at Tai Mo Shan with 45° orientation (i.e. NE-SW) are given in Table 6.1 for comparison. Table 10.5 lists the existing hydropower projects in China (水利部, 1995; 王國安, 1999; 王家祁, 2002) in which PMP estimates were investigated. PMP estimates from those projects are plotted in Figure 10.2. As shown in Figure 10.2, the 24-hour PMP updates in Hong Kong do not exceed the enveloping line of the relationship between 24-hour PMP estimates against the sizes of catchment areas for the existing hydropower projects.

Table of Contents
Table of Contents
Table of Contents
Table of Contents

Table 10.5 List of the Existing Hydropower Projects in China

No.	Project Name	No.	Project Name	No.	Project Name
1	Tingxia 亭下	11	Xin'an River 新安江	21	Chengbi River 澄碧河
2	Banqiao 板橋	12	Huangbi zhuang 黃碧莊	22	Daguangba 大廣壩
3	Bailianhe 白蓮河	13	Fuchun River 富春江	23	Xiashan 峽山
4	Yuqiao 於橋	14	Ankang 安康	24	Tuolin 拓林（台）
5	Zhanghe 漳河	15	Fengman 豐滿	25	Xin'an River 新安江
6	Daguangba 大廣壩	16	Tianshengqiao 天生橋	26	Fuchun River 富春江
7	Xiashan 峽山	17	Wuqiangxi 五強溪	27	Ankang 安康
8	Liuxihe 流溪河	18	Tingxia 亭下	28	Tongjiezi 銅街子
9	Xinfengjiang 新豐江	19	Banqiao 板橋		
10	Tuolin 拓林	20	Songtao 松濤		

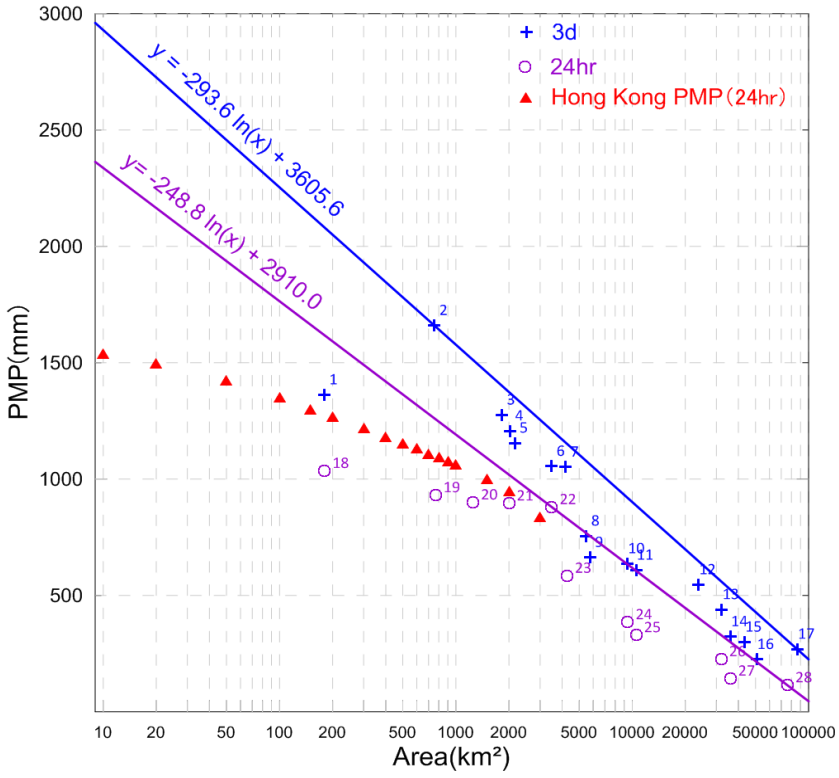

Note: Solid lines represent the envelopment of the relations between 24-hour in purple and 3-day in blue PMP estimates against the drainage area sizes for the existing hydropower projects, respectively. The corresponding names of the hydropower projects cited in the diagram are listed in Table 10.5.

Figure 10.2 Comparison of Hong Kong PMP Updates with PMP Estimates of Existing Hydropower Projects in China

Table of Contents
Table of Contents
Table of Contents
Table of Contents

10.4 Comparison of Hong Kong 24-hour PMP Updates with Previous Hong Kong PMP Estimates

Storm transposition was not adopted in the previous studies on 24-hour PMP estimates for Hong Kong and the DAD analyses with moisture maximization in these studies were based on local storms only. Therefore, there is no basis for comparison of the previous PMP estimates with the PMP updates in Hong Kong, which have been rigorously developed via storm transposition by targeting the most severe storm in the Southeast China region (i.e. the 2009 Typhoon Morakot storm in Taiwan).

Figure 10.3 provides a general view of the comparison on the basis of reciprocity between the PMP updates without storm transposition (i.e. the DAD analysis only) and the last update of PMP estimates in 1999 (1999 PMP).

(a) The 1999 PMP, which was based on the combination of the revised 1955 - 1965 PMP and 1966 - 1999 local storms, is lower than the 2013 master DAD based on 20 Hong Kong storms (from 1966 to 2010) except for area less than 30 km^2 where is controlled by the 1957 storm (not reassessed in this study). The higher 2013 master DAD is mainly due to the higher moisture maximization ratio (1.65 instead of 1.57) adopted for the controlling points corresponding to the 1993 storm and the use of DAD relation for the outstanding 1993 storm in a larger area range (i.e. > 80 km^2), which was previously limited to 80 km^2 only in the 1999 PMP study.

(b) The 2013 master DAD based on 20 Hong Kong storms plus two Guangdong storms is also shown in Figure 10.3. It is shown that the 2013 master DAD based on only 20 Hong Kong storms is closer to the 1999 PMP than the 2013 master DAD based on 20 Hong Kong storms plus two Guangdong storms for whole range of areal coverage.

10.5 Findings from the Comparison

The 24-hour PMP estimates from this study have been compared with local and worldwide data. Findings from this comparison are summarized as follows:

(a) The 24-hour Hong Kong PMP update is higher than the extreme rainfall records in Hong Kong to some noticeable extent.

(b) The 24-hour Hong Kong PMP update is higher than the rainfall records in Southeast China region including Zhejiang, Fujian, Guangdong, Guangxi and Hainan. It is approaching to the records in Taiwan.

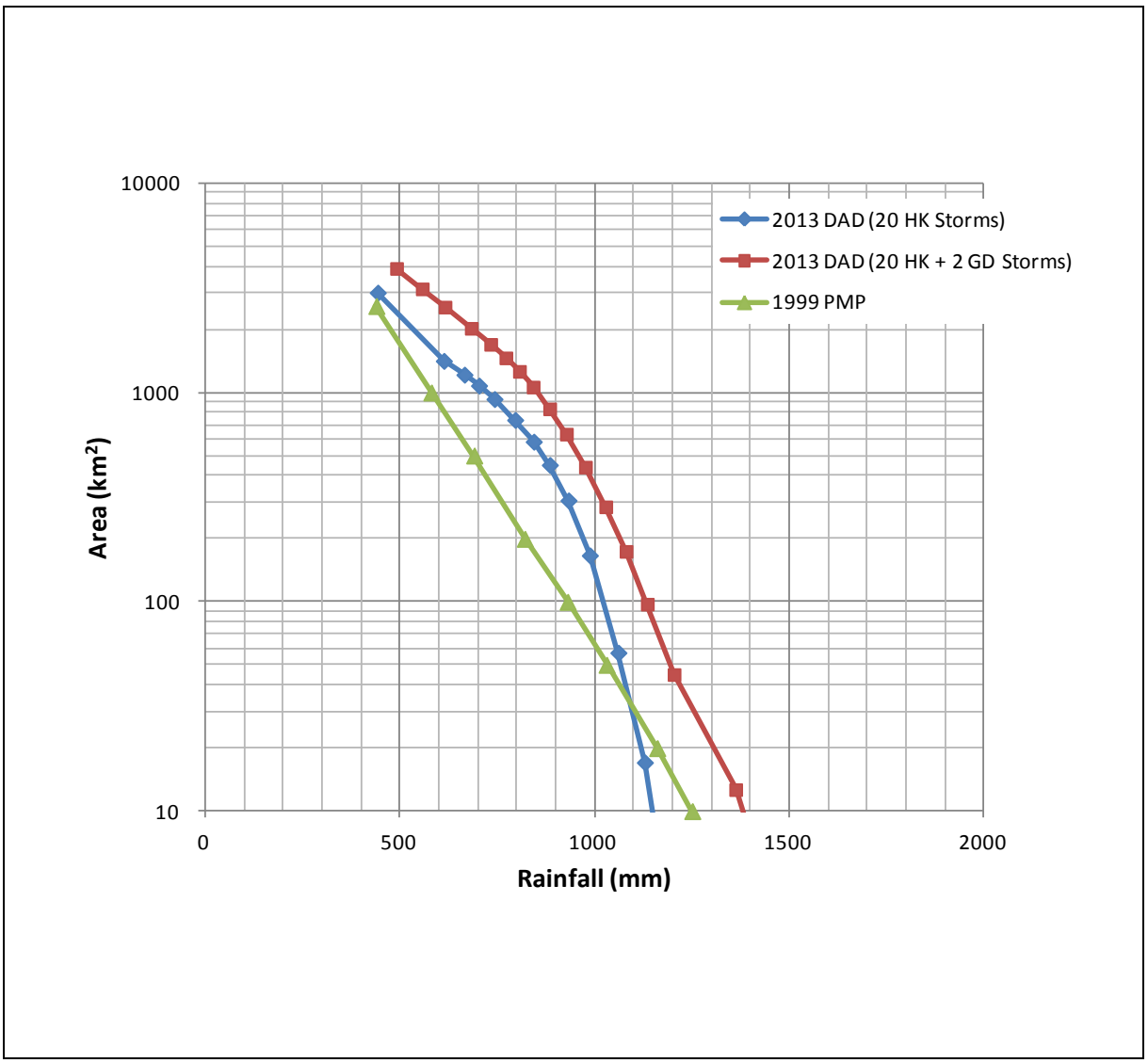

Figure 10.3 Comparison of the 1999 PMP with the 2013 Master DAD (without Storm Transposition) for 24-hour PMP

(c) The 24-hour Hong Kong PMP update is lower than the world records for 24 hours by about 17%.

(d) The 24-hour Hong Kong PMP update does not exceed the enveloping line of the relations between 24-hour PMP estimates against the size of catchment areas for the existing hydropower projects in China.

(e) Particularly, from Figure 10.2, the 24-hour Hong Kong PMP update is just slightly less than that of the project #22, Daguangba for the catchment size of 3,500 km^2, which was performed by Prof. Lin Bingzhang in 1987 for a World Bank's financed project. Nevertheless, the 24-hour Hong Kong PMP update of 1,600 mm is higher than the

Daguangba's 24-hour PMP of 1,324 mm for the centre (not shown in Figure 10.2). It should be noted that the design study of PMP for Daguangba was carried out in 1987 prior to the 2009 Typhoon Morakot.

(f) The current Hong Kong PMP updates are more reasonable, reliable and referable with support by the updated data and the technique developed based on all the four methods, involving moisture maximization, storm transposition, DAD analysis and statistical approach, which are the most common international practices for PMP estimation.

(g) Users are advised that uncertainties in the PMP estimates should be taken into account such as limited data, knowledge on mechanism of extreme storms and potential climate change impact, and etc., which will be further discussed in Section 11.

11 Discussions

11.1 Uncertainties and Limitations

11.1.1 Storm Survey (Storms for Transposition)

The systematic approach undertaken in the storm survey has been explained in Section 2.2. Efforts were made by the time of investigation of storms in the storm survey and collection of data in a wide region in Southeast China including Zhejiang, Fujian, Guangdong, Guangxi, Hainan, and Taiwan. Since the transposition method of PMP estimation is limited by availability of storm records, detailed investigation on major storms other than the four Taiwan storms was not conducted in this study. Nevertheless, the 24-hour rainfall (1,623.5 mm) recorded at Ahlishan brought by the 2009 Typhoon Morakot is the highest record in Taiwan and is close to the world record (WRA, 2009). In addition, as shown in Figure 4.6, the areal extent of rainfall brought by Typhoon Morakot was extensive. Hence, the selection of Typhoon Morakot for transposition in this study is justified. However, the PMP estimate may need to be further updated if a more intense rainstorm than Typhoon Morakot occurs in future.

11.1.2 Data Availability and Quality

Rainfall data for 389 raingauge stations (288 of CWB and 101 of WRA) in Taiwan out of total 462 stations have been acquired for storm observation and have been used to construct the isohyets for the four major Taiwan storms, viz Herb, Haitang, Aere, and Morakot. The acquired data have been examined for quality control. Overall speaking, the data are considered sufficiently complete and reliable. The isohyets constructed from the data should be accurate enough for the purpose of storm transposition.

11.1.3 Meteorological Similarity between Taiwan and Hong Kong Storms and Principles of SDOIF Method

Taiwan and Hong Kong are assumed meteorologically homogeneous in terms of typhoon-prone area in the Northwest pacific region. The principles of the SDOIF method as storm separation technique are justified to be effective and reasonable based on current science and technology and has been accepted by the WMO's expert panel for estimation of PMP. The above assumption is considered reasonable.

11.1.4 Selection of Base Stations

Selection of base stations is an issue in the use of the SDOIF method for storm separation, which leads to the establishment of the OIFs for different design durations before decoupling the target storm into two components, viz convergence and orographic. The base stations selected in the coastal or flat area in the moisture inflow route will affect the SDOIF values to some extent. However, if several eligible stations are selected for averaging, the uncertainties will be kept as minimum by reducing the sampling errors.

The selection of base stations for the target area (i.e. Taiwan) is considered appropriate as the five stations (namely 樸子 Puzi, 北門 Beimeng, 下營 Xiaying, 永康 Yongkang and 高雄 Gaoxiong) are located in the coast area of Southwest Taiwan with elevation below 20 m.

However, for the design area (i.e. Hong Kong), only three stations of Shenzhen, R30 and R22 are located in the relative flat area in the vicinity of northern Hong Kong that is in the prevailing route of the storm moisture inflow jet and is deemed almost not to be influenced by the topography in terms of the orographic intensification. In other words, due to the difficulty in data acquisition in South Guangdong (SGD), only one station (i.e. Shenzhen in SGD) is selected to join the R30 and R22 in northern Hong Kong for the "base averaging" r_0 in Equation 1.13. Therefore, the result of the "base averaging" for Taiwan is considered slightly better than that for Hong Kong.

11.1.5 Direction of Prevailing Moisture Inflow for Developing OIFs

Understanding of moisture flux direction for Taiwan's Morakot storm and for the local Hong Kong territory has been grained from other studies carried out by the Applied Hydrometeorological Research Institute (AHMRI) and other credential research institutions. Although the moisture inflow direction varies from storm to storm, the prevailing moisture flux direction for the worst or severe cases has been well studied for the target area, Taiwan, and the design area, Hong Kong, in regard of PMP estimation.

Target Area (Taiwan)

Since the prevailing moisture flux to Taiwan during the Morakot storm came from the West (W) and Southwest (SW), passing through the five coastal stations (永康 56，高雄 57，樸子 64，北門 65 and 下營 66) (See Figure 2.4). Figures 11.1 and 11.2 show the W and SW moisture flux during the Morakot Typhoon storm in different scales.

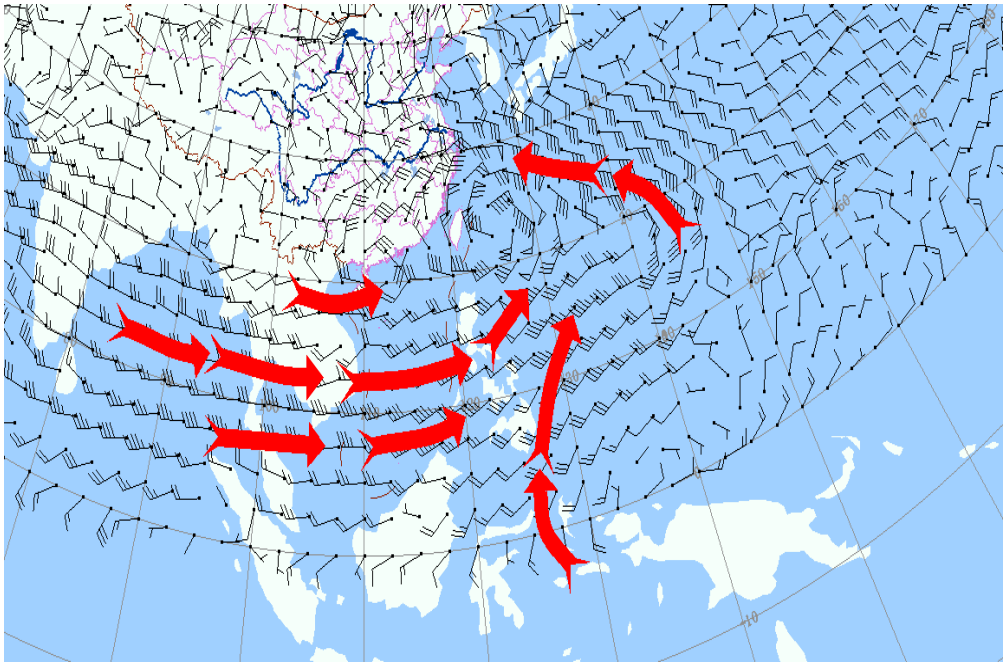

Source: (郭林, 2011)

Figure 11.1 Major Moisture Flux during 2009 Typhoon Morakot

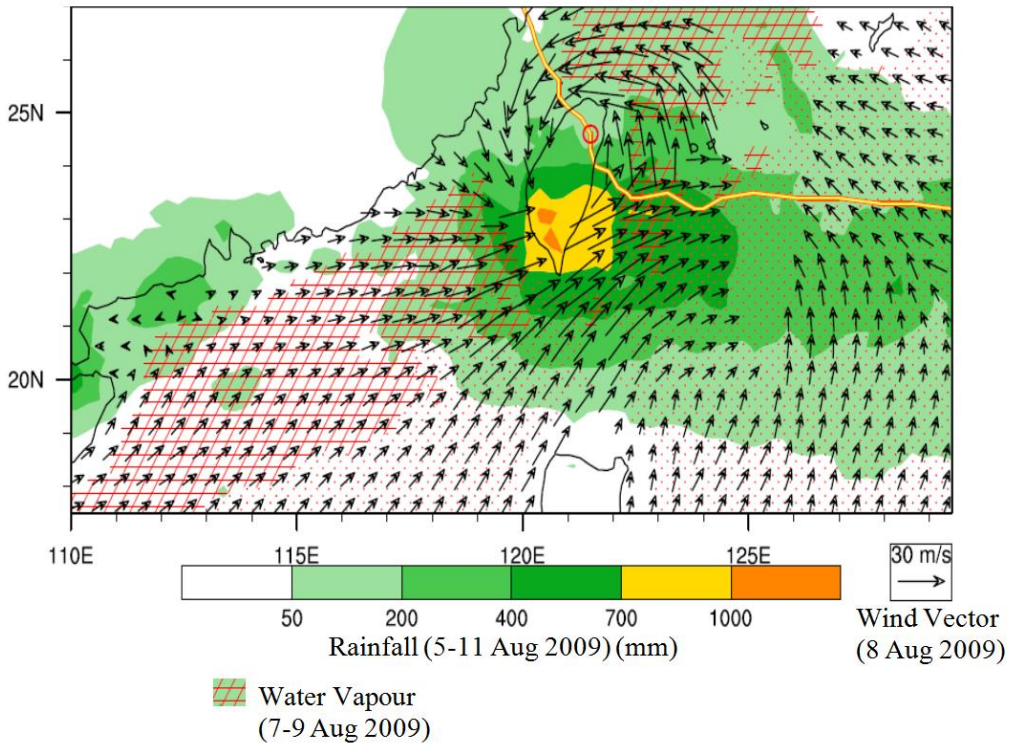

Source: (Hong et al, 2010)

Figure 11.2 Power Spectrum of the Western North Pacific Summer Monsoon Index

Design Area (Hong Kong)

During a typhoon invasion of Hong Kong, the prevailing moisture inflow mainly comes northeasterly and/or northerly, as shown an indicative diagram of Figure 11.3. As a result, one SGD station (Shenzhen) together with two Hong Kong stations (R22 & R30) located in the flat land and in the moisture flux route have been selected to form the base stations.

Two major factors affecting the selection of the base stations are:

(a) Worst situation which occurred or may occur in the future in terms of moisture inflow based on synoptic analysis; and

(b) Data availability of "base stations" in flat land or coastal area in the route of inflow moisture jet.

In principle, if the wind from southeast, south or southwest is considered, raingauge stations such as H15, N15, R13, R14 and R32 may be taken as potential base stations in view of data availability. However, since the means of annual maximum rainfall for these raingauge stations are generally higher than those of the raingauge stations associated with the northeasterly/northerly inflow, the northeasterly/northerly moisture pattern was finally selected as the prevailing moisture inflow for selection of base stations in order to produce the worst scenario from the viewpoints of landslide and flooding risks.

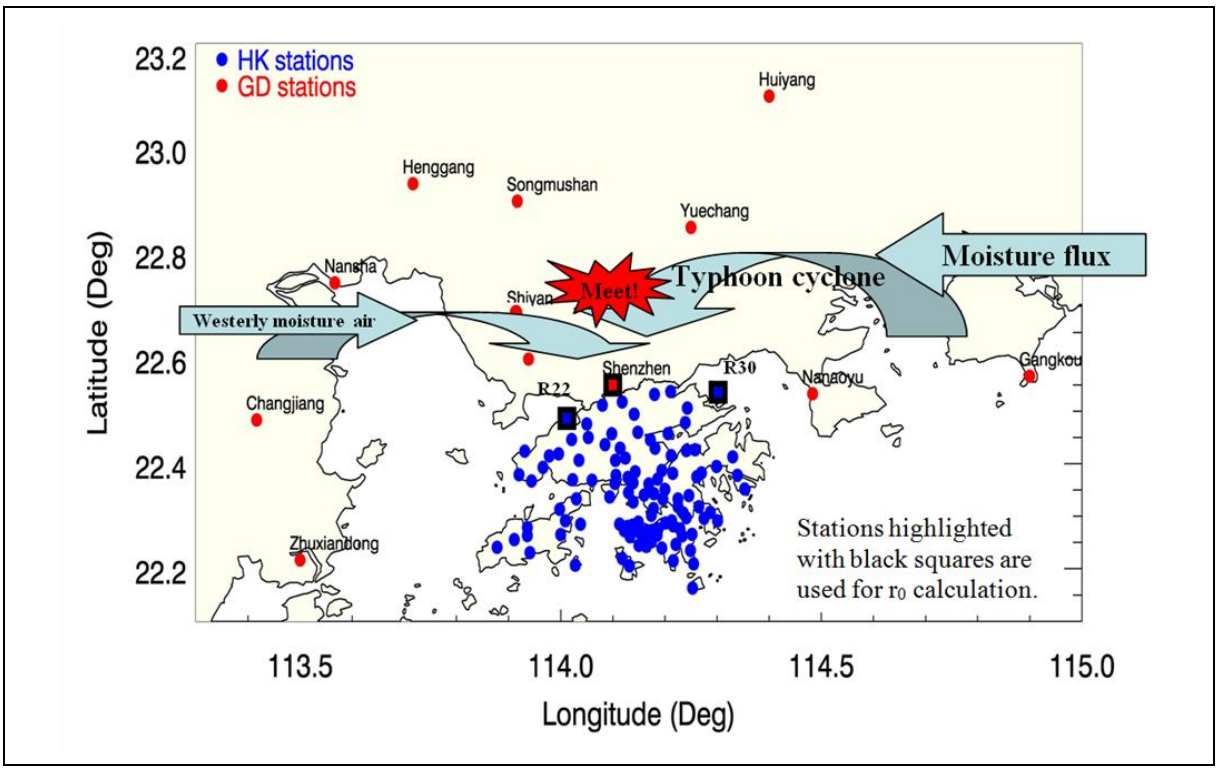

Figure 11.3 Indicative Diagram of Typhoon Moisture Inflow Jet to Hong Kong in the Event of PMP

11.1.6 Resolution with Respect to Spacing of Raingauge Stations and Grid Size

The uncertainties arisen from the grid size are related to the spacing of raingauges for which the rainfall data (of both storm data and annual historical data) were used in the storm transposition. However, as long as the raingauge stations selected are representative, the values of the SDOIF for grid size of 20 to 30 km^2 should be reasonably good. The more the stations are used, the better the resolution of OIF could be achieved.

11.1.7 Generalised Convergence Component

The pattern of generalised convergence component contains two parts, viz the shape and rainfall values assigned to each of the isohyets of the pattern. The rainfall values of the generalised convergence component pattern are based on the convergence component of Morakot. The shape of the pattern is based on the ratio of the major-axis to the minor-axis of the 300 mm isohyets of the convergence component of all four major Taiwan storms, viz Herb, Haitang, Aere and Morakot. This is an effective process of generating the generalised convergence component pattern.

11.1.8 Moisture Maximization

Several factors that may affect the estimation of the moisture maximization ratio are discussed in this section. Factors (b) and (c) are relevant to maximization for storm transposition while factors (a) and (d) affect the development of DAD with maximization for particular selected major storms.

(a) Normally, dew points at several points between the rainfall area and the moisture inflow jet should be selected and averaged to obtain the representative persisting 12-hour dew point to the storm. In this study, attempt was made to obtain the dew point data in the neighbouring Guangdong, but they were finally not available. In terms of the equation of the moisture maximization ratio ($r = (W_2/W_1)$), this may affect the representativeness of the estimate of precipitable water, W_1, for the selected storm and hence the moisture maximization ratio.

(b) For the same reason, in Hong Kong only the rainfall data at HKO can be used for calculation of the historical highest persisting 12-hour dew point as it has the longest data period of 63 years. All other stations have only data of 20 years more. This also will affect the determination of W_2, the historical highest precipitable water and hence the moisture maximization ratio.

(c) Normally, the time interval used to determine the representative highest persisting 12-hour dew point is within the 24-hour prior to the core rainfall intensity. However,

sometimes it is hard to locate the onset of the core rainfall intensity for different types of storm.

(d) Data availability and study depth are the major factors causing the uncertainties to a PMP estimate. The investigation and analysis of both W_2 and W_1 for the 1993 storm in Hong Kong is a good example. In the 1999 PMP Study, dew point data at HKO only were considered in assessing the moisture maximization ratio, but in the current study, the dew data at six stations, viz CCH, HKO, HKS, SHA, TKL and KP, were considered. All the factors such as moisture inflow direction, wind gust direction and core rainfall intensity were scrutinized in the current study. The moisture maximization ratio was 1.57 for the 1999 PMP Study and now it is 1.65 for the updated PMP.

According to a recent investigation (陳宏等, 2014) on sensitivity study of different methods to derivation of the precipitable water conducted by the AHMRI, the pseudo adiabatic method tends to overestimate the precipitable water while the empirical surface dew point method would underestimate it in comparison with the specific humidity stratification integral method which is considered more accurate due to its physical essence and the use of radiosonde data. As shown in Figure 11.4, the degree of overestimation would increase when the latitude of station decreases. The relative error on estimation of precipitable water is given in the following equation:

$$\text{Relative error} = \frac{\text{(pseudo adiabatic method's - specific humidity stratification integral method's)}}{\text{specific humidity stratification integral method's}} \times 100\%$$

Figure 11.4 indicates that the precipitable water in Gaoxiong with 22°34' N was overestimated by 14.01% and in Yongkang with 23°02' N is by 12.81% while the precipitable water in Hong Kong was overestimated by 16.16%. The average of the precipitable water in Gaoxiong and Yongkang is 13.41%. Therefore, the ratio of moisture maximization for Hong Kong would be reduced from 1.304 to 1.262.

$$\begin{aligned} r &= W_2 / W_1 = W_{27.17} / W_{24} \\ &= \frac{96.48}{74.0} \times \frac{1 - 16.16\%}{1 - 13.41\%} \\ &= 1.262 \end{aligned}$$

If this uncertainty in calculation of precipitable water is accounted for in the PMP estimation, the point PMP value at the centre of the design PMP pattern would be reduced to 1,548 mm from 1,600 mm (about 3% reduction).

24-hour: 1,227 mm x 1.262 = 1,548 mm

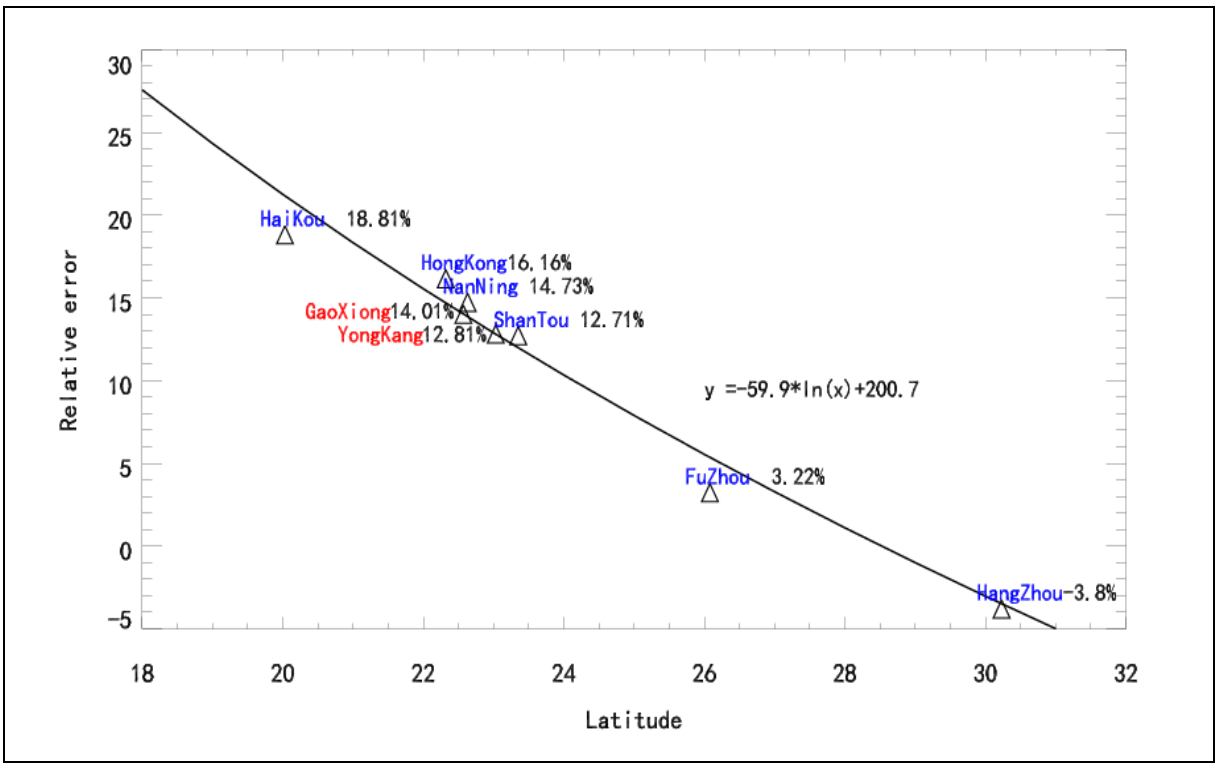

Figure 11.4 Relation of Relative Error in Estimation of Precipitable Water with Latitude

11.2 Twin Peak Values of OIF in Hong Kong (Analysis of Rainfall Pattern)

Referring to Figure 4.8, the highest OIF at Lantau is comparable with that at Tai Mo Shan. This pattern of twin-peaks was further investigated through analysis of the ratios of typhoons to non-typhoons relevant to the 24-hour annual maximum rainfalls at Tai Mo Shan and Lantau. The analysis, as shown in Appendix P, indicates that the above ratio at Tai Mo Shan is similar to that at Lantau (both around 4:6). No major difference in the synoptic weather patterns which affect the 24-hour annual maximum rainfalls at the two areas was noted.

From the viewpoint of PMP estimation, the size of Hong Kong is considered small unlike a catchment or river basin. Distinguishing two peaks at Lantau or Tai Mo Shan is not necessary as the geographic distance between the two spots is small in relation to the scale of a typical rainstorm.

11.3 Guangdong Storms for Comparison Purposes

The reason to include the two top Guangdong storms (i.e. the 2007 storm associated with Typhoon Pabuk and the 2010 storm associated with Typhoon Fanapi) in the development of the master DAD for Hong Kong is that they are the most severe storms in the vicinity of Hong Kong and are the same type of storm as Morakot. The feasibility to include two top Guangdong storms as target storms for transposition to Hong Kong was once investigated.

However, the trial was abandoned due to the unavailability of a complete set of both the storm-based and particularly the historical rainfall data for transposition analysis. The historical hourly rainfall data before 2000 are sporadic with low quality that would impose high uncertainties in developing the OIF for the purpose of transposition. However, it is worthwhile to take them into account in the DAD analysis (i.e. without transposition) based on the ground observations at 171 stations for Fanapi and 32 stations for Pabuk.

The DAD analysis is a relatively simple method that provides useful reference to compare the results from the transposition analysis which is based on Taiwan storms.

11.4 PMP Estimates Using Statistical Approach

As mentioned in Section 1.3.1.1, "this statistical estimation is particularly useful for making quick estimates of PMP. Obviously, the longer data series is welcomed for the method." The statistical PMP estimates are quick estimates for reference only and not recommended to be used as the final estimates for the purpose of engineering design study. The quality of the statistical estimates of PMP depends greatly upon the data quality, quantity and length in the study area, and the depth of the study as well. All historical data at stations used in this study are short with less than 30 years for Hong Kong stations except HKO and less than 40 years for SGD stations. Although much longer time period of data (116 years) is available at the station "HKO", it is the single station with such long data period in the whole study area and no exceptionally heavy (or highest) rainfall records were observed there. Therefore, it has just moderate representativeness in terms of PMP estimation via the statistical approach.

Their corresponding N_s (stable data length) required to get a stable estimate of the values of K_m should be longer than 80 years when K_m approaches T_m, but the reality is that the 30 to 40 years of data are available. Therefore, the PMP estimates inherently contain a high degree of uncertainty. However, the estimates have a good value for reference in regard to PMP estimation for Hong Kong area because all data available not only in Hong Kong but also in SGD have been used in the revised statistical approach with peer-reviewed rigorous criteria newly developed for application of the statistical approach (see Section 1.3.1.2).

"Regionalization" (see Section 3.2) in this context refers to the process of enveloping. PMP estimates were determined in a relatively wide area not only based on a single local raingauge. The purpose of presenting PMP estimates for Hong Kong and SGD data separately here is to show that the estimate based on SGD data represents less uncertainty (i.e. more stable sample size) but less representativeness. On the other hand, the estimate based on Hong Kong data only represents more uncertainty but more representativeness (i.e. more stations). Data from Hong Kong and SGD have different degree of uncertainty when they are applied to the statistical analysis. Uncertainties come from the relatively short period of data for Hong Kong and poor representativeness comes from a few raingauge stations for SGD. Normally, longer data would provide results with less uncertainty and more stations in a region would give better representativeness in statistical analysis. Highlighting the issues on uncertainties and representativeness reminds users of the limitations and the need to interpret the PMP based on statistical approach with care.

PMP estimates obtained from this statistical analysis represent point values.

Referring to Section 4.2.5 in Manual on Estimation of PMP (WMO, 2009), these point values could be applicable to areas up to 25 km^2 when they are compared with existing DAD curves or PMP estimates from storm transposition approach in study. To provide a quick estimate for the purpose of this study, only a single PMP value was provided over the territory of Hong Kong for the duration of 24-hour. Since the data used for PMP estimation via statistical approach are station-based but not area-average, the PMP estimate is a single PMP value. However, a limited regionalization was applied when the PMP value was computed. Therefore, the statistical approach to PMP could be conventionally considered as a transposition of parameters within a limited area.

The purpose of statistical estimation is to obtain information on the possible range of the 24-hour PMP. Results from the statistical approach were compared with results from the storm transposition approach for cross-checking and reference. In the study, the PMP estimate based on the storm transposition approach is considered a more realistic PMP estimate for Hong Kong.

The selection criteria for rainfall data are intended to reduce the statistical error due to short period of data. However, raingauge stations on Lantau Island were screened out because the length of data period did not meet the selection criteria. An uneven station distribution may lead to some degree of uncertainty in the statistical analysis.

11.5 4-hour PMP Estimates

Attempts have been made to apply the SDOIF method with the rainfall data of the four Taiwan storms, viz Herb, Aere, Haitang and Morakot as well as the "traditional" moisture maximization method with the new local storm data to update the PMP for 4-hour duration. New information about extreme rainfall events in Taiwan for short durations has just been discovered. According to a publication of the Taiwan National Science and Technology Centre for Disaster Reduction (龔楚嫈等, 2012) and a list of the top 30 3-hour rainfalls in Taiwan obtained from the CWB of Taiwan, the above four Taiwan storms are not the top storms for 3-hour duration in Taiwan though the quality of the newly discovered short duration storms is pending for verification. Although the 4-hour list is not available, it is expected that the same conclusion would apply to 4-hour duration. Hence, the PMP established from rainfall data of the four Taiwan storms may be underestimated. Nevertheless, the results are considered as an interim updating of the 4-hour PMP and for reference only. The analysis and the results are given in Appendices Q to W.

12 Conclusions and Recommendations

The previous 1999 24-hour PMP study covered local storms up to year 1999 while several severe storms have occurred in Hong Kong and Southeast China region since the 1999 PMP study. There is a need for updating the PMP using an improved PMP estimation technique as recommended in the 3rd Edition of Manual on Estimation of PMP published by WMO (2009).

In this study, the international best practice has been adopted by taking into account non-local storms in meteorologically similar area using storm transposition method.

Distinguishing from the previous PMP study, storm separation technique based on the SDOIF Method was applied to separate orographic effect from rainfall data for non-local storms. The convergence component was combined with local orographic factors to estimate a new 24-hour PMP in Hong Kong.

The storm transposition analysis based on Typhoon Morakot has been undertaken. The embryonic PMP was further adjusted by the moisture maximization ratio. The isohyets of 24-hour PMP centred at Tai Mo Shan and Lantau are given in Figures 6.1 and 7.1 respectively. The DAD curve of the updated 24-hour PMP, which is based on the average of the DAD curves for PMP centred at Tai Mo Shan and Lantau, is given in Figure 7.2 and Table 7.1. For this curve, the updated 24-hour PMP corresponding to a rainfall area of 10 km^2 is 1,510 mm. For landslide risk assessment, it is recommended that the elliptical-shaped isohyets with an aspect ratio of 1.6 and dimensions given in Table 7.2, which are derived from the average DAD curve, should be adopted for assessing landslide responses.

A literature review of the impact of climate change on PMP estimate and trend analyses of related climate parameters have been conducted. With relatively high uncertainties in the projections of extreme rainfalls, frequency and intensity of tropical cyclones, potential changes in precipitable water in our region as well as the relationship between extreme rainfalls and PMP, it is still difficult to ascertain and quantify the impact of climate change on the PMP in Hong Kong in the 21st century. More studies are required to further our understanding on this subject.

Updating of PMP is suggested in the future if other severe storms with extreme rainfall occur. To facilitate future updating study, keeping track of extreme rainfall events in meteorologically similar areas is recommended.

13 References

Bureau of Meteorology (2009). *Climate Change and Probable Maximum Precipitation, HRS Report No.12.* Bureau of Meteorology, Melbourne, Australia.

Chen, T.Y. (1969). *Supplement to Meteorological Results 1966 - the Severe Rainstorms in Hong Kong during June 1966.* Royal Observatory Hong Kong, 79 p.

China Water & Power Press (1995). *The Handbook of Design Floods for Water Resources and Hydropower Engineering.*

Hansen, E.M. (1987). Probable maximum precipitation for design floods in the United State. *J. Hydrol*., 96 p.

HKO (1999). *The Probable Maximum Precipitation Updating Study for Hong Kong.* Hong Kong Observatory, 32 p.

Hong, C.C., Hsu, H.H., Lee, M.Y. & Kuo, J.L. (2010). Role of sub-monthly disturbance and 40 - 50 day ISO on the extreme rainfall event associated with Typhoon Morakot (2009) in Southern Taiwan. *Geophysical Research Letters*, vol. 37, L08805, 6 pp.

IPCC (2013). *Technical Summary. In: Climate Change 2013: The Physical Science Basis.* Contribution of Working Group I to the Fifth Assessment Report of the Intergovernmental Panel on Climate Change.

Kung, C.S. (2010). *台灣地區颱風極端降雨特性,* Presentation at AHMRI of NUIST, Nanjing, 2010.5.

Kunkel, K.E., Karl, T.R., Easterling, D.R., Redmond, K., Young, J., Yin, X. & Hennon, P. (2013). Probable maximum precipitation and climate change. *Geophysical Research Letters,* vol. 40, pp 1402-1408.

Lee, T.C., Chan, K.Y., Chan, H.S. & Kok, M.H. (2011). Projection of extreme rainfall in Hong Kong in the 21st century, *Acta Meteorologica Sinica*, 25(6), 691-709, doi: 10.1007/s13351-011-0601-y.

Lin, B., Bonnin, G.M., Martin, D.L., Parzybok, T., Yekta, M. & Riley, D. (2006). Regional Frequency Studies of Annual Extreme Precipitation in the United States based on Regional L-moments Analysis. *Proceedings of the World Environmental and Water Resources Congress.* ASCE Conf. Proc., Omaha, Nebraska, USA, pp 1-11.

Lin, B. & Julian, L.T. (2001). Trend and shift statistics on annual maximum precipitation in the Ohio River Basin over the last century. *Symposium on Precipitation Extremes: Predictions, Impacts, and Responses, 81st AMS Annual Meeting*, Albuquerque, New Mexico.

Lin, B. & Vogel, J. (1993). A New Look at the Statistical Estimation of the PMP. *ASCE Proceedings*, Session S25, pp 629-634.

Maidment, D.R. (1992). *Handbook of Hydrology*. McGraw-Hill, New York, 17.30, 19.17 - pp 19.18.

O'Gorman, P.A. (2012). Sensitivity of tropical precipitation extremes to climate change, *Nature Geoscience*, 5(10), pp 697-700.

WMO (2009). *Manual on Estimation of Probable Maximum Precipitation (PMP) (WMO-No. 1045).* World Meteorological Organization, 257 p.

Wong, M.C., Mok, H.Y. & Lee, T.C. (2011). Observed Changes in Extreme Weather Indices in Hong Kong. *Int. J. Climatol*., 31, 2300-2311, DOI: 10.1002/joc.2238.

WRA (2009). *莫拉克颱風暴雨量及洪流量分析.* Water Resources Agency, Ministry of Economic Affairs, Taiwan (台灣經濟部水利署), 33 p.

Ying, M., Knutson, T.R., Kamahori, H. & Lee, T.C. (2012). Impacts of Climate Change on Tropical Cyclones in the Western North Pacific Basin. Part II: Late twenty-first Century Projections. *Tropical Cyclone Research and Review,* vol. 1, no. 2. pp 231-241.

王家祁 (2002). *中國暴雨*. 北京市. 中國水利水電出版社.

王國安 (1999). *可能最大暴雨和洪水計算原理與方法*. 鄭州市. 黃河水利出版社.

水利部 (長江水水利委員會水文局, 水利部南京水文水資源研究所) (1995). *水利水電工程設計洪水計算手冊*. 北京市. 中國水利水電出版社. 1995.10.

林炳章 (1981). 統計估算法在可能最大降水研究中的應用. *河海大學學報*. 1981.1. 南京.

林炳章 (1987). *海南島昌化江大廣壩工程 PMP-PMF 估算綜合報告*. 河海大學.

林炳章 (1988). 分時段地形增強因數法在山區PMP 估算中的應用. *河海大學學報*. 1988, 16(3). pp 40-52.

林炳章，邵月紅，閆桂霞 & 張葉暉 (2012). 水文氣象促進工程水文計算核心課題研究的發展[A]. *2012 中國水文學術討論會論文集*[C]. 南京：河海大學出版社, 2012. 50-63.

郭林 (2011). *2009 年“莫拉克”颱風超強降水原因初步分析*. 廈門氣象局. “氣候變化對可能最大降水估算影響及防洪對策”第一次學術研討會文集，2011 年 3 月 30-31 日，廈門，中國.

陳宏、林炳章 & 張葉暉 (2014). *PMP 估算中大氣可降水量計算方法的探討*. 《水文》2014 年第三期, 中國水利水電出版社，2014.6 北京.

龔楚嫕、於宜強、李宗融 & 林李 (2012). 短延時致災降雨事件分析. *災害防救電子報*, 2012/04, 第 081 期. 國家災害防救科技中心 (NCDR), 台灣, 11 p.

Appendix A

Detailed Description on Major Severe Non-local Storms

Contents

List of Tables

List of Figures

A.1 Storms Investigated in Southeast China

A.1.1 Typhoon Pabuk

Typhoon Pabuk (帕布颱風, Figure A1) 9-12 August 2007

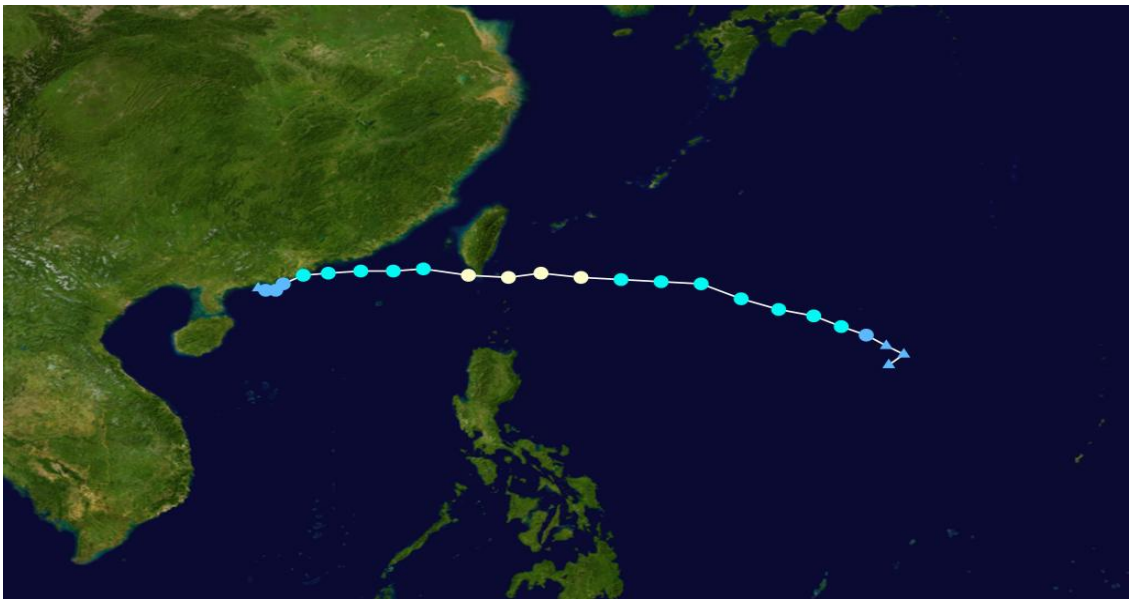

Figure A1 Typhoon Track for Pabuk in Guangdong

Typhoon Pabuk passed the southern end of Taiwan, and crossed South China Sea to Guangdong Province and Hong Kong. It further moved westward near Hainan Island, weakened to a tropical depression, then moved reversely to eastward along the coast of South China Sea and East China Sea along mainland China. The typhoon was not so strong in intensity, but it came with well-developed clouds bringing heavy rains to many places in China from Guangdong Province to Fujian Province.

According to the Central Meteorological Office, Leizhou Peninsula recorded a heavy rain once in 200 years, which recorded 1-hour precipitation of 213 mm, 24-hour precipitation of 1,188.2 mm, recorded as the maximum 24-hour rainfall record in the mainland China.

The total rainfall for the period of 10-12 August 2007 is 1,348.9 mm based on the hourly rainfall observations for Typhoon Pabuk that the Applied Hydrometeorological Research Institute (AHMRI) have collected from the Guangdong Hydrological Bureau (HB), as shown in the isohyets chart below (Figure A2).

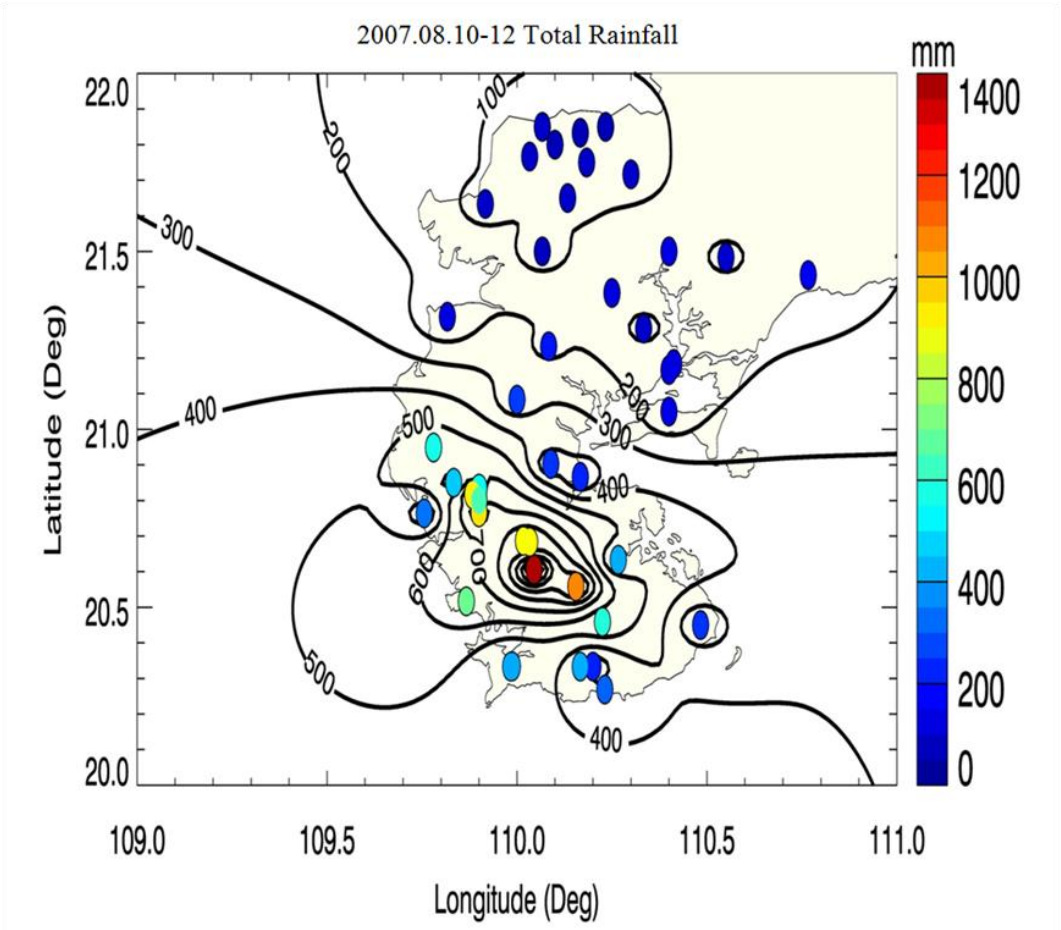

Figure A2 Isohyets Chart of Total Rainfall for Typhoon Pabuk in Guangdong

The isohyets charts for 24-hour rainfall of 1,188.2 mm and 4-hour rainfall of 396.2 mm of Typhoon Pabuk are given in Figures A3 and A4 below:

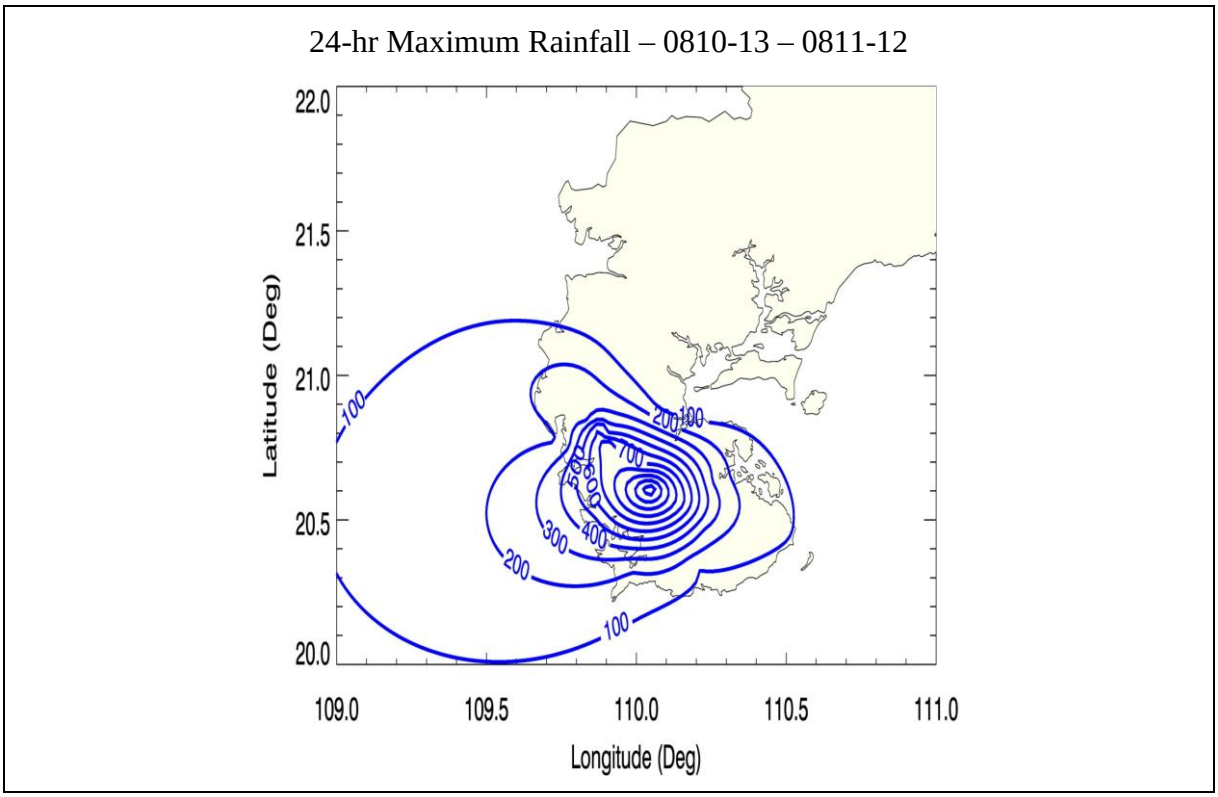

Figure A3 Isohyets Chart of 24-hour Rainfall for Typhoon Pabuk

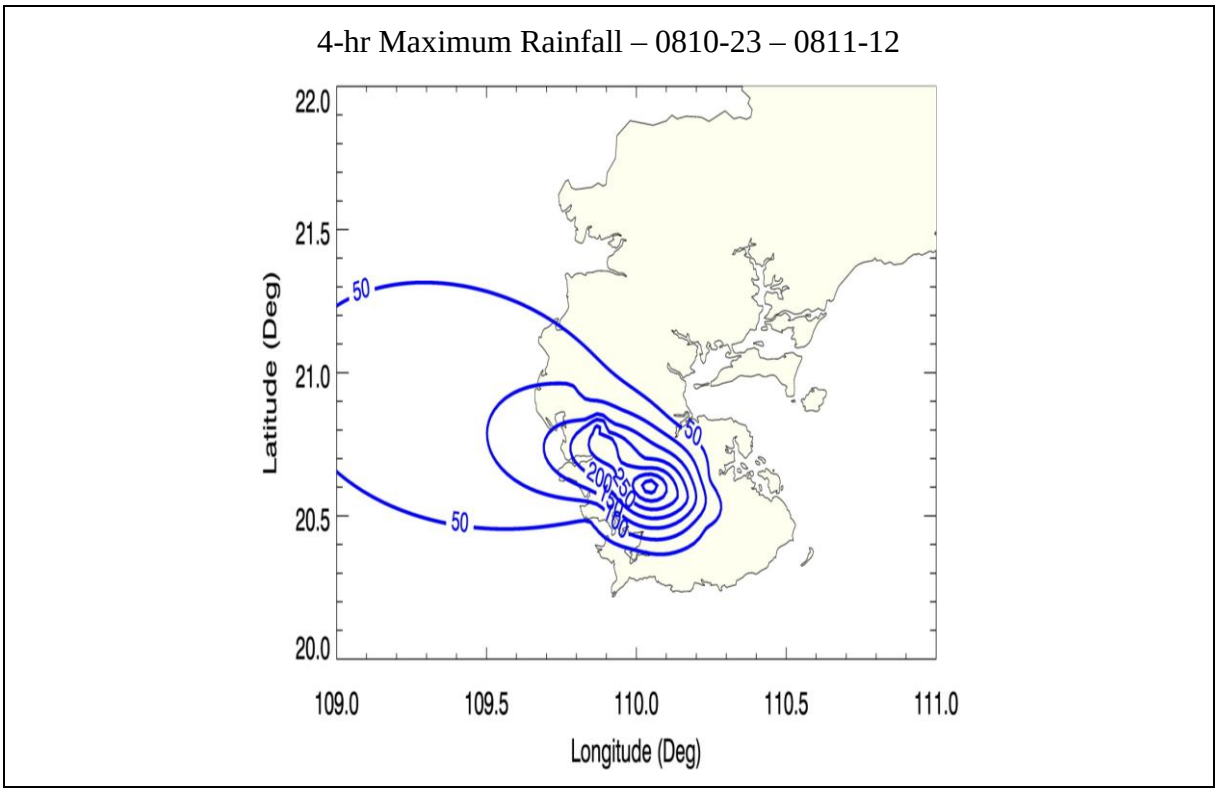

Figure A4 Isohyets Chart of 4-hour Rainfall for Typhoon Pabuk

A.1.2 Typhoon Fanapi

Typhoon Fanapi (凡那比颱風, Figure A5) 21-23 September 2010

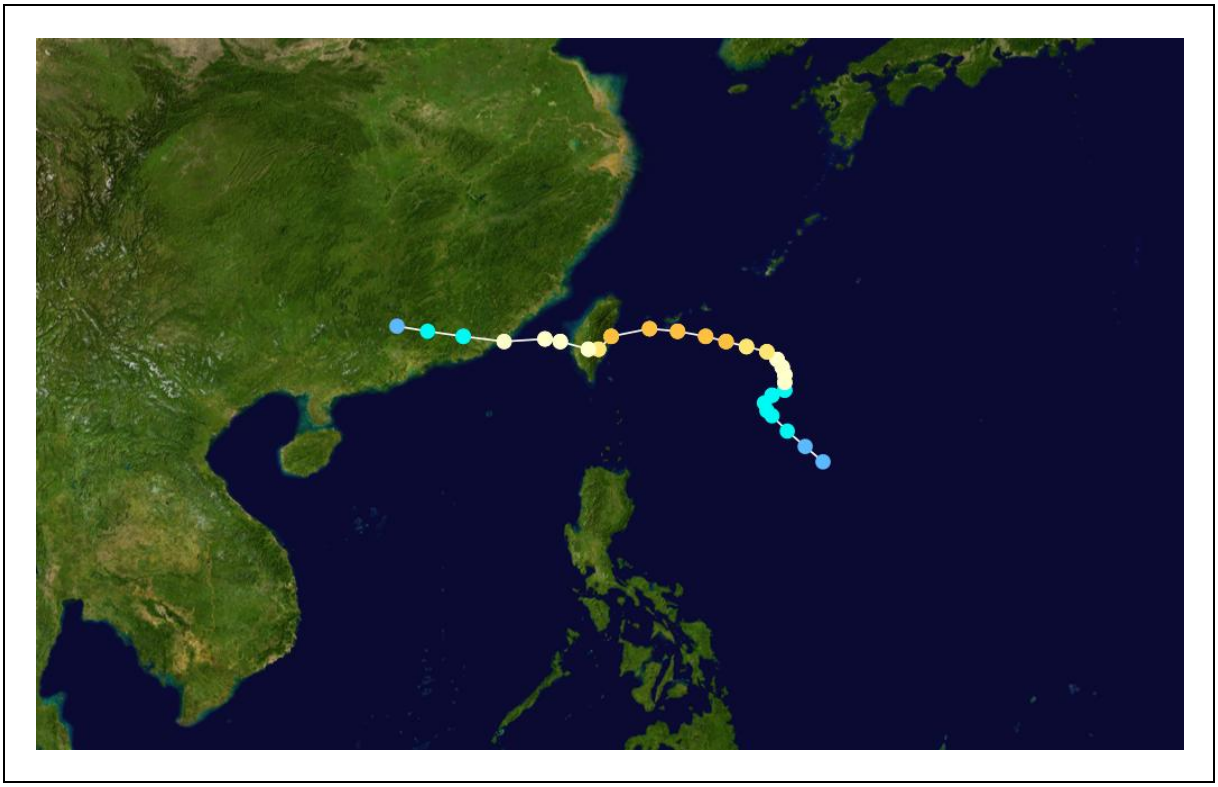

Figure A5 Typhoon Track for Fanapi in Guangdong

After landfall in Taiwan for about nine hours, Fanapi moved across Taiwan Strait and made its second landfall over Zhangpu in Fujian, China. Late on 20 September, Fanapi weakened into a tropical depression over Guangdong, China, and it dissipated completely on the next day.

Regarding the rainfall, the stations with large 6-hour rainfall are Magui, Gaozhou City with 427.5 mm and Maoming, Yangchun City with 434 mm; the stations with large 12-hour rainfall are Magui, Gaozhou City with 673.5 mm and Maoming, Yangchun City with 784 mm; the stations with large 24-hour rainfall are Magui, Gaozhou City with 706.5 mm and Maoming, Yangchun City with 814 mm.

The total rainfall for the period of 21-23 September 2010 is 972 mm based on the hourly rainfall observations for Typhoon Fanapi that the AHMRI have collected from the Guangdong HB as shown in the isohyets chart below (Figure A6).

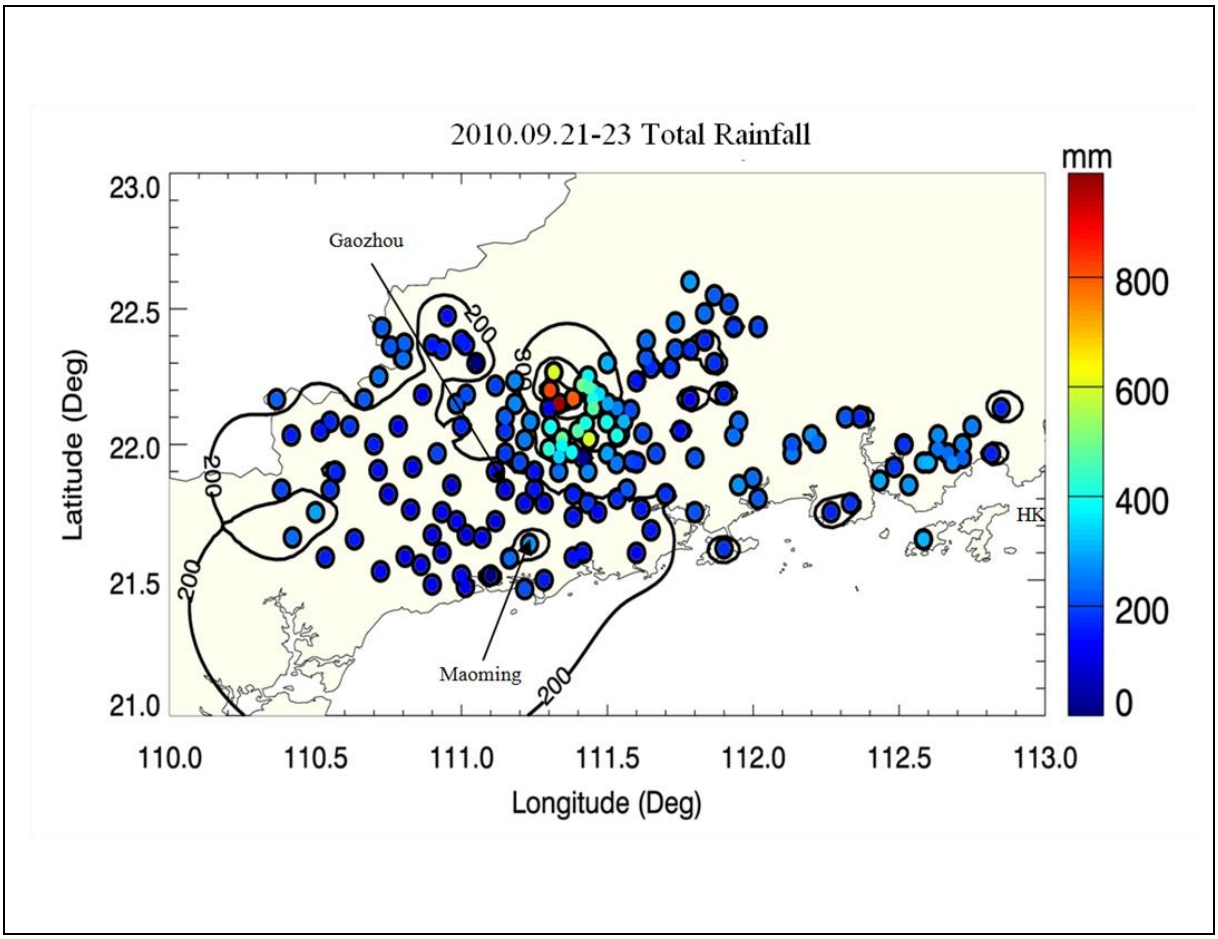

Figure A6 Isohyets Chart of Total Rainfall for Typhoon Fanapi in Guangdong

The isohyets charts for 24-hour rainfall of 839.5 mm and 4-hour rainfall of 416.5 mm of Typhoon Fanapi are given in Figures A7 and A8 below:

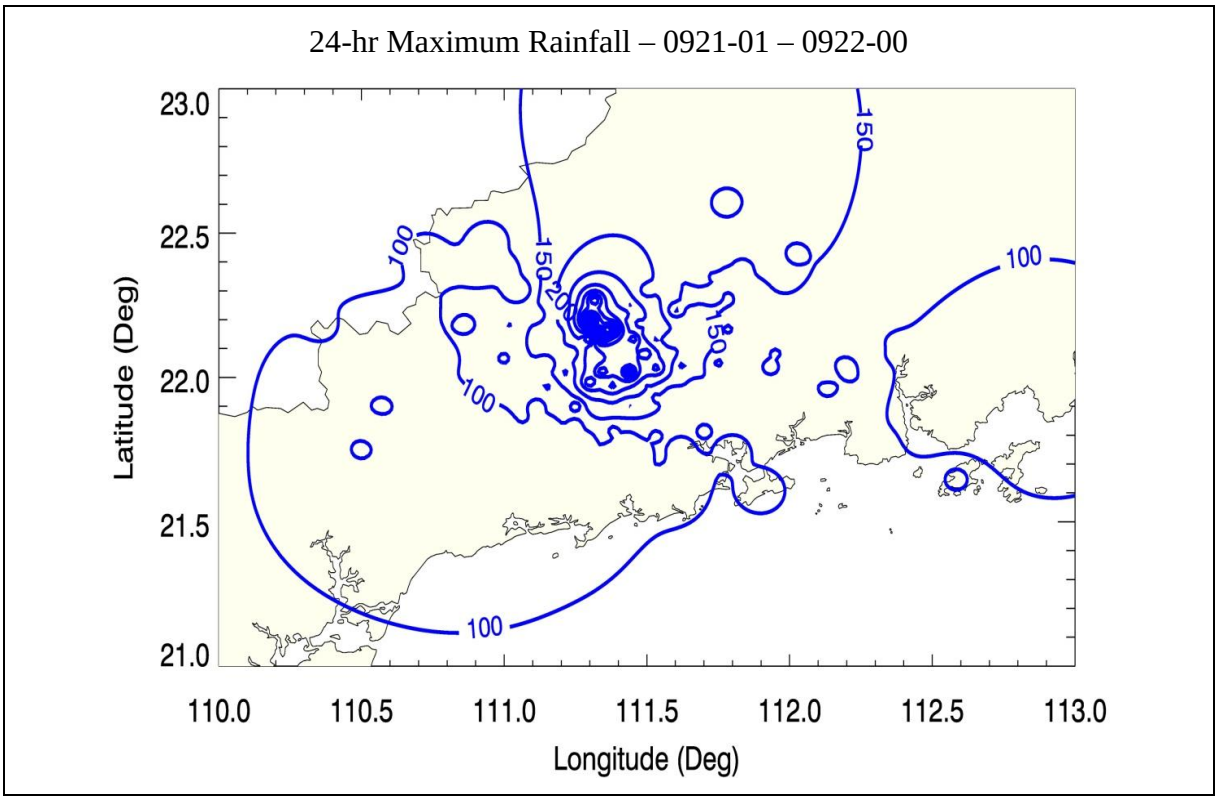

Figure A7 Isohyets Chart of 24-hour Rainfall for Typhoon Fanapi

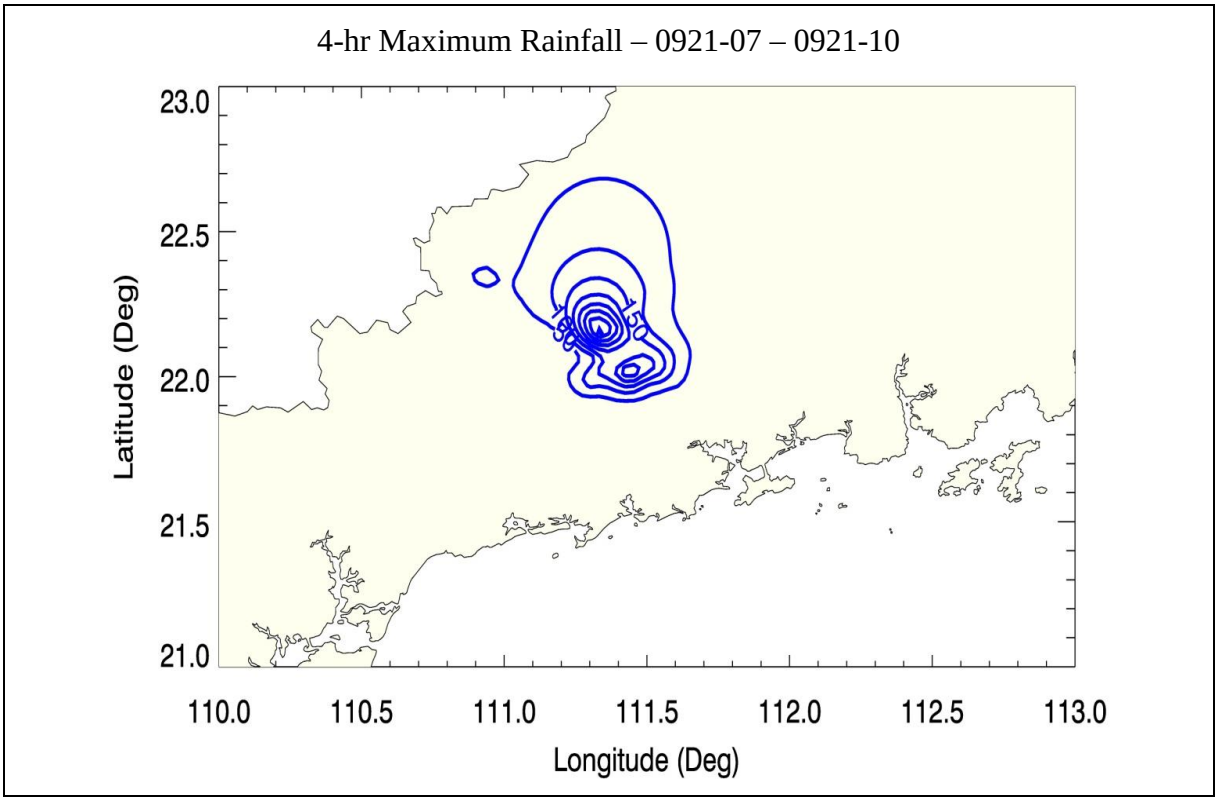

Figure A8 Isohyets Chart of 4-hour Rainfall for Typhoon Fanapi

A.2 Storms Investigated in Taiwan

A.2.1 Typhoon Herb

Typhoon Herb (賀伯颱風, Figure A9) 29 July to1 August 1996

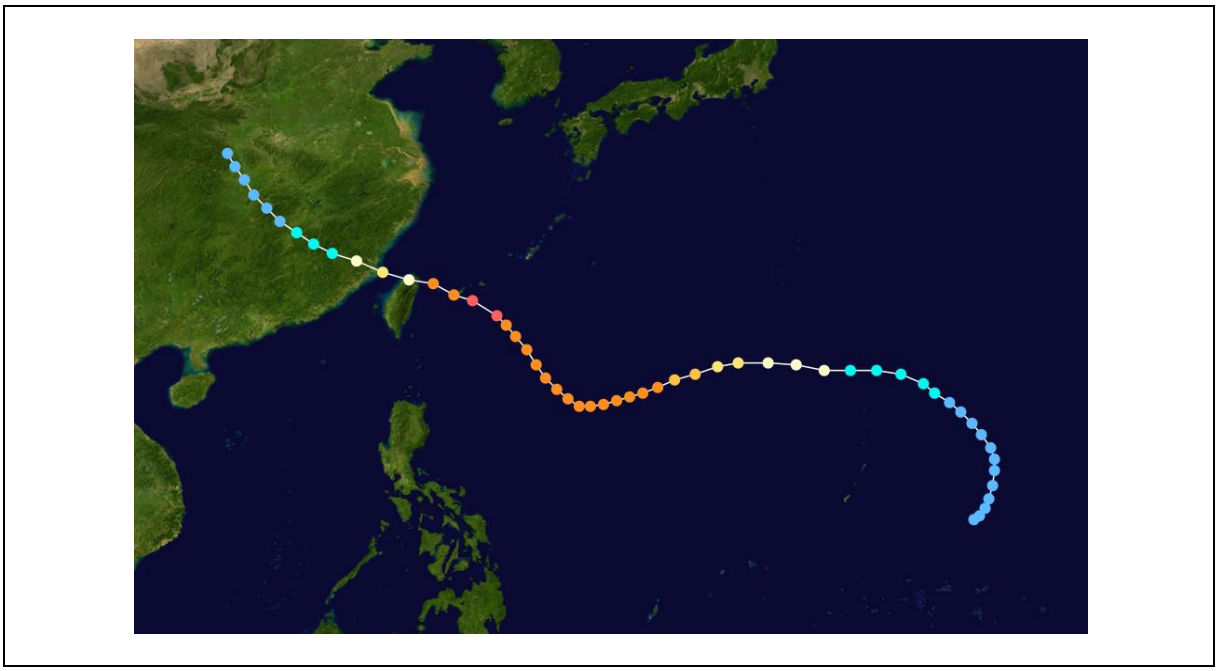

Figure A9 Typhoon Track for Herb

The active monsoon trough that spawned Typhoons Frankie (08W) and Gloria (09W) consolidated into a third area well east of the other two to develop Tropical Depression 10W near Saipan on 23 July. It moved northward at first, then westward in response to the subtropical ridge to its north. Tropical Depression 10W was upgraded to Tropical Storm Herb on 24 July. Tropical Storm Herb moved west, growing in size and strengthening to Typhoon Herb on 25 July before 48 hours later reaching Category 4 (125 knots). An interaction with Typhoon Gloria (in what is known as the "Fujiwhara effect") saw Herb downgraded to 115 knots. Shortly afterward Herb began to intensify again, and became a Category 5 super typhoon (140 knots) on 30 July. Herb also became a very large typhoon: the largest typhoon in July and the 8th largest typhoon since 1977.

Herb struck the Ryūkyū Islands and made landfall in northern Taiwan as a Category 4 Super Typhoon (130 knots) on 31 July. The eye of the storm passed directly over Taipei, Taiwan. Herb weakened as it crossed Taiwan and then the Taiwan Strait, to make landfall in China as a strong Category 2. Herb rapidly weakened over the country and dissipated on 3 August.

Regarding the rainfall, the accumulative rainfall at Nantou, Alishan and Taozhumiao mountainous region are all more than 1,000 mm. The raingauge station at Alishan recorded the daily rainfall of 1,094.5 mm on 31 July and 892 mm on 1 August. Typhoon Herb left a 24-hour and 48-hour rainfall accumulation of 1,749 and 1,987 mm respectively, recorded at

the Central Weather Bureau Alishan weather station.

There are some missing data in this storm records from Central Weather Bureau (CWB) of Taiwan and many "big numbers" for hourly data, such as 789.0 mm for Station C01090 at 1996.08.02.16 for Herb, which are deemed to be suspicious, as shown in Table A1. It seems that these "big numbers" probably represent the total ranfall over the previous hours, which show "-9996" that stands for missing records and are cumulated in the later hour. Hence, these suspicious records are not used in the subsequent analysis.

Table A1 Example of "Big Numbers" in CWB's Records for Typhoon Herb

Station	Date/Time	Rainfall
C0I010	1996083124	0.0
C0I090	1996080101	-9996
C0I090	1996080102	-9996
C0I090	1996080103	-9996
C0I090	1996080104	-9996
C0I090	1996080105	-9996
C0I090	1996080106	-9996
C0I090	1996080107	-9996
C0I090	1996080108	-9996
C0I090	1996080109	-9996
C0I090	1996080110	-9996
C0I090	1996080111	-9996
C0I090	1996080112	-9996
C0I090	1996080113	-9996
C0I090	1996080114	-9996
C0I090	1996080115	-9996
C0I090	1996080116	-9996
C0I090	1996080117	-9996
C0I090	1996080118	-9996
C0I090	1996080119	-9996
C0I090	1996080120	-9996
C0I090	1996080121	-9996
C0I090	1996080122	-9996
C0I090	1996080123	-9996
C0I090	1996080124	-9996
C0I090	1996080201	-9996
C0I090	1996080202	-9996
C0I090	1996080203	-9996
C0I090	1996080204	-9996
C0I090	1996080205	-9996
C0I090	1996080206	-9996
C0I090	1996080207	-9996
C0I090	1996080208	-9996
C0I090	1996080209	-9996
C0I090	1996080210	-9996
C0I090	1996080211	-9996
C0I090	1996080212	-9996
C0I090	1996080213	-9996
C0I090	1996080214	-9996
C0I090	1996080215	-9996
C0I090	1996080216	789.0
C0I090	1996080217	0.0

The maximum 4-hour and 24-hour isohyets charts for Typhoon Herb are given in Figures A10 and A11 below:

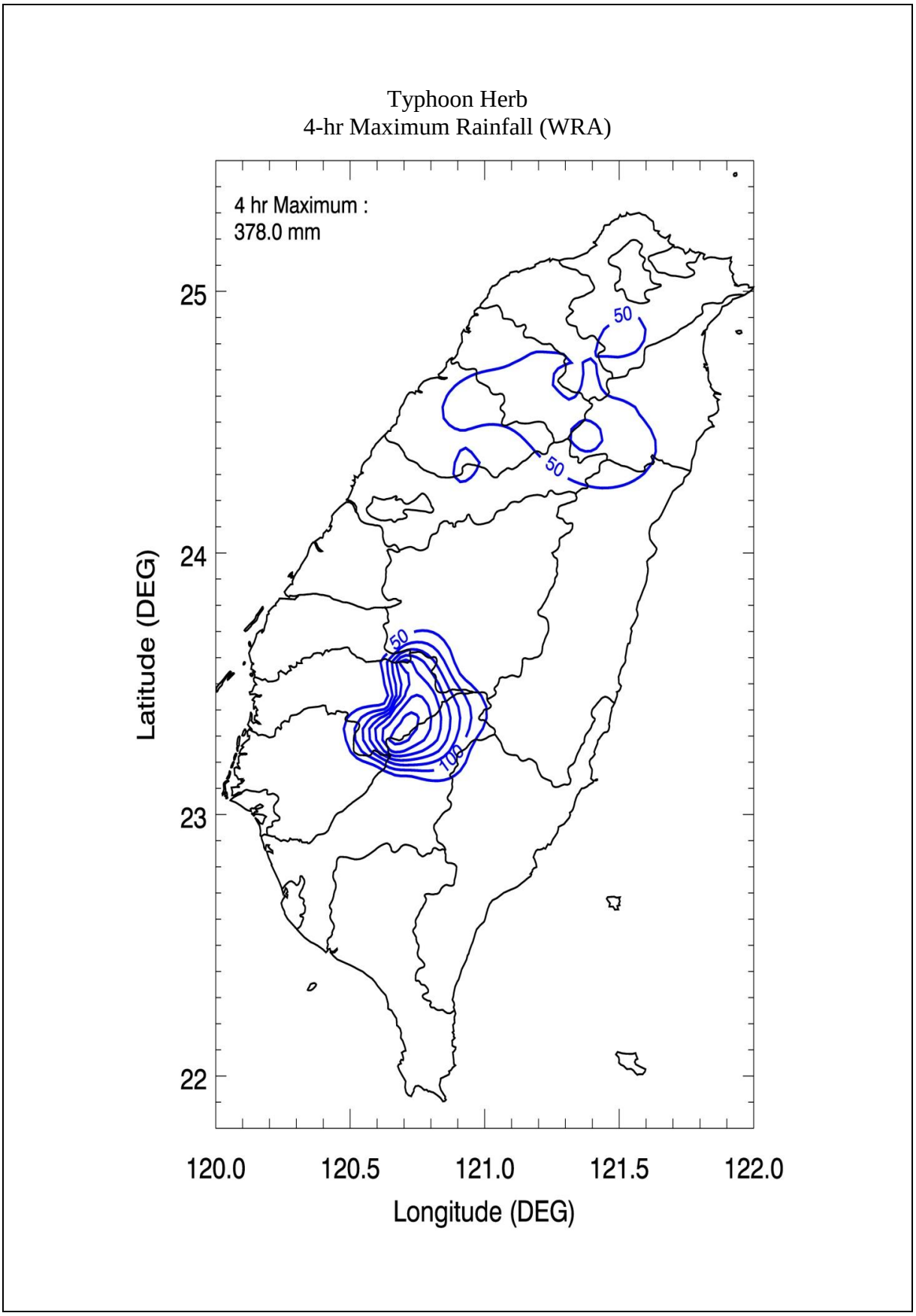

Figure A10 Isohyets Chart of 4-hour Rainfall for Typhoon Herb

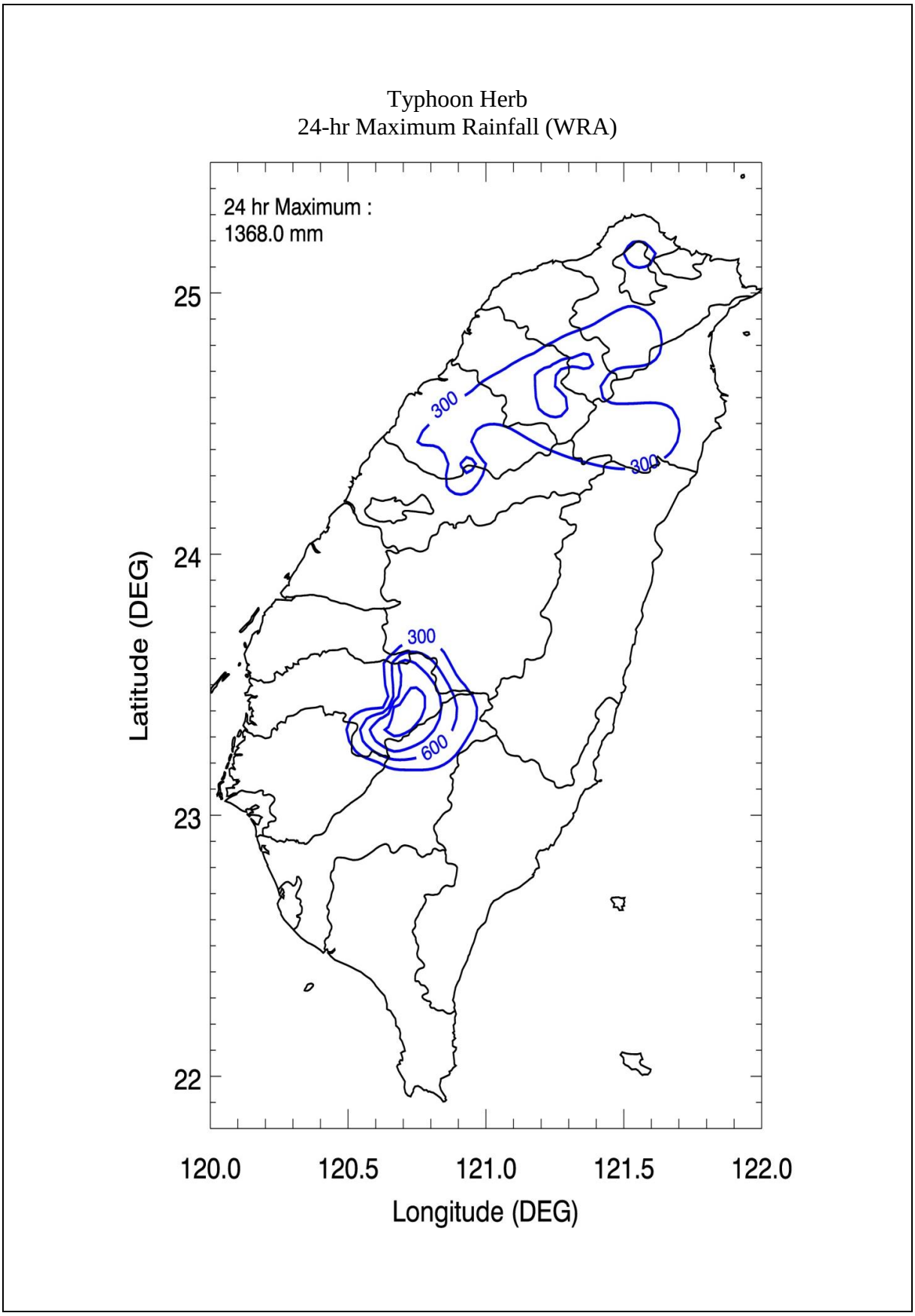

Figure A11 Isohyets Chart of 24-hour Rainfall for Typhoon Herb

A.2.2 Typhoon Aere

Typhoon Aere (艾莉颱風, Figure A12) 23-26 August 2004

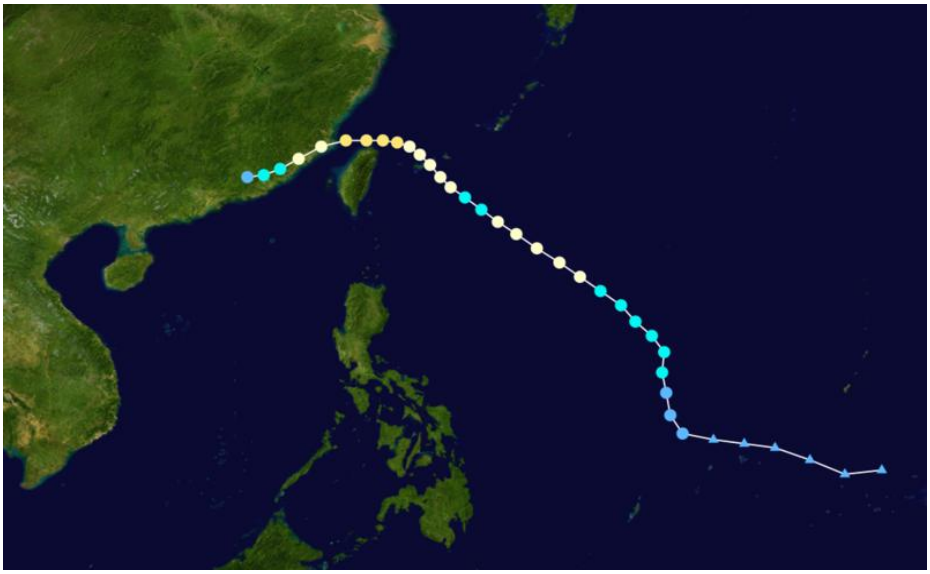

Figure A12 Typhoon Track for Aere

An area of convection developed approximately 250 miles east of Pohnpei late on August 13. By August 16, the disturbance had passed 40 miles north of Chuuk. It developed enough organization to be designated a tropical depression on 19 August, about 400 miles west of Guam. From there, it moved northwest at 12 mph along the southwestern periphery of a mid-level steering ridge. The system reached tropical storm status on August 20, gaining the name Aere.

Tropical Storm Aere was upgraded to typhoon intensity on 21 August, and its strength levelled off during 21 August and 22 August. On 23 August, the typhoon was briefly downgraded to a tropical storm due to vertical wind shear while located 200 miles south of Naha, Okinawa. Aere quickly regained typhoon status and maintained its intensity for the rest of 23 August and developed a 50-mile wide eye. The tropical cyclone reached its peak intensity of 100 mph late on 24 August, when the pressure lowered to 955 mb.

As the storm crossed the northern tip of Taiwan, it began to weaken. Typhoon Aere turned west-southwestward on the 25 August and made its closest approach to Taipei, Taiwan, passing only 30 miles to the city's north. Aere turned southwestward later that day, a trajectory that carried the storm past Xiamen early the next day and close to Shantou later that day before weakening to tropical storm intensity. The remnants of Typhoon Aere remained a tropical depression until 31 August. (Wikipedia)

The maximum 4-hour and 24-hour isohyets charts for Typhoon Aere are given in Figures A13 and A14 below:

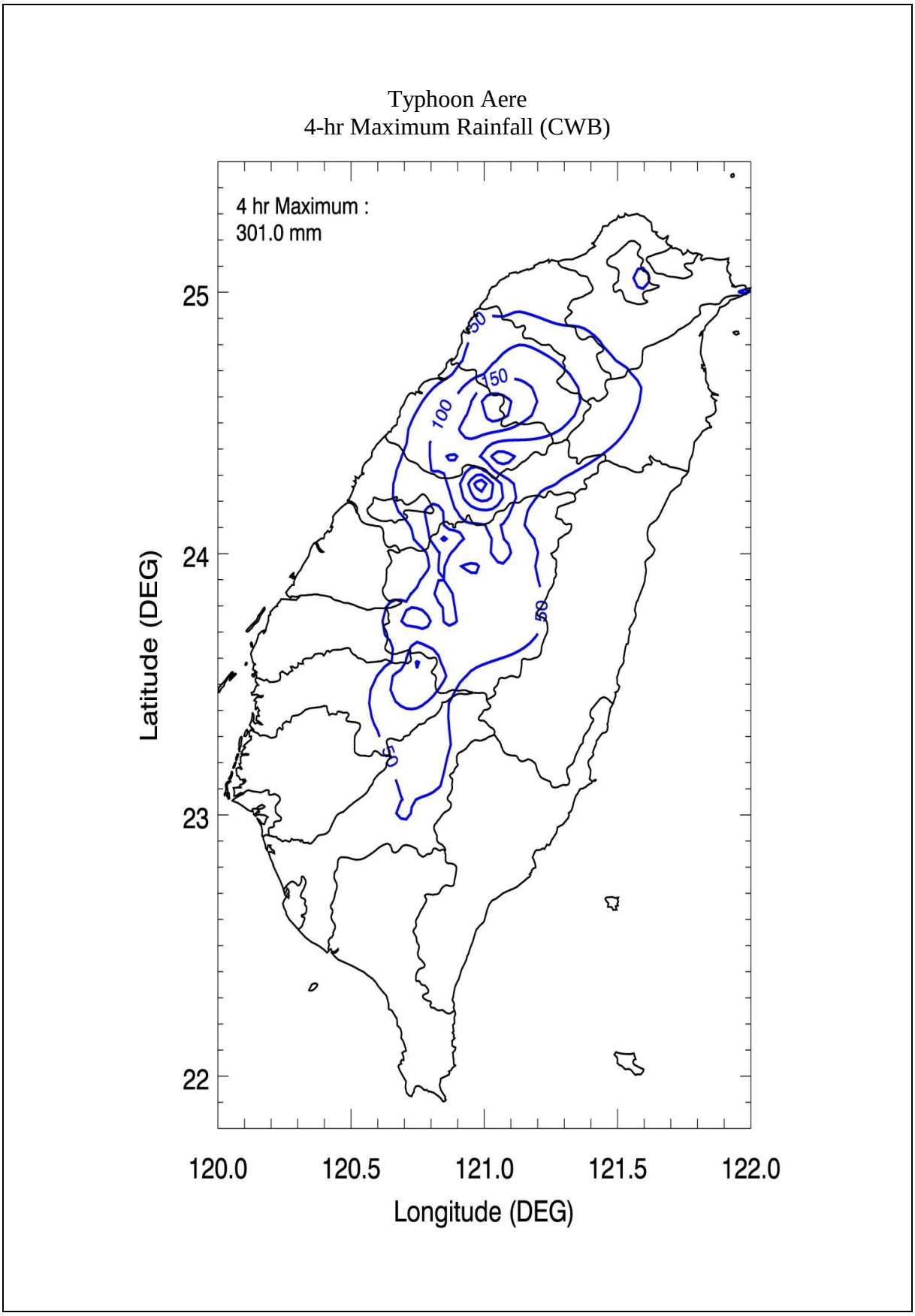

Figure A13 Isohyets Chart of 4-hour Rainfall for Typhoon Aere

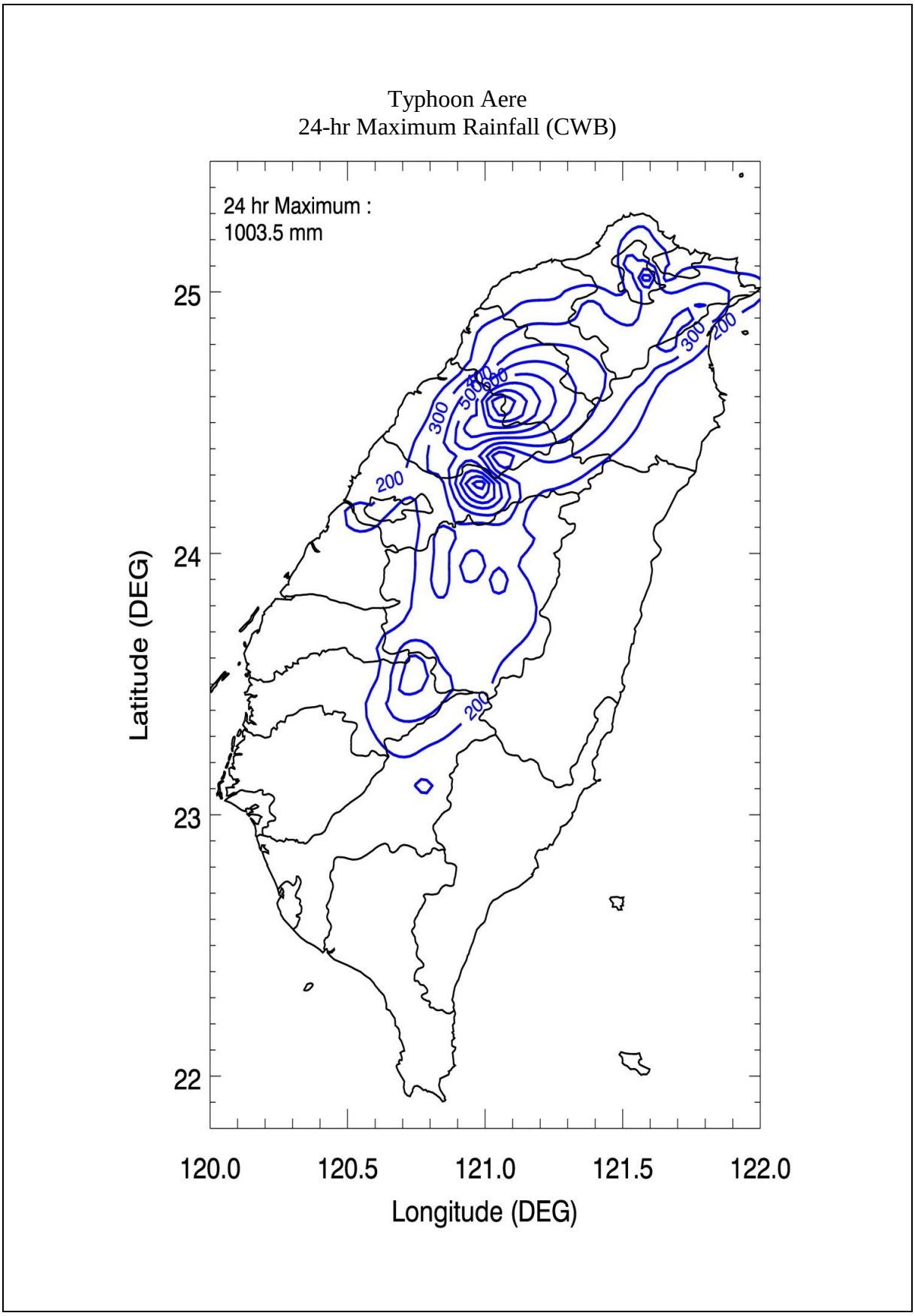

Figure A14 Isohyets Chart of 24-hour Rainfall for Typhoon Aere

A.2.3 Typhoon Haitang

Typhoon Haitang (海棠颱風, Figure A15) 16-20 July 2005

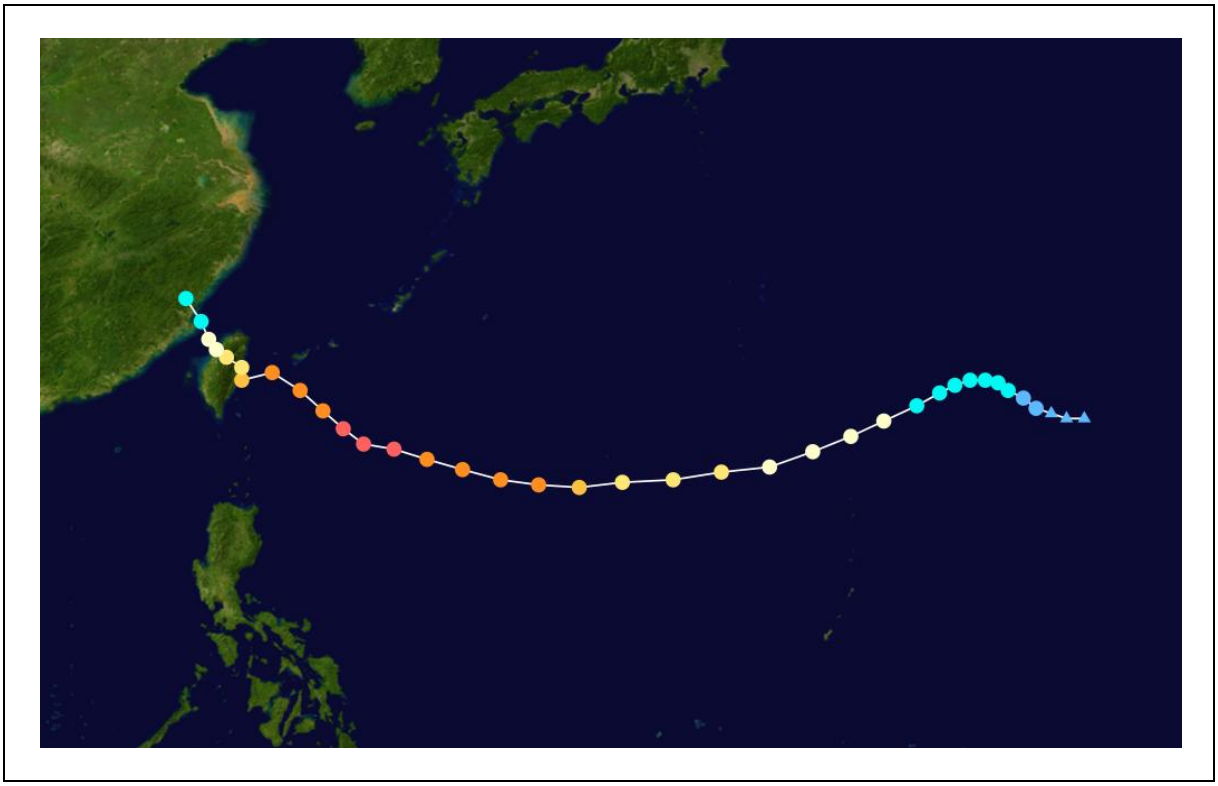

Figure A15 Typhoon Track for Haitang

The storm formed on the evening of 11 July as a poorly organized depression about 280 km west of Marcus Island, Japan at 1200 UTC (2000 Japan Standard Time (JST)). By 1800 UTC (0300 JST 13 July), it had reached a high, destructive tropical storm strength and was named Haitang, a Chinese name for flowering crabapple. It grew to typhoon strength at 1800 UTC (0300 JST 14 July) the following day.

As it moved westward it continued to gain in strength, reaching Category 3 status as it entered the Philippine area of responsibility. By 16 July, the storm continued tracking west and became a threat to Taiwan and Japan's Sakishima Islands. On 17 July it continued west, sparing Sakishima a direct hit but aiming directly for Taiwan. Typhoon Haitang made landfall near Hualian, Taiwan at 0000 UTC (0800 HKT) on the morning of 18 July. Taking a full day to cross the island and it caused flash floods and landslides as it passed over the interior mountains. Weakening to a tropical storm as it entered the South China Sea, it reorganized into a minimal typhoon as it approached the southeast China coast. Haitang made landfall for the second time near Wenzhou China on 19 July at 1200 UTC (2000 HKT). Moving inland, it rapidly lost its strength and dissipated. PAGASA stopped issuing advisories for the storm near Jiangxi on 20 July. (Wikipedia)

There are some missing data in this storm records from CWB and many "big numbers" for hourly data, such as 202.5 mm for Station C1R330 at 2005.07.19.15 for Haitang, which are deemed to be suspicious, as shown in Table A2. It seems that these "big numbers" probably represent the total ranfall over the previous hours, which show "-9996" that stands for missing records and are cumulated in the later hour. Hence, these suspicious records were not used in subsequent analysis.

Table A2 Example of "Big Numbers" in CWB's Records for Typhoon Haitang

Station	Date/Time	Rainfall
C1R330	2005071911	12.5
C1R330	2005071912	5.0
C1R330	2005071913	10.0
C1R330	2005071914	0.5
C1R330	2005071915	3.0
C1R330	2005071916	-9996
C1R330	2005071917	-9996
C1R330	2005071918	-9996
C1R330	2005071919	-9996
C1R330	2005071920	-9996
C1R330	2005071921	-9996
C1R330	2005071922	-9996
C1R330	2005071923	-9996
C1R330	2005071924	-9996
C1R330	2005072001	-9996
C1R330	2005072002	-9996
C1R330	2005072003	-9996
C1R330	2005072004	-9996
C1R330	2005072005	-9996
C1R330	2005072006	-9996
C1R330	2005072007	-9996
C1R330	2005072008	-9996
C1R330	2005072009	-9996
C1R330	2005072010	-9996
C1R330	2005072011	-9996
C1R330	2005072012	-9996
C1R330	2005072013	-9996
C1R330	2005072014	-9996
C1R330	2005072015	202.5
C1R330	2005072016	0.0
C1R330	2005072017	0.0

The maximum 4-hour and 24-hour isohyets charts for Typhoon Haitang are given in Figures A16 and A17 below:

Table of Contents
Table of Contents
Table of Contents
Table of Contents

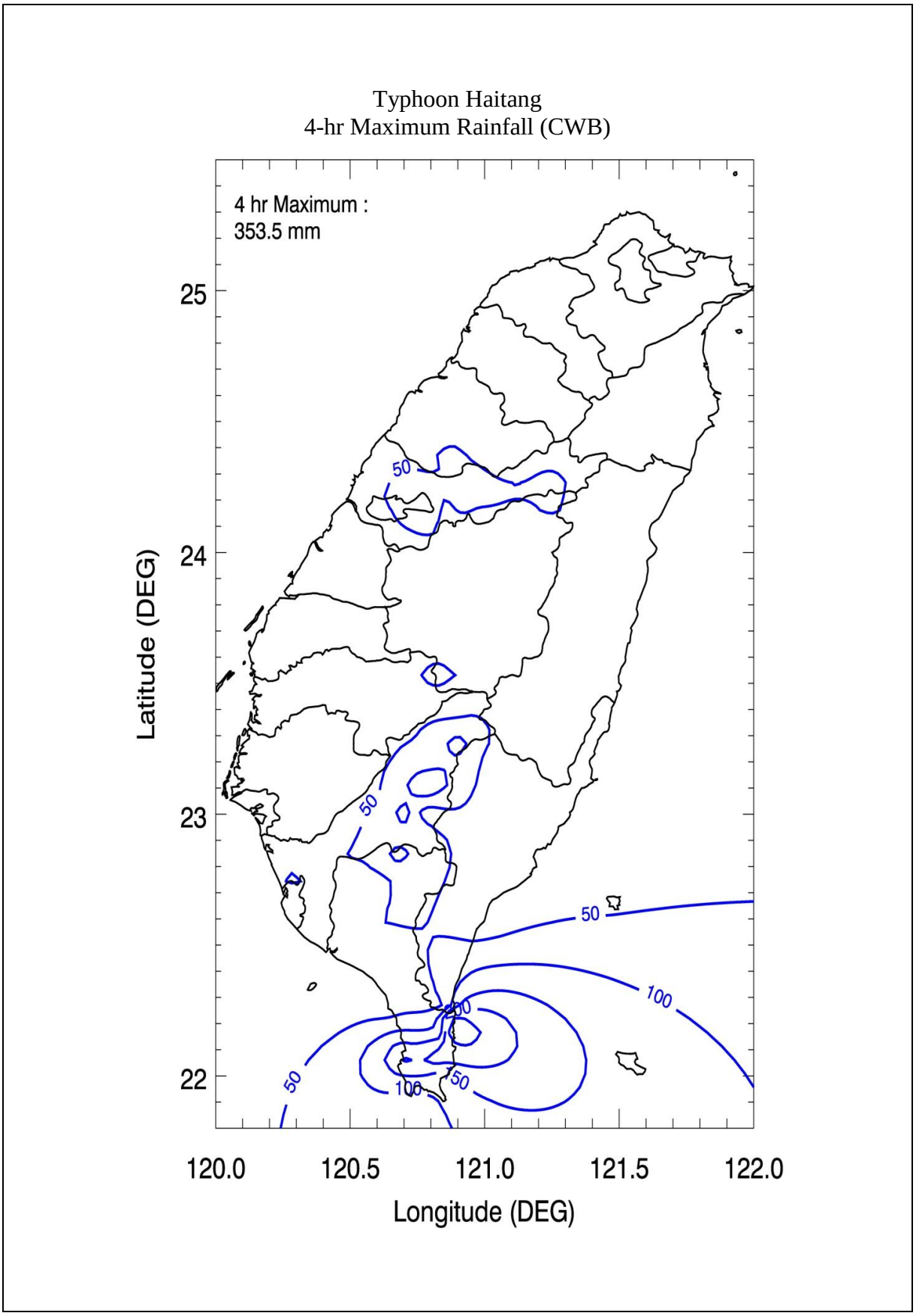

Figure A16 Isohyets Chart of 4-hour Rainfall for Typhoon Haitang

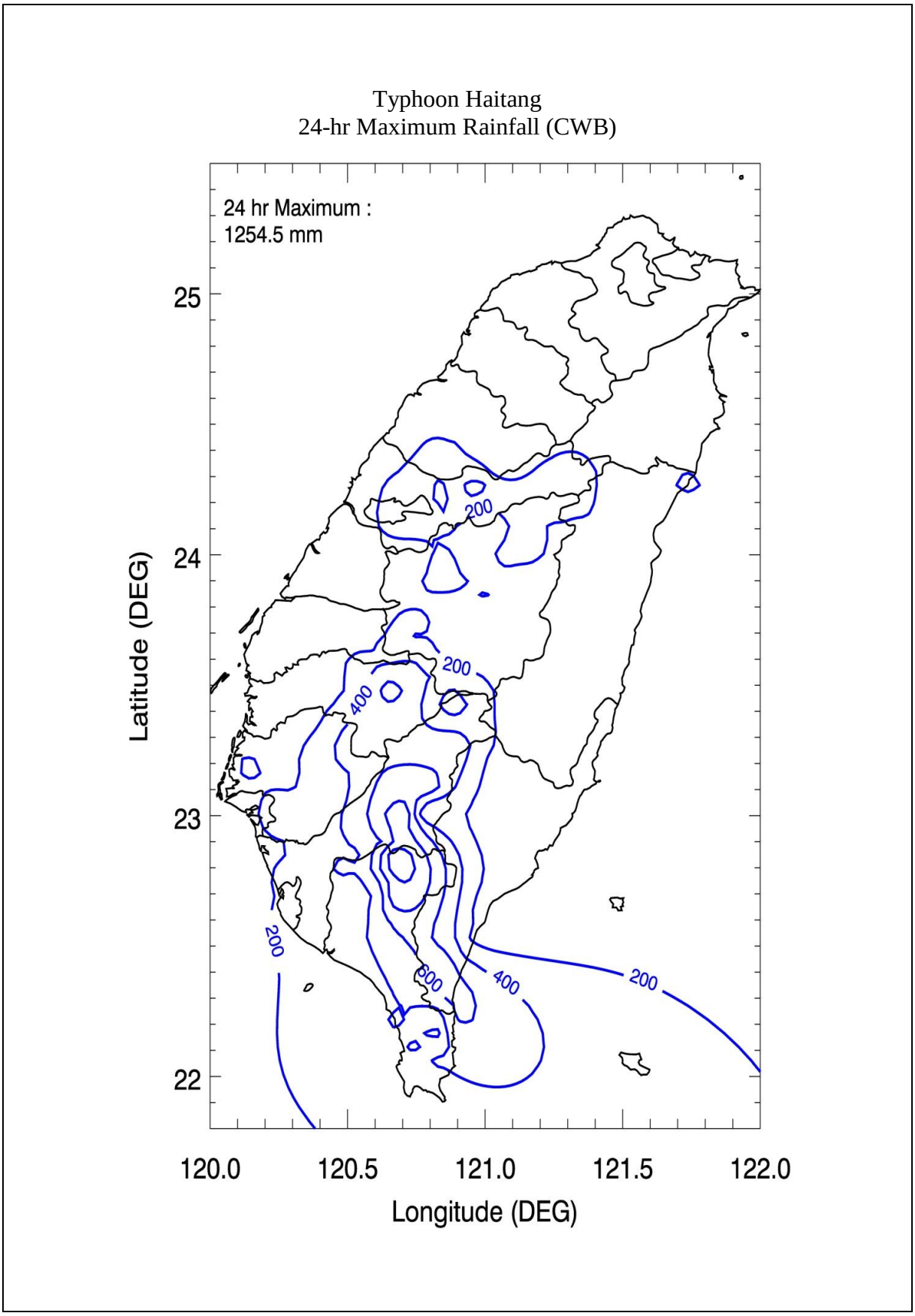

Figure A17 Isohyets Chart of 24-hour Rainfall for Typhoon Haitang

A.2.4 Typhoon Morakot

Typhoon Morakot (莫拉克颱風, Figure A18) 6-10 August 2009

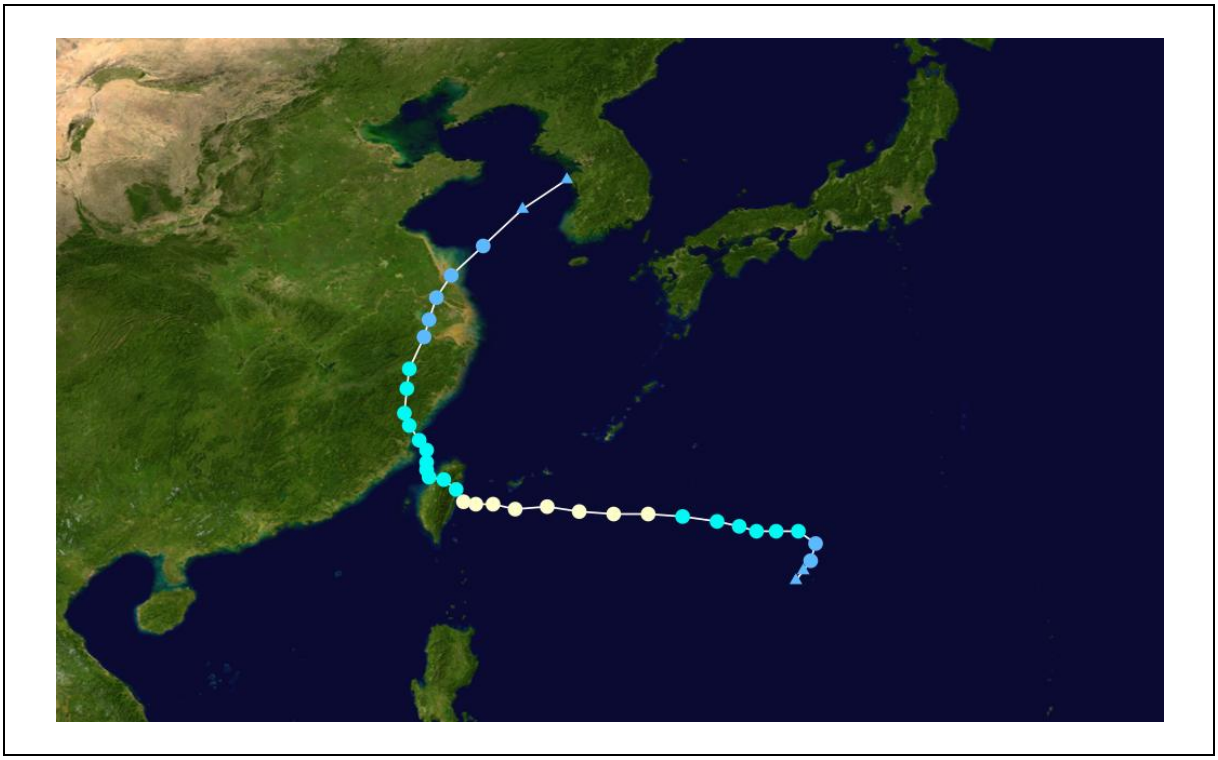

Figure A18 Typhoon Track for Morakot

Typhoon Morakot was the deadliest typhoon to impact Taiwan in recorded history. It formed early on 2 August, 2009 as an unnamed tropical depression. During that day the depression gradually developed before being upgraded to a tropical storm and assigned the name Morakot, by the Japan Meteorological Agency late on 3 August. The large system gradually intensified as it tracked westward towards Taiwan. Early on 7 August, the storm attained its peak intensity with winds of 140 km/h according to the Japan Meteorological Agency. Morakot weakened slightly before making landfall in central Taiwan later that day. Roughly 24 hours later, the storm emerged back over water into the Taiwan Strait and weakened to a severe tropical storm before making landfall in Mainland China on 9 August. The storm gradually weakened as it continued to slowly track inland. The remnants of the typhoon eventually dissipated on 11 August. (Wikipedia)

Although Morakot was only a moderate intensity typhoon at landfall, it was a large and relatively slow-moving storm, and it produced extreme rainfall over southern parts of Taiwan, reaching 1,404 mm in 24 hours at Weiliao Mountain in Pingtung County, and a three day storm total of 2,884 mm at Alishan, both of which are records for Taiwan and relatively close to world record values.

The maximum 4-hour and 24-hour isohyets charts for Typhoon Morakot are given in Figures A19 and A20 below:

Table of Contents
Table of Contents
Table of Contents
Table of Contents

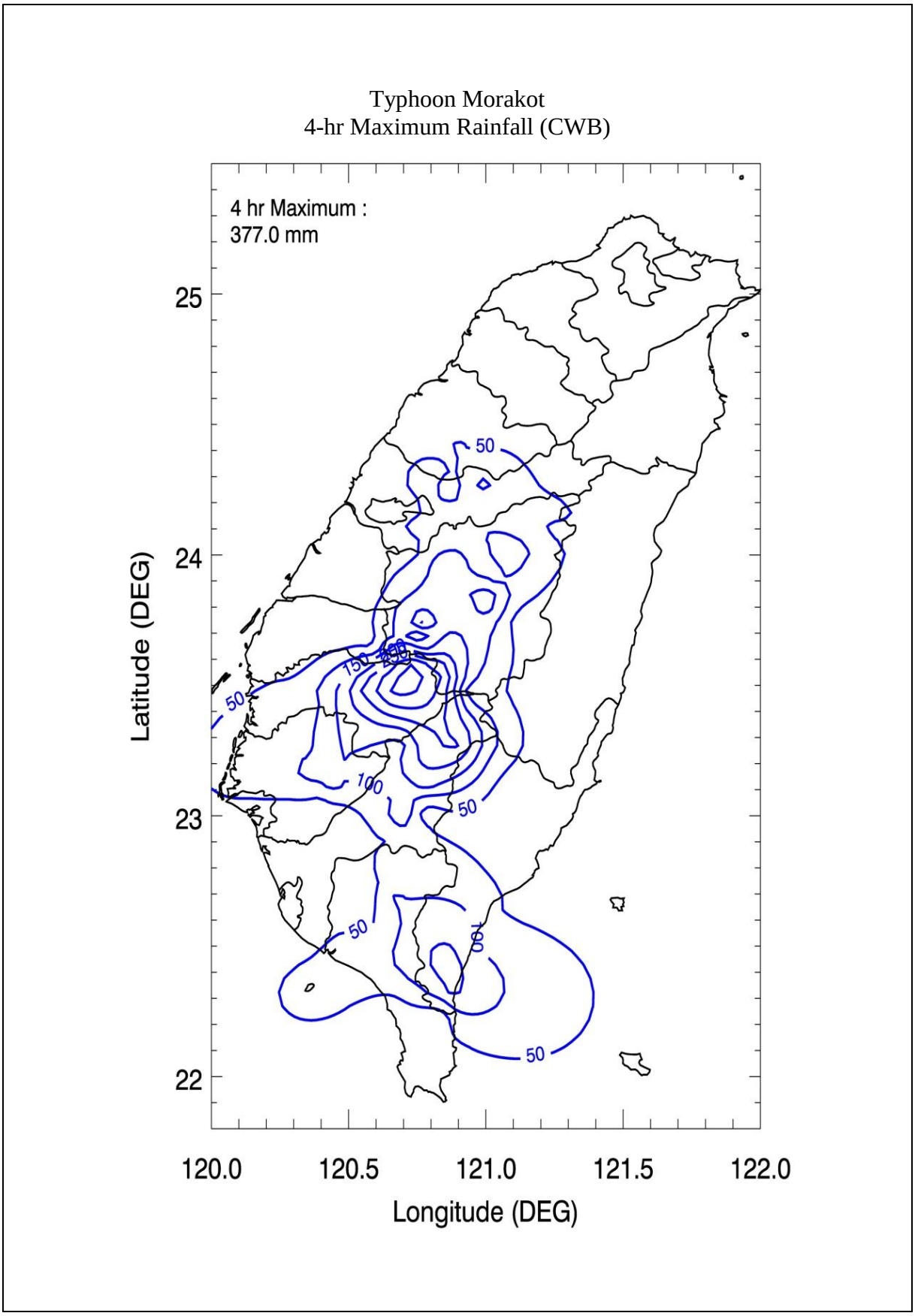

Figure A19 Isohyets Chart of 4-hour Rainfall for Typhoon Morakot

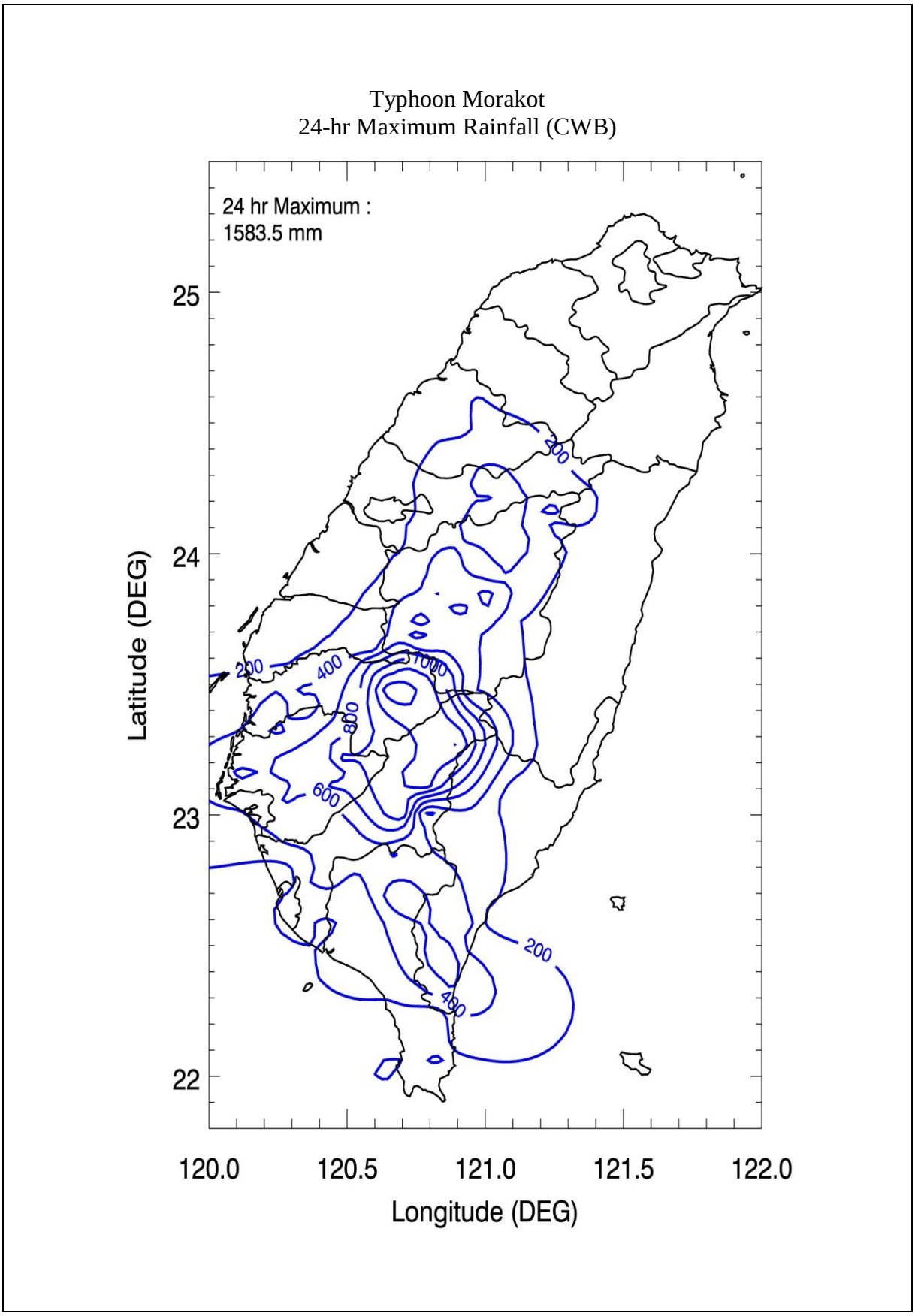

Figure A20 Isohyets Chart of 24-hour Rainfall for Typhoon Morakot

Appendix B

Period and Type of Historical Data

Contents

List of Tables

B.1 Period and Type of Historical Data

Table B1 Period and Type of Historical Data for Hong Kong

No.	Station ID	Period of Time	Type
Stations with data length of 27-year or more			
1 - 19	H01, H02, H03, H04, H05, H06, H07, H08, H09, H10, H12, H14, H15, H16, H17, H18, H19, H20, H21	Yr 1984 - 2010	5-min
20 - 27	K01, K02, K03, K04, K05, K06, K07, K08	Yr 1984 - 2010	5-min
28 - 42	N01, N02, N03, N04, N05, N06, N07, N08, N09, N10, N11, N12, N13, N14, N15	Yr 1984 - 2010	5-min
43	HKO	Yr 1987 - 2010	5-min
		Yr 1885 - 1986 (Yr 1940 - 1946 data missing for the World War II)	1-hr
Stations with data length less than 27 years			
44	H27	Yr 2000 - 2001	5-min
45 - 50	H23, H24, H25, H26, H28 H29	Yr 2000 - 2010	5-min
51 - 53	H11, H13, H22	Yr 1984 - 1999	5-min
54 - 55	K09, K10	Yr 2000 - 2010	5-min
56	N51	Yr 2003 - 2010	5-min
57	R33	Yr 1994 - 1999	5-min
58	R40	Yr 1996 - 2005	5-min
59 - 90	N19, N20, N21, N22, N23, N24, N25, N26, N27, N28, N29, N30, N31, N32, N33, N34, N35, N36, N37, N38, N39, N40, N41, N42, N43, N44, N45, N46, N47, N48, N49, N50	Yr 2000 - 2010	5-min
91 - 92	N17, N18	Yr 1992 - 2010	5-min
93	N16	Yr 1986 - 2010	5-min
94 - 95	R15, R16	Yr 1987 - 1999	5-min
96	R42	Yr 1993 - 2005	5-min
97	R19	Yr 1993 - 2010	5-min
98	R30	Yr 1987 - 2008	5-min
99 - 116	R01, R11, R12, R13, R14, R17, R18, R21, R22, R23, R24, R25, R26, R27, R28, R29, R31, R32	Yr 1987 - 2010	5-min

Table B2 Period and Type of Historical Data for South Guangdong

No.	Station	Period of Time (missing)	No. of Years	Type (Annual Maximum Series)
1	Nanaoyu 南澳圩	1973 - 2010	38	1, 3, 4, 6, 12, 24-hr
2	Shiyan 石岩	1974 - 2010	37	1, 3, 6, 12, 24-hr
3	Henggang 橫崗	1976 - 2010	35	1, 3, 6, 12, 24-hr
4	Xili 西瀝	1975 - 2010	36	1, 3, 6, 12, 24-hr
5	Changjiang 長江	1976 - 2010	35	1, 3, 6, 12, 24-hr
6	Songmushan 松木山	1976 - 2010 (1982, 1985)	33	1, 3, 6, 12, 24-hr
7	Zhuxiandong 竹仙洞	1982 - 2010 (1987)	28	1, 3, 6, 12, 24-hr
8	Shenzhen 深圳	1981 - 2010 (1990)	29	1, 3, 6, 12, 24-hr
9	Huiyang 惠陽	1971 - 2010 (1997)	39	1, 3, 4, 6, 12, 24-hr
10	Gangkou 港口	1975 - 2010	36	1, 3, 4, 6, 12, 24-hr
11	Nansha 南沙	1981 - 2010 (1982 - 1984)	27	1, 3, 6, 12, 24-hr
12	Yuechang 約場	1971 - 2010 (1990)	39	1, 3, 4, 6, 12, 24-hr

Table of Contents
Table of Contents
Table of Contents

Appendix C

Details of Historical Maxima of the 12 South Guangdong Stations

Contents

List of Tables

Table C1 Historical Maxima of Station Nanaoyu 南澳圩站

STCD	YR	HMXP1	HMXP3	HMXP4	HMXP6	HMXP12	HMXP24
81622640	1966	-	-	-	82.5	125.7	183.6
81622640	1973	45.5	95.5	-	110.2	178.3	226.4
81622640	1974	80.6	128.1	-	153.3	225.3	327.4
81622640	1975	51.7	100.8	-	113.7	135.8	245.4
81622640	1976	51.6	87.6	-	164.3	251.9	342.0
81622640	1977	41.0	70.1	-	74.3	78.5	120.5
81622640	1978	41.0	76.4	-	84.1	95.1	194.0
81622640	1979	54.8	107.8	-	172.1	239.1	313.5
81622640	1980	51.6	105.4	-	156.6	180.6	237.9
81622640	1981	62.7	138.9	-	180.3	190.1	193.2
81622640	1982	51.8	88.6	91.8	110.7	138.4	244.4
81622640	1983	72.2	123.2	129.1	143.5	165.2	193.3
81622640	1984	56.0	94.7	97.2	108.9	130.3	164.3
81622640	1985	57.5	83.5	83.9	114.6	171.6	187.3
81622640	1986	81.0	116.2	118.6	129.9	157.0	193.5
81622640	1987	79.0	105.2	107.1	117.2	154.1	182.1
81622640	1988	47.1	64.4	67.4	69.1	76.9	124.6
81622640	1989	64.0	100.0	105.6	142.2	189.6	226.0
81622640	1990	38.8	55.6	58.5	74.9	101.3	154.1
81622640	1991	60.6	90.1	103.8	116.4	136.7	173.5
81622640	1992	56.2	92.3	-	102.8	110.4	121.3
81622640	1993	64.5	110.4	118.9	134.5	212.9	254.8
81622640	1994	62.2	111.5	135.8	154.9	217.9	308.1
81622640	1995	73.2	149.6	175.4	230.9	261.1	400.8
81622640	1996	72.3	111.2	119.4	128.2	161.6	228.8
81622640	1997	80.5	152.9	165.3	170.9	193.6	207.1
81622640	1998	75.8	118.5	133.0	142.5	218.1	302.6
81622640	1999	72.1	165.0	213.2	267.9	320.7	443.6
81622640	2000	77.0	139.1	151.0	154.8	258.9	350.7
81622640	2001	113.8	243.4	262.5	299.2	342.4	595.0
81622640	2002	50.5	101.9	106.4	122.4	131.7	137.2
81622640	2003	86.3	155.4	169.1	215.0	237.9	339.3
81622640	2004	51.9	91.1	92.7	96.5	109.7	116.6
81622640	2005	63.1	80.0	83.2	106.9	195.2	337.9
81622640	2006	36.7	82.4	-	104.7	151.8	219.3
81622640	2007	58.5	116.0	-	148.0	148.0	149.5
81622640	2008	75.5	148.5	-	177.5	184.5	242.0
81622640	2009	60.0	82.5	-	131.0	142.5	165.5
81622640	2010	47.5	91.5	-	97.5	99.0	100.5

Table C2 Historical Maxima of Station Shiyan 石岩站

STCD	YR	HMXP1	HMXP3	HMXP6	HMXP12	HMXP24
81222600	1974	30.1	37.7	61.0	93.0	165.8
81222600	1975	60.5	118.9	140.0	143.5	143.5
81222600	1976	45.2	118.5	132.3	141.7	174.5
81222600	1977	39.4	65.4	75.8	84.0	105.8
81222600	1978	30.2	43.4	53.0	78.2	136.4
81222600	1979	42.1	55.6	94.0	147.7	168.5
81222600	1980	85.0	117.3	151.3	155.7	163.4
81222600	1981	43.1	75.0	84.9	92.8	212.5
81222600	1982	25.4	43.7	68.8	73.3	84.9
81222600	1983	71.9	109.3	128.0	145.6	181.1
81222600	1984	30.4	50.6	70.6	86.3	106.5
81222600	1985	40.4	56.6	90.7	118.7	146.3
81222600	1986	50.3	101.3	125.9	139.9	165.5
81222600	1987	98.0	202.5	301.4	340.0	340.2
81222600	1988	42.3	86.3	123.5	124.7	126.9
81222600	1989	30.3	81.7	142.1	247.3	343.2
81222600	1990	71.4	131.6	134.8	139.8	150.0
81222600	1991	88.5	97.7	97.7	110.3	112.8
81222600	1992	36.2	52.1	67.5	93.0	134.8
81222600	1993	59.2	97.5	132.8	136.7	159.2
81222600	1994	52.8	104.4	108.0	139.9	171.8
81222600	1995	53.9	69.9	95.9	109.2	115.2
81222600	1996	44.8	84.4	154.9	189.2	266.6
81222600	1997	38.5	80.6	99.9	138.6	145.4
81222600	1998	35.7	66.1	81.6	93.8	123.1
81222600	1999	45.6	58.0	61.6	80.7	127.5
81222600	2000	74.1	83.7	92.1	174.5	213.2
81222600	2001	78.2	97.2	97.2	115.5	138.3
81222600	2002	39.6	43.2	45.6	61.9	98.6
81222600	2003	38.5	82.8	94.0	134.0	195.3
81222600	2004	37.0	63.1	73.4	110.3	129.8
81222600	2005	53.2	97.8	166.7	203.5	251.8
81222600	2006	56.0	93.5	147.5	179.0	205.0
81222600	2007	69.5	78.5	83.5	107.0	107.0
81222600	2008	79.5	143.5	195.5	381.0	479.5
81222600	2009	46.0	87.5	121.0	144.0	169.0
81222600	2010	63.0	69.0	99.5	100.5	120.0

Table C3 Historical Maxima of Station Henggang 横岗站

STCD	YR	HMXP1	HMXP3	HMXP6	HMXP12	HMXP24
81221120	1976	71.8	161.4	182.9	197.1	201.6
81221120	1977	36.1	48.1	52.1	66.0	95.1
81221120	1978	26.3	37.4	43.3	80.9	88.7
81221120	1979	46.1	67.9	70.5	77.1	93.9
81221120	1980	56.7	62.1	72.5	74.6	103.6
81221120	1981	67.0	169.0	245.4	310.5	493.4
81221120	1982	50.8	62.7	66.1	68.6	74.8
81221120	1983	47.0	78.0	158.2	170.2	197.2
81221120	1984	65.7	102.7	125.6	146.8	161.1
81221120	1985	34.6	68.1	68.3	77.8	88.1
81221120	1986	47.1	64.1	95.5	112.6	154.0
81221120	1987	45.9	60.3	103.3	110.8	129.6
81221120	1988	59.6	66.1	83.5	133.2	139.7
81221120	1989	41.2	109.2	160.0	254.5	318.1
81221120	1990	63.0	73.7	73.9	76.5	89.3
81221120	1991	36.8	49.5	64.8	65.0	69.8
81221120	1992	43.3	51.9	80.2	113.5	157.1
81221120	1993	60.2	89.1	99.7	150.2	192.0
81221120	1994	80.9	86.0	113.7	135.3	135.7
81221120	1995	41.6	78.6	88.3	100.3	167.4
81221120	1996	60.6	117.7	144.2	182.4	189.8
81221120	1997	47.9	103.1	110.0	112.5	159.3
81221120	1998	72.4	104.6	144.6	160.4	160.6
81221120	1999	48.4	76.7	87.8	128.9	191.4
81221120	2000	68.5	88.5	97.9	98.4	165.7
81221120	2001	59.0	87.9	95.7	97.3	158.1
81221120	2002	59.0	81.0	81.5	81.5	81.5
81221120	2003	59.0	86.5	101.0	106.5	112.0
81221120	2004	74.5	86.5	124.0	148.0	167.5
81221120	2005	70.5	106.0	128.5	134.5	197.5
81221120	2006	48.5	110.5	149.5	183.0	221.5
81221120	2007	63.5	142.5	142.5	142.5	155.0
81221120	2008	58.5	167.5	193.5	256.0	291.0
81221120	2009	47.5	77.5	92.5	101.0	102.5
81221120	2010	77.5	118.5	162.5	163.0	163.0

Table C4 Historical Maxima of Station Xili 西瀝站

STCD	YR	HMXP1	HMXP3	HMXP6	HMXP12	HMXP24
81222720	1975	-	-	105.0	105.0	137.3
81222720	1976	-	49.8	73.5	112.3	191.2
81222720	1977	-	48.4	67.3	86.6	119.2
81222720	1978	36.1	44.9	45.4	61.3	81.0
81222720	1979	31.2	55.0	77.5	119.7	140.5
81222720	1980	52.3	103.5	126.3	198.0	215.8
81222720	1981	60.8	76.0	85.3	130.7	158.4
81222720	1982	31.0	44.5	51.3	90.7	110.8
81222720	1983	27.0	45.9	61.9	84.6	132.7
81222720	1984	35.3	59.8	68.5	86.5	119.0
81222720	1985	54.7	77.3	103.2	119.7	152.4
81222720	1986	40.0	60.6	78.3	89.2	140.7
81222720	1987	41.9	77.7	82.6	129.9	170.5
81222720	1988	49.5	86.0	116.0	145.2	155.2
81222720	1989	50.2	115.2	187.8	305.3	383.4
81222720	1990	29.3	43.8	51.1	52.3	54.7
81222720	1991	33.8	50.7	55.9	60.4	60.5
81222720	1992	59.4	110.5	136.4	163.7	170.4
81222720	1993	60.1	74.6	105.4	155.6	201.6
81222720	1994	36.5	82.2	120.2	194.8	227.6
81222720	1995	49.5	97.9	174.1	191.4	223.8
81222720	1996	59.3	66.9	67.0	101.5	101.5
81222720	1997	37.0	64.3	84.4	122.1	145.2
81222720	1998	88.8	137.8	170.8	176.8	176.8
81222720	1999	38.3	65.0	86.0	102.4	190.8
81222720	2000	51.1	96.6	163.9	267.7	312.8
81222720	2001	61.9	86.2	106.5	139.0	147.8
81222720	2002	44.4	82.9	82.9	82.9	94.9
81222720	2003	40.6	72.4	83.1	133.0	237.0
81222720	2004	52.3	68.5	93.0	131.2	161.8
81222720	2005	55.0	126.2	181.4	226.9	266.0
81222720	2006	48.0	75.5	98.0	126.0	164.5
81222720	2007	45.0	65.5	70.0	97.0	119.5
81222720	2008	68.2	128.3	170.4	224.8	292.8
81222720	2009	81.0	105.5	123.5	140.5	151.5
81222720	2010	46.5	74.0	96.5	97.0	100.5

Table C5 Historical Maxima of Station Changjian 長江站

STCD	YR	HMXP1	HMXP3	HMXP6	HMXP12	HMXP24
81320400	1976	-	-	135.7	171.8	214.7
81320400	1977	-	-	107.6	152.0	175.8
81320400	1978	-	-	71.0	103.5	126.5
81320400	1979	-	-	82.7	110.3	125.5
81320400	1980	-	-	101.1	129.1	129.1
81320400	1981	-	-	101.1	149.7	183.6
81320400	1982	47.9	60.6	70.9	91.5	110.1
81320400	1983	40.8	46.9	58.3	105.2	129.5
81320400	1984	49.9	59.0	95.3	102.3	109.5
81320400	1985	43.5	57.0	66.6	106.3	146.0
81320400	1986	41.0	55.5	82.2	131.5	216.8
81320400	1987	84.8	129.1	184.3	198.8	242.2
81320400	1988	43.6	102.8	114.6	123.3	164.5
81320400	1989	53.7	98.1	159.8	222.7	299.2
81320400	1990	78.0	181.0	223.2	223.2	233.4
81320400	1991	35.3	68.0	79.9	83.3	92.4
81320400	1992	31.7	62.1	104.2	121.8	164.4
81320400	1993	60.6	126.2	171.2	207.2	320.6
81320400	1994	62.3	120.0	170.7	215.2	235.2
81320400	1995	22.2	54.0	90.0	112.0	142.0
81320400	1996	67.8	89.7	99.3	143.0	201.0
81320400	1997	33.2	69.1	91.1	121.8	166.6
81320400	1998	52.3	105.8	145.4	193.2	202.5
81320400	1999	58.2	83.8	141.0	192.8	221.8
81320400	2000	48.4	71.0	119.0	171.7	247.4
81320400	2001	45.2	96.2	117.8	146.9	185.0
81320400	2002	42.0	84.0	147.5	171.0	233.5
81320400	2003	71.5	136.5	151.0	249.0	351.5
81320400	2004	43.5	72.5	92.0	161.0	195.5
81320400	2005	39.5	92.5	102.5	103.0	113.0
81320400	2006	48.5	122.0	167.5	194.0	199.0
81320400	2007	41.0	53.5	64.5	80.0	106.5
81320400	2008	53.0	115.0	154.0	177.0	227.0
81320400	2009	53.0	92.5	121.5	143.5	159.0
81320400	2010	50.5	89.5	112.5	128.0	130.5

Table C6 Historical Maxima of Station Songmushan 松木山站

STCD	YR	HMXP1	HMXP3	HMXP6	HMXP12	HMXP24
81221080	1976	68.3	95.5	144.6	164.3	218.9
81221080	1977	55.3	98.6	128.7	226.5	260.7
81221080	1978	70.7	94.5	98.8	98.8	113.4
81221080	1979	38.7	65.6	70.1	100.3	126.4
81221080	1980	45.4	78.6	116.2	132.8	140.2
81221080	1981	60.9	125.6	170.6	204.1	255.5
81221080	1982	-	-	-	-	-
81221080	1983	64.7	95.8	104.5	119.9	140.7
81221080	1984	53.2	89.3	95.4	104.6	104.7
81221080	1985	-	-	-	-	-
81221080	1986	46.5	74.7	78.6	109.1	179.5
81221080	1987	48.1	85.9	94.6	128.8	164.0
81221080	1988	50.4	81.2	105.9	132.5	146.1
81221080	1989	38.5	60.9	65.5	85.5	135.9
81221080	1990	33.5	49.1	51.6	58.3	63.2
81221080	1991	40.3	67.7	120.9	121.6	121.6
81221080	1992	75.6	97.2	98.6	111.5	131.1
81221080	1993	52.4	118.1	150.7	200.0	263.4
81221080	1994	52.4	85.4	107.0	129.1	216.8
81221080	1995	34.6	48.6	70.8	104.0	132.5
81221080	1996	44.6	67.0	93.0	120.7	185.4
81221080	1997	66.2	104.4	104.6	118.1	146.0
81221080	1998	68.6	80.5	117.9	130.5	145.4
81221080	1999	67.2	118.1	181.8	233.3	296.1
81221080	2000	82.7	117.6	133.9	134.8	142.3
81221080	2001	41.3	82.8	93.2	94.4	121.2
81221080	2002	71.0	71.5	74.0	74.0	132.0
81221080	2003	70.0	70.5	90.5	130.5	178.0
81221080	2004	31.5	55.5	84.0	108.5	122.5
81221080	2005	58.0	98.0	135.5	170.5	203.0
81221080	2006	76.5	191.0	238.5	324.0	339.5
81221080	2007	55.0	85.5	109.0	117.5	160.5
81221080	2008	47.5	108.5	150.0	221.5	270.0
81221080	2009	41.0	69.0	97.0	125.0	140.0
81221080	2010	59.5	70.0	80.0	81.5	96.0

Table C7 Historical Maxima of Station Zhuxiandong 竹仙洞站

STCD	YR	HMXP1	HMXP3	HMXP6	HMXP12	HMXP24
81320700	1976	-	-	-	-	-
81320700	1977	-	-	-	-	-
81320700	1978	-	-	-	-	-
81320700	1979	-	-	-	-	-
81320700	1980	-	-	-	-	-
81320700	1981	-	-	-	-	-
81320700	1982	90.5	197.5	244.1	272.3	522.7
81320700	1983	94.2	150.7	226.4	289.5	294.3
81320700	1984	93.1	169.5	194.3	206.8	208.6
81320700	1985	45.8	90.6	100.5	149.3	193.4
81320700	1986	92.1	184.9	198.2	230.9	275.2
81320700	1987	-	-	-	-	-
81320700	1988	73.8	85.3	134.5	240.4	276.6
81320700	1989	117.8	193.6	235.5	236.9	276.5
81320700	1990	23.3	32.2	43.9	54.2	64.1
81320700	1991	87.3	103.7	111.0	112.0	151.6
81320700	1992	59.5	94.9	111.0	158.3	177.2
81320700	1993	56.1	98.7	128.8	187.5	215.0
81320700	1994	86.5	190.4	308.9	437.3	505.9
81320700	1995	89.2	174.7	207.1	227.3	263.4
81320700	1996	170.4	369.6	436.5	489.7	519.9
81320700	1997	123.5	189.0	203.1	211.6	218.4
81320700	1998	44.5	93.9	137.8	171.5	217.7
81320700	1999	57.7	110.8	126.6	188.4	242.6
81320700	2000	99.2	230.6	381.5	411.8	467.4
81320700	2001	73.6	114.7	148.5	202.8	232.1
81320700	2002	65.0	129.5	150.0	185.0	187.0
81320700	2003	64.0	167.0	198.0	210.0	266.0
81320700	2004	58.0	99.5	143.0	178.5	192.5
81320700	2005	51.5	114.0	197.0	209.5	213.0
81320700	2006	56.0	139.0	168.5	179.0	181.0
81320700	2007	45.0	66.0	89.5	127.5	168.0
81320700	2008	46.5	100.5	143.0	206.5	291.0
81320700	2009	69.5	134.5	176.5	191.5	214.5
81320700	2010	69.0	120.5	141.5	176.5	196.5

Table C8 Historical Maxima of Station Shenzhen 深圳站

STCD	YR	HMXP1	HMXP3	HMXP4	HMXP6	HMXP12	HMXP24
81222740	1976	-	-	-	-	-	-
81222740	1977	-	-	-	-	-	-
81222740	1978	-	-	-	-	-	-
81222740	1979	-	-	-	-	-	-
81222740	1980	-	-	-	-	-	-
81222740	1981	47.5	82.8	97.2	102.6	105.8	141.8
81222740	1982	92.6	126.1	129.8	183.6	200.3	220.2
81222740	1983	56.6	77.8	78.0	86.6	106.6	133.9
81222740	1984	47.9	62.9	75.1	83.7	106.3	153.1
81222740	1985	39.9	47.9	57.6	65.2	115.6	145.8
81222740	1986	72.0	79.9	81.8	86.5	106.6	177.4
81222740	1987	53.1	75.5	75.6	88.0	92.5	123.8
81222740	1988	50.6	105.2	125.4	130.2	176.9	219.1
81222740	1989	53.4	104.1	105.2	122.6	182.1	237.5
81222740	1990	-	-	-	-	-	-
81222740	1991	66.7	74.2	96.2	130.2	161.1	162.2
81222740	1992	42.1	78.6	-	108.0	136.7	154.2
81222740	1993	73.5	159.0	181.6	198.3	262.5	345.4
81222740	1994	96.8	157.4	167.7	225.2	306.2	386.2
81222740	1995	53.3	92.9	98.1	109.9	139.8	167.3
81222740	1996	75.7	96.5	96.5	96.5	118.8	155.1
81222740	1997	40.4	61.8	72.2	98.7	179.9	231.9
81222740	1998	64.0	148.9	177.1	226.8	278.7	280.7
81222740	1999	68.4	169.6	183.0	219.2	276.4	350.0
81222740	2000	66.6	126.6	167.2	209.5	255.1	292.6
81222740	2001	66.1	108.0	115.8	149.5	197.2	212.3
81222740	2002	61.7	79.0	83.9	88.6	100.7	130.0
81222740	2003	60.0	92.8	104.9	112.3	151.2	193.6
81222740	2004	81.7	82.9	83.4	87.2	115.0	115.0
81222740	2005	52.5	101.3	119.6	136.9	178.0	244.0
81222740	2006	57.0	81.5	-	107.5	129.5	166.0
81222740	2007	49.0	83.0	-	93.5	142.5	180.5
81222740	2008	58.5	131.5	-	170.0	201.0	278.5
81222740	2009	35.5	57.0	-	78.5	119.5	147.0
81222740	2010	72.0	104.5	-	141.5	173.5	184.0

Table C9 Historical Maxima of Station Huiyan 惠陽站

STCD	YR	HMXP1	HMXP3	HMXP4	HMXP6	HMXP12	HMXP24
81124700	1971	36.0	60.0	64.0	71.0	131.0	155.0
81124700	1972	65.1	72.6	73.5	73.7	92.8	155.4
81124700	1973	59.5	102.3	107.7	114.0	121.2	243.5
81124700	1974	41.5	77.4	92.7	120.6	178.7	243.3
81124700	1975	48.0	70.8	73.7	78.6	125.4	166.9
81124700	1976	53.6	71.9	76.3	81.9	120.2	180.2
81124700	1977	49.0	64.3	68.4	89.1	105.4	106.0
81124700	1978	66.3	81.7	90.5	100.2	101.3	103.1
81124700	1979	67.8	160.9	186.9	218.4	329.2	403.8
81124700	1980	68.8	90.6	94.5	106.4	168.8	181.6
81124700	1981	46.7	58.8	61.5	95.9	101.5	131.3
81124700	1982	33.3	51.9	56.7	65.1	77.1	113.9
81124700	1983	49.0	93.8	111.2	131.1	158.6	176.7
81124700	1984	58.4	78.7	84.8	101.7	128.6	179.1
81124700	1985	41.9	55.1	61.6	94.3	129.8	184.0
81124700	1986	56.6	93.2	102.3	117.4	131.7	154.5
81124700	1987	54.2	90.5	94.7	98.9	127.9	135.2
81124700	1988	71.8	119.5	134.7	149.2	176.8	192.6
81124700	1989	35.8	47.2	51.5	64.1	68.6	105.4
81124700	1990	72.0	104.4	106.0	132.1	139.5	139.8
81124700	1991	63.6	99.4	105.6	119.8	145.6	150.3
81124700	1992	34.3	52.2	59.2	61.1	83.2	105.7
81124700	1993	39.7	95.4	106.5	117.6	157.5	187.4
81124700	1994	46.8	51.1	51.4	54.1	54.7	80.7
81124700	1995	36.9	40.6	45.8	50.6	68.6	86.7
81124700	1996	55.2	65.1	71.1	97.8	110.5	111.4
81124700	1997	-	-	-	-	-	-
81124700	1998	57.2	90.2	90.5	94.4	102.2	134.5
81124700	1999	45.6	79.6	94.6	110.2	191.3	221.2
81124700	2000	72.8	111.8	116.8	130.9	169.8	183.4
81124700	2001	75.4	94.7	102.5	124.2	146.3	157.2
81124700	2002	34.3	40.7	41.4	57.6	78.6	111.7
81124700	2003	47.0	63.5	77.0	86.0	96.0	110.5
81124700	2004	62.5	84.0	88.0	90.5	90.5	107.0
81124700	2005	77.0	131.5	137.0	158.5	188.5	217.0
81124700	2006	75.0	113.0	-	126.5	220.5	271.5
81124700	2007	73.5	81.5	-	91.5	120.5	147.5
81124700	2008	37.0	68.0	-	93.0	119.0	230.0
81124700	2009	54.5	70.0	-	72.0	86.5	113.5
81124700	2010	36.0	50.5	-	63.5	78.0	95.5

Table C10 Historical Maxima of Station Gangkou 港口站

STCD	YR	HMXP1	HMXP3	HMXP4	HMXP6	HMXP12	HMXP24
81622540	1975	102.5	147.7	148.0	152.9	174.8	229.1
81622540	1976	35.2	68.6	82.3	99.7	154.4	207.4
81622540	1977	50.7	79.5	88.4	100.8	113.9	114.0
81622540	1978	62.4	80.3	98.2	101.2	104.4	113.5
81622540	1979	44.8	79.3	83.8	100.2	160.9	232.0
81622540	1980	59.4	91.3	114.7	138.1	161.7	199.8
81622540	1981	74.7	93.6	94.8	104.0	116.0	145.7
81622540	1982	51.1	79.7	82.7	112.1	117.3	213.0
81622540	1983	57.7	82.9	89.9	109.5	154.0	164.9
81622540	1984	33.6	55.0	73.3	78.9	84.0	97.2
81622540	1985	41.4	64.5	64.5	97.8	155.1	179.5
81622540	1986	68.0	107.2	107.2	110.6	152.7	246.9
81622540	1987	78.2	192.1	219.1	291.4	341.5	343.2
81622540	1988	70.7	118.5	137.0	152.4	174.6	191.2
81622540	1989	44.3	47.4	480.0	50.8	65.9	94.0
81622540	1990	85.4	126.1	133.7	145.4	151.8	233.4
81622540	1991	61.9	79.9	81.3	81.5	107.2	134.2
81622540	1992	48.0	104.9	-	122.8	126.4	132.5
81622540	1993	65.8	90.3	126.4	140.1	192.6	274.1
81622540	1994	52.8	92.1	113.2	118.5	121.8	122.7
81622540	1995	129.8	257.5	287.3	357.4	390.3	481.4
81622540	1996	65.3	96.0	102.5	114.0	126.9	146.2
81622540	1997	66.4	112.0	116.3	117.3	170.8	245.0
81622540	1998	53.1	113.8	119.6	131.6	169.0	222.2
81622540	1999	89.8	206.9	226.8	244.0	259.2	264.9
81622540	2000	61.2	110.7	130.8	162.6	188.7	273.1
81622540	2001	57.0	105.7	124.1	151.0	212.0	245.3
81622540	2002	70.1	92.6	97.2	110.3	145.8	151.1
81622540	2003	57.7	90.2	96.8	104.4	107.3	149.8
81622540	2004	68.5	70.0	80.5	107.0	107.0	107.0
81622540	2005	73.5	194.5	213.0	221.5	233.5	233.5
81622540	2006	76.0	147.0	-	231.0	297.5	312.5
81622540	2007	39.0	63.4	-	86.2	91.3	117.3
81622540	2008	45.5	87.5	-	110.5	157.0	259.0
81622540	2009	39.5	51.0	-	63.5	68.5	103.5
81622540	2010	41.0	96.0	-	172.0	203.5	258.5

Table C11 Historical Maxima of Station Nansha 南沙站

STCD	YR	HMXP1	HMXP3	HMXP6	HMXP12	HMXP24
81322420	1976	-	-	-	-	-
81322420	1977	-	-	-	-	-
81322420	1978	-	-	-	-	-
81322420	1979	-	-	-	-	-
81322420	1980	-	-	-	-	-
81322420	1981	59.2	125.8	206.3	251.5	418.6
81322420	1982	-	-	-	-	-
81322420	1983	-	-	-	-	-
81322420	1984	-	-	-	-	-
81322420	1985	63.0	94.2	109.2	124.6	128.6
81322420	1986	71.5	121.0	139.0	189.2	257.2
81322420	1987	130.4	132.5	133.2	150.4	254.0
81322420	1988	84.6	109.2	117.2	118.4	119.3
81322420	1989	70.4	80.0	91.4	105.2	177.7
81322420	1990	29.7	38.2	44.0	47.7	76.9
81322420	1991	32.9	65.0	97.1	105.9	109.2
81322420	1992	49.8	60.0	71.2	106.5	143.4
81322420	1993	39.2	84.8	134.5	187.1	238.4
81322420	1994	44.7	54.7	67.8	100.9	131.2
81322420	1995	62.2	126.4	198.3	224.7	256.9
81322420	1996	78.5	129.7	146.7	207.0	208.4
81322420	1997	60.9	90.6	122.4	130.4	149.4
81322420	1998	68.0	108.0	162.8	182.5	191.0
81322420	1999	48.4	72.0	96.4	117.3	159.8
81322420	2000	40.8	55.6	75.7	89.9	118.2
81322420	2001	57.6	88.8	119.4	129.5	149.0
81322420	2002	52.0	66.8	68.8	69.4	77.6
81322420	2003	60.5	68.0	78.0	116.5	144.0
81322420	2004	51.0	79.5	129.0	188.5	236.5
81322420	2005	31.5	69.0	73.0	85.5	111.5
81322420	2006	64.5	118.0	157.5	206.0	247.0
81322420	2007	43.5	65.0	65.5	85.5	86.5
81322420	2008	47.5	101.5	188.5	269.0	293.0
81322420	2009	38.5	58.0	77.0	91.0	96.0
81322420	2010	65.5	81.0	88.5	89.0	102.0

Table C12 Historical Maxima of Station Yuechang 約場站

STCD	YR	HMXP1	HMXP3	HMXP4	HMXP6	HMXP12	HMXP24
81124540	1971	65.0	88.0	89.0	116.0	118.0	147.0
81124540	1972	68.0	130.0	153.0	163.0	199.0	223.0
81124540	1973	82.1	104.8	110.3	140.9	175.4	202.2
81124540	1974	63.0	91.8	94.8	96.7	97.5	134.4
81124540	1975	64.8	65.5	88.8	107.4	162.2	201.1
81124540	1976	59.7	83.5	91.7	96.3	126.9	197.3
81124540	1977	47.7	73.4	80.9	115.0	195.2	230.9
81124540	1978	62.5	74.3	77.6	77.6	96.2	159.6
81124540	1979	70.7	86.3	119.1	149.7	200.4	205.5
81124540	1980	101.1	186.2	209.1	231.2	268.1	285.8
81124540	1981	63.5	145.7	168.7	179.8	210.6	213.4
81124540	1982	47.3	79.6	95.0	95.5	97.3	114.1
81124540	1983	50.8	86.8	87.3	88.7	88.8	130.5
81124540	1984	90.3	171.5	178.4	203.7	244.4	275.5
81124540	1985	51.9	97.2	127.9	131.9	133.3	161.1
81124540	1986	72.1	120.8	139.4	171.8	208.9	328.9
81124540	1987	57.8	103.2	105.8	108.2	123.4	123.7
81124540	1988	86.4	119.7	121.6	124.9	128.8	129.2
81124540	1989	31.7	62.5	62.5	71.2	105.9	125.0
81124540	1990	-	-	-	-	-	-
81124540	1991	-	-	-	75.4	96.3	96.3
81124540	1992	-	-	-	113.0	113.0	129.1
81124540	1993	-	-	-	62.0	124.0	237.4
81124540	1994	-	-	-	84.5	84.5	135.0
81124540	1995	-	-	-	143.0	143.0	167.0
81124540	1996	-	-	-	36.3	72.5	145.0
81124540	1997	-	-	-	104.0	104.0	191.0
81124540	1998	-	-	-	88.6	91.3	97.6
81124540	1999	-	-	-	81.0	81.0	106.0
81124540	2000	-	-	-	93.4	113.8	126.3
81124540	2001	-	-	-	80.7	80.7	125.6
81124540	2002	47.5	111.0	-	125.0	145.0	171.0
81124540	2003	39.0	58.5	-	76.5	103.0	168.0
81124540	2004	47.0	63.5	-	78.5	113.5	139.5
81124540	2005	67.5	106.0	-	112.5	135.0	173.5
81124540	2006	43.5	70.0	-	83.0	136.0	149.5
81124540	2007	66.5	86.5	-	93.5	133.0	143.5
81124540	2008	42.0	96.0	-	126.0	176.0	261.0
81124540	2009	48.0	79.0	-	114.5	126.0	162.5
81124540	2010	78.0	103.0	-	125.5	165.5	220.5

Table of Contents
Table of Contents
Table of Contents

Appendix D

Calculation for Statistical Estimate of 24-hour PMP

Contents

List of Tables

D.1 Sorted Statistical Estimation of 24-hour PMP

Statistical estimation of 24-hour PMP for Hong Kong and South Guangdong are recorded in the following tables:

Table D1 24-hour Statistical Estimation of PMP for Hong Kong

Hong Kong 24-hr

Station	Data n (year)	Xm	$\bar{X}_{n-1}$	S_{n-1}	$\bar{X}_n$	S_n	$C_v = \frac{S_n}{\bar{X}_n}$	Adjusted mean $(1+\frac{3C_{vm}}{\sqrt{n}})*\bar{X}_n$	$K_m = \frac{X_m - \bar{X}_{n-1}}{S_{n-1}}$	$\Phi_m = \frac{X_m - \bar{X}_n}{S_n}$	$\Phi_m^2 + 2$	$n \geq (\Phi_m^2 + 2)$	required n_i when $K_m --> \phi_m$	
N14	27	956	302.8846	119.5233	327.0741	171.8571	0.5254	426.2958	5.4643	3.6596	15.3926	√	89	
~~N09~~	~~27~~	~~800~~	~~236.9231~~	~~78.1749~~	~~257.7778~~	~~132.7368~~	~~0.5149~~	~~334.4134~~	~~7.2028~~	~~4.0849~~	~~18.6868~~	~~√~~	~~108~~	(Out)
HK0	119	697.1	228.7708	88.8074	220.3972	98.2743	0.4459	247.7708	5.2735	4.8507	25.5296	√	147	
N02	27	587.5	240.2115	82.8633	253.0741	105.2105	0.4157	313.8174	4.1911	3.1786	12.1037	√	70	
N01	27	570	256.3462	92.8217	267.9630	109.2161	0.4076	331.0189	3.3791	2.7655	9.6480	√	56	
~~N15~~	~~27~~	~~562~~	~~221.0577~~	~~58.6060~~	~~233.6852~~	~~87.2228~~	~~0.3732~~	~~284.0433~~	~~5.8175~~	~~3.7641~~	~~16.1684~~	~~√~~	~~93~~	(Out)
K02	27	508	248.6538	95.2023	258.2593	105.8584	0.4099	319.3767	2.7242	2.3592	7.5658	√	43	
N06	27	508	251.8462	92.0211	261.3333	102.8220	0.3935	320.6976	2.7836	2.3990	7.7550	√	45	
K06	27	506.5	235.1731	84.6223	245.2222	98.0414	0.3998	301.8265	3.2063	2.6650	9.1021	√	52	
H01	27	496	212.9231	80.5872	223.4074	95.9812	0.4296	278.8222	3.5127	2.8401	10.0660	√	58	
N10	27	492	228.0769	86.7214	237.8519	99.0513	0.4164	295.0392	3.0433	2.5658	8.5834	√		
H17	27	486	242.1538	78.4842	251.1852	90.1394	0.3589	303.2272	3.1069	2.6050	8.7861	√		
K04	27	484.5	238.2115	75.1141	247.3333	87.5883	0.3541	297.9025	3.2789	2.7077	9.3319	√		
H02	27	483.5	230.9038	85.0873	240.2593	96.5636	0.4019	296.0103	2.9687	2.5190	8.3452	√		
H04	27	477	247.7308	84.9175	256.2222	94.2362	0.3678	310.6295	2.6999	2.3428	7.4888	√		
K07	27	473.5	246.0192	91.9384	254.4444	100.2205	0.3939	312.3068	2.4743	2.1857	6.7774	√		
N04	27	470.5	228.2308	76.2177	237.2037	88.0885	0.3714	288.0616	3.1786	2.6484	9.0142	√		
N08	27	468.5	236.5385	71.2025	245.1296	82.8711	0.3381	292.9753	3.2578	2.6954	9.2651	√		
H08	27	468	239.0000	81.7675	247.4815	91.4933	0.3697	300.3052	2.8006	2.4102	7.8091	√		
H16	27	468	240.7500	76.3937	249.1667	86.7423	0.3481	299.2474	2.9747	2.5228	8.3645	√		
N11	27	467.5	214.7308	73.9788	224.0926	87.3427	0.3898	274.5199	3.4168	2.7868	9.7663	√		
N03	27	466	238.6923	80.2732	247.1111	90.0533	0.3644	299.1034	2.8317	2.4307	7.9081	√		
H12	27	465	248.8462	80.3533	256.8519	89.0999	0.3469	308.2937	2.6900	2.3361	7.4575	√		
H14	27	460	207.5000	51.2855	216.8519	69.9313	0.3225	257.2267	4.9234	3.4770	14.0892	√		
N12	27	458.5	203.2308	77.6378	212.6852	90.6047	0.4260	264.9958	3.2880	2.7130	9.3606	√		
H06	27	457.5	238.8654	84.2336	246.9630	92.6974	0.3753	300.4818	2.5956	2.2712	7.1585	√		
H10	27	457.5	245.7500	81.0894	253.5926	89.3490	0.3523	305.1783	2.6113	2.2821	7.2082	√		
N13	27	452	235.7308	64.6341	243.7407	75.8235	0.3111	287.5174	3.3461	2.7466	9.5440	√		
K01	27	447.5	231.0192	87.9140	239.0370	95.7461	0.4005	294.3160	2.4624	2.1772	6.7404	√		
H09	27	433	250.0769	82.1370	256.8519	87.8994	0.3422	307.6006	2.2270	2.0040	6.0159	√		
H07	27	432	232.0000	78.9277	239.4074	86.4376	0.3610	289.3122	2.5340	2.2281	6.9645	√		
K03	27	426	227.5577	84.6425	234.9074	91.3635	0.3889	287.6561	2.3445	2.0916	6.3746	√		
H03	27	424	208.7885	67.2277	216.7593	77.8533	0.3592	261.7079	3.2012	2.6619	9.0859	√		
K05	27	420	227.6538	73.7632	234.7778	81.2527	0.3461	281.6891	2.6076	2.2796	7.1965	√		
N05	27	419.5	211.4615	72.7878	219.1667	81.8367	0.3734	266.4151	2.8582	2.4480	7.9925	√		
H19	27	419	226.4038	69.4775	233.5370	77.5583	0.3321	278.3153	2.7721	2.3913	7.7182	√		
H18	27	410.5	231.9231	67.8592	238.5370	74.8923	0.3140	281.7762	2.6316	2.2961	7.2722	√		
N07	27	399.5	204.2885	93.5358	211.5185	99.1153	0.4686	268.7427	2.0870	1.8966	5.5971	√		
H21	27	395.5	204.4615	64.8440	211.5370	73.4487	0.3472	253.9427	2.9461	2.5046	8.2733	√		
K08	27	390	224.0769	76.8099	230.2222	81.8076	0.3553	277.4539	2.1602	1.9531	5.8146	√		
H05	27	388.5	223.2308	70.3736	229.3519	75.9842	0.3313	273.2213	2.3485	2.0945	6.3869	√		
H15	27	385.5	210.0192	54.6760	216.5185	63.3639	0.2926	253.1017	3.2095	2.6668	9.1120	√		
H20	27	355.5	205.1538	65.1189	210.7222	70.1040	0.3327	251.1968	2.3088	2.0652	6.2650	√		
Maximum							0.5254	426.2958	5.4643					
	$X_{pmp}=(1+K_m*CV_m)*\phi_m$		1650.263127											
			(24-h PMP)											
			(HK data)											

Table D2 24-hour Statistical Estimation of PMP for South Guangdong

Guangdong 24-hr

Station	Data n (year)	Xm	$\bar{X}_{n-1}$	S_{n-1}	$\bar{X}_n$	S_n	$C_v=\frac{S_n}{\bar{X}_n}$	Adjusted mean $(1+\frac{3C_m}{\sqrt{n}})*\bar{X}_n$	daily to 24-hr *1.13	$\Phi_m=\frac{X_m-\bar{X}_n}{S_n}$	Φ_m^2+2	$n\geq(\Phi_m^2+2)$	$K_m=\frac{X_m-\bar{X}_{n-1}}{S_{n-1}}$	required n, when K_m --> ϕ_m
南澳屿	39	595	227.7000	84.4264	237.1179	101.9778	0.4301	295.9948	334.4742	3.5094	14.3160	√	4.3505	82
竹仙洞	28	522.7	248.4963	102.6587	258.2893	113.2862	0.4386	323.6951	365.7754	2.3340	7.4476	√	2.6710	43
横岗	35	493.4	152.1529	57.1017	161.9029	80.5719	0.4977	208.4211	235.5158	4.1143	18.9275	√	5.9761	109
港口	36	481.4	193.0629	67.1604	201.0722	81.7988	0.4068	248.2988	280.5776	3.4270	13.7446	√	4.2933	79
石岩	37	479.5	163.8722	59.9719	159.4432	78.6714	0.4934	204.8642	231.4965	4.0683	18.5509	√	5.2629	107
惠阳	39	403.8	154.4789	48.3681	160.8718	62.2236	0.3868	196.7966	222.3802	3.9041	17.2421	√	5.1547	99
深圳	29	386.2	197.9607	64.5922	204.4517	72.4224	0.3542	246.2648	278.2793	2.5096	8.2979	√	2.9143	48
西沥	36	383.4	165.3229	60.0079	166.9472	60.0079	0.3594	201.5928	227.7998	3.6071	15.0110	√	3.6341	86
长江	35	351.5	180.8618	56.0822	185.7371	62.3268	0.3356	221.7216	250.5454	2.6596	9.0733	√	3.0426	52
松木山	33	339.5	164.1563	56.5630	169.4697	63.4907	0.3746	206.1261	232.9224	2.6780	9.1719	√	3.1000	53
约场	39	328.9	168.5421	49.1813	172.6538	54.9045	0.3180	204.3530	230.9188	2.8458	10.0985	√	3.2605	
南沙	26	293	158.7880	60.6548	163.9500	64.9972	0.3964	201.4762	227.6681	1.9855	5.9421	√	2.2127	
	Maximum						0.4977		365.7754				5.9761	
		Xpmp=(1+Km*CVn)*xn		1453.612299										
				(24-h PMP)										
				(S GD data)										

Table of Contents
Table of Contents
Table of Contents

Appendix E

Comparison of Rainfall Data for Haitang Storm

Contents

E.1 Comparison of Rainfall Data for Haitang Storm

Results from two datasets (Water Resources Agency (WRA) and Central Weather Bureau (CWB)) have been compared for Haitang storm by referring to the figures below. There is only one (or two) stations in the storm center in WRA data. Spatial interpolation cannot be undertaken only based on these one or two stations as it would cause much uncertainty. On the other hand, it is found out during a data quality control that some spurious records in CWB data are observed (see Section A.2.3) but the results from CWB have been compared with some reports about this storm online. At least, the 24-hour results are similar to different sources, which indicate the validity of CWB data. Therefore, CWB is finally selected for the analysis. Actually, isohyets of 24-hour from Haitang storm are not used in transposition but the isohyets pattern of Morakot.

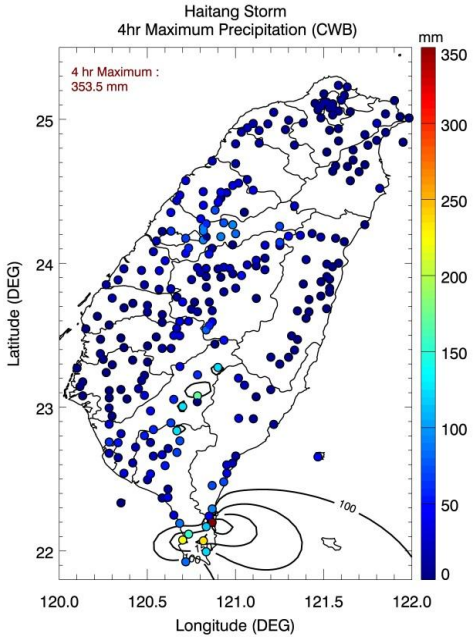

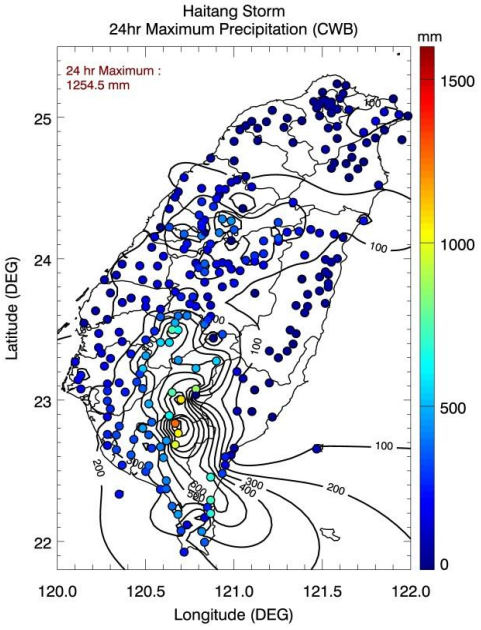

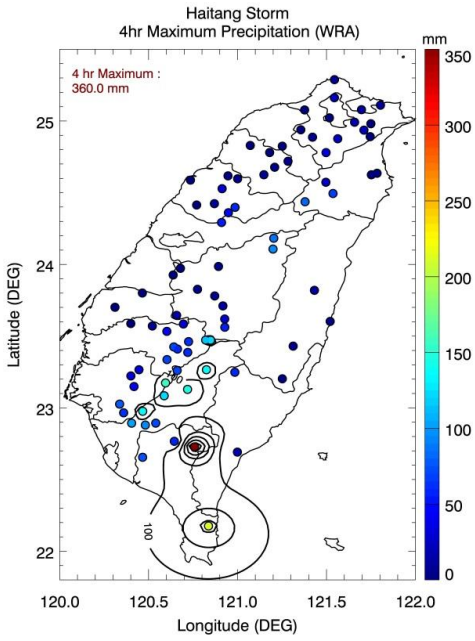

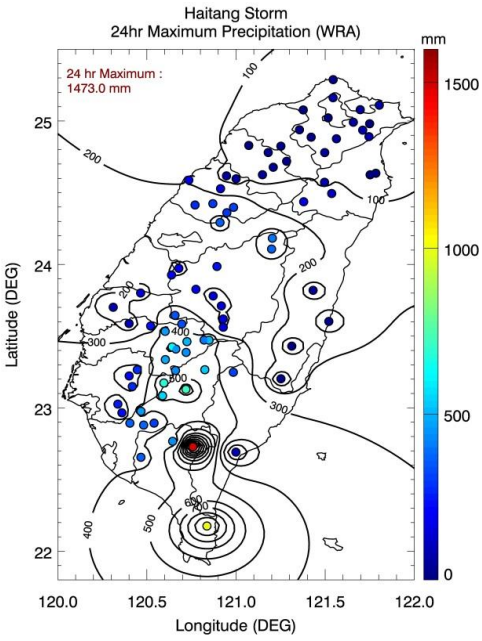

Table of Contents
Table of Contents
Table of Contents

Appendix F

Complete Set of Orientation of Convergence Pattern on HK 24-hour OIF

Contents

List of Figures

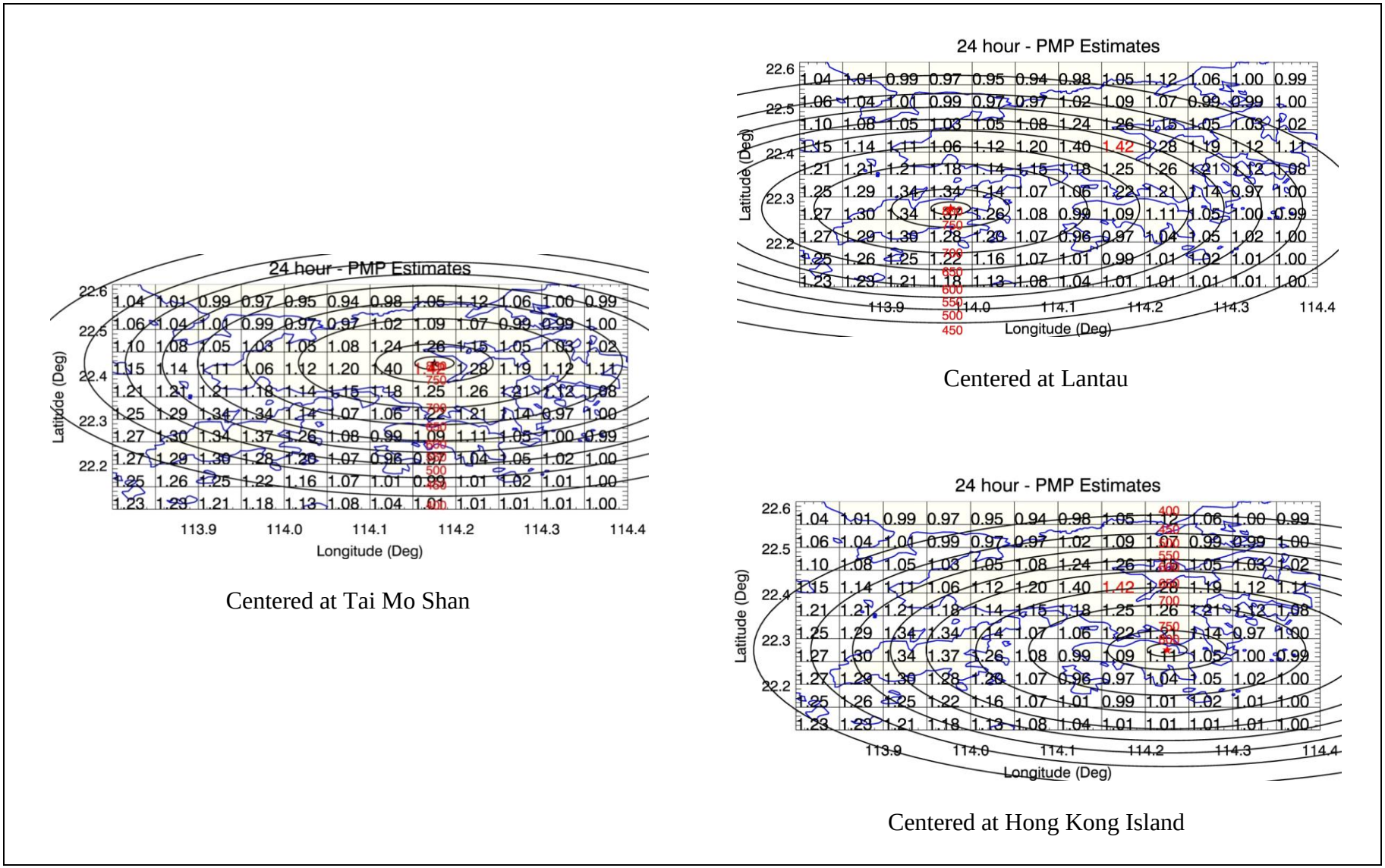

Figure F1 E-W Orientation 0° - 24-hour (Embryonic PMP)

Table of Contents
Table of Contents
Table of Contents

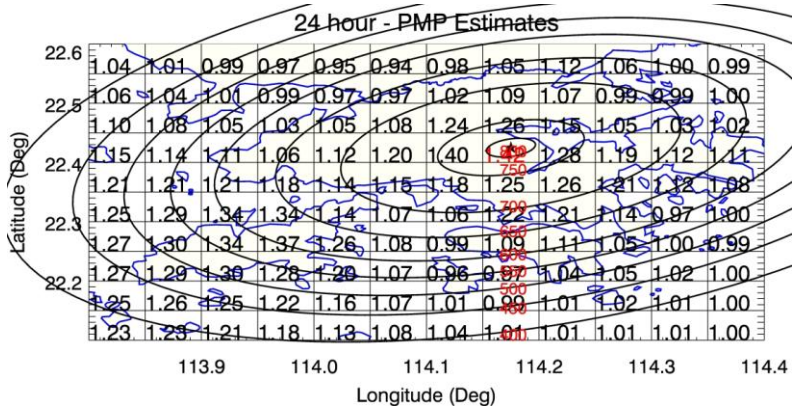

Centered at Tai Mo Shan

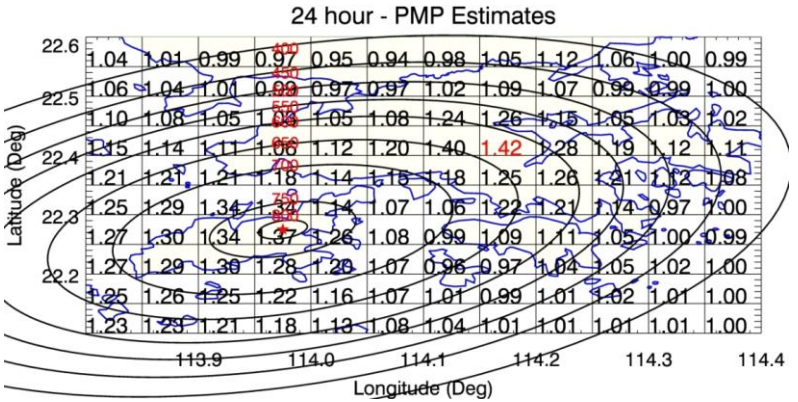

Centered at Lantau

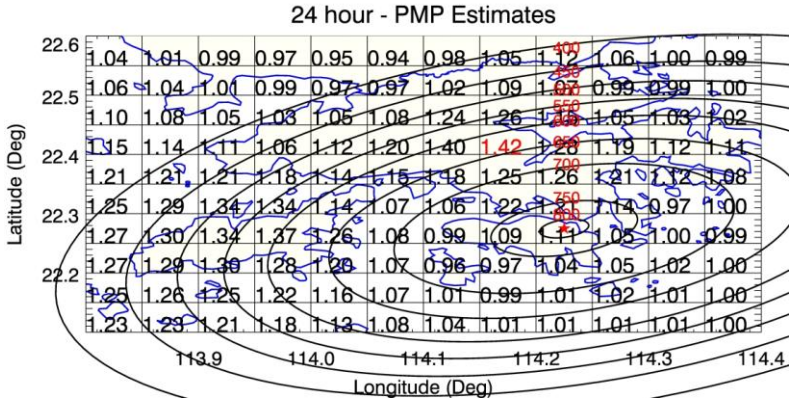

Centered at Hong Kong Island

Figure F2 ENE-WSW Orientation 22.5° - 24-hour (Embryonic PMP)

Table of Contents
Table of Contents
Table of Contents

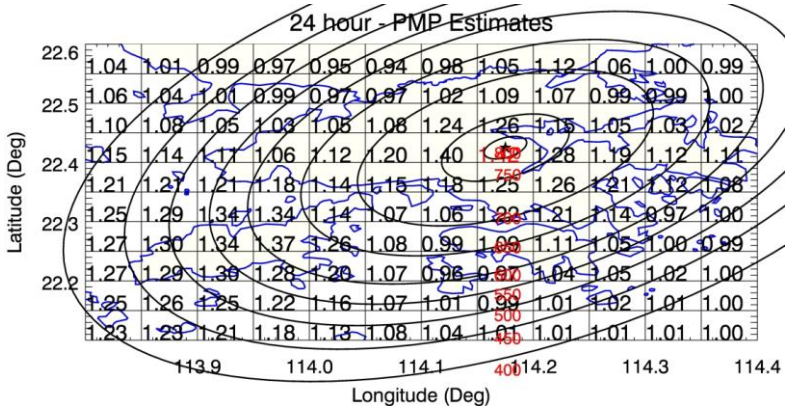

Centered at Tai Mo Shan

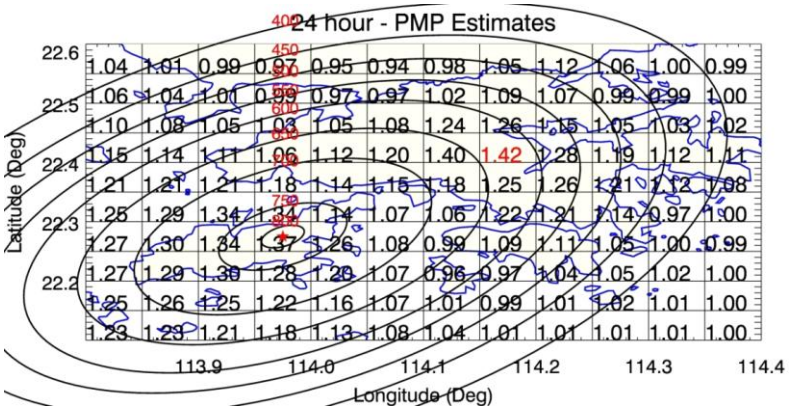

Centered at Lantau

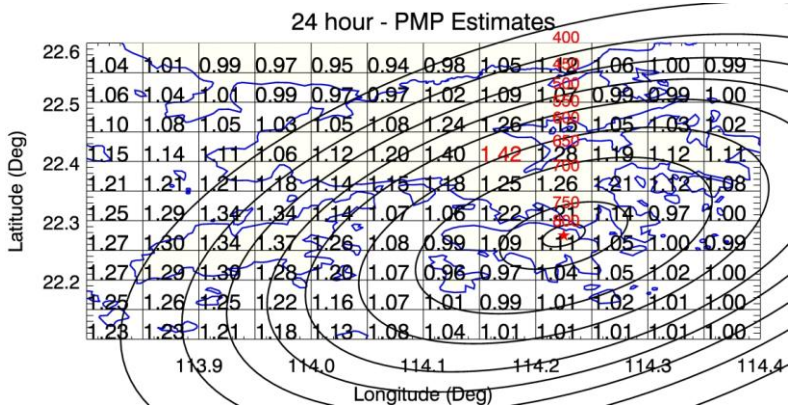

Centered at Hong Kong Island

Figure F3 NE-SW Orientation 45° - 24-hour (Embryonic PMP)

Table of Contents
Table of Contents
Table of Contents

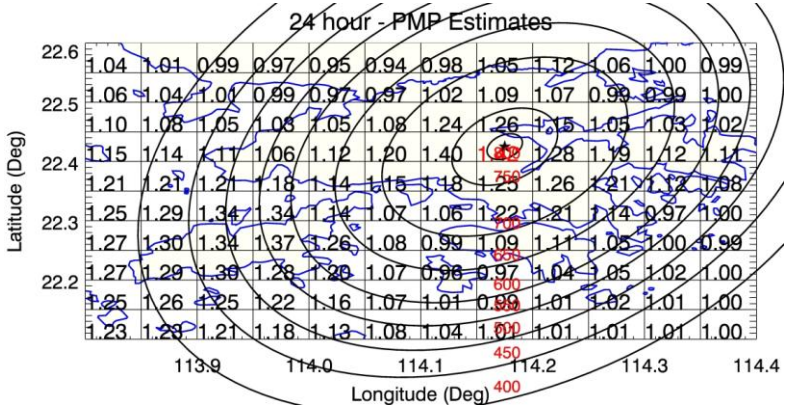

Centered at Tai Mo Shan

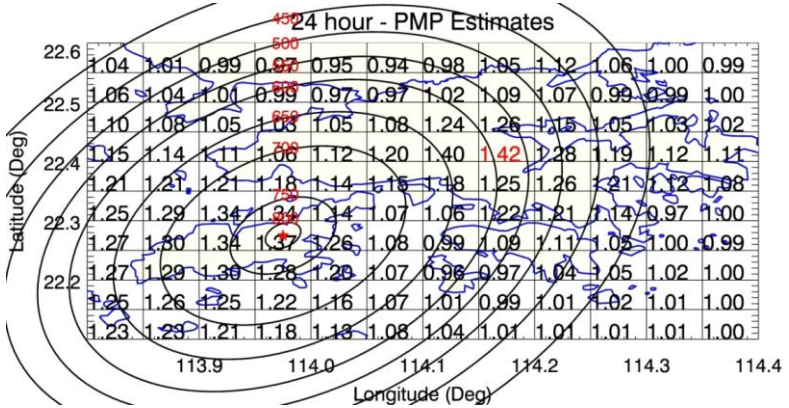

Centered at Lantau

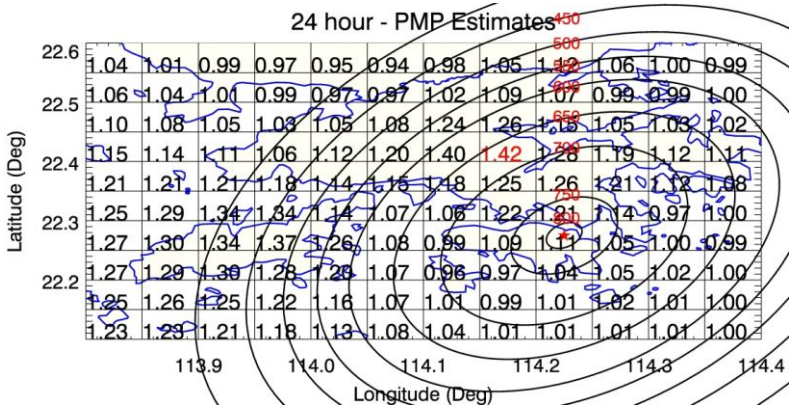

Centered at Hong Kong Island

Figure F4 NNE-SSW Orientation 67.5° - 24-hour (Embryonic PMP)

Table of Contents
Table of Contents
Table of Contents

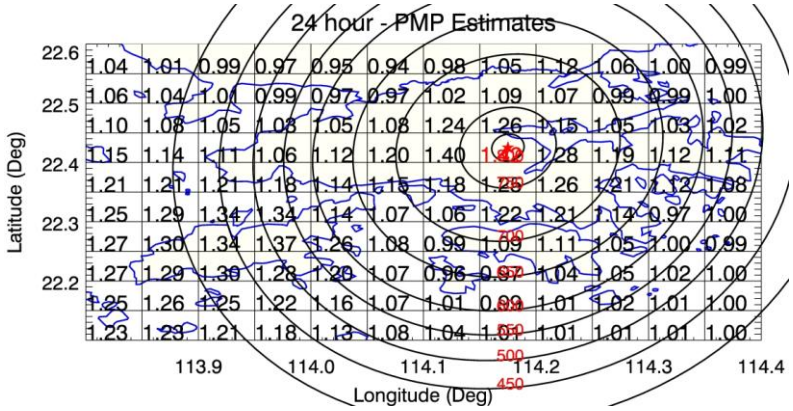

Centered at Tai Mo Shan

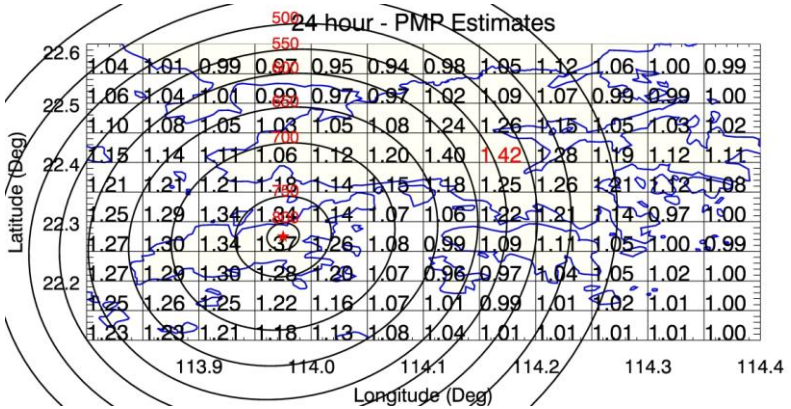

Centered at Lantau

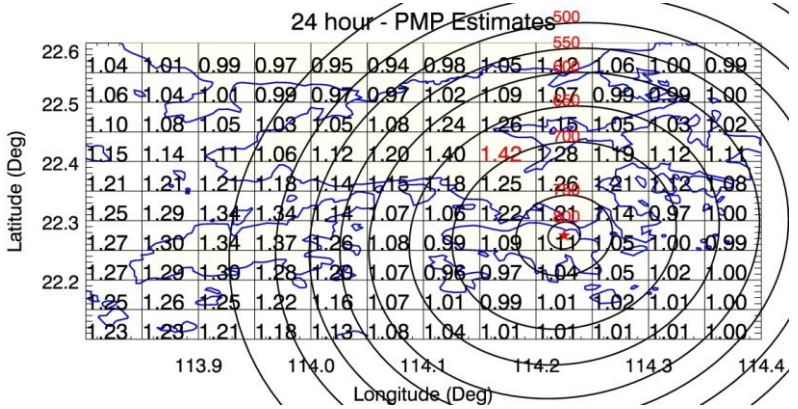

Centered at Hong Kong Island

Figure F5 N-S Orientation 85° - 24-hour (Embryonic PMP)

Table of Contents
Table of Contents
Table of Contents

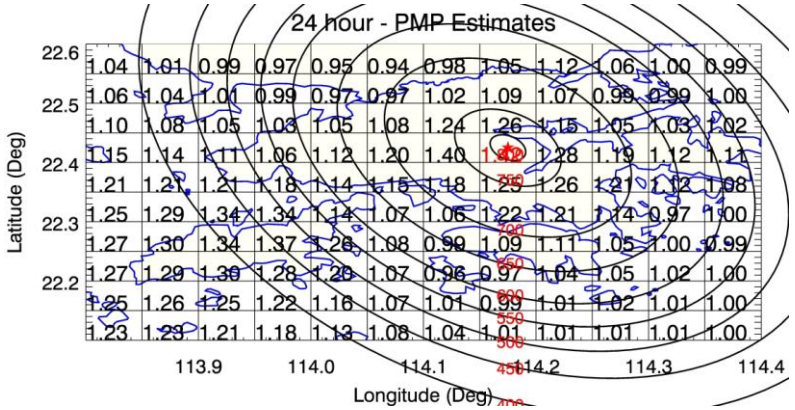

Centered at Tai Mo Shan

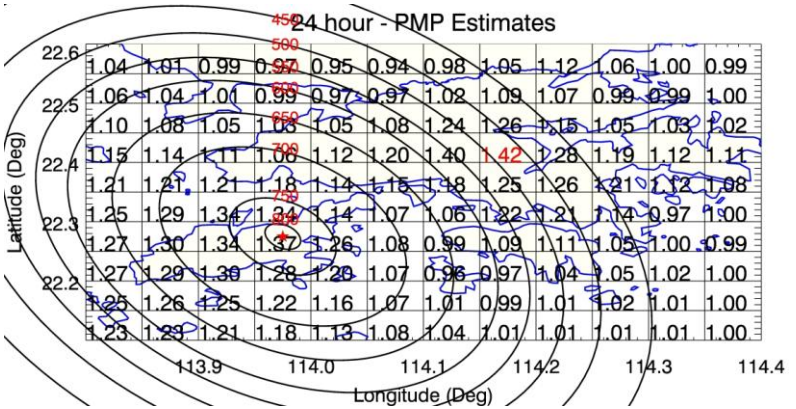

Centered at Lantau

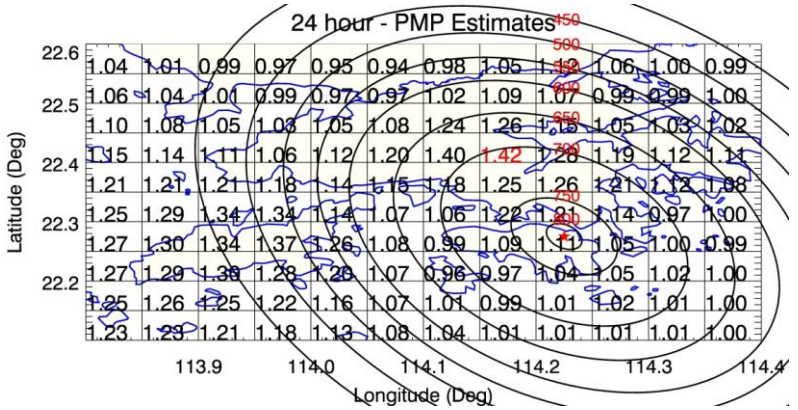

Centered at Hong Kong Island

Figure F6 NNW-SSE Orientation 112.5° - 24-hour (Embryonic PMP)

Table of Contents
Table of Contents
Table of Contents

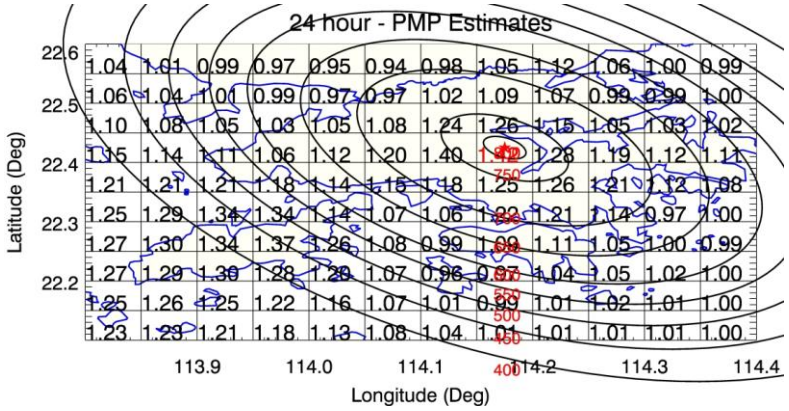

Centered at Tai Mo Shan

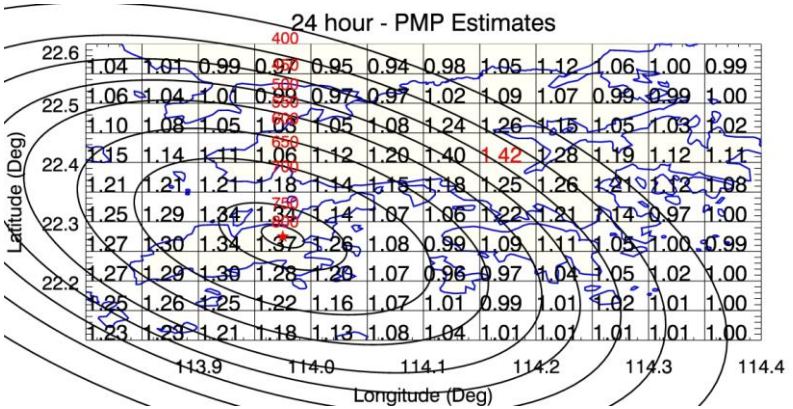

Centered at Lantau

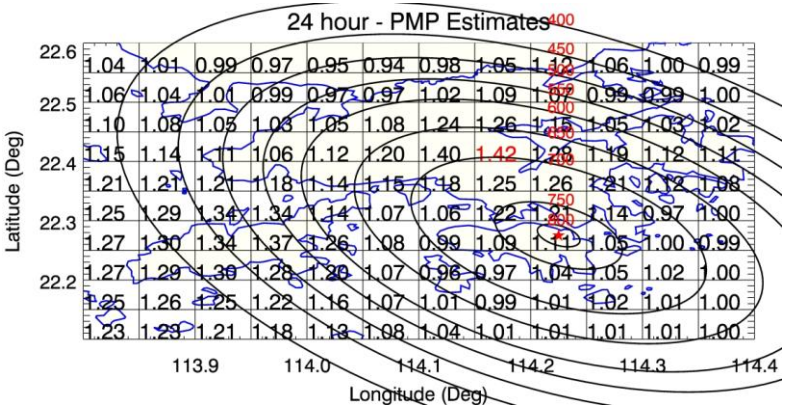

Centered at Hong Kong Island

Figure F7 NW-SE Orientation 135° - 24-hour (Embryonic PMP)

Table of Contents
Table of Contents
Table of Contents

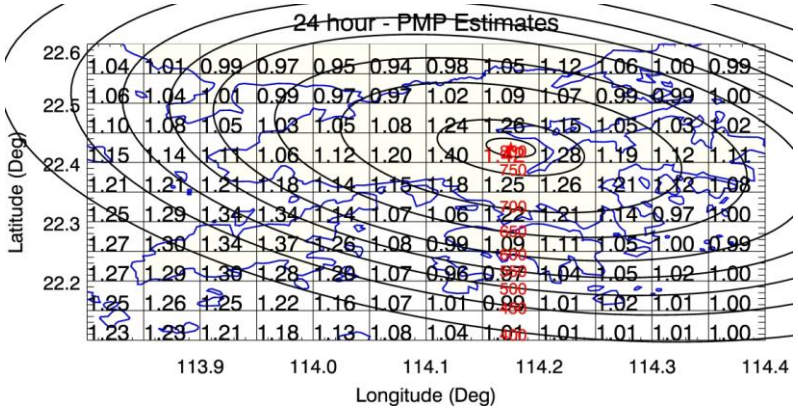

Centered at Tai Mo Shan

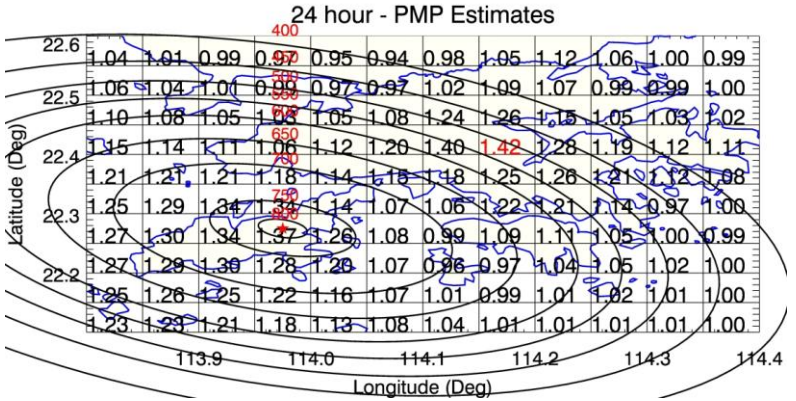

Centered at Lantau

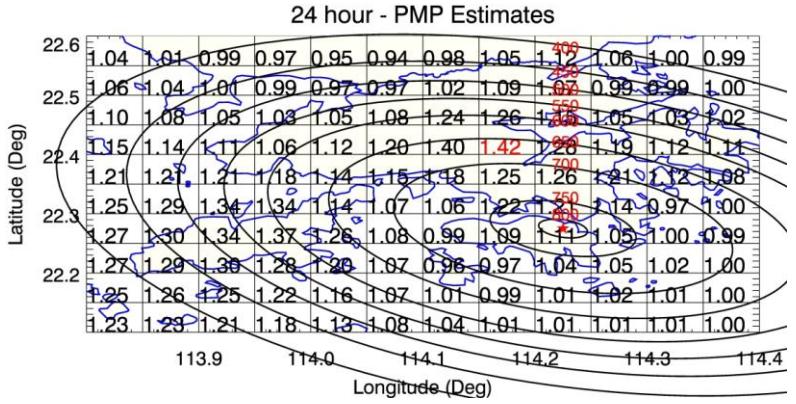

Centered at Hong Kong Island

Figure F8 WNW-ESE Orientation 157.5° - 24-hour (Embryonic PMP)

Table of Contents
Table of Contents
Table of Contents

Table of Contents
Table of Contents
Table of Contents

Appendix G

Embryonic 24-hour PMP in Grids and Isohyets with the Generalized Convergence Pattern Centred at Tai Mo Shan for a Complete Set of Orientation Adjustments

Contents

List of Figures

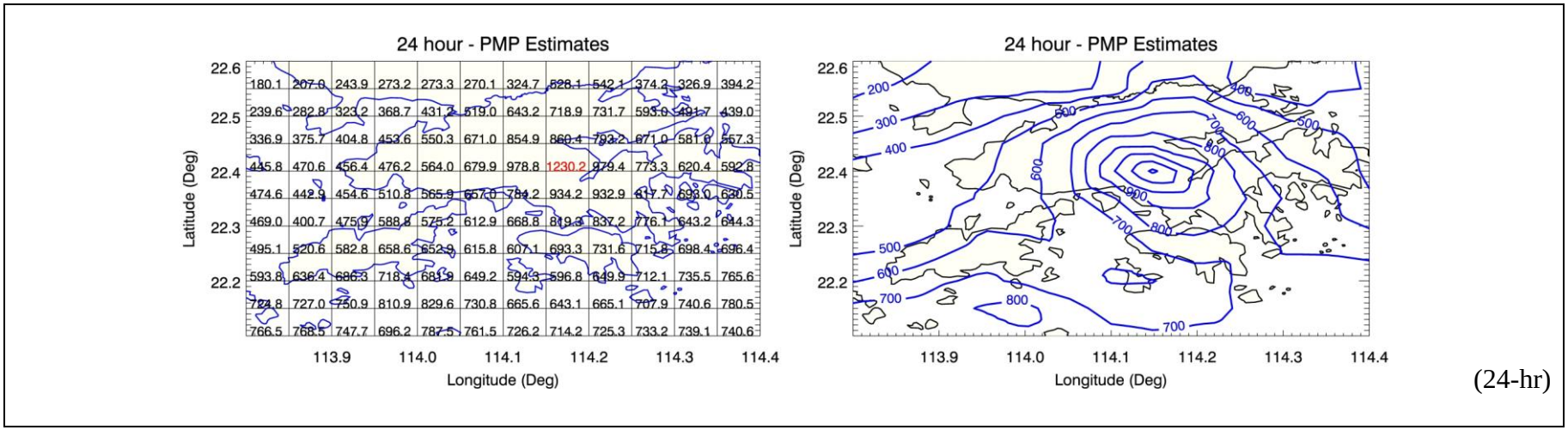

(24-hr)

Figure G1 Embryonic PMP Centred at Tai Mo Shan, E-W Orientation - 0°

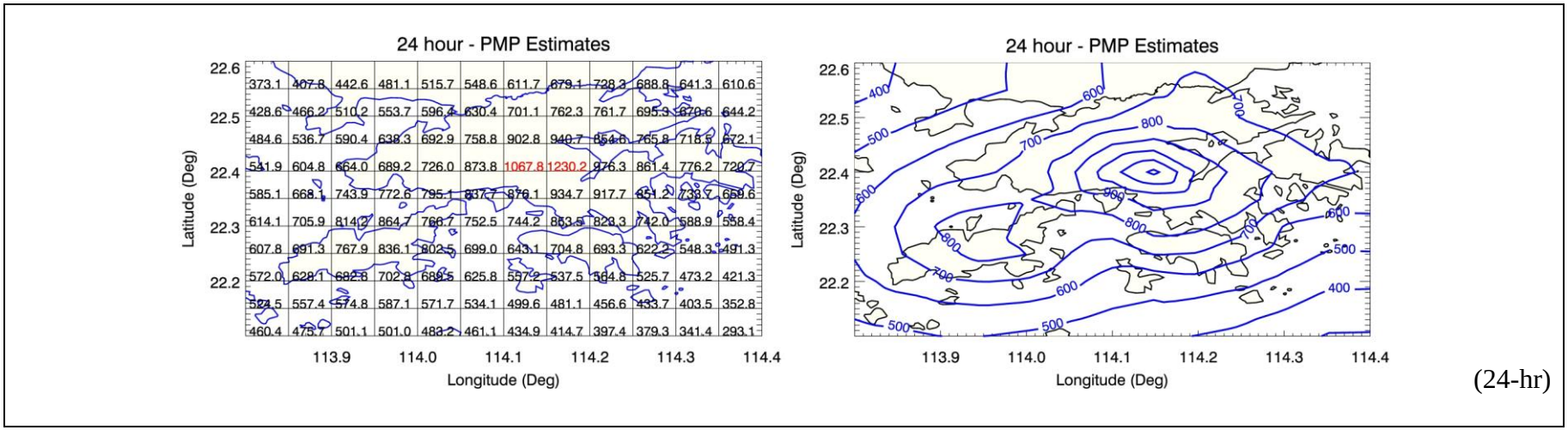

(24-hr)

Figure G2 Embryonic PMP Centred at Tai Mo Shan, ENE-WSW Orientation - 22.5°

Table of Contents
Table of Contents
Table of Contents

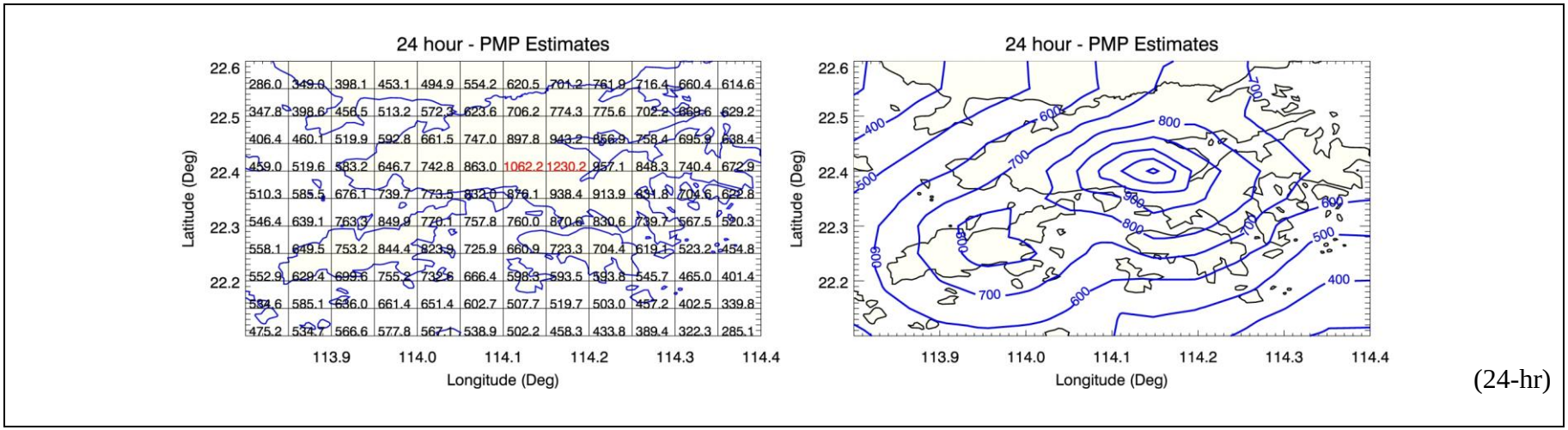

(24-hr)

Figure G3 Embryonic PMP Centred at Tai Mo Shan, NE-SW Orientation - 45°

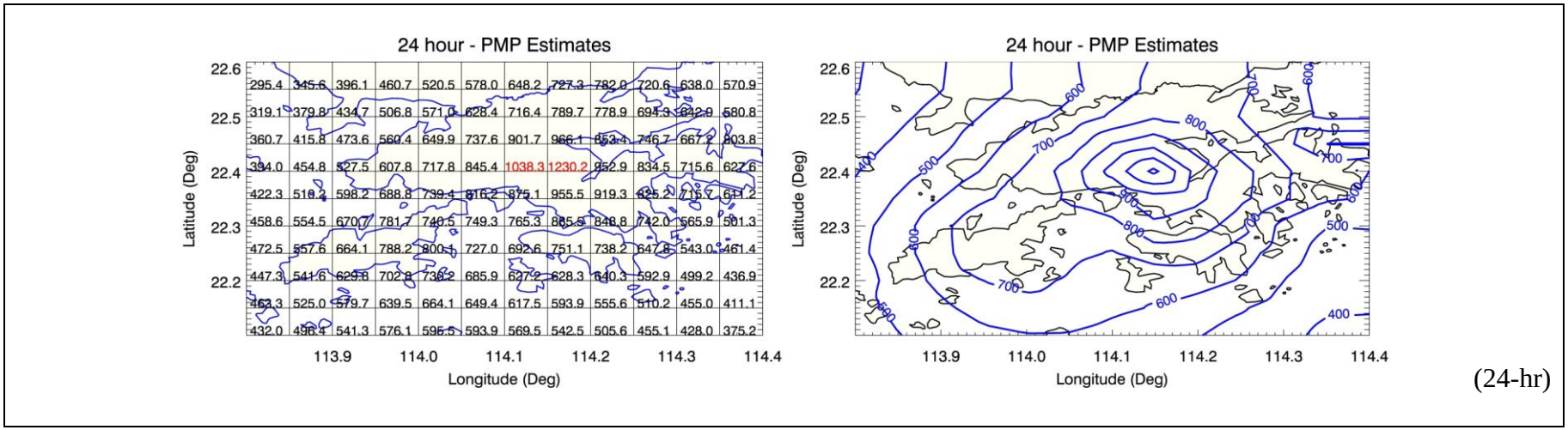

(24-hr)

Figure G4 Embryonic PMP Centred at Tai Mo Shan, NNE-SSW Orientation - 67.5°

Table of Contents
Table of Contents
Table of Contents

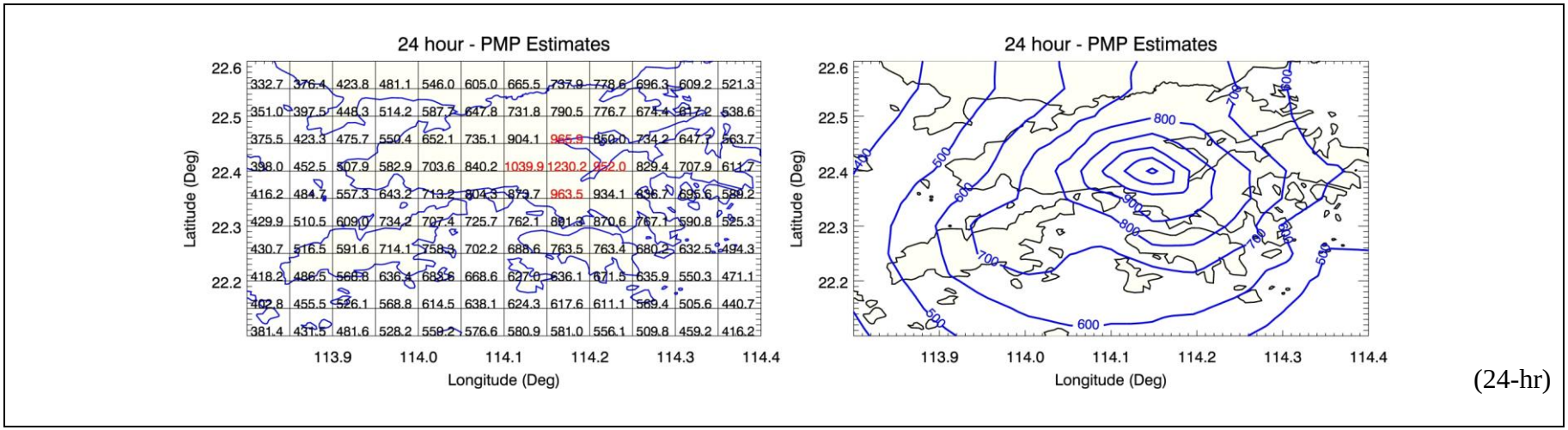

(24-hr)

Figure G5 Embryonic PMP Centred at Tai Mo Shan, N-S Orientation - 85°

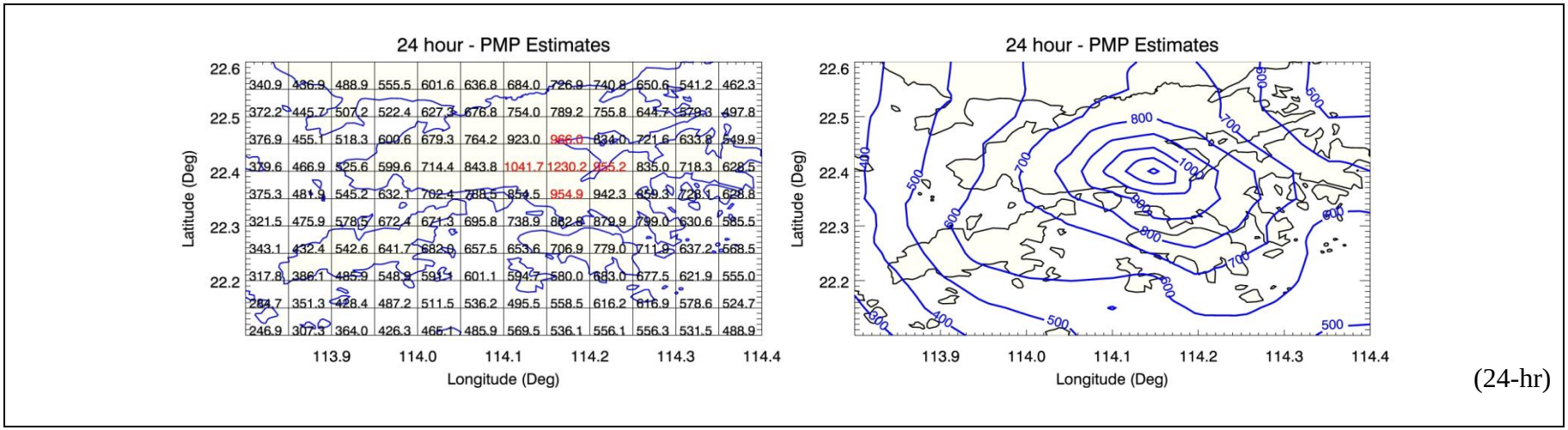

(24-hr)

Figure G6 Embryonic PMP Centred at Tai Mo Shan, NNW-SSE Orientation - 112.5°

Table of Contents
Table of Contents
Table of Contents

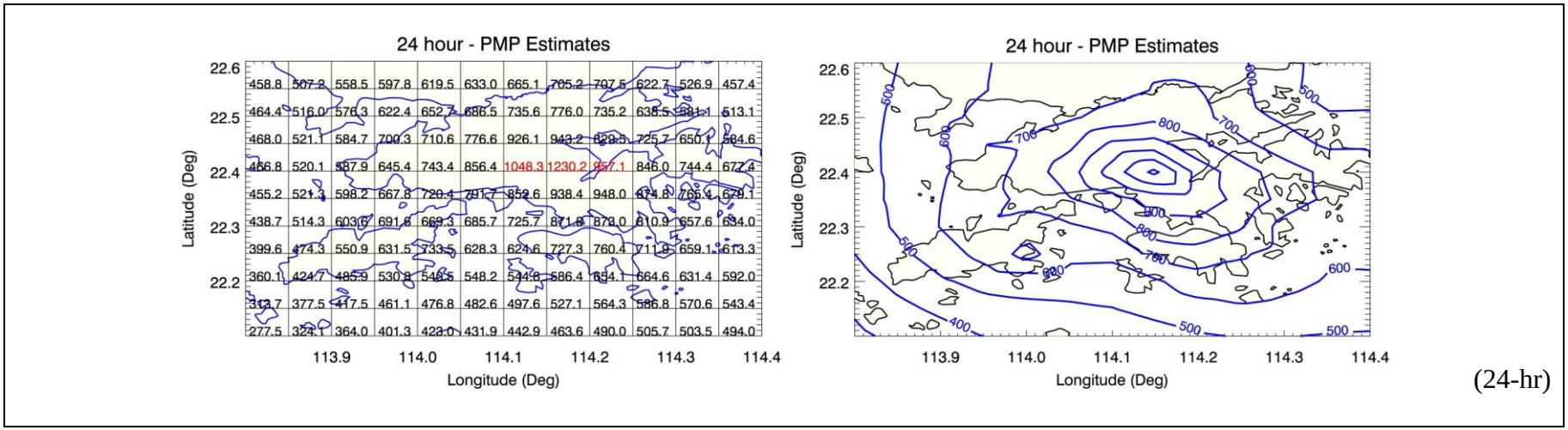

Figure G7 Embryonic PMP Centred at Tai Mo Shan, NW-SE Orientation - 135°

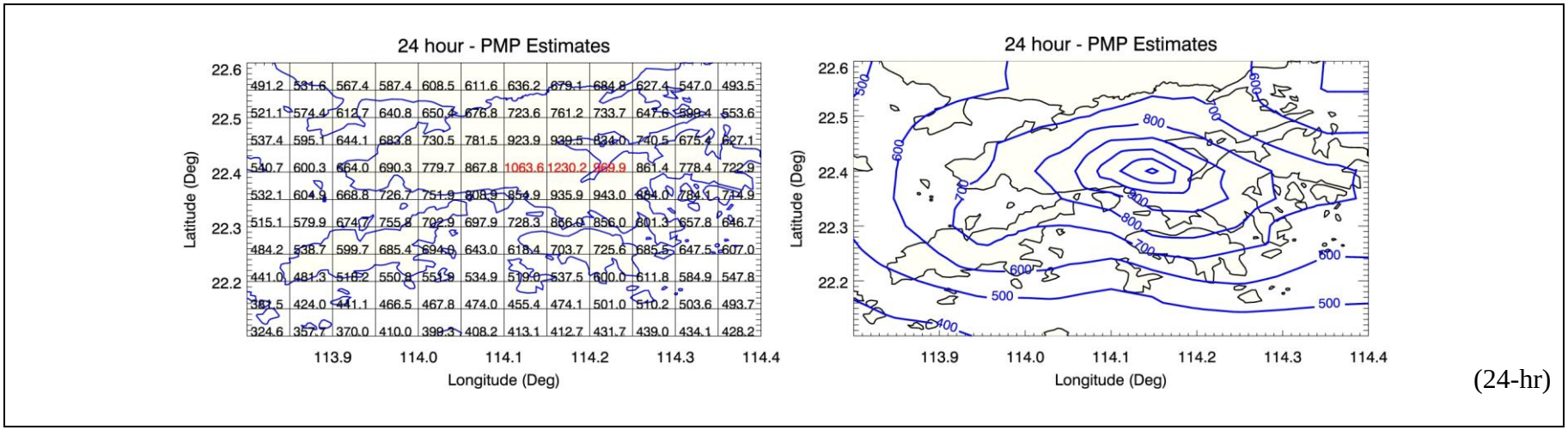

Figure G8 Embryonic PMP Centred at Tai Mo Shan, WNW-ESE Orientation - 157.5°

Table of Contents
Table of Contents
Table of Contents

Appendix H

Embryonic 24-hour PMP in Grids and Isohyets with the Generalized Convergence Pattern Centred at Lantau for a Complete Set of Orientation Adjustments

Contents

List of Figures

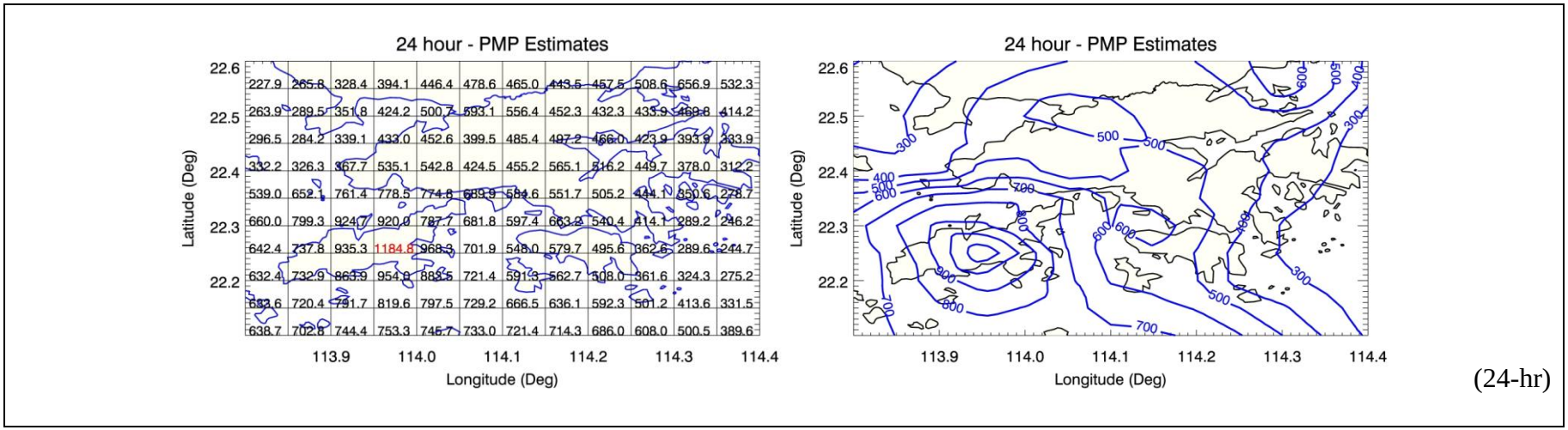

Figure H1 Embryonic PMP Centred at Lantau, E-W Orientation - 0°

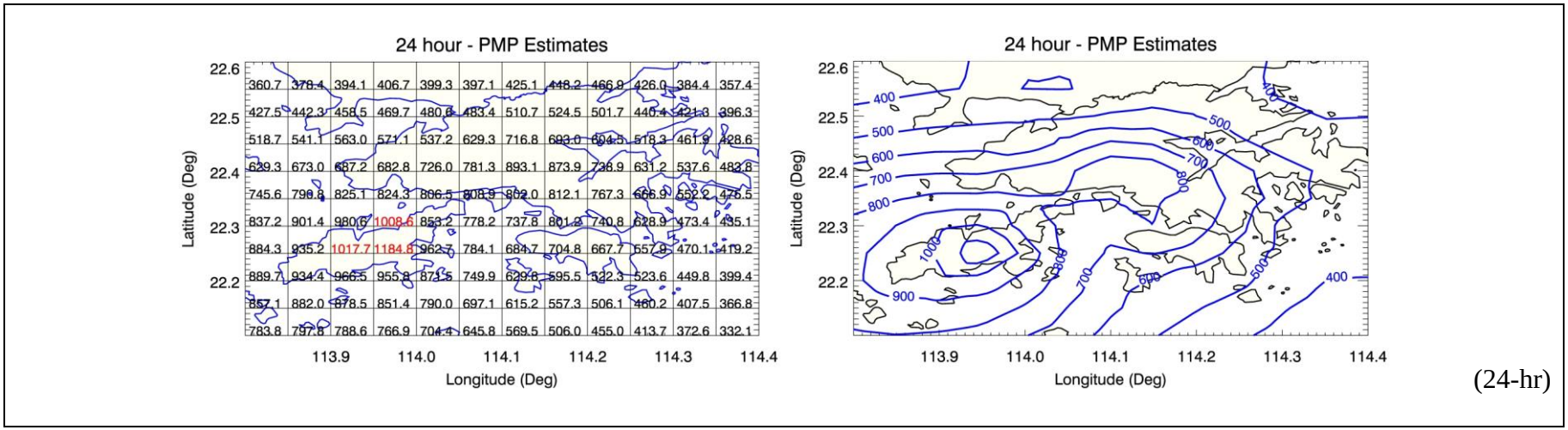

Figure H2 Embryonic PMP Centred at Lantau, ENE-WSW Orientation - 22.5°

Table of Contents
Table of Contents
Table of Contents

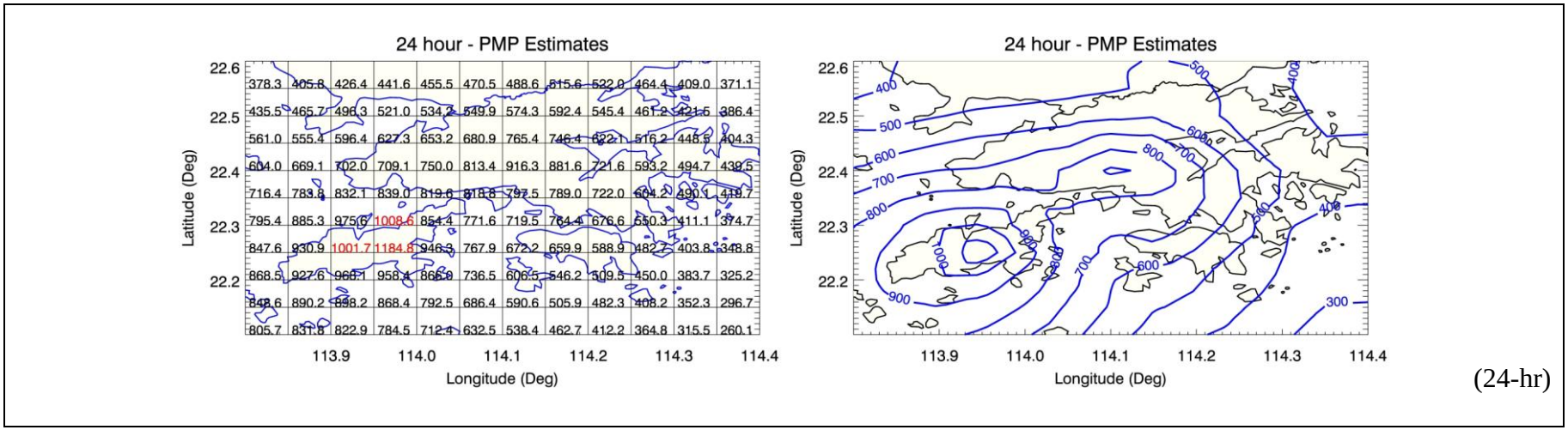

Figure H3 Embryonic PMP Centred at Lantau, NE-SW Orientation - 45°

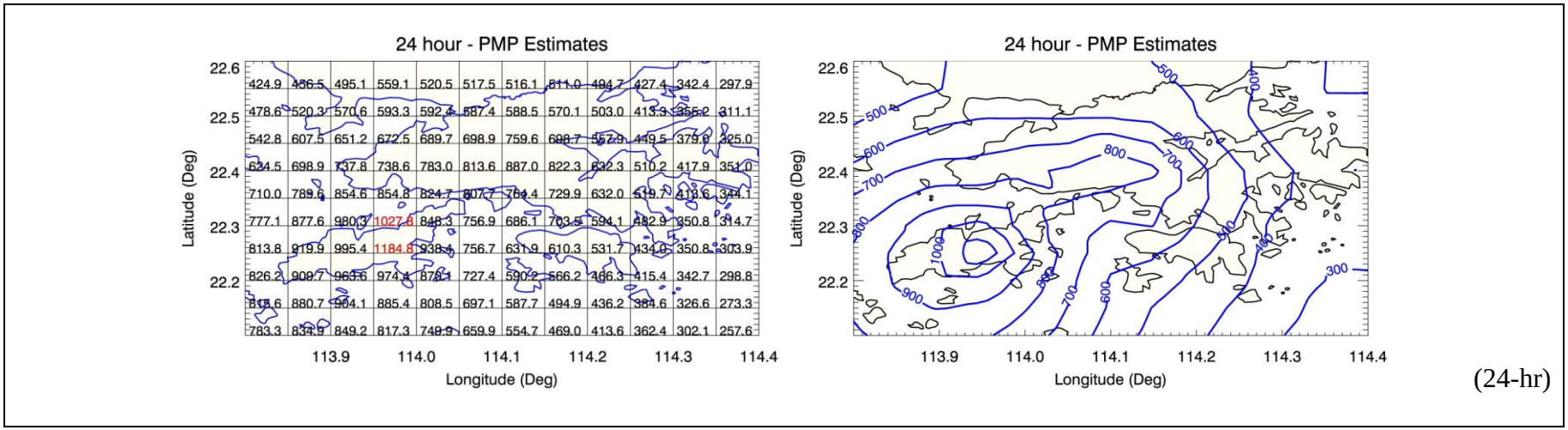

Figure H4 Embryonic PMP Centred at Lantau, NNE-SSW Orientation - 67.5°

Table of Contents
Table of Contents
Table of Contents

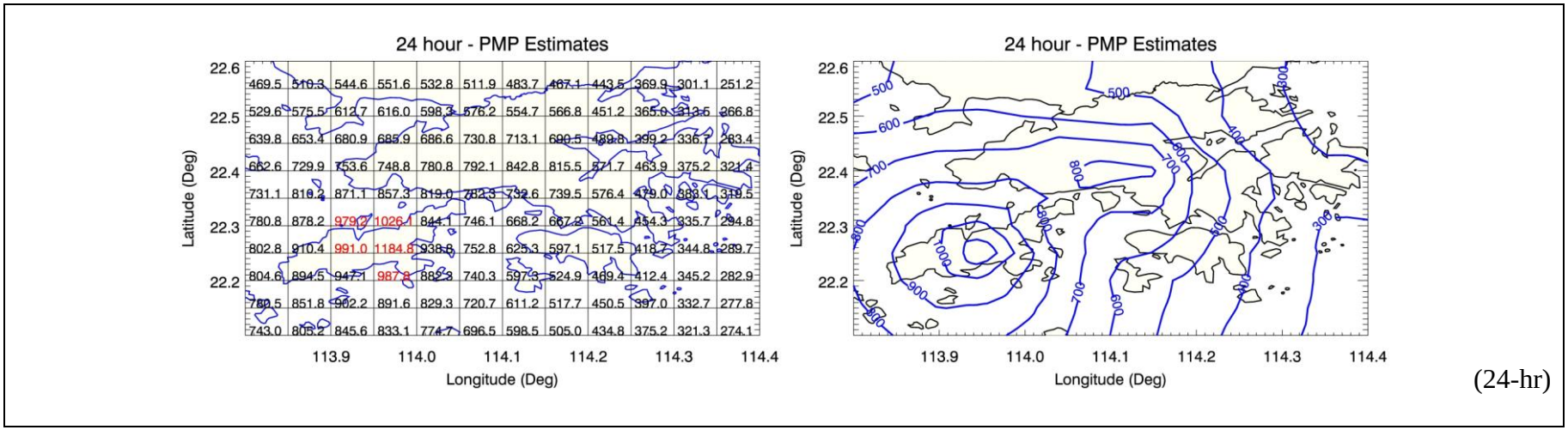

Figure H5 Embryonic PMP Centred at Lantau, N-S Orientation - 85°

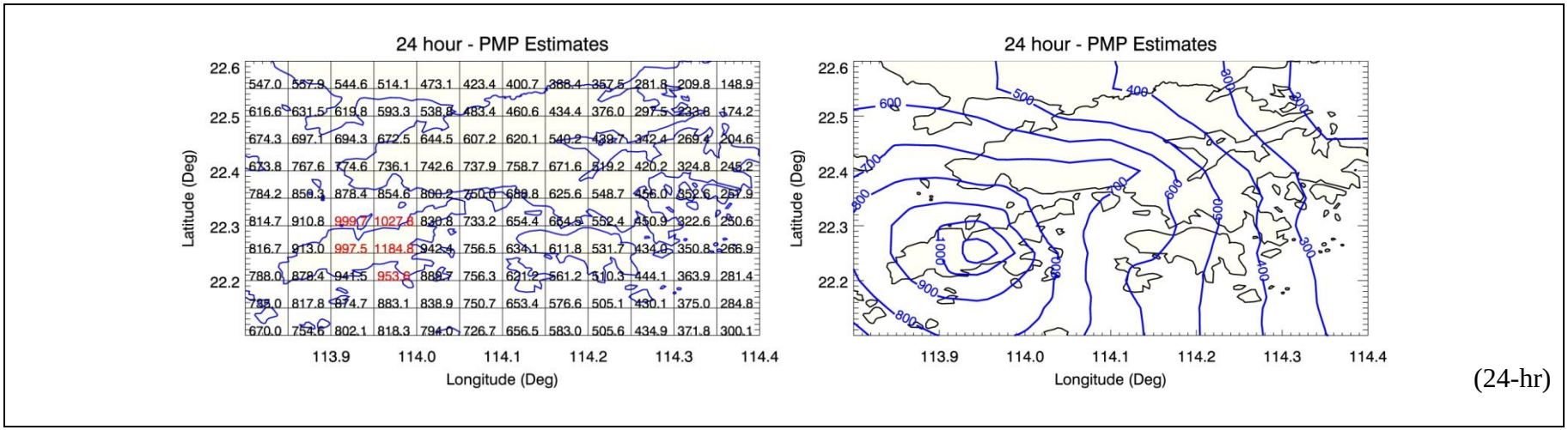

Figure H6 Embryonic PMP Centred at Lantau, NNW-SSE Orientation - 112.5°

Table of Contents
Table of Contents
Table of Contents

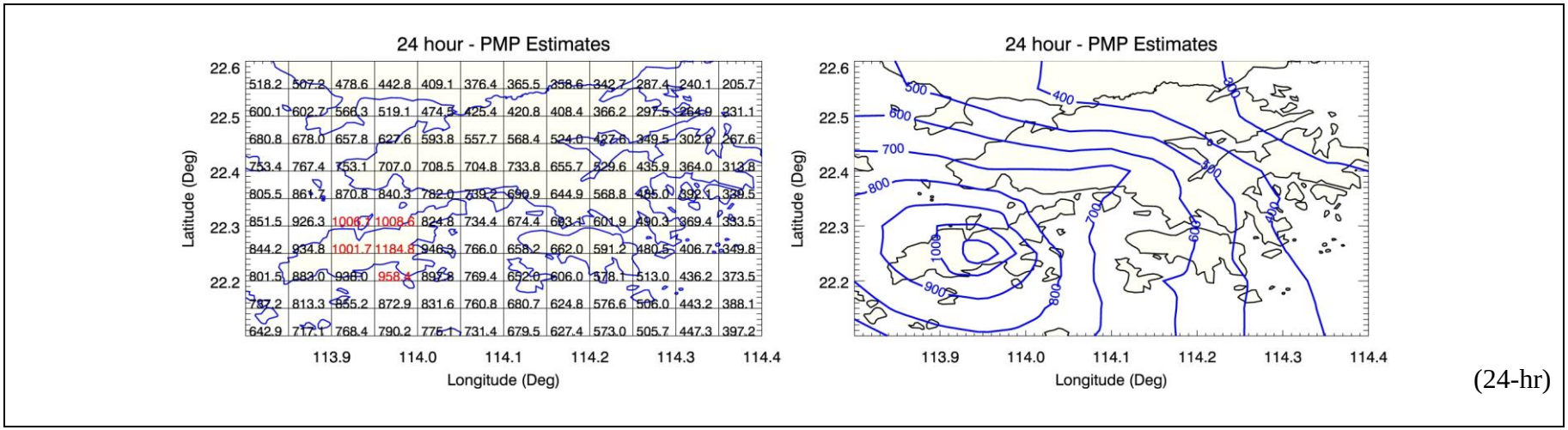

Figure H7 Embryonic PMP Centred at Lantau, NW-SE Orientation - 135°

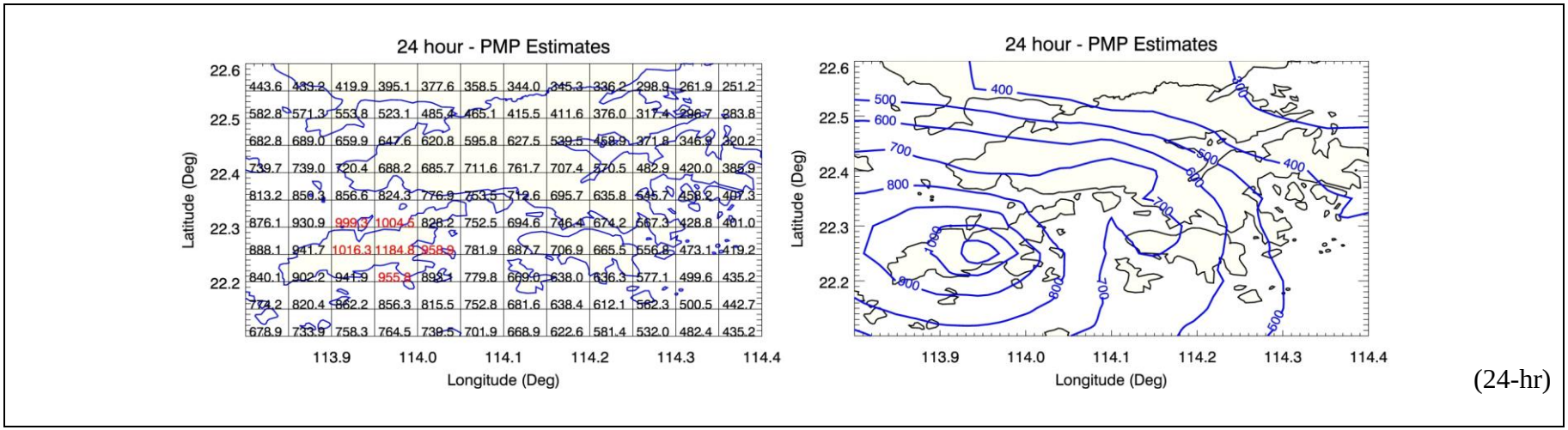

Figure H8 Embryonic PMP Centred at Lantau, WNW-ESE Orientation - 157.5°

Table of Contents
Table of Contents
Table of Contents

Table of Contents
Table of Contents
Table of Contents

Appendix I

Embryonic 24-hour PMP in Grids and Isohyets with the Generalized Convergence Pattern Centred at Hong Kong Island for a Complete Set of Orientation Adjustments

Contents

List of Figures

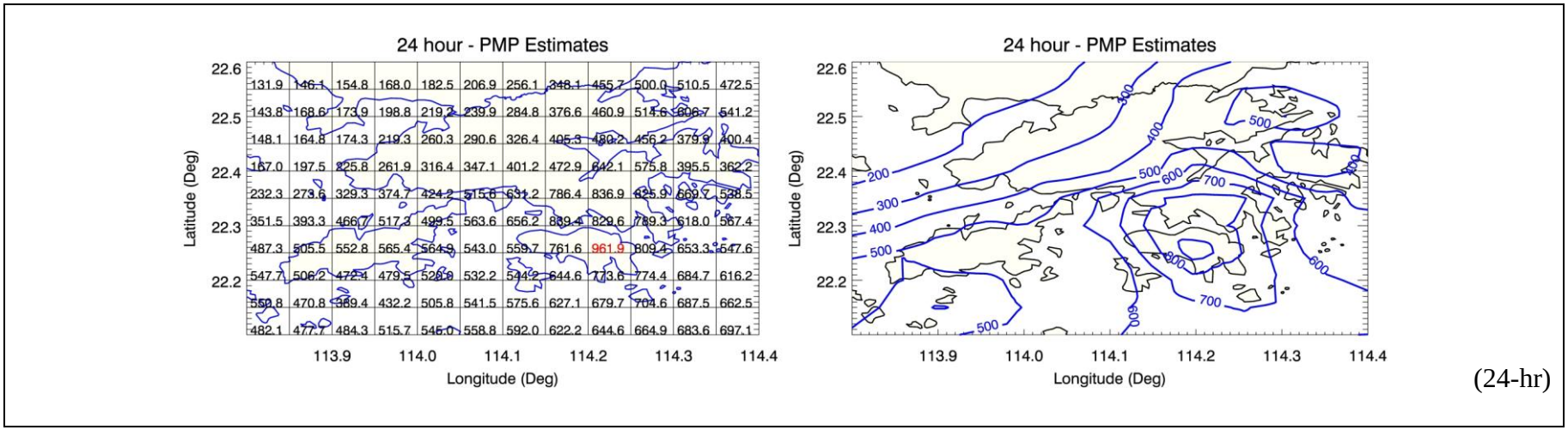

Figure I1 Embryonic PMP Centred at Hong Kong Island, E-W Orientation - 0°

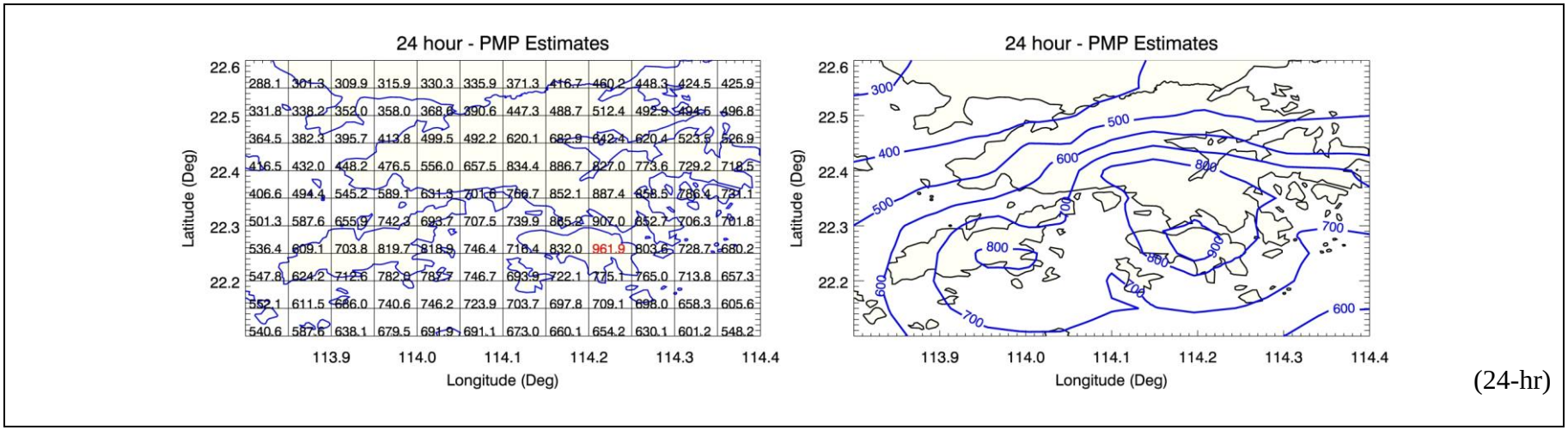

Figure I2 Embryonic PMP Centred at Hong Kong Island, ENE-WSW Orientation - 22.5°

Table of Contents
Table of Contents
Table of Contents

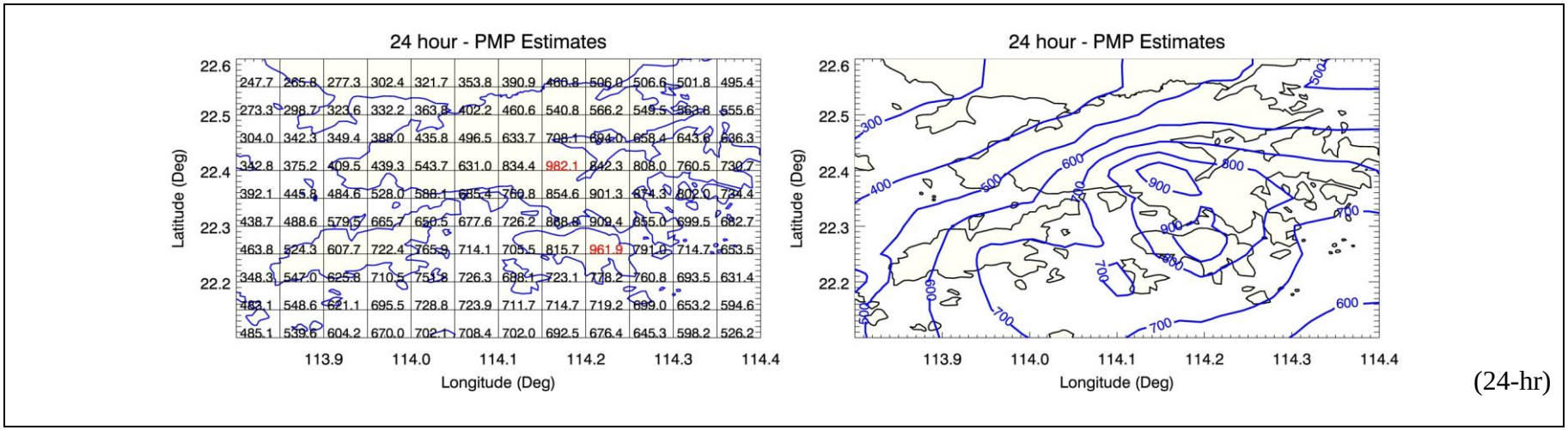

Figure I3 Embryonic PMP Centred at Hong Kong Island, NE-SW Orientation - 45°

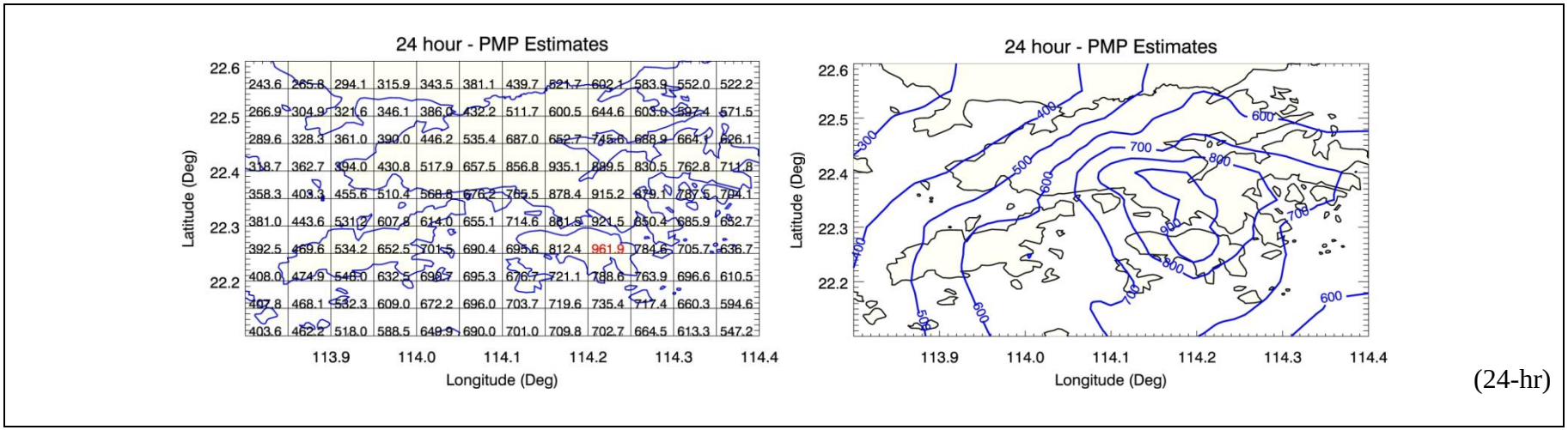

Figure I4 Embryonic PMP Centred at Hong Kong Island, NNE-SSW Orientation - 67.5°

Table of Contents
Table of Contents
Table of Contents

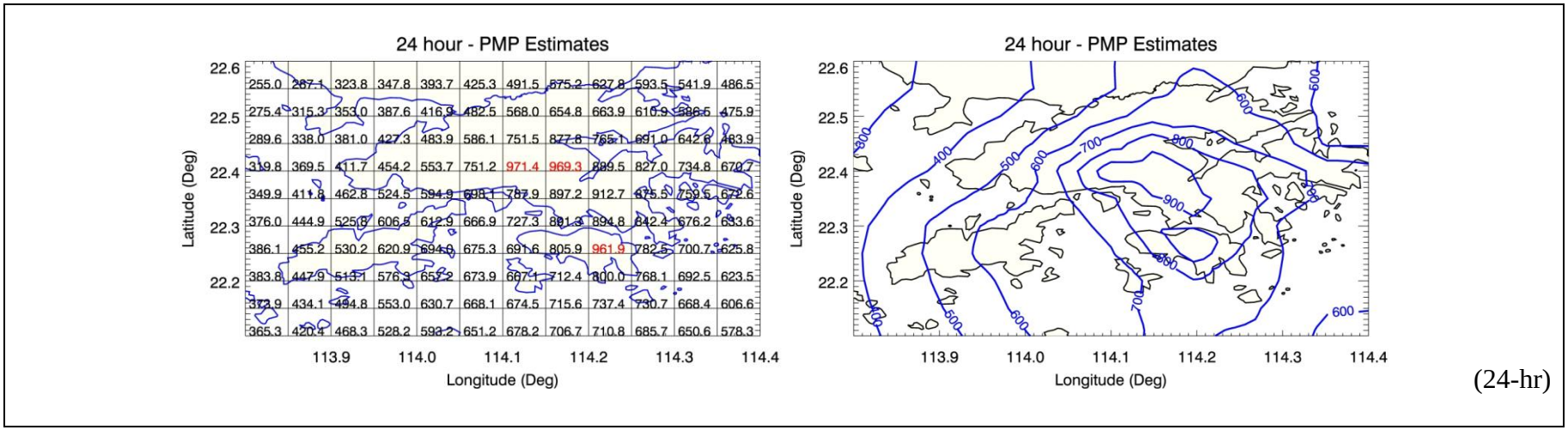

Figure I5 Embryonic PMP Centred at Hong Kong Island, N-S Orientation - 85°

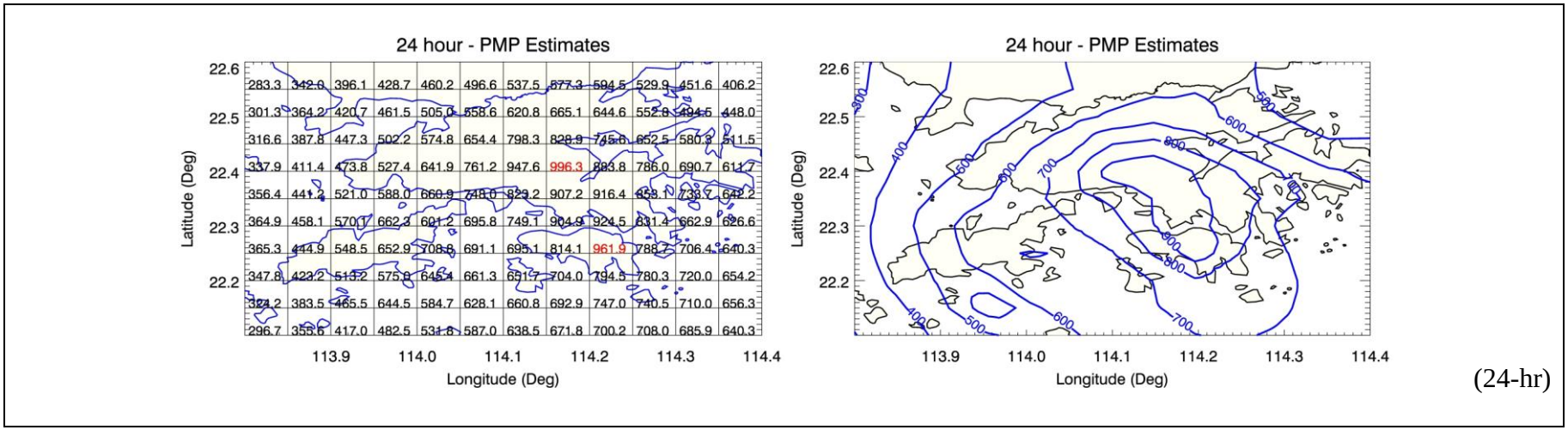

Figure I6 Embryonic PMP Centred at Hong Kong Island, NNW-SSE Orientation - 112.5°

Table of Contents
Table of Contents
Table of Contents

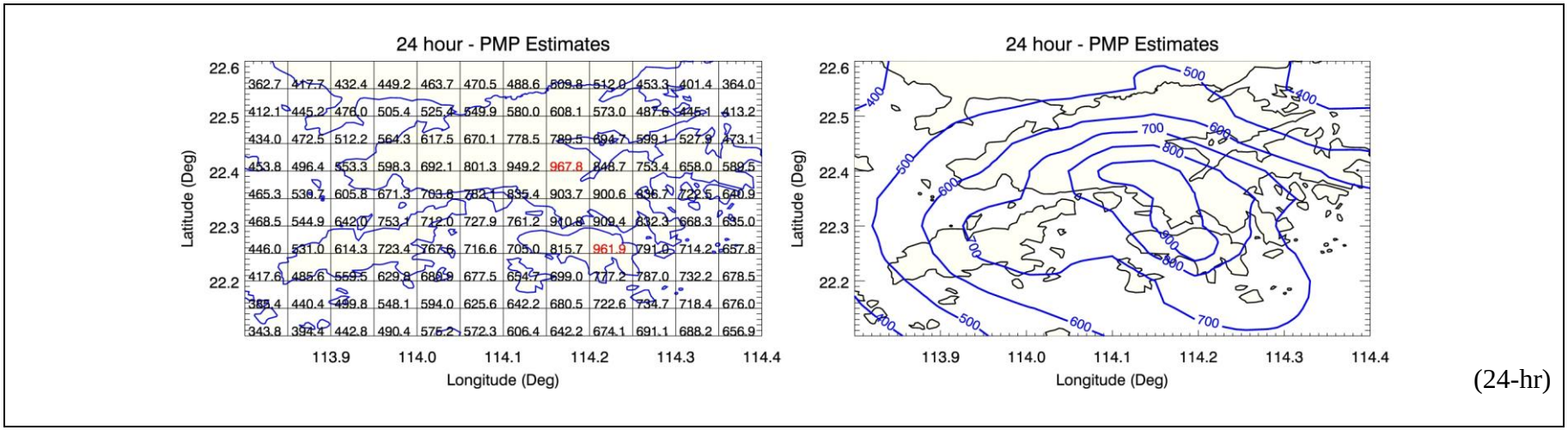

Figure I7 Embryonic PMP Centred at Hong Kong Island, NW-SE Orientation - 135°

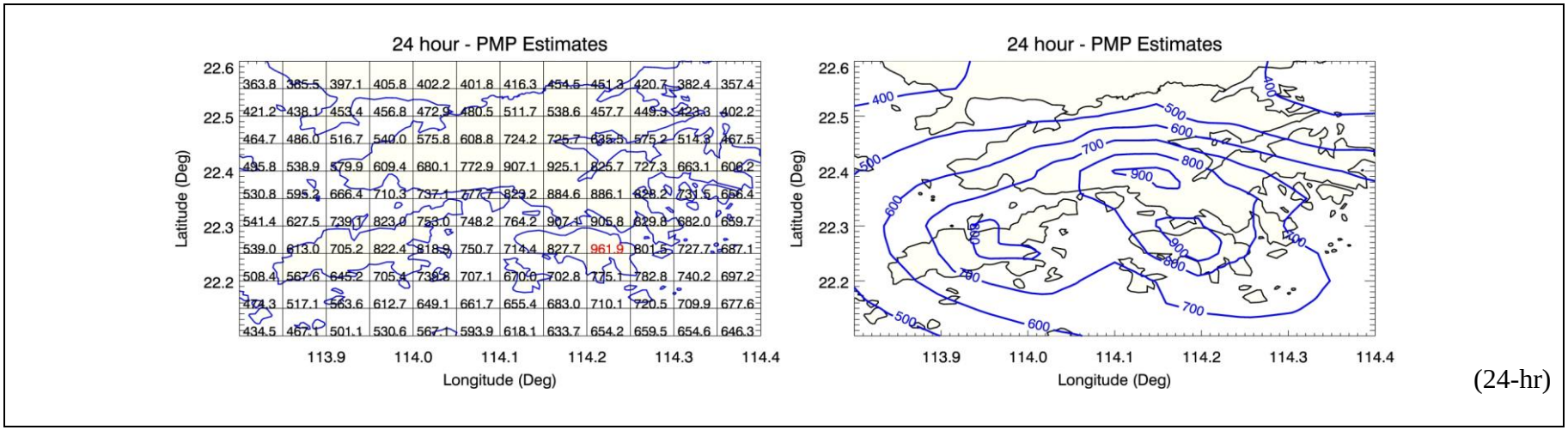

Figure I8 Embryonic PMP Centred at Hong Kong Island, WNW-ESE Orientation - 157.5°

Table of Contents
Table of Contents
Table of Contents

Table of Contents
Table of Contents
Table of Contents

Appendix J

Assessment of Precipitable Water for the Representative Storm Morakot

Contents

List of Tables

Table J1 Assessment of Precipitable Water for the Representative Storm Morakot

							Date_Time								
No.	ID	Name	ELE(m)	WGS84_X	WGS84_Y		0806_00	0806_06	0806_12	0806_18	0807_00	0807_06	0807_12	0807_18	0808_00
1	467420	Yongkang永康(#56)	8.1	120.22	23.04	Pressure (hPa)	1001.7	999.9	999	994.9	992.2	986	981.5	979.3	975.2
						Elevation Difference (m)	17	-1	-10	-51	-78	-140	-185	-207	-248
						Dew Point Observation Td (℃)	23.5	23	24.3	23.1	23.3	25.2	24.9	25.6	25.4
						Calculated 1000hPa Td (℃)	23.6	23	24.3	23.3	23.6	25.8	25.6	26.4	26.4
						1000hPa Td (℃) based on design charts	23.5	23	24.3	23.2	23.4	25.4	25.2	26.2	26.1
2	467440	Gaoxiong高雄(#57)	2.3	120.30	22.57	Pressure (hPa)	1001.4	999.3	997.9	993.7	991.9	985.9	981.8	980	977.7
						Elevation Difference (m)	14	-7	-21	-63	-81	-141	-182	-200	-223
						Dew Point Observation Td (℃)	26	24.3	25.2	24.3	25.1	25.6	25.9	26.5	26
						Calculated 1000hPaTd (℃)	26.1	24.3	25.3	24.6	25.4	26.2	26.6	27.3	26.9
						1000hPaTd (℃) based on design charts	26	24.3	25.2	24.4	25.2	26	26.3	26.9	26.7
3	466990	Hualian花蓮(#60)	16	121.60	23.98	Pressure (hPa)	999.1	996.9	992.7	990.5	983	976.4	970.6	968.2	968.6
						Dew Point Observation Td (℃)	23.7	23.4	24.9	23.4	23.5	22.9	24.1	25.4	26.3
						Calculated 1000hPa Td (℃)	23.8	23.5	25	23.5	23.6	23	24.2	25.5	26.4
						1000hPa Td (℃) based on design charts									
4	467080	Yilan宜蘭(#61)	7.2	121.73	24.77	Pressure (hPa)	1000	998.5	996.1	992.4	989	983.6	980.1	977.2	974.9
						Dew Point Observation Td (℃)	22.6	21.9	24	24.7	24.3	24.6	25.2	24.7	25.8
						Calculated 1000hPa Td (℃)	22.6	21.9	24	24.7	24.3	24.6	25.2	24.7	25.8
						1000hPa Td (℃) based on design charts									

Beginning of Core Rainfall

(Note: Representative Highest Persisting 12-hr Dew Point prior to Core Rainfall: Yongkang 23.3°C, Gaoxiong 24.60°C, Average 24.0°C)

Appendix K

Computer Outputs from Three Tests for Selecting GEV Distribution to Best Fit the Dew Point Series

Computer Output for Test 1: Monte Carlo Simulation Test

```
  1-day, Annual Maximum, YR                                    1 SITES

 No.    n     stnID      LAT          LONG       ELV    L-CV   L-SKEW  L-KURT   D(I)
  1     50  01-0001 114.17000000  22.30000000   32    0.0076  0.0588  0.0823   1.00

    WEIGHTED MEANS        0.0076  0.0588  0.0823

PARAMETERS OF REGIONAL KAPPA DISTRIBUTION    0.9915  0.0171  0.3401  0.3452


***** GOODNESS-OF-FIT MEASURES *****
(NUMBER OF SIMULATIONS  =  1000)

 1 GEN. LOGISTIC       (GLO)   L-KURTOSIS= 0.170   Z VALUE=  2.21 (Fail *)
 2 GEN. EXTREME VALUE  (GEV)   L-KURTOSIS= 0.116   Z VALUE=  0.87 (Pass  ) (the best)
 3 GEN. NORMAL         (GNO)   L-KURTOSIS= 0.126   Z VALUE=  1.10 (Pass  )
 4 PEARSON TYPE III    (PE3)   L-KURTOSIS= 0.123   Z VALUE=  1.05 (Pass  )
 5 GEN. PARETO         (GPA)   L-KURTOSIS= 0.015   Z VALUE= -1.67 (Fail *)
 6 GUMBEL              (GUM)   L-KURTOSIS= 0.150   Z VALUE=  1.73 (Fail *)
 7 NORMAL              (NOR)   L-KURTOSIS= 0.123   Z VALUE=  1.03 (Pass  )


PARAMETER ESTIMATES FOR DISTRIBUTIONS ACCEPTED AT THE 90% LEVEL

GEN. EXTREME VALUE      0.995     0.013     0.181
GEN. NORMAL             0.999     0.013    -0.120
PEARSON TYPE III        1.000     0.014     0.360
NORMAL                  1.000     0.013     0.000
WAKEBY                  0.974     0.083     8.367     0.025    -0.482

QUANTILE ESTIMATES
                     0.010  0.020  0.050  0.100  0.200  0.500  0.900  0.950  0.990  0.999
GEN. EXTREME VALUE   0.972  0.975  0.979  0.983  0.988  0.999  1.018  1.024  1.034  1.044
GEN. NORMAL          0.972  0.975  0.979  0.983  0.988  0.999  1.018  1.024  1.035  1.049
PEARSON TYPE III     0.972  0.975  0.979  0.983  0.988  0.999  1.018  1.024  1.035  1.049
NORMAL               0.969  0.972  0.978  0.983  0.989  1.000  1.017  1.022  1.031  1.042
WAKEBY               0.975  0.976  0.979  0.983  0.988  0.999  1.019  1.024  1.030  1.034


ALL DATA PROCESSED
```

Computer Output for Test 2: Root Mean Square Error of the Sample L-moments Test

The input file is: am01d_00.4cr

==========The results are: ============

DT4	MEAN	MNAB	RMSE		
-0.03435	-0.03435	0.03435	0.03435	--- GEV	
-0.08725	-0.08725	0.08725	0.08725	--- GLO	
0.06726	0.06726	0.06726	0.06726	--- GPA	
-0.04320	-0.04320	0.04320	0.04320	--- GNO	
-0.04115	-0.04115	0.04115	0.04115	--- PE3	
-0.03435	-0.03435	0.03435	0.03435	--- GEV	(1)
-0.04115	-0.04115	0.04115	0.04115	--- PE3	(2)
-0.04320	-0.04320	0.04320	0.04320	--- GNO	(3)
0.06726	0.06726	0.06726	0.06726	--- GPA	(4)
-0.08725	-0.08725	0.08725	0.08725	--- GLO	(5)

Computer Output for Test 3: Real-data-check Test

```
 The input data name: dur01.max                                          The conversion factor =    1.000

 ========================================================================
 This input file is a composite data set of one 1day-set with one 24hour-set.
 The 1-day data will be multiplied by the factor to convert to 24-hour.
 ========================================================================

 Start searching missing data in input file:


 No missing data found!


 ============================================================================

REGIONAL ANALYSIS, UNBIASED L-MOMENTS


The real input data:

Number of eligible stations, Name of state:   1,    1-day, Annual Maximum, YR

                                                      MEAN    LAMBDA2    L-Cv     L-Cs     L-Ck     TAU5

SITE    1 (011961) 01-0001 ANMAX         N= 50    L-M. RATIOS: 26.1480   0.1988   0.0076   0.0588   0.0823   0.0054

 The sum of means=  26.15;  nsite=    1;  The average mean=  26.15


Average number of years=          50
Maximum number of years=          50
Minimum number of years=          50


REGIONAL AVERAGE L-MOMENT RATIOS    1.0000    0.0076    0.0588    0.0823    0.0054
```

```
--------------------------------End of L-moment ratios------------------------------------------------------

################################################## List   of Quantiles ######## ###########################################

PARAMETER ESTIMATION: FAIL FLAG**


==================================================================================================================================================
### ( 1) When the distribution you selected to fit is Exponential (EXP)

Plotting position parameters of P=(m+A)/(n+B): A= 0.00     B= 0.00

Number of  daily  and  hourly stations:    1;   0

REGIONAL exp PARAMETERS      0.9848      0.0152      0.0000      0.0000      0.0000

                                                                                                          QUANTILES
NON-EXCEEDANCE PROBABILITY:                                        0.3680 0.5000 0.8000 0.9000 0.9600 0.9800 0.9900 0.9950 0.9980 0.9990 0.99980.9999
RETURN YEARS:                                                      1.58-Y  2-YR   5-YR  10-Y   25-Y   50-Y   100-Y  200-Y  500-Y  1000Y  5000y 10000y

 No  stnID    LAT     LONG     ELEV TYPE  N  Reg   max     mean
-----------------------------------------------------------------------------------------------------------------------------------------------------
REGIONAL GROWTH FACTORS:                                           0.992  0.995  1.009  1.020  1.034  1.044  1.055  1.065  1.079  1.090  1.114  1.125

  1 01-0001 114.1700  22.3000   32  01D  50 Rda ( 26.90) [ 26.15]  25.93  26.03  26.39  26.67  27.03  27.31  27.58  27.86  28.22  28.50  29.14  29.41

PARAMETER ESTIMATION: FAIL FLAG**


==================================================================================================================================================
### ( 2) When the distribution you selected to fit is Gamma (GAM)

Plotting position parameters of P=(m+A)/(n+B): A= 0.00     B= 0.00

Number of  daily  and  hourly stations:    1;   0

REGIONAL gam PARAMETERS   5507.8438      0.0002      0.0000      0.0000      0.0000
```


Table of Contents
Table of Contents
Table of Contents

QUANTILES

NON-EXCEEDANCE PROBABILITY:											0.3680	0.5000	0.8000	0.9000	0.9600	0.9800	0.9900	0.9950	0.9980	0.9990	0.99980.9999
RETURN YEARS:											1.58-Y	2-YR	5-YR	10-Y	25-Y	50-Y	100-Y	200-Y	500-Y	1000Y	5000y 10000y
No	stnID	LAT	LONG	ELEV	TYPE	N	Reg	max	mean												
REGIONAL GROWTH FACTORS:											0.995	1.000	1.011	1.017	1.024	1.028	1.032	1.035	1.039	1.042	1.048 1.051
1	01-0001	114.1700	22.3000	32	01D	50	Rda	(26.90)	[26.15]		26.03	26.15	26.44	26.60	26.77	26.88	26.97	27.06	27.17	27.25	27.41 27.48

PARAMETER ESTIMATION: FAIL FLAG**

==

(3) When the distribution you selected to fit is Gumbel (GUM)

Plotting position parameters of P=(m+A)/(n+B): A= 0.00   B= 0.00

Number of daily and hourly stations: 1;   0

REGIONAL gum PARAMETERS   0.9937   0.0110   0.0000   0.0000   0.0000

QUANTILES

NON-EXCEEDANCE PROBABILITY:											0.3680	0.5000	0.8000	0.9000	0.9600	0.9800	0.9900	0.9950	0.9980	0.9990	0.99980.9999
RETURN YEARS:											1.58-Y	2-YR	5-YR	10-Y	25-Y	50-Y	100-Y	200-Y	500-Y	1000Y	5000y 10000y
No	stnID	LAT	LONG	ELEV	TYPE	N	Reg	max	mean												
REGIONAL GROWTH FACTORS:											0.994	0.998	1.010	1.018	1.029	1.036	1.044	1.052	1.062	1.069	1.087 1.095
1	01-0001	114.1700	22.3000	32	01D	50	Rda	(26.90)	[26.15]		25.98	26.09	26.41	26.63	26.90	27.10	27.30	27.50	27.76	27.96	28.42 28.62

PARAMETER ESTIMATION: FAIL FLAG**

==

(4) When the distribution you selected to fit is Normal (NOR)

Plotting position parameters of P=(m+A)/(n+B): A= 0.00   B= 0.00

Table of Contents
Table of Contents
Table of Contents

Number of daily and hourly stations: 1; 0

REGIONAL nor PARAMETERS 1.0000 0.0135 0.0000 0.0000 0.0000

						QUANTILES						
NON-EXCEEDANCE PROBABILITY:	0.3680	0.5000	0.8000	0.9000	0.9600	0.9800	0.9900	0.9950	0.9980	0.9990	0.9998	0.9999
RETURN YEARS:	1.58-Y	2-YR	5-YR	10-Y	25-Y	50-Y	100-Y	200-Y	500-Y	1000Y	5000y	10000y
REGIONAL GROWTH FACTORS:	0.995	1.000	1.011	1.017	1.024	1.028	1.031	1.035	1.039	1.042	1.048	1.050

No	stnID	LAT	LONG	ELEV	TYPE	N	Reg	max	mean										
1	01-0001	114.1700	22.3000	32	01D	50	Rda	(26.90)	[26.15]	26.03	26.15	26.44	26.60	26.76	26.87	26.97	27.06	27.16	27.24	27.40	27.46

==========

(5) When the distribution you selected to fit is Kappa (KAP)

Plotting position parameters of P=(m+A)/(n+B): A= 0.00 B= 0.00

Number of daily and hourly stations: 1; 0

REGIONAL kap PARAMETERS 0.9915 0.0171 0.3401 0.3454 0.0000

						QUANTILES						
NON-EXCEEDANCE PROBABILITY:	0.3680	0.5000	0.8000	0.9000	0.9600	0.9800	0.9900	0.9950	0.9980	0.9990	0.9998	0.9999
RETURN YEARS:	1.58-Y	2-YR	5-YR	10-Y	25-Y	50-Y	100-Y	200-Y	500-Y	1000Y	5000y	10000y
REGIONAL GROWTH FACTORS:	0.994	0.999	1.012	1.018	1.025	1.028	1.031	1.033	1.036	1.037	1.039	1.039

No	stnID	LAT	LONG	ELEV	TYPE	N	Reg	max	mean										
1	01-0001	114.1700	22.3000	32	01D	50	Rda	(26.90)	[26.15]	26.00	26.12	26.46	26.63	26.80	26.89	26.96	27.02	27.08	27.11	27.16	27.18

==========

(6) When the distribution you selected to fit is Wakeby (WAK)

Plotting position parameters of P=(m+A)/(n+B): A= 0.00 B= 0.00

Number of daily and hourly stations: 1; 0

REGIONAL wak PARAMETERS 0.9744 0.0834 8.3833 0.0248 -0.4825

							QUANTILES						
NON-EXCEEDANCE PROBABILITY:							0.3680	0.5000	0.8000	0.9000	0.9600	0.9800	0.9900
RETURN YEARS:							1.58-Y	2-YR	5-YR	10-Y	25-Y	50-Y	100-Y

No	stnID	LAT	LONG	ELEV	TYPE	N	Reg	max	mean													
REGIONAL GROWTH FACTORS:										0.994	0.999	1.012	1.019	1.025	1.028	1.030	1.032	1.033	1.034	1.035	1.035
1	01-0001	114.1700	22.3000	32	01D	50	Rda	(26.90)	[26.15]	26.00	26.12	26.46	26.64	26.80	26.88	26.94	26.98	27.02	27.04	27.06	27.07

==========

(7) When the distribution you selected to fit is Generalized Extreme Value (GEV)

Plotting position parameters of P=(m+A)/(n+B): A= 0.00 B= 0.00

Number of daily and hourly stations: 1; 0

REGIONAL gev PARAMETERS 0.9947 0.0126 0.1809 0.0000 0.0000

							QUANTILES						
NON-EXCEEDANCE PROBABILITY:							0.3680	0.5000	0.8000	0.9000	0.9600	0.9800	0.9900
RETURN YEARS:							1.58-Y	2-YR	5-YR	10-Y	25-Y	50-Y	100-Y

No	stnID	LAT	LONG	ELEV	TYPE	N	Reg	max	mean													
REGIONAL GROWTH FACTORS:										0.995	0.999	1.011	1.018	1.025	1.030	1.034	1.038	1.042	1.044	1.050	1.051
1	01-0001	114.1700	22.3000	32	01D	50	Rda	(26.90)	[26.15]	26.01	26.13	26.44	26.62	26.81	26.93	27.04	27.13	27.24	27.31	27.44	27.49

==========

(8) When the distribution you selected to fit is Generalized Logistic (GLO)

Plotting position parameters of P=(m+A)/(n+B): A= 0.00 B= 0.00

Number of daily and hourly stations: 1; 0

REGIONAL glo PARAMETERS 0.9993 0.0076 -0.0588 0.0000 0.0000

						QUANTILES						
NON-EXCEEDANCE PROBABILITY:	0.3680	0.5000	0.8000	0.9000	0.9600	0.9800	0.9900	0.9950	0.9980	0.9990	0.9998	0.9999
RETURN YEARS:	1.58-Y	2-YR	5-YR	10-Y	25-Y	50-Y	100-Y	200-Y	500-Y	1000Y	5000y	10000y
No stnID LAT LONG ELEV TYPE N Reg max mean												
REGIONAL GROWTH FACTORS:	0.995	0.999	1.010	1.017	1.026	1.032	1.039	1.046	1.056	1.064	1.083	1.092
1 01-0001 114.1700 22.3000 32 01D 50 Rda (26.90) [26.15]	26.02	26.13	26.41	26.59	26.82	26.99	27.17	27.36	27.61	27.81	28.31	28.54

==========

(9) When the distribution you selected to fit is Generalized Normal (GNO)

Plotting position parameters of P=(m+A)/(n+B): A= 0.00 B= 0.00

Number of daily and hourly stations: 1; 0

REGIONAL gno PARAMETERS 0.9992 0.0134 -0.1205 0.0000 0.0000

						QUANTILES						
NON-EXCEEDANCE PROBABILITY:	0.3680	0.5000	0.8000	0.9000	0.9600	0.9800	0.9900	0.9950	0.9980	0.9990	0.9998	0.9999
RETURN YEARS:	1.58-Y	2-YR	5-YR	10-Y	25-Y	50-Y	100-Y	200-Y	500-Y	1000Y	5000y	10000y
No stnID LAT LONG ELEV TYPE N Reg max mean												
REGIONAL GROWTH FACTORS:	0.995	0.999	1.011	1.018	1.025	1.030	1.035	1.040	1.045	1.049	1.058	1.062
1 01-0001 114.1700 22.3000 32 01D 50 Rda (26.90) [26.15]	26.01	26.13	26.44	26.61	26.81	26.94	27.07	27.18	27.33	27.44	27.67	27.77

==========

(10) When the distribution you selected to fit is Generalized Pareto (GPA)

Plotting position parameters of P=(m+A)/(n+B): A= 0.00 B= 0.00

Number of daily and hourly stations: 1; 0

REGIONAL gpa PARAMETERS 0.9789 0.0375 0.7778 0.0000 0.0000

							QUANTILES						
NON-EXCEEDANCE PROBABILITY:						0.3680	0.5000	0.8000	0.9000	0.9600	0.9800	0.9900	0.9950	0.9980	0.9990	0.9998	0.9999
RETURN YEARS:						1.58-Y	2-YR	5-YR	10-Y	25-Y	50-Y	100-Y	200-Y	500-Y	1000Y	5000y	10000y
No	stnID	LAT	LONG	ELEV	TYPE N Reg	max	mean										
REGIONAL GROWTH FACTORS:						0.993	0.999	1.013	1.019	1.023	1.025	1.026	1.026	1.027	1.027	1.027	1.027
?	1	01-0001	114.1700	22.3000	32 01D 50 Rda (26.90) [26.15]	25.97	26.12	26.50	26.65	26.75	26.80	26.82	26.84	26.85	26.85	26.86	26.86

==========

(11) When the distribution you selected to fit is Pearson III (PE3)

Plotting position parameters of P=(m+A)/(n+B): A= 0.00 B= 0.00

Number of daily and hourly stations: 1; 0

REGIONAL pe3 PARAMETERS 1.0000 0.0135 0.3606 0.0000 0.0000

							QUANTILES						
NON-EXCEEDANCE PROBABILITY:						0.3680	0.5000	0.8000	0.9000	0.9600	0.9800	0.9900	0.9950	0.9980	0.9990	0.9998	0.9999
RETURN YEARS:						1.58-Y	2-YR	5-YR	10-Y	25-Y	50-Y	100-Y	200-Y	500-Y	1000Y	5000y	10000y
No	stnID	LAT	LONG	ELEV	TYPE N Reg	max	mean										
REGIONAL GROWTH FACTORS:						0.995	0.999	1.011	1.018	1.025	1.030	1.035	1.039	1.045	1.049	1.057	1.061
	1	01-0001	114.1700	22.3000	32 01D 50 Rda (26.90) [26.15]	26.01	26.13	26.44	26.61	26.81	26.94	27.06	27.18	27.32	27.42	27.65	27.74

##########End of List of Quantiles##########

=====Summary of Regional Growth Factors=========

PROBABILITY:	0.6320	0.5000	0.2000	0.1000	0.0400	0.0200	0.0100	0.0050	0.0020	0.0010	0.0002	0.0001

REGIONAL GROWTH FACTORS:	0.992	0.995	1.009	1.020	1.034	1.044	1.055	1.065	1.079	1.090	1.114	1.125	--- exp
REGIONAL GROWTH FACTORS:	0.995	1.000	1.011	1.017	1.024	1.028	1.032	1.035	1.039	1.042	1.048	1.051	--- gam
REGIONAL GROWTH FACTORS:	0.994	0.998	1.010	1.018	1.029	1.036	1.044	1.052	1.062	1.069	1.087	1.095	--- gum
REGIONAL GROWTH FACTORS:	0.995	1.000	1.011	1.017	1.024	1.028	1.031	1.035	1.039	1.042	1.048	1.050	--- nor
REGIONAL GROWTH FACTORS:	0.994	0.999	1.012	1.018	1.025	1.028	1.031	1.033	1.036	1.037	1.039	1.039	--- kap
REGIONAL GROWTH FACTORS:	0.994	0.999	1.012	1.019	1.025	1.028	1.030	1.032	1.033	1.034	1.035	1.035	--- wak
REGIONAL GROWTH FACTORS:	0.995	0.999	1.011	1.018	1.025	1.030	1.034	1.038	1.042	1.044	1.050	1.051	--- gev
REGIONAL GROWTH FACTORS:	0.995	0.999	1.010	1.017	1.026	1.032	1.039	1.046	1.056	1.064	1.083	1.092	--- glo
REGIONAL GROWTH FACTORS:	0.995	0.999	1.011	1.018	1.025	1.030	1.035	1.040	1.045	1.049	1.058	1.062	--- gno
REGIONAL GROWTH FACTORS:	0.993	0.999	1.013	1.019	1.023	1.025	1.026	1.026	1.027	1.027	1.027	1.027	--- gpa
REGIONAL GROWTH FACTORS:	0.995	0.999	1.011	1.018	1.025	1.030	1.035	1.039	1.045	1.049	1.057	1.061	--- pe3

----THE RESULTS OF REALDATA CHECK ARE AS FOLLOWING:

	2-YR	5-YR	10-YR	25-YR	50-YR	100-YR	
Theoretical probabilities:	0.5000	0.2000	0.1000	0.0400	0.0200	0.0100	
Empirical frequencies:	0.5800	0.2800	0.0800	0.0000	0.0000	0.0000	--- exp
Relative errors (%):	16.00	40.00	20.00	100.00	100.00	100.00	
Empirical frequencies:	0.4800	0.2400	0.0800	0.0600	0.0200	0.0000	--- gam
Relative errors (%):	4.00	20.00	20.00	50.00	0.00	100.00	
Empirical frequencies:	0.5800	0.2400	0.0800	0.0200	0.0000	0.0000	--- gum
Relative errors (%):	16.00	20.00	20.00	50.00	100.00	100.00	

```
Empirical frequencies:      0.4800  0.2400  0.1400  0.0600  0.0200  0.0000  --- nor
Relative errors ( % ):        4.00   20.00   40.00   50.00    0.00  100.00

Empirical frequencies:      0.4800  0.2400  0.0800  0.0600  0.0200  0.0000  --- kap
Relative errors ( % ):        4.00   20.00   20.00   50.00    0.00  100.00

Empirical frequencies:      0.4800  0.2400  0.0800  0.0600  0.0200  0.0000  --- wak
Relative errors ( % ):        4.00   20.00   20.00   50.00    0.00  100.00

Empirical frequencies:      0.4800  0.2400  0.0800  0.0200  0.0000  0.0000  --- gev
Relative errors ( % ):        4.00   20.00   20.00   50.00  100.00  100.00

Empirical frequencies:      0.4800  0.2400  0.1400  0.0200  0.0000  0.0000  --- glo
Relative errors ( % ):        4.00   20.00   40.00   50.00  100.00  100.00

Empirical frequencies:      0.4800  0.2400  0.0800  0.0200  0.0000  0.0000  --- gno
Relative errors ( % ):        4.00   20.00   20.00   50.00  100.00  100.00

Empirical frequencies:      0.4800  0.2400  0.0800  0.0600  0.0600  0.0200  --- gpa
Relative errors ( % ):        4.00   20.00   20.00   50.00  200.00  100.00

Empirical frequencies:      0.4800  0.2400  0.0800  0.0200  0.0000  0.0000  --- pe3
Relative errors ( % ):        4.00   20.00   20.00   50.00  100.00  100.00

================================================================================

 Rank       2-year              5-year             10-year             25-year             50-year

      DIS    RE  SCORE    DIS    RE  SCORE    DIS    RE  SCORE    DIS    RE  SCORE    DIS    RE  SCORE

  1   gev  4.00   3.0     gev 20.00   3.0     gev 20.00   3.5     gev 50.00   3.5     gev100.00   3.5
  2   glo  4.00   3.0     glo 20.00   3.0     gno 20.00   3.5     glo 50.00   3.5     glo100.00   3.5
```

3	gno	4.00	3.0	gno	20.00	3.0	gpa	20.00	3.5	gno	50.00	3.5	gno100.00	3.5
4	gpa	4.00	3.0	gpa	20.00	3.0	pe3	20.00	3.5	pe3	50.00	3.5	pe3100.00	3.5
5	pe3	4.00	3.0	pe3	20.00	3.0	glo	40.00	1.0	gpa	50.00	1.0	gpa200.00	1.0

The final score for each of the five distributions: (The higher score, the better DIS.)

GEV score = 16.5
GLO score = 14.0
GNO score = 16.5
GPA score = 11.5
PE3 score = 16.5

If there is a tie on score, the 100-year Relative errrs (%) will serve as tie-break.
(The lower RE, the better DIS.)

Table of Contents
Table of Contents
Table of Contents

Appendix L

Southeast China Sea Surface Temperature (SST) Isolines

Data type: Monthly average of SST isolines (Jan - Dec)
Location: SE China
Data period: 1960 - 2010
Source: NOAA global SST data

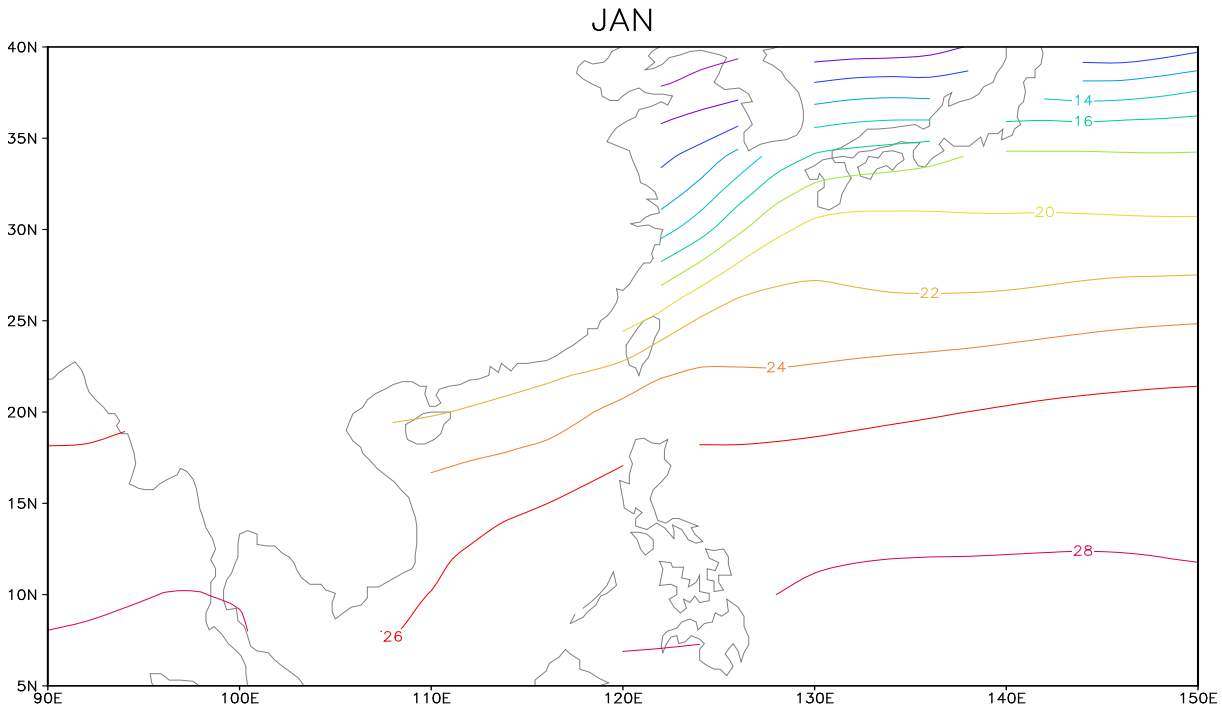

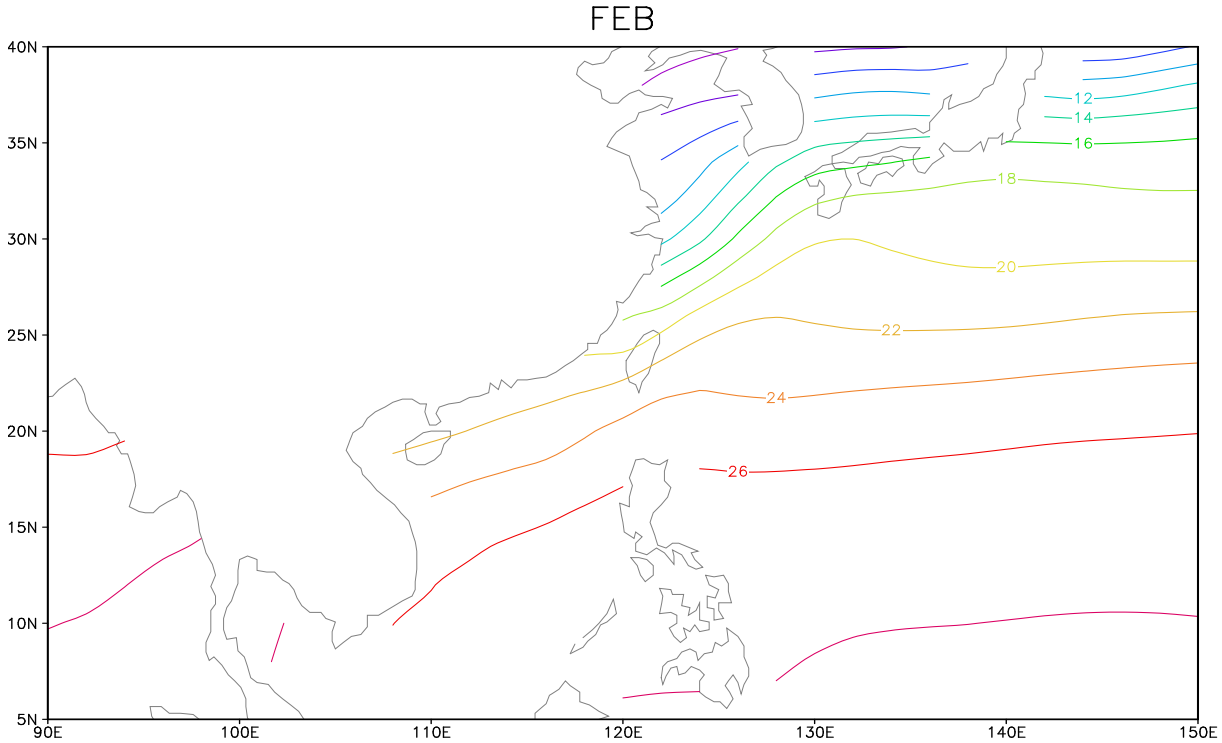

Table of Contents
Table of Contents
Table of Contents
Table of Contents

MAR

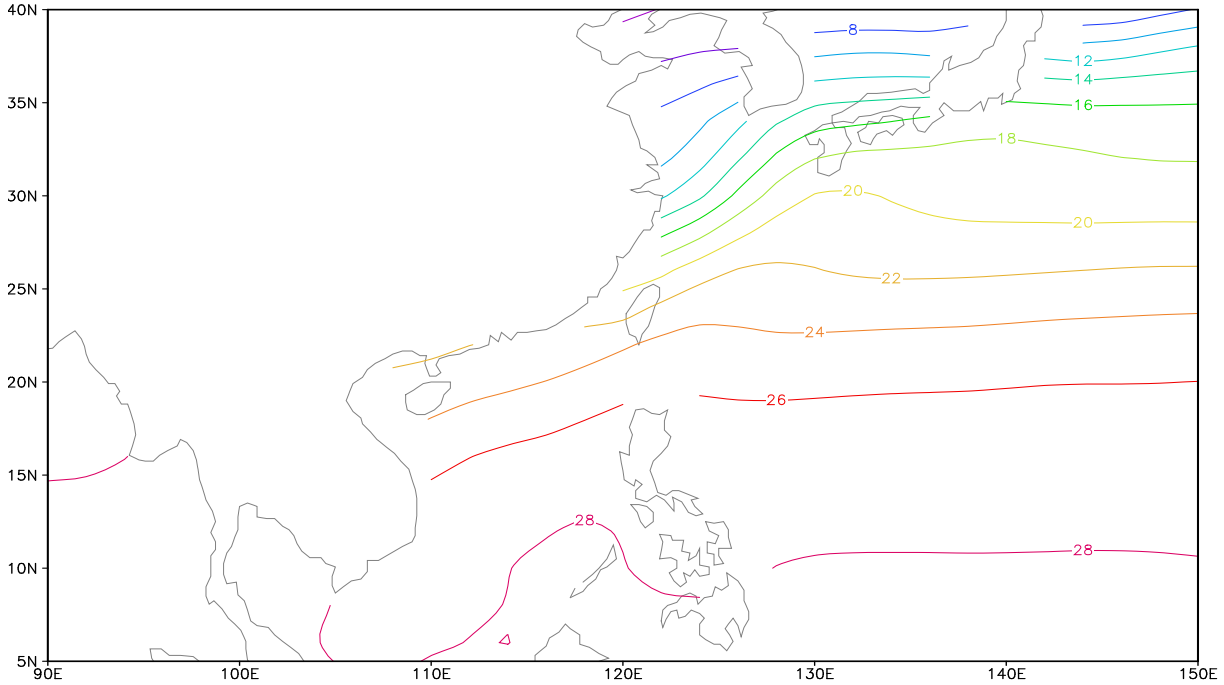

APR

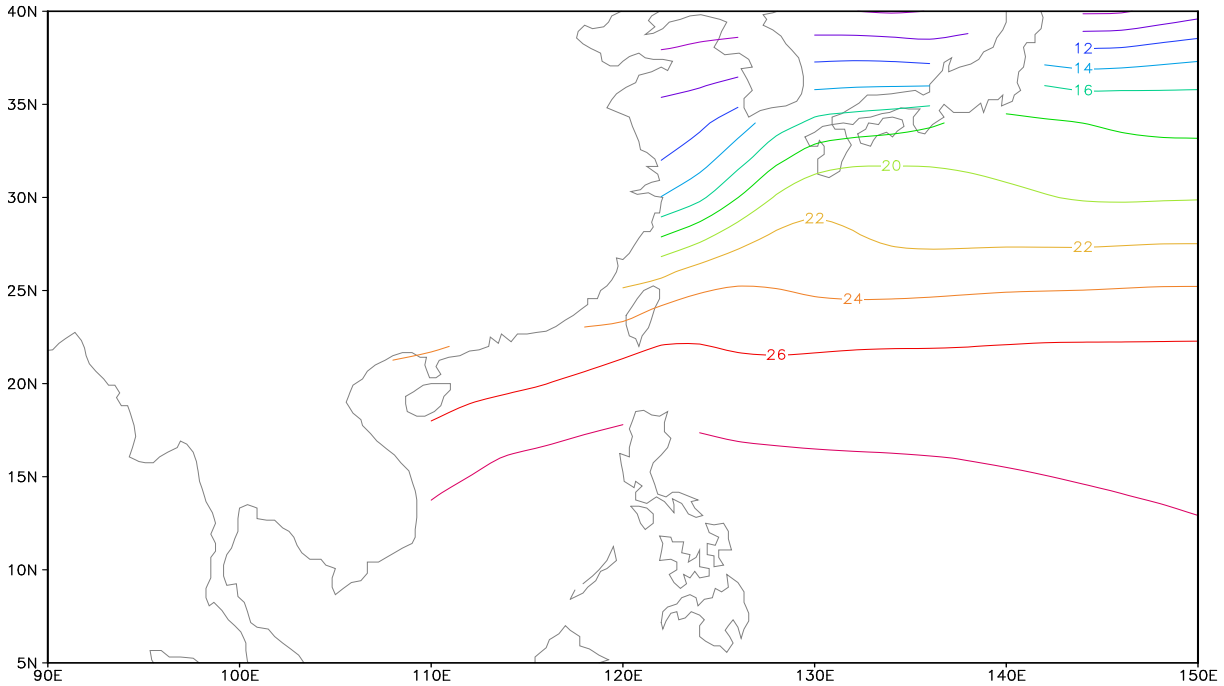

MAY

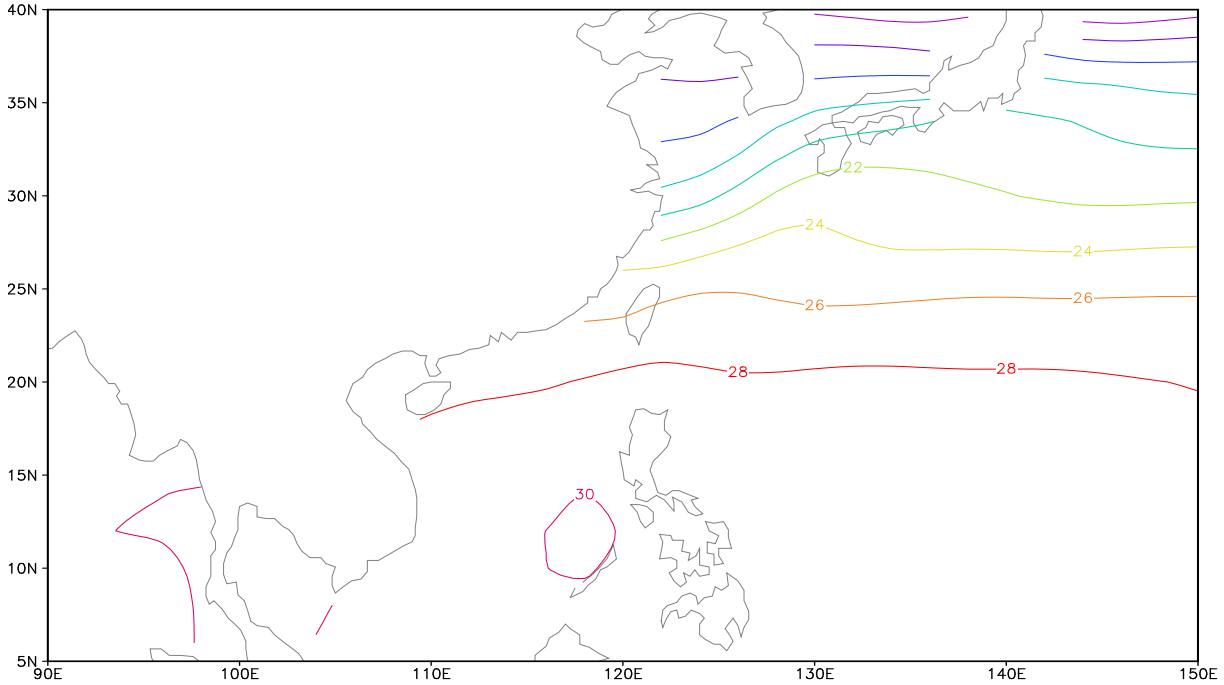

JUN

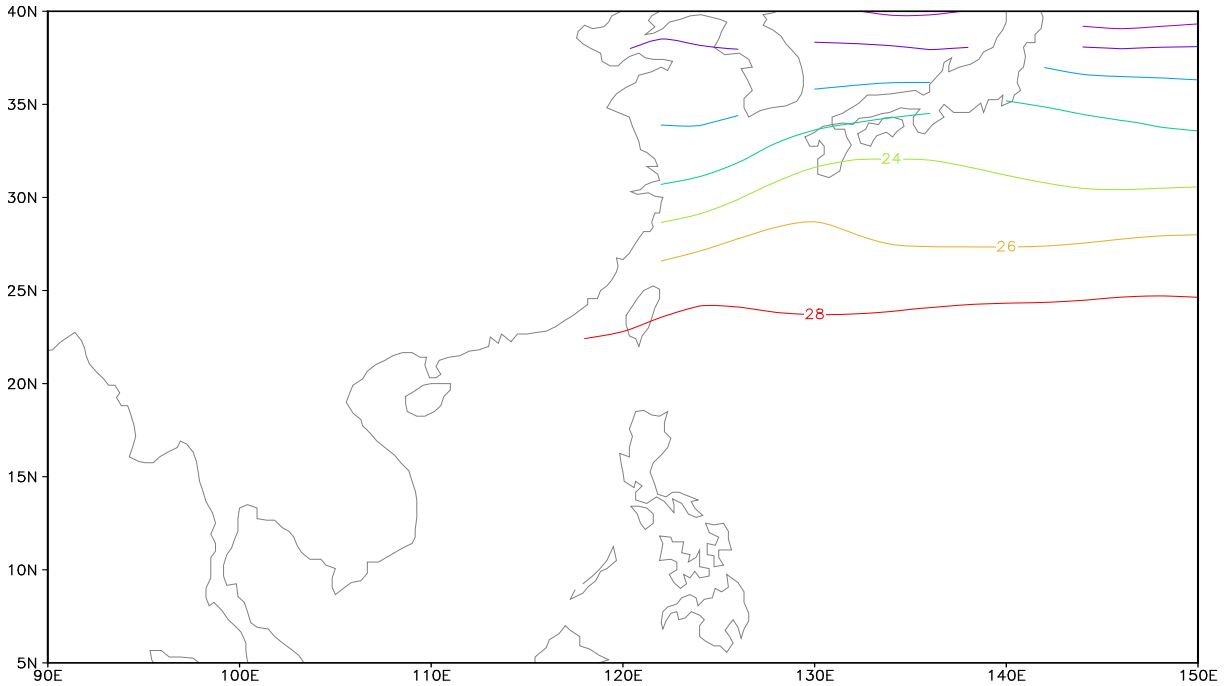

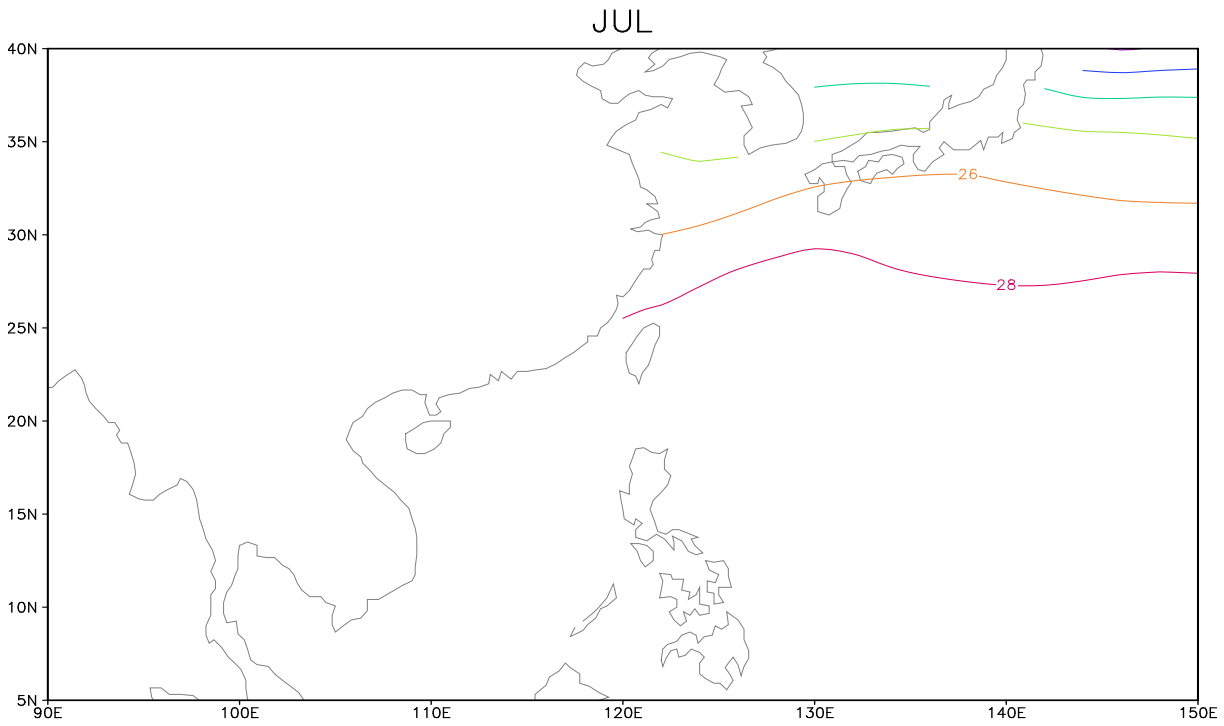

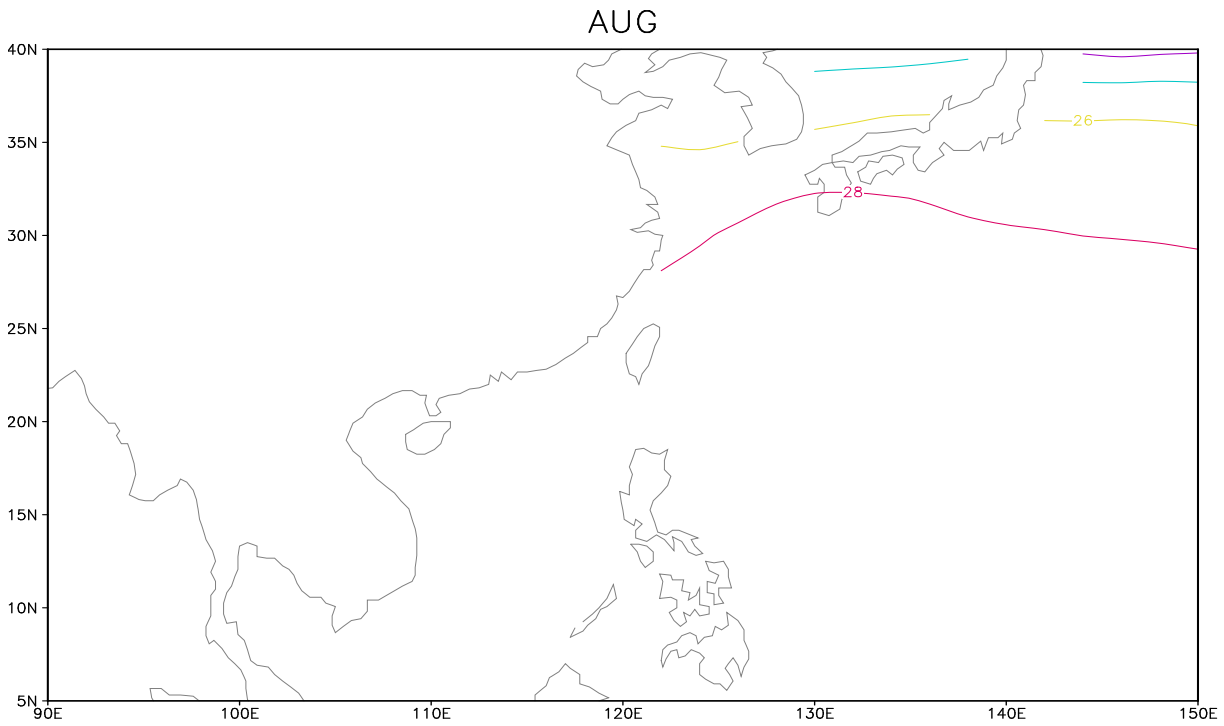

Table of Contents
Table of Contents
Table of Contents
Table of Contents

SEP

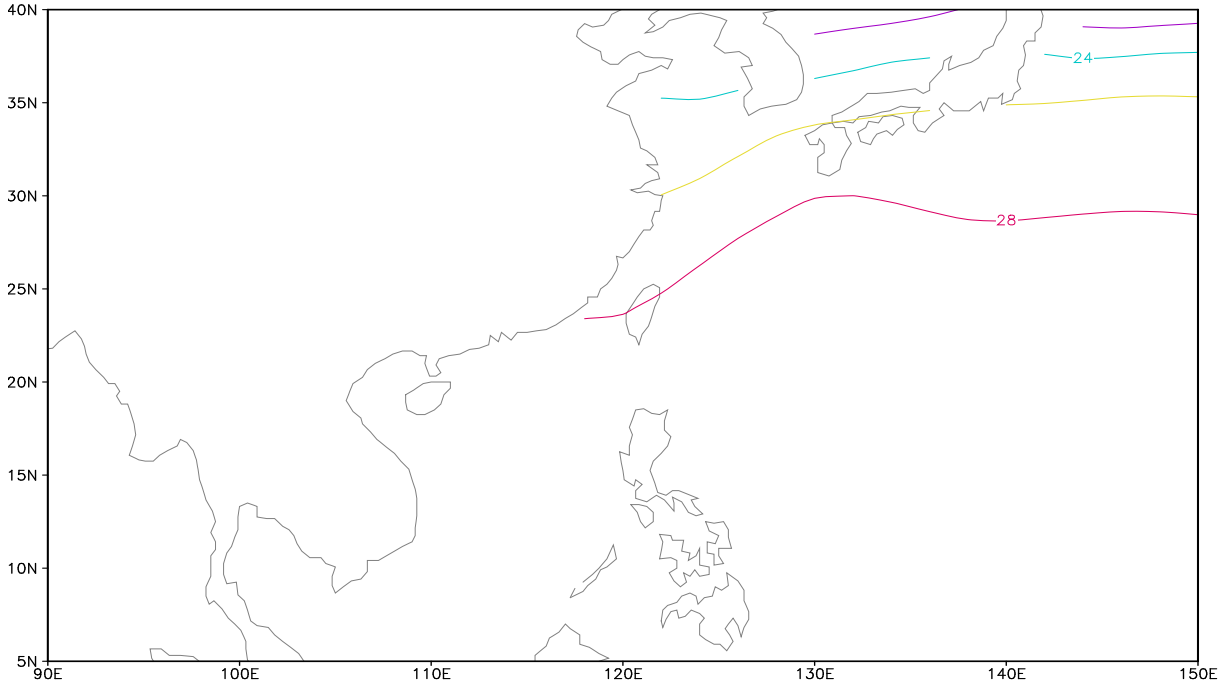

OCT

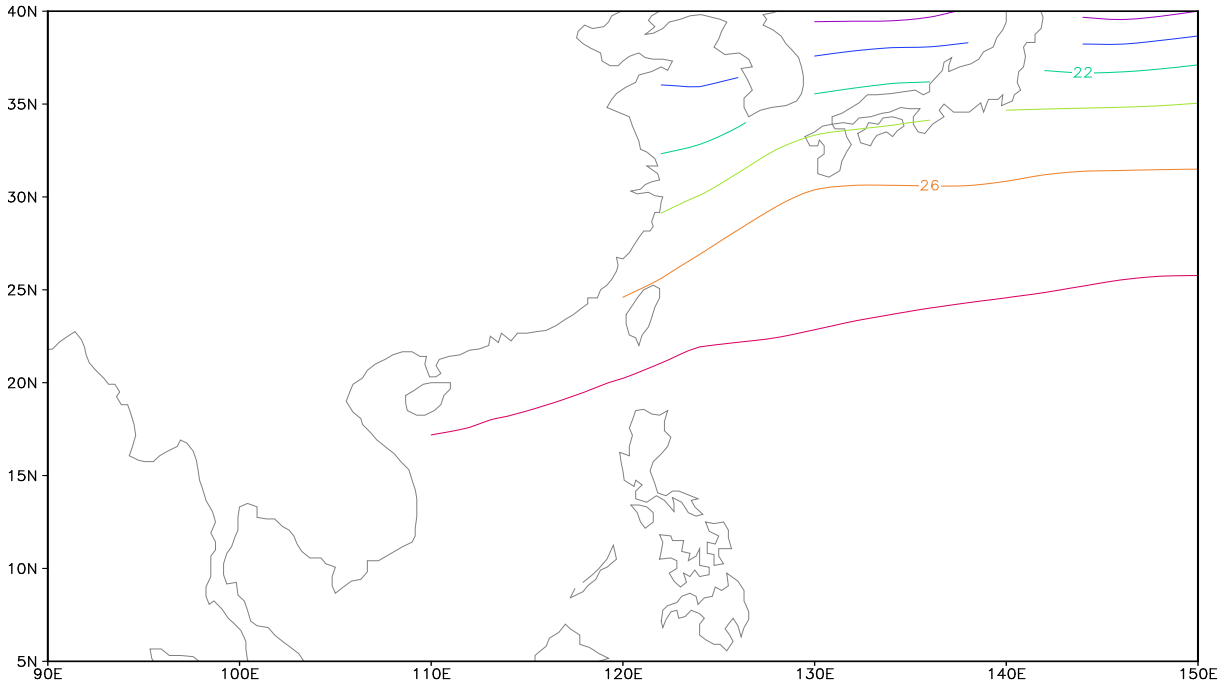

NOV

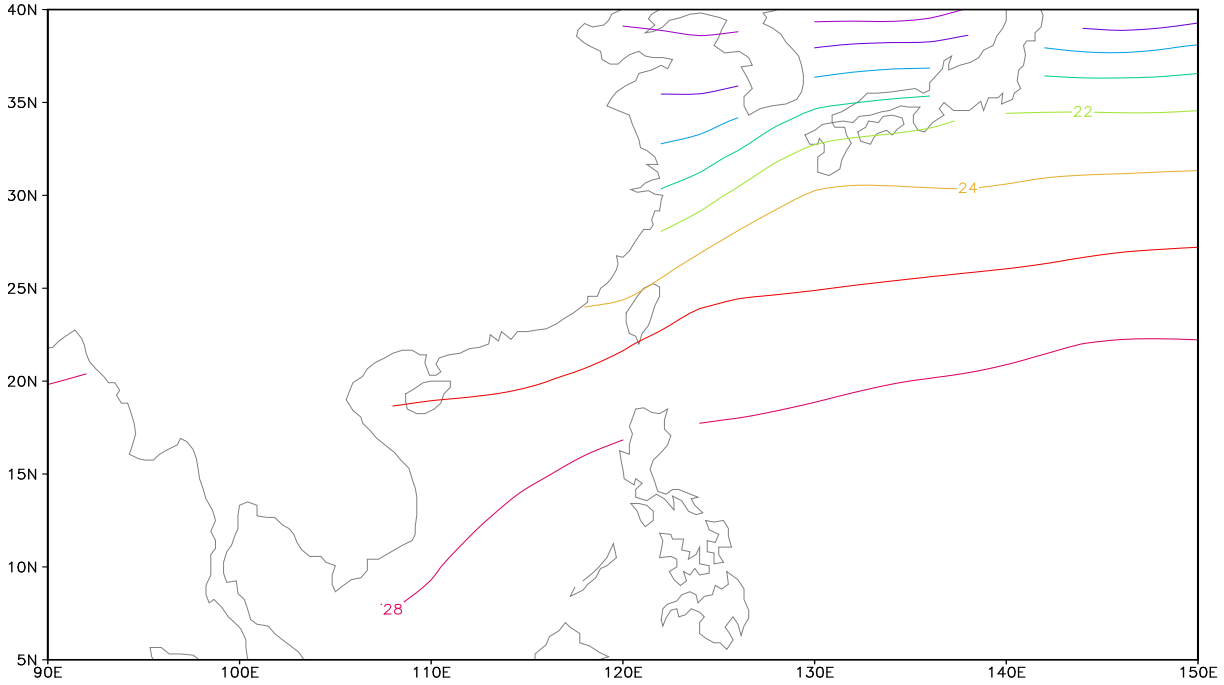

DEC

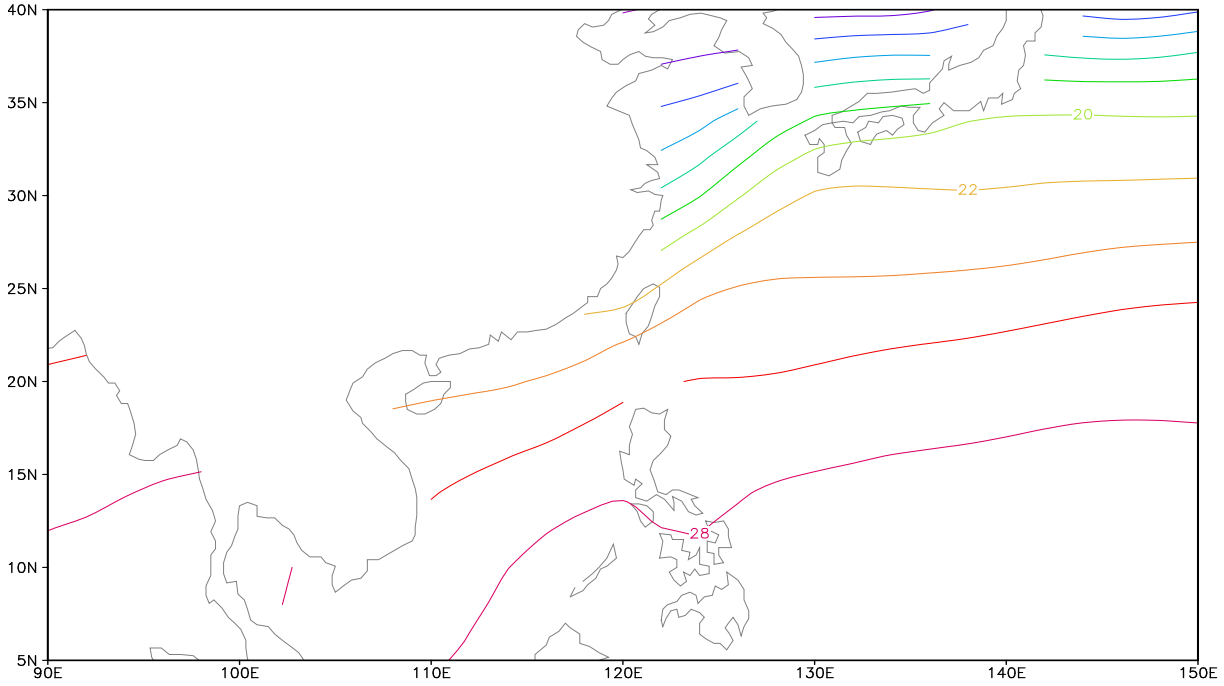

Table of Contents
Table of Contents
Table of Contents

Appendix M

24-hour Isohyets from Storm Transposition with Moisture Maximization

Contents

M.1 Moisture-maximized 24-hour Isohyets for Storm Transposition Centered at Tai Mo Shan

E-W orientation - 0°

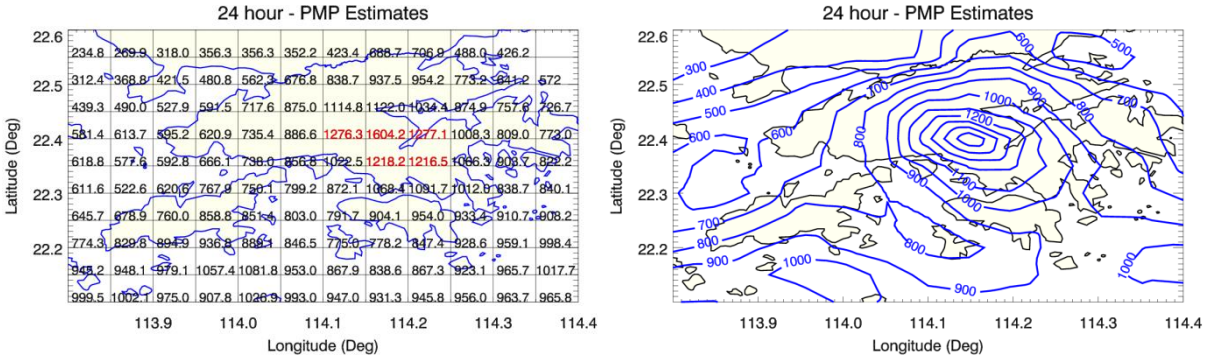

ENE-WSW orientation - 22.5°

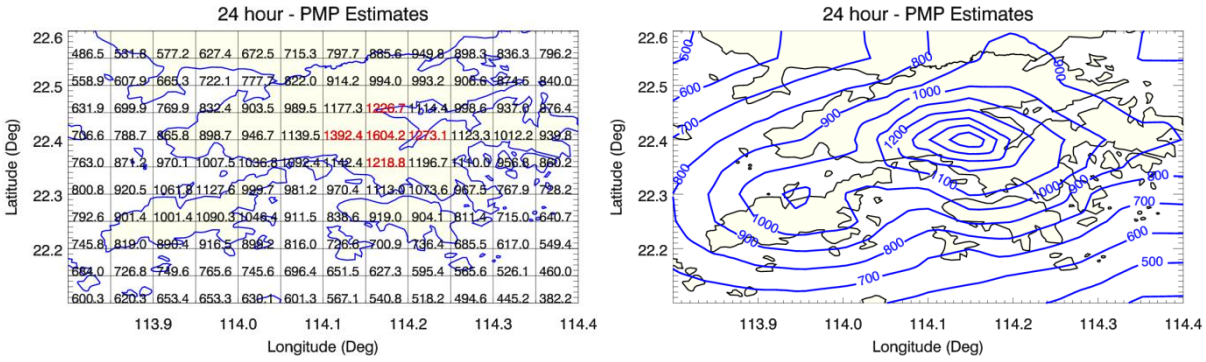

NE-SW orientation - 45°

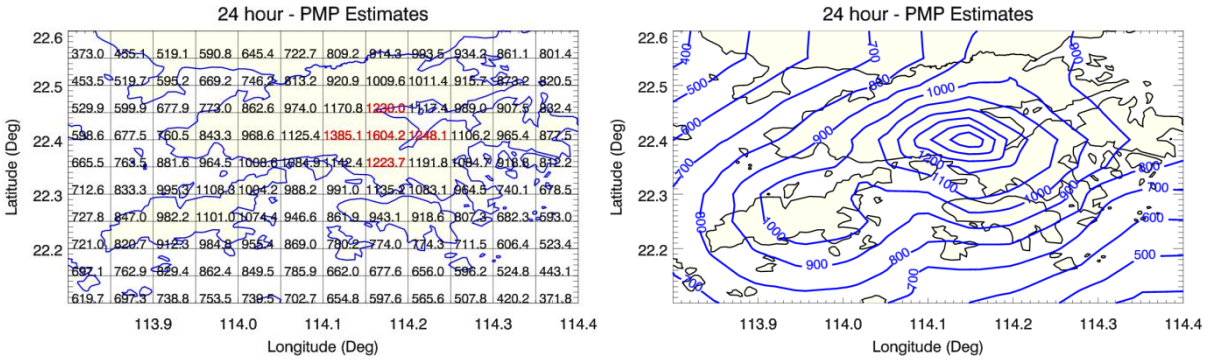

NNE-SSW orientation - 67.5°

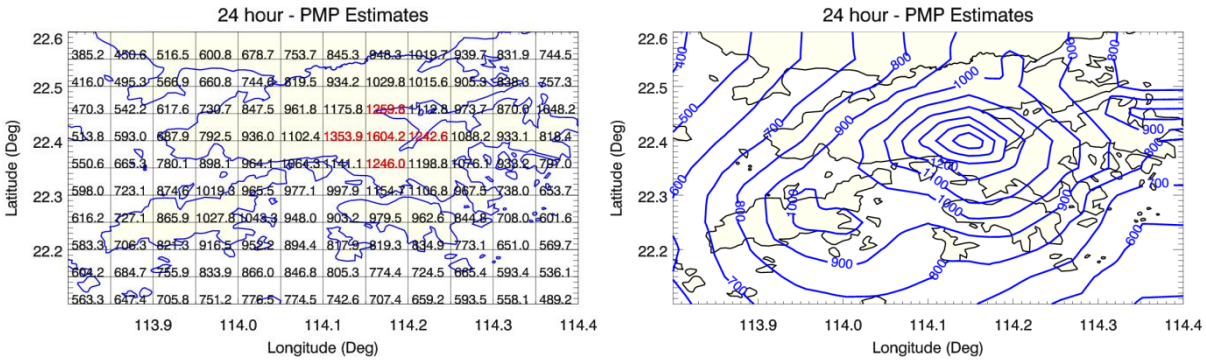

Table of Contents
Table of Contents
Table of Contents
Table of Contents

N-S orientation - 85°

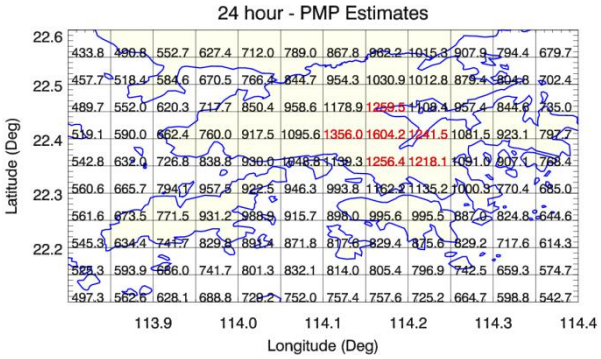

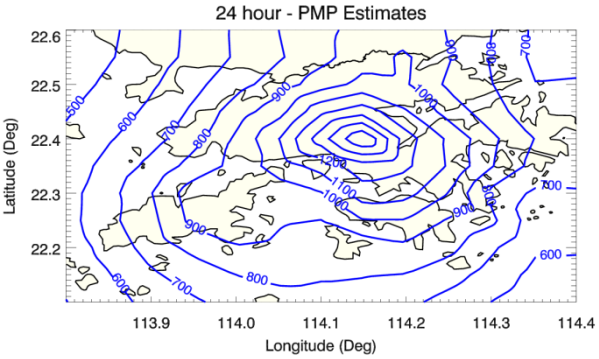

NNW-SSE orientation - 112.5°

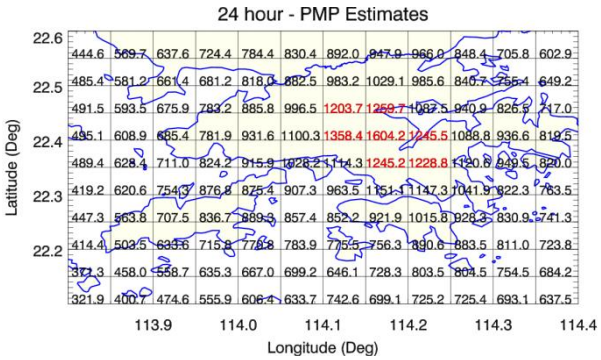

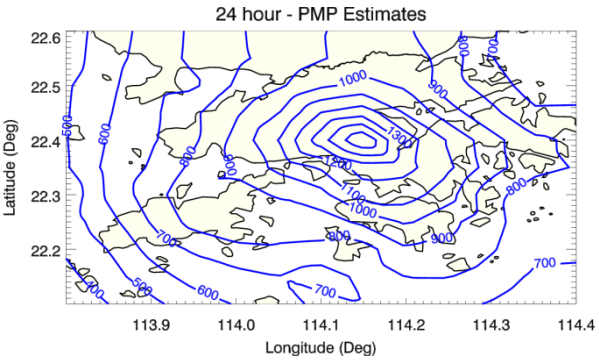

NW-SE orientation - 135°

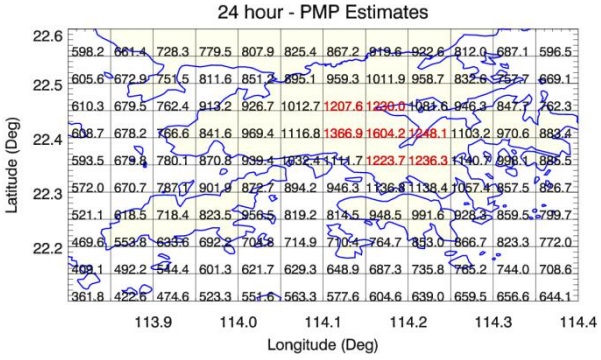

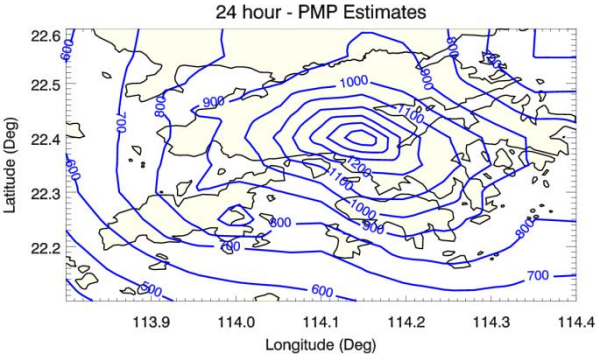

WNW-ESE orientation - 157.5°

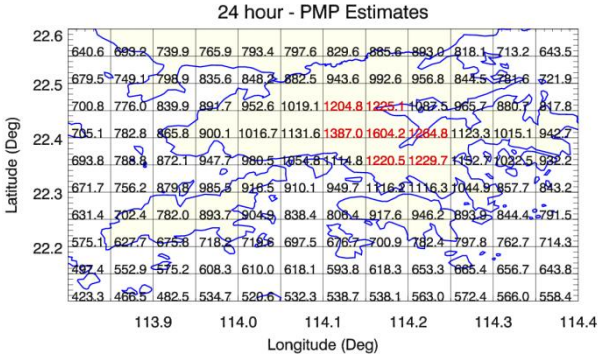

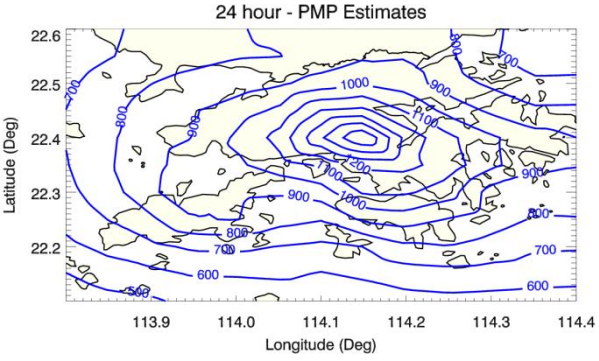

Table of Contents
Table of Contents
Table of Contents
Table of Contents

M.2 Moisture-maximized 24-hour Isohyets for Storm Transposition Centered at Lantau

E-W orientation - 0°

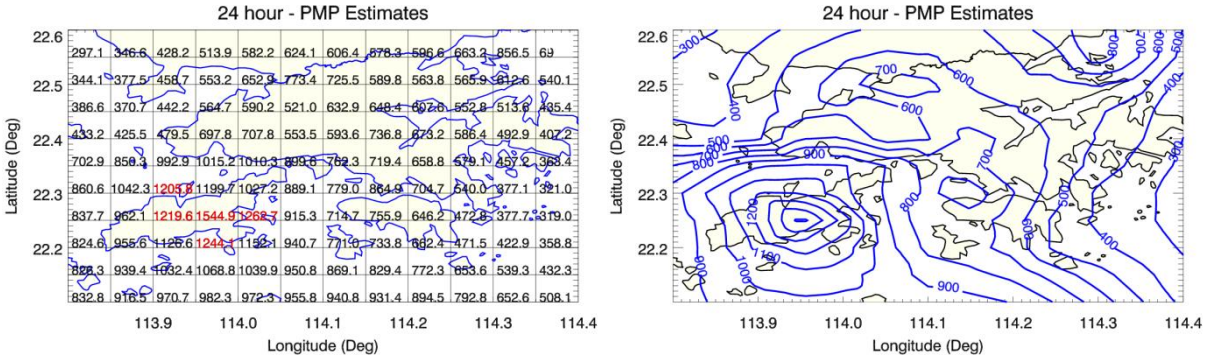

ENE-WSW orientation - 22.5°

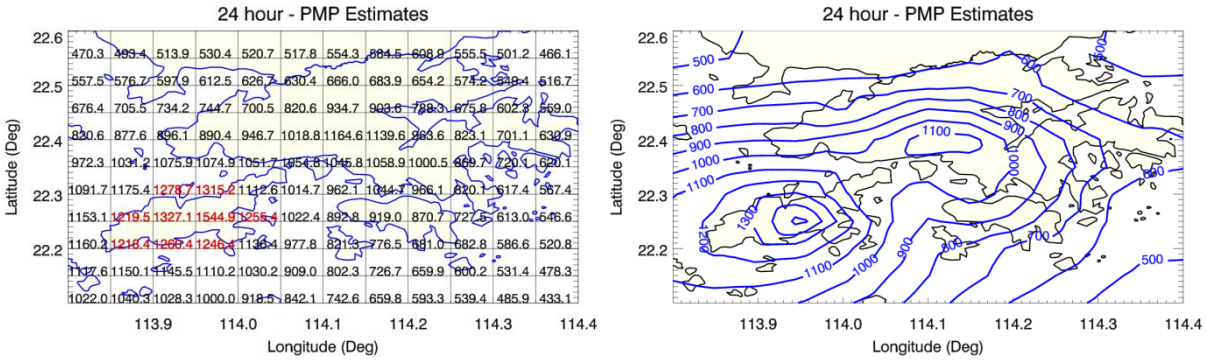

NE-SW orientation - 45°

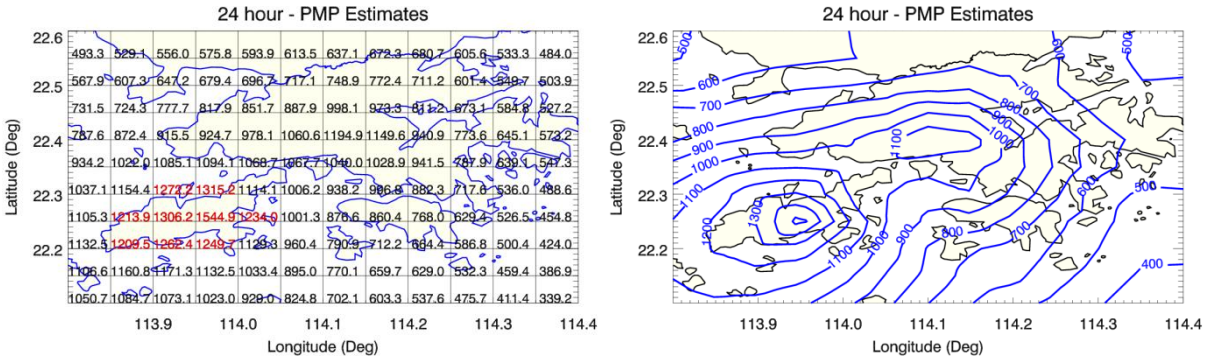

NNE-SSW orientation - 67.5°

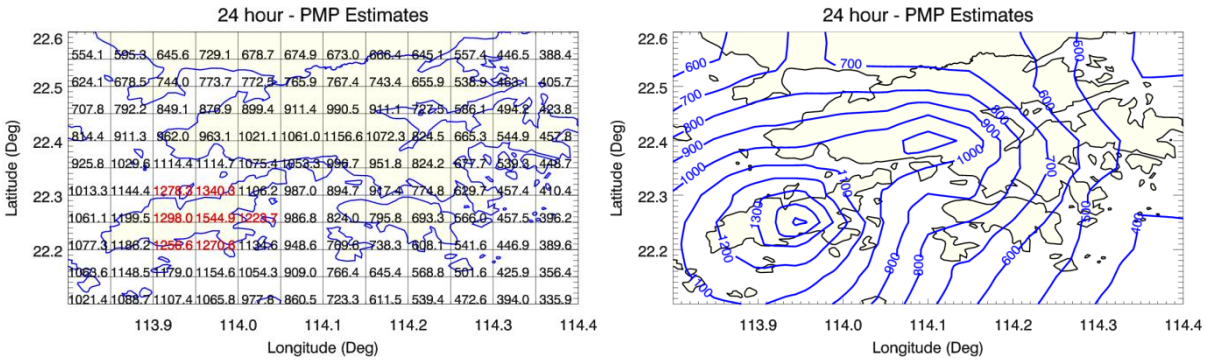

Table of Contents
Table of Contents
Table of Contents
Table of Contents

N-S orientation - 85°

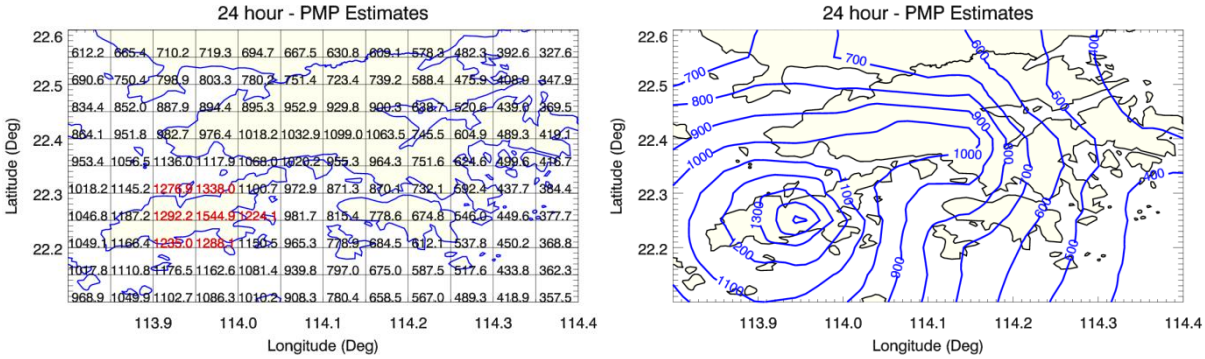

NNW-SSE orientation - 112.5°

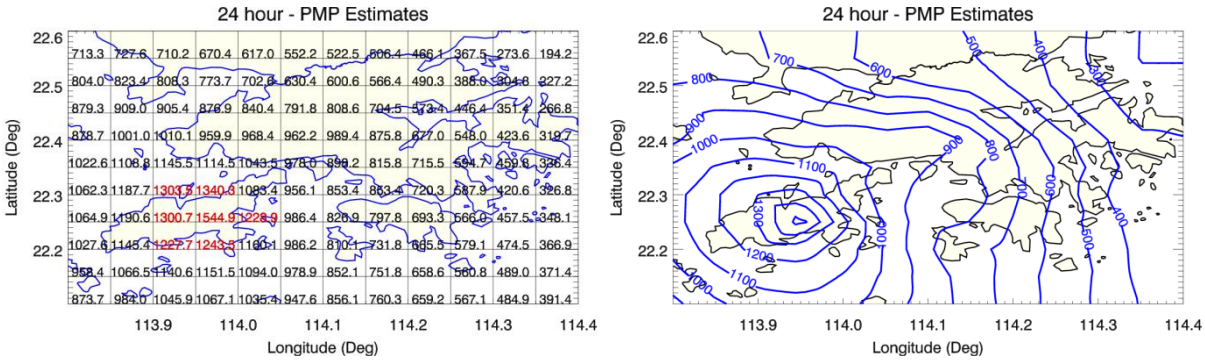

NW-SE orientation - 135°

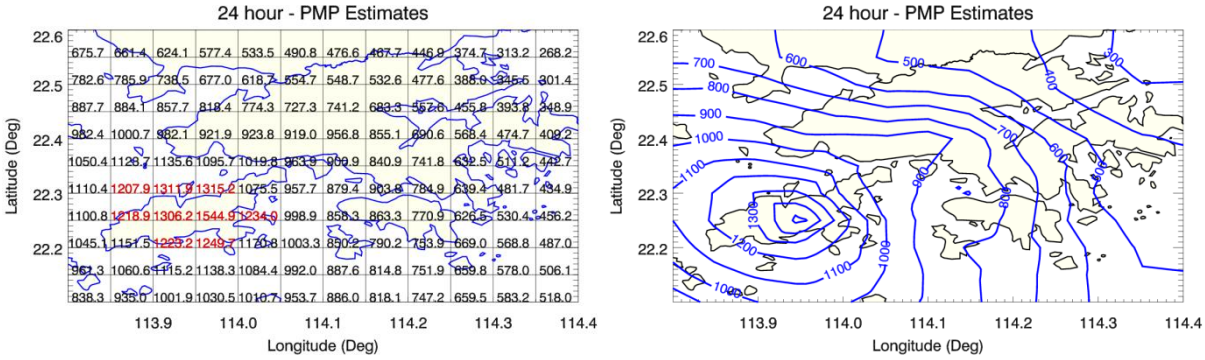

WNW-ESE orientation - 157.5°

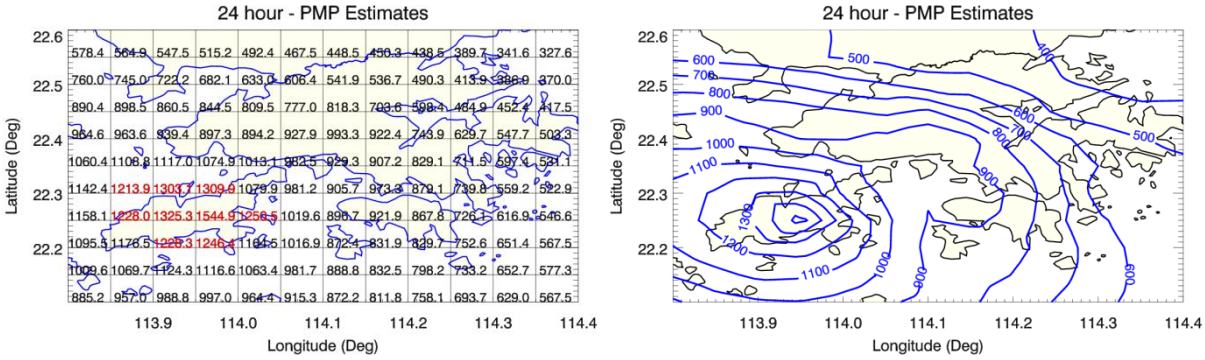

Table of Contents
Table of Contents
Table of Contents
Table of Contents

M.3 Moisture-maximized 24-hour Isohyets for Storm Transposition Centered at Hong Kong Island

E-W orientation - 0°

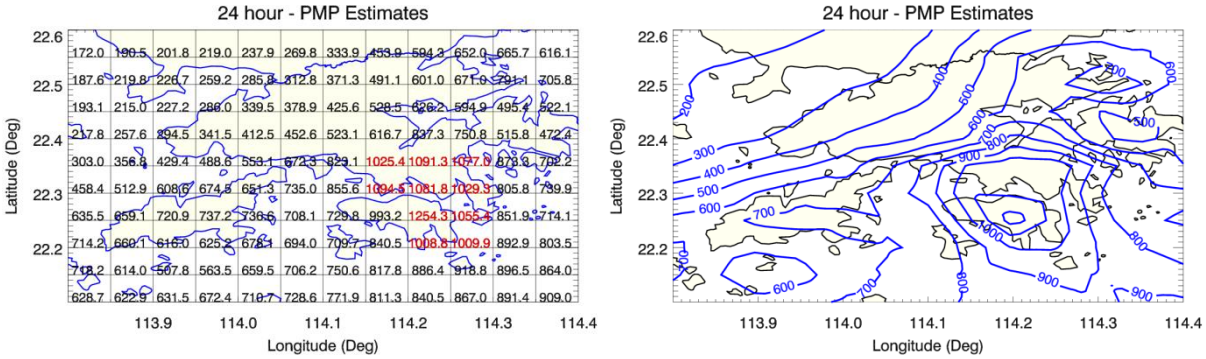

ENE-WSW orientation - 22.5°

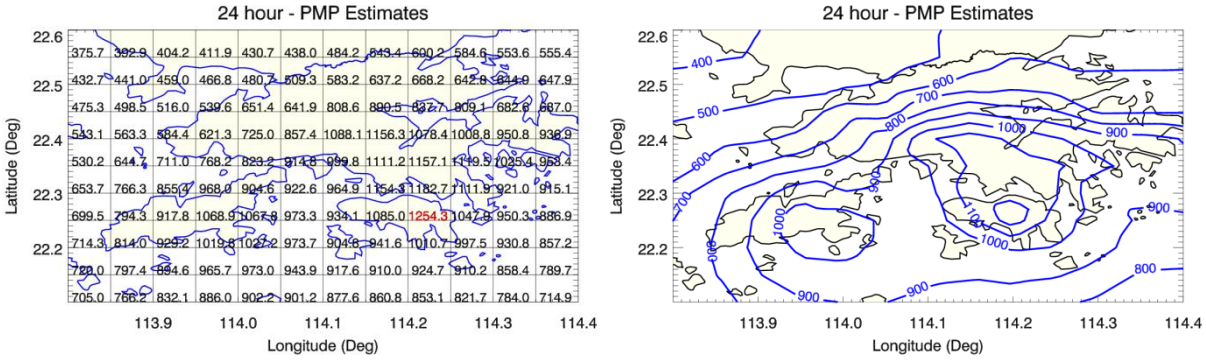

NE-SW orientation - 45°

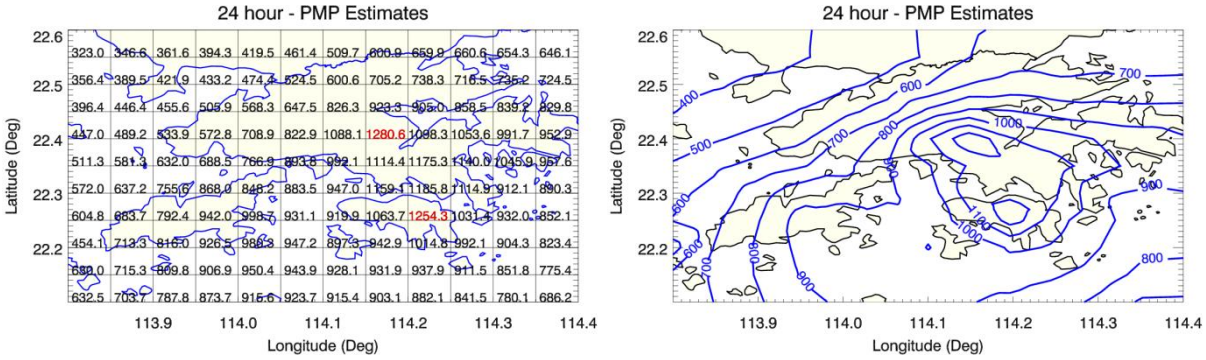

NNE-SSW orientation - 67.5°

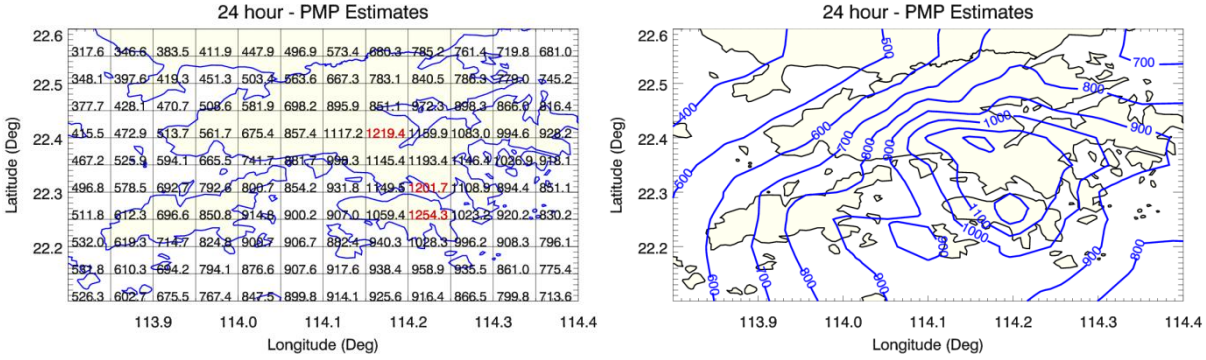

Table of Contents
Table of Contents
Table of Contents
Table of Contents

N-S orientation - 85°

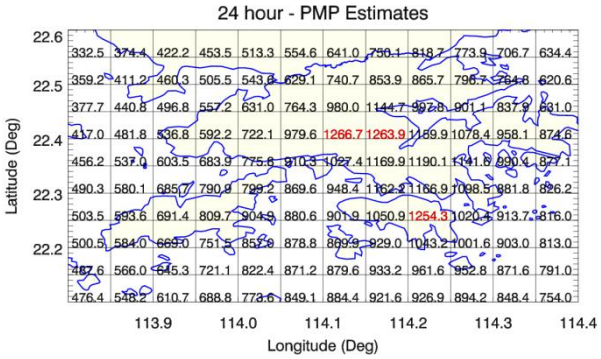

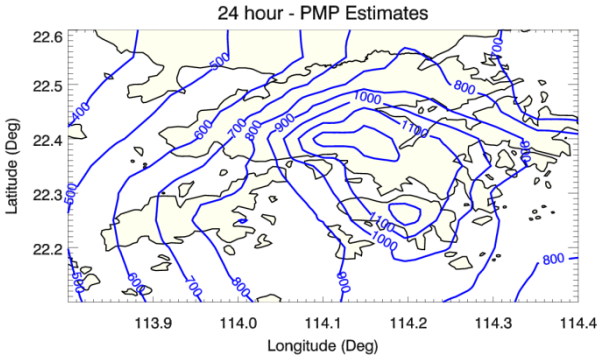

NNW-SSE orientation - 112.5°

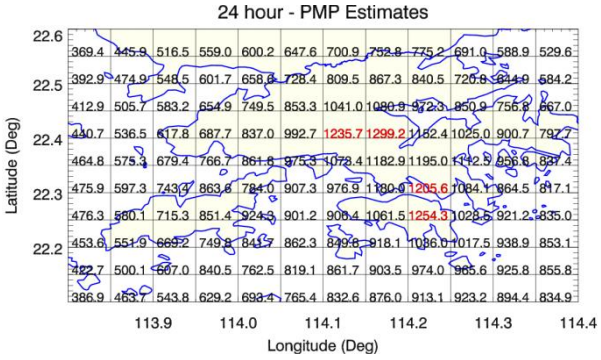

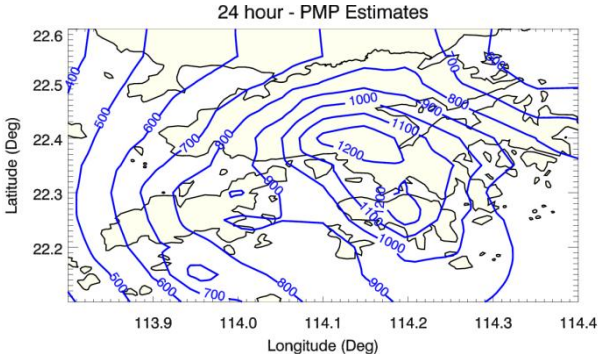

NW-SE orientation - 135°

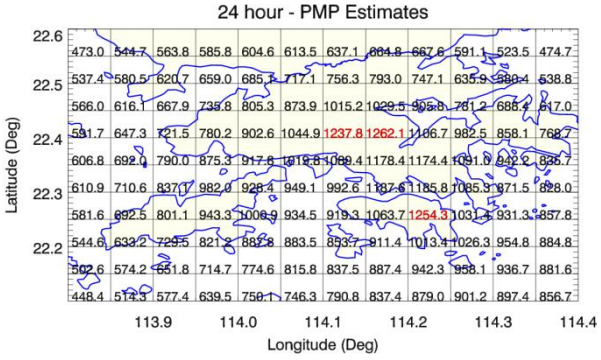

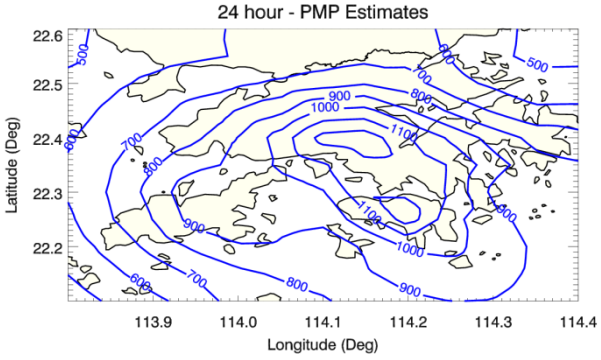

WNW-ESE orientation - 157.5°

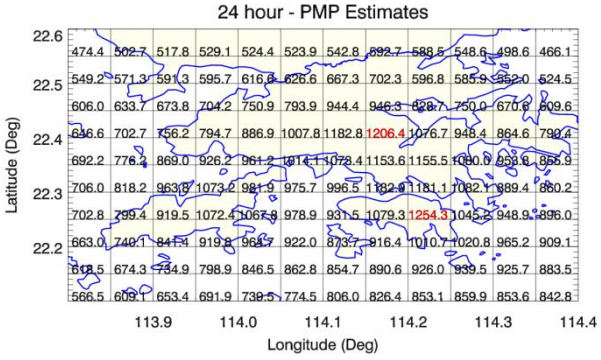

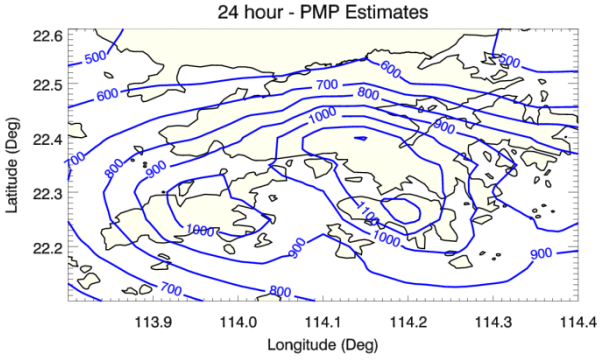

Table of Contents
Table of Contents
Table of Contents
Table of Contents

Appendix N

Steps for Calculation of Moisture Maximization Ratios for Local Storms

Contents

N.1 Steps for Calculation Moisture Maximization Ratios for Local Storms

1. Calculate the maximum mean 12-hour dew point map [(1)].

2. Choose the stations with 12-hour maximum consistent dew points.

1966	HKO					
	23.8					
1976	HKO					
	24.1					
1993	CCH	HKO	HKS	SHA	TKL	KP
	22	21.3	21.3	20.8	21.3	20.8
1994	HKO	SKG				
	24.8	24.9				
2008	HKS	WGL	TYW	CCH		
	23	23.2	23.8	23.8		
1970	HKO					
	24.9					
1971	HKO					
	24.2					
1972 (1)	HKO					
	23.0					
1972 (2)	HKO					
	25.6					
1972 (3)	HKO					
	24.2					
1973	HKO					
	25.3					
1981	HKO					
	24.0					
1983	HKO					
	24.7					
1989	HKO					
	22.7					
1997	CCH	HKO				
	26.1	25.3				
2003	CCH	HKS				
	23.6	23.7				
2005	LFS	SEK	SSH	TKL		
	25.0	25.6	25.1	25.1		

[(1)] Use a 12-hour window to pick up the maximum persisting 12-hour dew point from a period of 24-hour prior to the onset of the corresponding major intensified rainfall.

3. Calculate the corresponding 1000 hPa dew points.

1966	HKO						Mean Dew Point
	23.93						23.93
1976	HKO						
	24.23						24.23
1993	CCH (72 m)	HKO	HKS	SHA	TKL	KP	
	22.384	21.4707	21.3267	20.84	21.38	21.1467	21.42
1994	HKO	SKG					
	24.93	24.9167					24.92
2008	HKS (5 m)	WGL (56 m)	TYW (5 m)	CCH (72 m)			
	23.02	23.43	23.82	24.10			23.59
1970	HKO						
	25.03						25.03
1971	HKO						
	24.33						24.33
1972 (1)	HKO						
	23.13						23.13
1972 (2)	HKO						
	25.73						25.73
1972 (3)	HKO						
	24.33						24.33
1973	HKO						
	25.43						25.43
1981	HKO						
	24.13						24.13
1983	HKO						
	24.83						24.83
1989	HKO						
	22.87						22.87
1997	CCH	HKO					
	26.39	25.43					25.91
2003	CCH	HKS					
	23.90	23.72					23.81
2005	LFS	SEK	SSH	TKL			
	25.12	25.66	25.14	25.16			25.27

4. HKO station is chosen for calculation the historical 12-hour maximum consistent dew point, which is then converted it to the corresponding 1000 hPa dew point.

   The 100-yr return period of the historical 12-hour maximum consistent dew point at HKO, which is calculated based on the newest data from HKO data between 1961 and 2010 that were best fitted by GEV distribution via regional L-moments Analysis, is 27.04. The corresponding 1000 hPa dew point is 27.17.

5. Find the PW values through the Table A1 of (WMO, 2009).

1966	73.13 mm
1976	75.06 mm
1993	58.535 mm
1994	79.596 mm
2008	70.909 mm
1970	80.290 mm
1971	75.697 mm
1972 (1)	68.070 mm
1972 (2)	85.237 mm
1972 (3)	75.697 mm
1973	83.065 mm
1981	74.417 mm
1983	78.985 mm
1989	66.484 mm
1997	86.557 mm
2003	72.325 mm
2005	81.983 mm
Historical Max	**96.48 mm**

6. Use the equation $r = (W_2/W_1)$ to calculate the maximization factor.

1966	1.32
1976	1.29
1993	1.65
1994	1.21
2008	1.36
1970	1.20
1971	1.27
1972 (1)	1.42
1972 (2)	1.13
1972 (3)	1.27
1973	1.16
1981	1.30
1983	1.22
1989	1.45
1997	1.11
2003	1.33
2005	1.18

Appendix O

Results of DAD Analyses

Contents

List of Tables

List of Figures

Based on the lists of top storms for 24-hour rainfalls as shown in Tables 2.1, 2.2 and 2.4, the following DAD curves are produced:

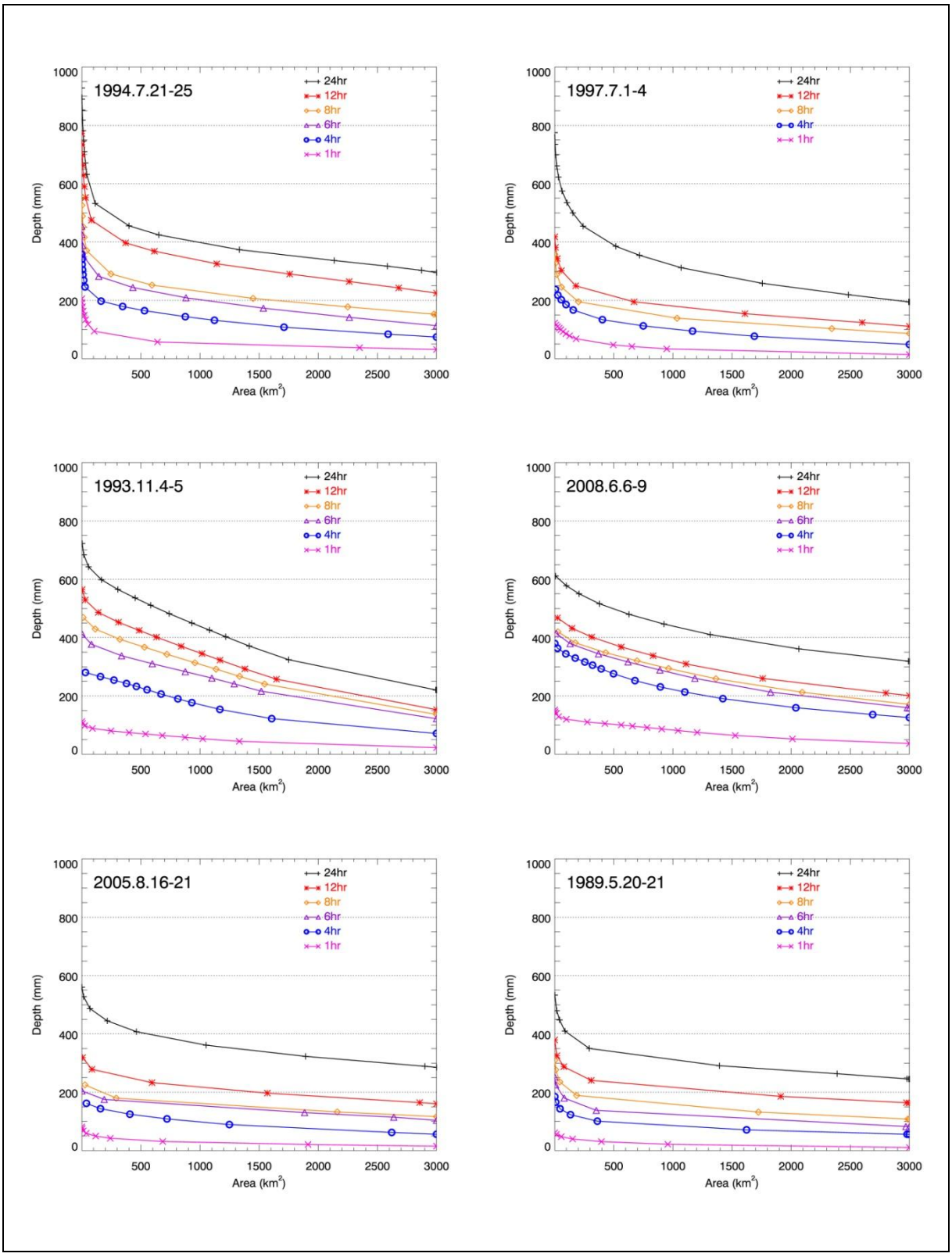

Figure O1 DAD Curves for Top 10 Storms between 1984 and 2010 (Sheet 1 of 2)

Table of Contents
Table of Contents
Table of Contents
Table of Contents

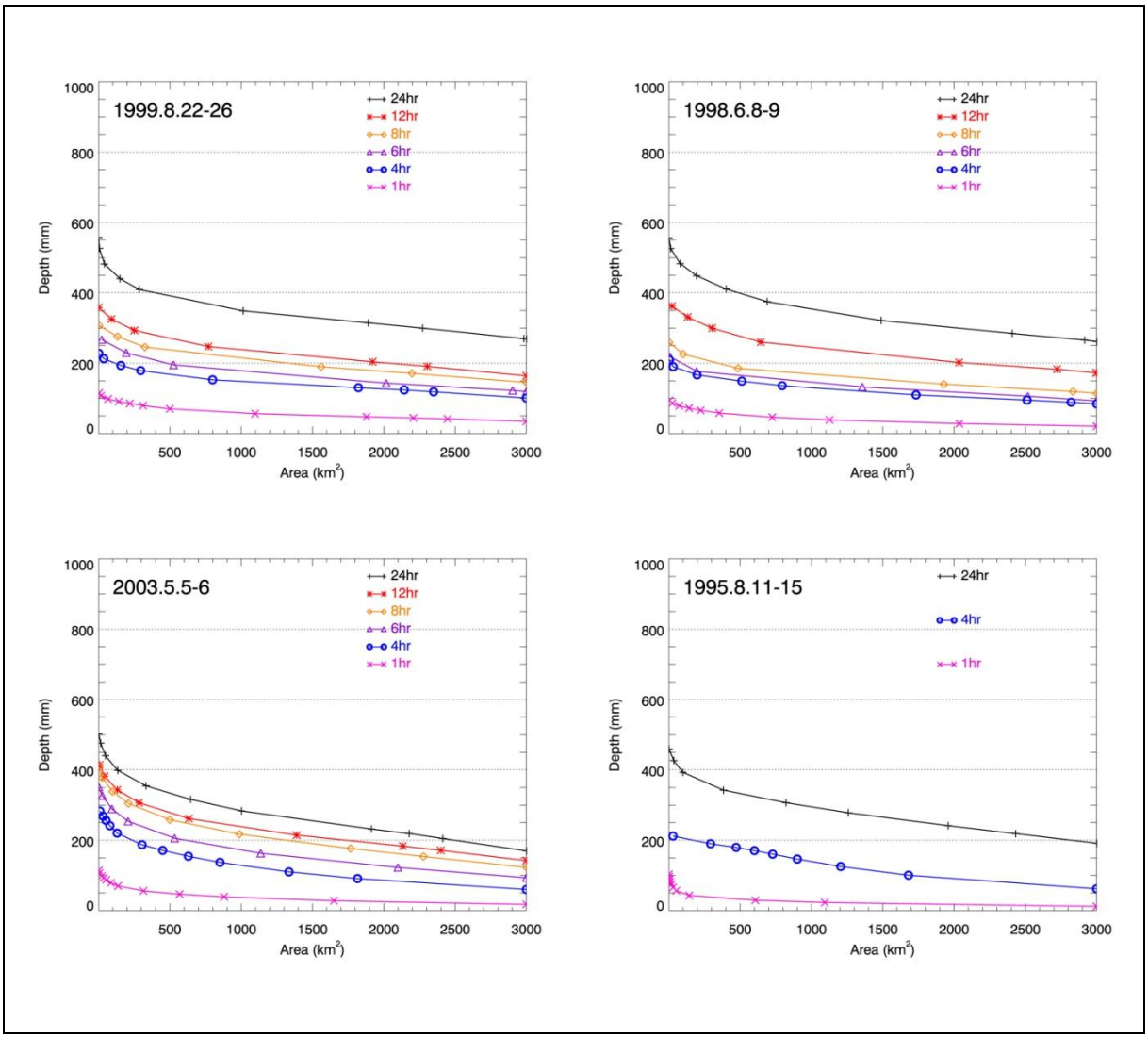

Figure O1 DAD Curves for Top 10 Storms between 1984 and 2010 (Sheet 2 of 2)

Table of Contents
Table of Contents
Table of Contents
Table of Contents

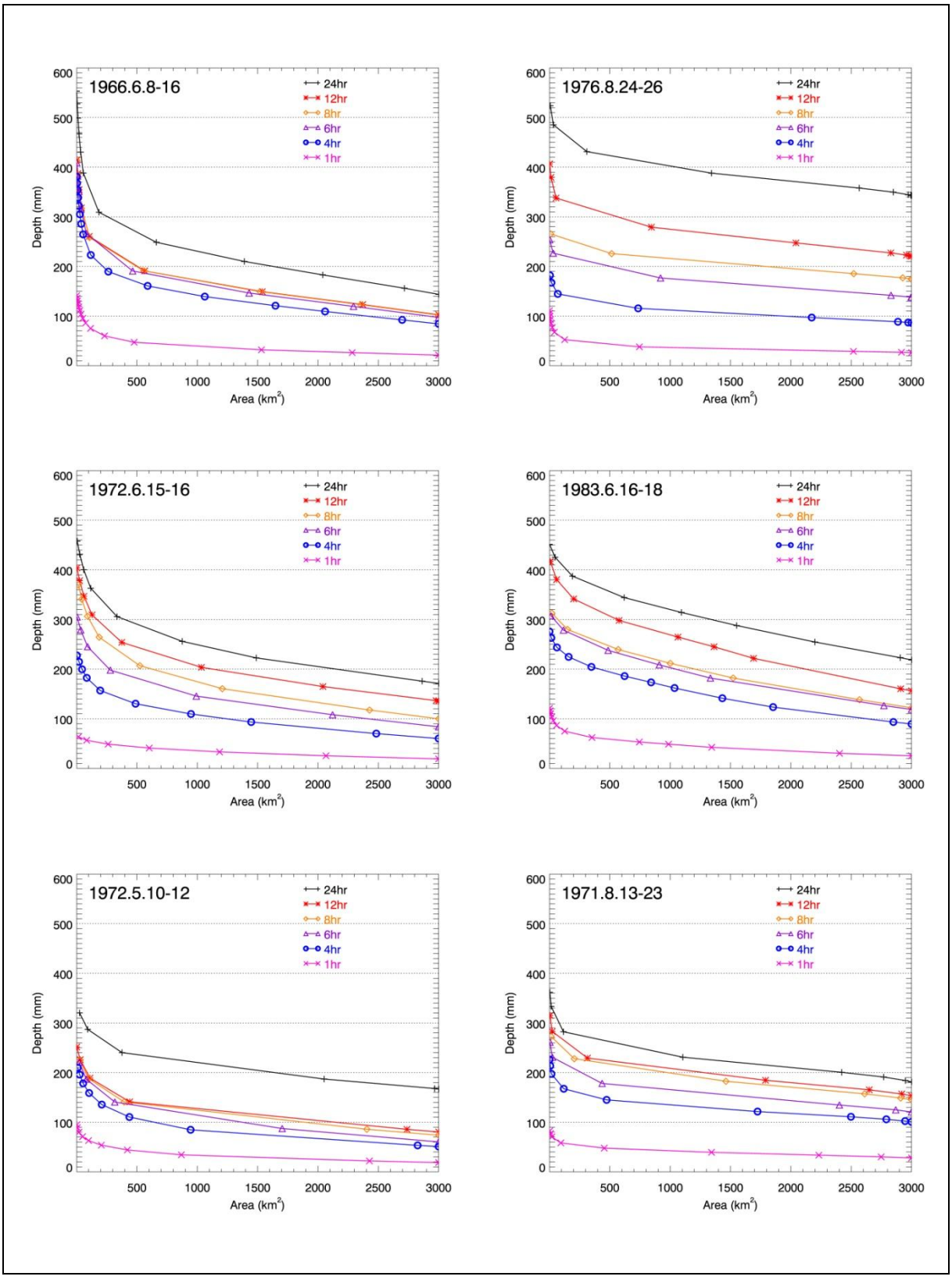

Figure O2 DAD Curves for Top 10 Storms between 1966 and 1984 (Sheet 1 of 2)

Table of Contents
Table of Contents
Table of Contents
Table of Contents

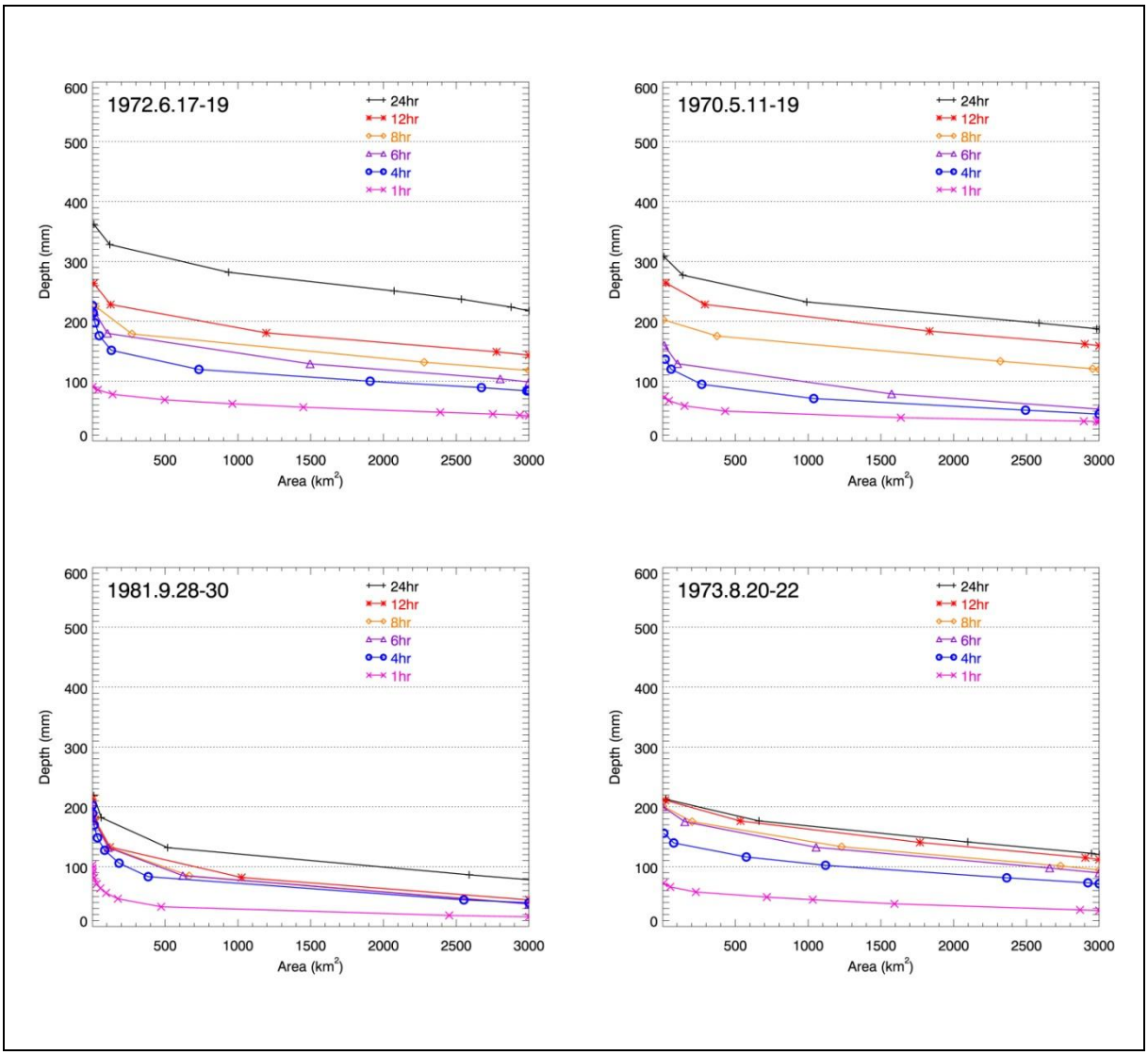

Figure O2 DAD Curves for Top 10 Storms between 1966 and 1984 (Sheet 2 of 2)

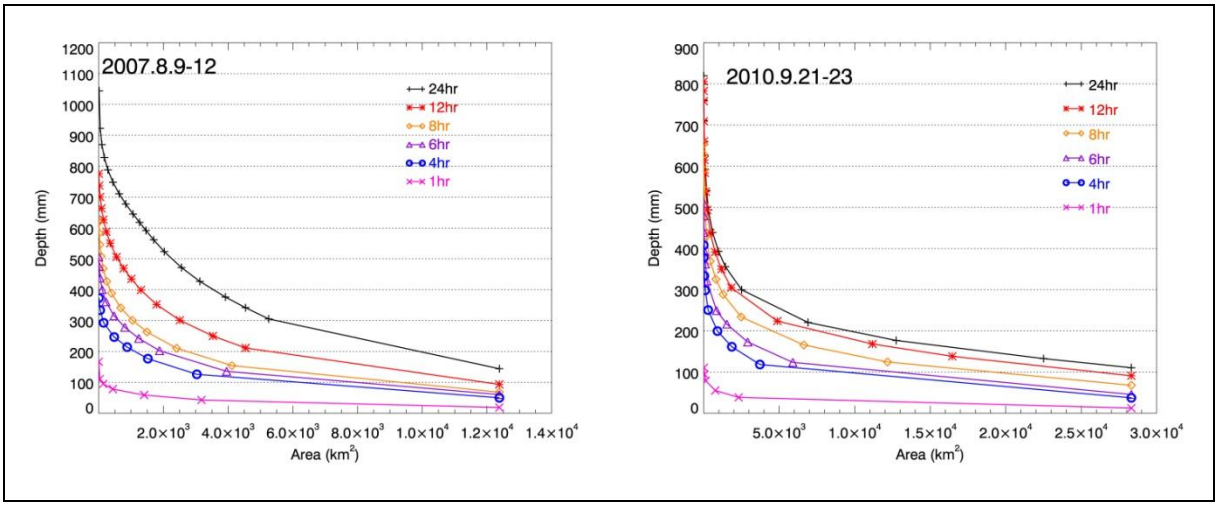

Figure O3 DAD Curves for 2 Representative Guangdong Storms

Table of Contents
Table of Contents
Table of Contents
Table of Contents

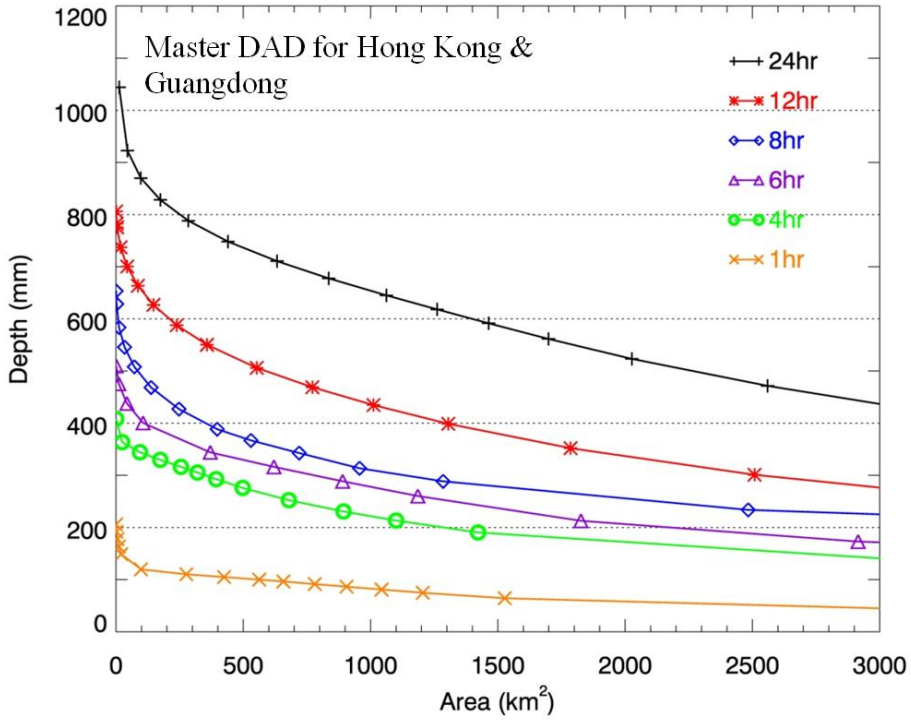

Note: The above master DAD curves are based on 20 local storms, which are the top 10 between 1966 and 1983 and the top 10 between 1984 and 2010 for 24-hour rainfalls, and 2 major Guangdong storms (Typhoons Pabuk and Fanapi).

Figure O4 Master DAD Curves without Moisture Maximization Representing the Hong Kong and Its Vicinity

Table O1 Master DAD Based on 20 Hong Kong and 2 Guangdong Storms with Moisture Maximization

24-hr		12-hr		8-hr		6-hr		4-hr		1-hr	
A (km^2)	D (mm)	A (km^2)	D (mm)	A (km^2)	D (mm)	A (km^2)	D (mm)	A (km^2)	D (mm)	A (km^2)	D (mm)
12.67	1044.10[1]	0.63	806.00[2]	0.31	653.50[2]	0.63	509.75[2]	0.63	408.25[2]	0.24	205.75[5]
44.93	922.69[1]	2.51	782.75[2]	2.51	628.56[2]	10.83	475.65[1]	24.28	363.51[4]	1.96	191.93[5]
97.46	870.04[1]	4.38	775.55[1]	11.98	583.62[1]	43.08	437.73[1]	94.24	344.20[4]	5.60	177.68[5]
174.18	828.18[1]	17.97	737.31[1]	33.64	545.88[1]	106.21	400.45[1]	173.80	329.69[4]	11.52	163.45[5]
284.31	788.21[1]	44.01	700.45[1]	72.12	508.06[1]	370.36	344.06[4]	255.12	316.24[4]	20.56	148.74[5]
440.06	748.14[1]	86.17	663.53[1]	137.78	468.47[1]	620.20	316.24[4]	320.36	305.30[4]	98.36	119.7[4]
632.68	710.65[1]	147.23	626.82[1]	247.22	427.10[1]	890.16	288.57[4]	393.60	292.68[4]	276.16	110.25[4]
835.43	677.73[1]	238.69	587.80[1]	397.67	388.47[1]	1185.80	260.25[4]	497.80	275.90[4]	424.64	104.92[4]
1061.91	645.16[1]	357.58	550.30[1]	530.00	367.00[3]	1826.20	212.82[4]	679.12	252.30[4]	562.60	100.03[4]
1261.90	618.19[1]	552.96	506.03[1]	719.48	342.77[3]	2915.23	172.95[2]	893.84	230.73[4]	657.72	96.41[4]
1463.73	591.55[1]	771.38	468.92[1]	956.72	313.57[3]			1100.60	213.21[4]	781.00	91.45[4]
1698.97	561.57[1]	1011.69	434.74[1]	1285.13	288.49[2]			1422.36	190.43[4]	905.48	86.44[4]
2026.60	523.32[1]	1305.22	398.81[1]	2483.40	233.73[2]			3721.49	118.23[2]	1043.36	80.97[4]
2559.51	471.62[1]	1785.60	352.05[1]							1205.32	74.79[4]
3127.45	426.83[1]	2508.36	301.04[1]							1527.12	64.30[4]
3914.96	376.18[1]	3531.57	250.03[1]							3175.60	42.72[1]

Notes:
(1) A for Area; D for Depth.
(2) [1] Guangdong 2007 storm; [2] Guangdong 2010 storm; [3] Hong Kong 1993 storm; [4] Hong Kong 2008 storm; [5] Hong Kong 1994 storm.
(3) The above master DAD curves are based on 20 local storms, which are the top 10 between 1966 and 1983 and the top 10 between 1984 and 2010 for 24-hour rainfalls, and 2 major Guangdong storms (Typhoons Pabuk and Fanapi).

Table of Contents
Table of Contents
Table of Contents

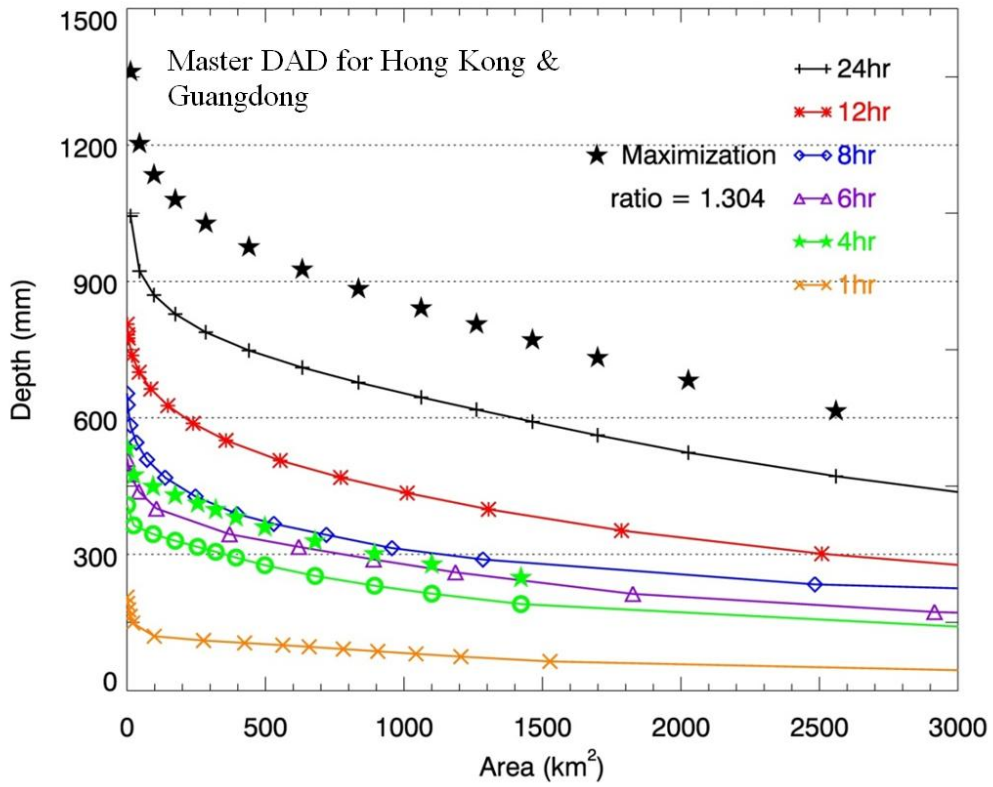

Notes:

(1) Points with star indicate the moisture-maximized values for corresponding points at 24-hour DAD curve in black and at 4-hour DAD curve in green respectively by multiplying by 1.304.

(2) The above master DAD curves are based on 20 local storms, which are the top 10 between 1966 and 1983 and the top 10 between 1984 and 2010 for 24-hour rainfalls, and 2 major Guangdong storms (Typhoons Pabuk and Fanapi).

Figure O5 Master DAD Curves Representing the Hong Kong and Its Vicinity with Moisture Maximization

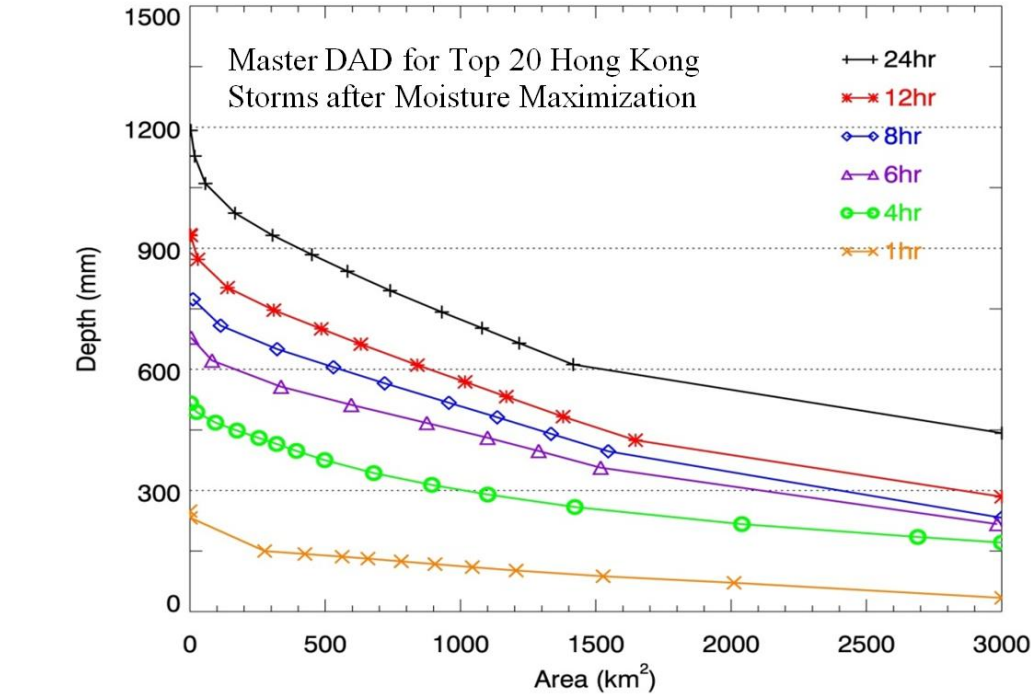

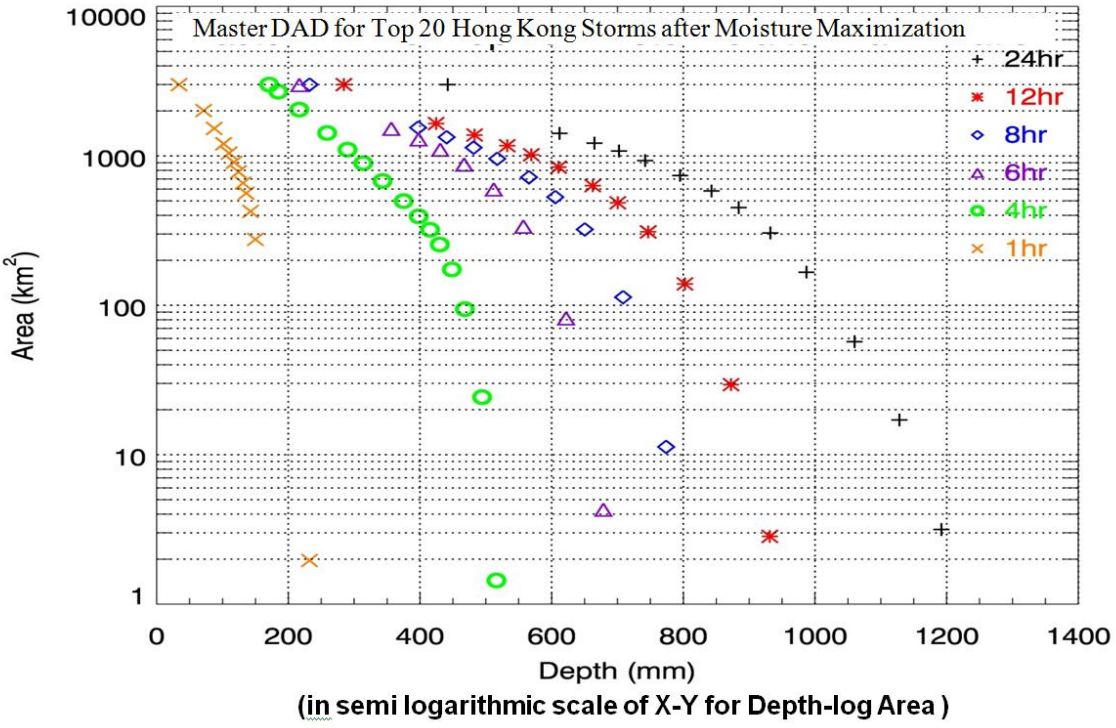

Note: The above master DAD curves are based on 20 local storms, which are the top 10 between 1966 and 1983 and the top 10 between 1984 and 2010 for 24-hour rainfalls, and 2 major Guangdong storms (Typhoons Pabuk and Fanapi).

Figure O6 Master DAD Curves Based on Top 20 Local Storms

Table of Contents
Table of Contents
Table of Contents
Table of Contents

Table O2 Master DAD Based on 20 Hong Kong Storms with Moisture Maximization

24-hr		12-hr		8-hr		6-hr		4-hr		1-hr	
Area (km^2)	Depth (mm)	Area (km^2)	Depth (mm)	Area (km^2)	Depth (mm)	Area (km^2)	Depth (mm)	Area (km^2)	Depth (mm)	Area (km^2)	Depth (mm)
3.16	1192.13[2]	0.32	933.82[1]	11.28	773.85[2]	4.28	678.56[2]	1.44	516.12[3]	0.24	248.96[1]
17.08	1128.25[2]	2.84	931.42[2]	113.24	708.48[2]	81.72	621.88[2]	24.28	494.37[3]	1.96	232.23[1]
57.12	1060.26[2]	29.44	872.54[2]	322.04	650.30[2]	336.52	557.04[2]	94.24	468.11[3]	276.16	149.94[3]
166.60	986.98[2]	138.96	802.56[2]	530.00	605.55[2]	596.12	512.06[2]	173.80	448.38[3]	424.64	142.69[3]
305.12	932.17[2]	309.96	746.67[2]	719.48	565.57[2]	875.36	467.14[2]	255.12	430.09[3]	562.60	136.04[3]
450.72	884.22[2]	485.32	700.45[2]	956.72	517.39[2]	1099.72	430.75[2]	320.36	415.20[3]	657.72	131.12[3]
582.24	842.89[2]	631.48	662.44[2]	1135.32	481.42[2]	1288.64	397.84[2]	393.60	398.05[3]	781.00	124.38[3]
739.52	795.22[2]	840.44	610.56[2]	1334.20	440.40[2]	1517.76	356.46[2]	497.80	375.22[3]	905.48	117.56[3]
930.68	742.03[2]	1016.76	569.06[2]	1545.68	397.08[2]	2982.68	216.76[3]	679.12	343.12[3]	1043.36	110.11[3]
1079.36	702.32[2]	1169.08	532.54[2]	3000.00	232.28[3]			893.84	313.79[3]	1205.32	101.71[3]
1216.88	664.91[2]	1378.92	482.88[2]					1100.60	289.97[3]	1527.12	87.44[3]
1416.00	612.01[4]	1646.52	424.51[2]					1422.36	258.98[3]	2010.92	71.31[3]
3000.00	442.26[4]	3000.00	284.46[4]					2039.88	216.61[3]	3000.00	33.96[4]
								2689.80	184.81[3]		
								3000.00	170.97[3]		

Notes: (1) [1]Hong Kong 1994 storm (r = 1.21); [2] Hong Kong 1993 storm (r = 1.65); [3] Hong Kong 2008 storm (r = 1.36); [4] Hong Kong 1976 storm (r = 1.29).

(2) The above master DAD curves are based on 20 local storms, which are the top 10 between 1966 and 1983 and the top 10 between 1984 and 2010 for 24-hour rainfalls.

Table of Contents
Table of Contents
Table of Contents

Appendix P

Rainfall Pattern Analysis

Contents

List of Tables

Table P1 Storm Types of Annual Maxima of 24-hour Rainfall in Hong Kong

	Beginning of 24-hour Period								No. of Storms			
	Year	Month	Day	Hour	Minute	Station	24-hr Rainfall (mm)	Remarks	Non-Typhoon	(%)	Typhoon	(%)
Lantau	1987	4	5	17	5	R11	190.5	non-typhoon				
	1988	7	19	3	35	R11	192.5	Typhoon (Super Typhoon) WARREN				
	1989	5	20	5	45	R12	265	Typhoon BRENDA				
	1990	9	10	7	45	R12	207.5	non-typhoon				
	1991	9	3	21	30	N18	199.5	Severe Tropical Storm JOEL				
	1992	7	17	17	20	N17	454	Tropical Storm FAYE				
	1993	11	4	9	45	N17	745	Typhoon (Severe Typhoon) IRA				
	1994	7	22	6	5	N17	364	non-typhoon				
	1995	8	2	21	15	N18	212	trough; Outer rainbands of Severe Tropical Storm “Gary”				
	1996	9	14	7	40	N17	181.5	non-typhoon				
	1997	8	2	9	35	R11	274.5	Typhoon VICTOR				
	1998	7	12	6	5	R11	735.5	non-typhoon				
	1999	8	22	15	20	N18	470	Typhoon SAM				
	2000	4	22	18	55	N18	232.5	non-typhoon				
	2001	7	6	1	20	N21	301	Typhoon UTOR				
	2002	8	5	13	5	N24	212	non-typhoon (few hours after a typhoon)				
	2003	5	4	18	45	N23	372	non-typhoon				
	2004	8	28	14	20	N17	246.5	non-typhoon (1 day after a typhoon)				
	2005	8	19	18	30	N18	463.5	non-typhoon				
	2006	6	2	4	45	N23	237	non-typhoon				
	2007	5	19	14	10	N19	210	non-typhoon				
	2008	6	6	10	30	N19	622.5	non-typhoon				
	2009	7	18	12	50	N21	221	Typhoon MOLAVE				
	2010	9	3	4	15	N21	263	Severe Tropical Storm LIONROCK	14	(58)	10	(42)
Tai Mo Shan	1984	8	20	12	45	N14	177.5	Severe Tropical Storm GERALD				
	1985	9	5	13	5	N14	305.5	Typhoon TESS				
	1986	7	11	13	55	N14	314.5	Typhoon (Super Typhoon) PEGGY				
	1987	7	29	3	55	N14	169	non-typhoon				
	1988	7	19	3	15	N14	282	Typhoon (Super Typhoon) WARREN				
	1989	5	20	8	50	N14	566	Typhoon BRENDA				
	1990	9	10	6	50	N14	201	non-typhoon				
	1991	7	23	14	15	N14	150.5	Severe Tropical Storm BRENDAN				
	1992	7	17	17	25	N14	275.5	Tropical Storm FAYE				
	1993	9	26	0	0	N14	373.5	Typhoon DOT				
	1994	7	21	16	10	N14	956	non-typhoon				
	1995	10	5	8	40	N14	406.5	non-typhoon (2 days after typhoon)				
	1996	9	14	7	20	N14	202.5	non-typhoon				
	1997	7	2	3	20	N14	487.5	non-typhoon				
	1998	6	8	18	30	N14	405.5	non-typhoon				
	1999	8	22	12	15	N14	565	Typhoon SAM				
	2000	4	13	14	30	N14	324.5	non-typhoon				
	2001	6	9	9	10	N14	261	non-typhoon				
	2002	8	9	7	40	N14	191.5	non-typhoon				
	2003	5	4	10	30	N14	263	non-typhoon				
	2004	8	28	18	55	N14	212.5	non-typhoon (1 day after typhoon)				
	2005	8	19	19	50	N14	360.5	non-typhoon				
	2006	9	12	23	50	N14	342.5	Tropical Depression				
	2007	6	9	16	55	N14	150.5	non-typhoon				
	2008	6	6	19	5	N14	428	non-typhoon				
	2009	9	14	15	0	N14	204	Typhoon KOPPU				
	2010	7	22	8	0	N14	255	Typhoon CHANTHU	15	(56)	12	(44)

Table of Contents
Table of Contents
Table of Contents
Table of Contents

Table P2 Storm Types of Annual Maxima of 4-hour Rainfall in Hong Kong

Beginning of 4-hour Period									No. of Storms			
	Year	Month	Day	Hour	Minute	Station	4-hr Rainfall (mm)	Remarks	Non-Typhoon	(%)	Typhoon	(%)
Lantau	1987	4	5	16	45	R11	94	non-typhoon				
	1988	8	18	7	25	R12	102	non-typhoon				
	1989	5	2	9	20	R12	127.5	non-typhoon				
	1990	9	11	2	35	R12	116	non-typhoon				
	1991	9	4	15	15	N18	178	Severe Tropical Storm JOEL				
	1992	7	18	7	55	N17	312.5	Typhoon (Severe Typhoon) NAT				
	1993	11	5	1	25	R11	285.5	non-typhoon (1 hour after a typhoon)				
	1994	7	23	2	10	N17	182.5	non-typhoon				
	1995	7	25	17	25	R11	121	non-typhoon				
	1996	5	5	4	35	N17	164.5	non-typhoon				
	1997	6	22	23	35	N18	197.5	non-typhoon				
	1998	7	12	15	35	R11	258	non-typhoon				
	1999	8	23	4	55	R12	209.5	Typhoon SAM				
	2000	4	22	23	0	N18	171.5	non-typhoon				
	2001	7	15	13	0	N22	209.5	non-typhoon				
	2002	8	6	5	15	N24	158	non-typhoon (1 day after a typhoon)				
	2003	5	5	4	50	N23	279	non-typhoon				
	2004	5	8	2	55	N21	130.5	non-typhoon				
	2005	8	19	18	30	N18	173.5	non-typhoon				
	2006	6	2	9	20	N23	201	non-typhoon				
	2007	6	10	2	50	N19	130	non-typhoon				
	2008	6	7	4	30	N19	384	non-typhoon				
	2009	7	19	1	15	N21	169.5	Typhoon MOLAVE				
	2010	7	28	14	15	N18	154	non-typhoon	20	(83)	4	(17)
Tai Mo Shan	1984	4	17	10	0	N14	88	non-typhoon				
	1985	8	25	22	35	N14	118	non-typhoon				
	1986	5	11	13	30	N14	197	non-typhoon				
	1987	7	22	18	55	N14	76.5	non-typhoon				
	1988	7	19	3	10	N14	157.5	Typhoon (Super Typhoon) WARREN				
	1989	5	20	20	35	N14	194.5	Typhoon BRENDA				
	1990	7	14	11	35	N14	87.5	non-typhoon				
	1991	8	21	4	40	N14	59.5	non-typhoon				
	1992	7	18	9	10	N14	156	Tropical Storm FAYE				
	1993	6	16	9	55	N14	176.5	non-typhoon				
	1994	7	22	6	50	N14	365	non-typhoon				
	1995	8	14	0	55	N14	187.5	non-typhoon (2 days after typhoon)				
	1996	9	14	23	20	N14	103	non-typhoon				
	1997	8	12	10	10	N14	226	non-typhoon				
	1998	6	9	2	30	N14	179	non-typhoon				
	1999	8	23	5	10	N14	227.5	Typhoon SAM				
	2000	4	14	5	35	N14	212.5	non-typhoon				
	2001	6	9	7	40	N14	169	non-typhoon				
	2002	5	20	19	50	N14	107.5	non-typhoon				
	2003	6	10	23	35	N14	129.5	non-typhoon				
	2004	7	17	1	40	N14	99	non-typhoon (hours after typhoon)				
	2005	6	24	3	50	N14	119	non-typhoon				
	2006	6	2	9	5	N14	212.5	non-typhoon				
	2007	6	10	2	20	N14	80	non-typhoon				
	2008	4	19	16	25	N14	159	non-typhoon				
	2009	7	19	0	50	N14	117	Typhoon MOLAVE				
	2010	7	22	14	55	N14	232.5	Typhoon CHANTHU	21	(78)	6	(22)

Table of Contents
Table of Contents
Table of Contents
Table of Contents

Appendix Q

Interim Update of 4-hour PMP

Contents

List of Tables

List of Figures

Q.1 Results of Storm Survey for 4-hour Rainfall (Non-local Storms)

A list of the top 30 3-hour rainfalls in Taiwan obtained from Central Weather Bureau (CWB) of Taiwan is given in Table Q1. As shown, the four Taiwan storms (Typhoons Herb, Haitang, Aere and Morakot) are not the top storms for 3-hour rainfalls in Taiwan. Although the 4-hour list is not available, it is expected that the above four Taiwan storms should not be the top storms for 4-hour rainfalls in Taiwan. Hence, the PMP established from rainfall data of the 4 Taiwan storms may be underestimated. Nevertheless, the results are considered as an interim updating of the 4-hour PMP for reference. The analysis and the results of transposition of the above four Taiwan storms for 4-hour rainfall are given in Appendices Q to W.

Table Q1 List of Top 30 3-hour Rainfalls in Taiwan

排序	站 名	測站站碼	降水量(mm)	開始發生日期	影響天氣系統
1	彭佳嶼	46695	476.0	2002/07/10	娜克莉颱風
2	蘇澳	46706	444.0	2010/10/21	梅姬颱風
3	甲仙	C0V25	389.0	2008/07/17	卡梅基颱風
4	光復	C0T96	380.0	2001/07/29	桃芝颱風
5	新發	C1V24	368.5	2008/07/17	卡梅基颱風
6	土場	C1U70	347.5	2001/09/17	納莉颱風
7	關山	C1088	347.0	2008/07/17	卡梅基颱風
8	天祥	C0T82	337.0	1997/08/29	安珀颱風
9	瑪家	C1R14	335.5	2010/09/19	凡那比颱風
10	左營	C1V43	328.5	2001/07/11	潭美颱風
11	鳳凰	C0109	328.0	2001/07/30	桃芝颱風
12	阿里山	46753	325.5	2009/08/09	莫拉克颱風
13	澎湖	46735	324.0	1974/07/06	西南氣流
14	北寮	C1083	324.0	2008/07/17	卡梅基颱風
15	高雄	46744	318.1	1962/07/23	凱蒂颱風
16	岡山	C1V41	316.5	2010/09/19	凡那比颱風
17	高中	C1V23	315.0	2008/07/17	卡梅基颱風
18	布洛灣	C1T83	312.0	1997/08/29	安珀颱風
19	三地門	C0R15	312.0	2007/08/13	西南氣流
20	阿里山	46753	311.5	1996/07/31	賀伯颱風
21	土場	C1U70	310.5	2001/09/17	納莉颱風
22	瑪家	C1R14	309.0	2007/08/13	西南氣流
23	阿里山	46753	308.5	1996/08/01	賀伯颱風
24	岡山	C1V41	308.5	2010/09/19	凡那比颱風
25	馬頭山	C0M41	307.5	2008/07/17	卡梅基颱風
26	阿里山	46753	305.0	1996/08/01	賀伯颱風
27	阿里山	46753	305.0	2009/08/08	莫拉克颱風
28	瑪家	C1R14	305.0	2007/08/18	聖帕颱風
29	來義	C1R24	305.0	2009/08/08	莫拉克颱風
30	楠西	C1092	300.5	2008/07/17	卡梅基颱風

Source: Central Weather Bureau of Taiwan

Q.2 Historical Rainfall Data Adopted for Transposition Analysis

Historical Hourly Rainfall Series

(1) Taiwan

Table Q2 4-hour Mean of Annual Maximum Rainfalls in Taiwan (Sheet 1 of 2)

	No	ID	Name	Long	Lat	Elevation	N-yr	4-hr Mean of Annual Maximum Rainfall
	1	00F390	雙崎 Shuangqi(2)	120.91	24.29	543	46	131.30
	2	00H540	龍神橋 Longshenqiao	120.87	23.78	322	47	127.82
	3	00H710	集集 Jiji(2)	120.78	23.83	9	56	131.46
	4	00J810	北港 Beigang(2)	120.30	23.58	215	54	116.78
	5	00P470	旗山 Qishan(4)	120.48	22.88	64	50	120.67
	6	00Q070	屏東 Pingdong(5)	120.47	22.65	25	60	135.19
	7	00S120	鹿鳴橋 Lumingqiao	121.09	22.90	190	49	118.99
	8	01A160	林口 Linkou(1)	121.38	25.08	250	35	99.75
	9	01A200	火燒寮 Huoshaoliao	121.75	24.98	380	55	133.18
	10	01A430	福山 Fushan(3)	121.50	24.78	500	32	146.03
	11	01D100	太閣南 Taigenan	121.15	24.63	940	45	116.58
	12	01E030	橫龍山 Henglongshan	120.97	24.47	550	38	138.78
	13	01E330	大坪頂 Dapingding	120.73	24.43	190	30	113.76
	14	01F100	八仙山 baxianshan(1)	121.00	24.13	1600	20	142.74
	15	01F350	雪嶺 Xueling	121.03	24.28	2575	38	128.46
WRA	16	01F680	頭汴坑 Toubiankeng	120.81	24.12	480	42	133.58
	17	01G240	萬興 Wanxing(2)	120.42	23.96	11	43	106.29
	18	01H310	翠峰 Cuifeng	121.20	24.11	2303	45	96.32
	19	01H390	望鄉 Wangxiang	120.93	23.62	2200	49	124.51
	20	01H440	卡奈托灣 Kanaituowan(2)	121.09	23.75	1390	41	91.77
	21	01H470	西巒 Xiluan	120.92	23.71	1666	49	112.32
	22	01H590	六分寮 Liufengliao	120.64	23.93	427	43	123.17
	23	01H680	北山 Beishan(2)	120.89	23.99	339	42	116.63
	24	01J100	西螺 Xiluo(2)	120.47	23.80	30	48	107.28
	25	01J930	林內 Linnei(1)	120.61	23.76	82	49	115.43
	26	01J960	大埔 Dapu	120.62	23.63	205	51	134.10
	27	01K060	褒忠 Baozhong(2)	120.31	23.70	13	49	103.37
	28	01L390	大湖山 Dahushan	120.62	23.48	725	53	176.54
	29	01L480	樟腦寮 Zhangnaoliao(2)	120.60	23.53	545	48	168.56
	30	01L910	中坑 Zhongkeng(3)	120.52	23.57	95	48	128.05
	31	01O070	關子嶺 Guanziling(2)	120.51	23.33	350	52	157.35

Table of Contents
Table of Contents
Table of Contents
Table of Contents

Table Q2 4-hour Mean of Annual Maximum Rainfalls in Taiwan (Sheet 2 of 2)

	No	ID	Name	Long	Lat	Elevation	N-yr	4-hr Mean of Annual Maximum Rainfall
WRA	32	01P190	木柵 Mushan	120.47	22.98	78	52	135.06
	33	01P500	阿蓮 Ahlian(2)	120.33	22.88	21	50	134.13
	34	01P660	甲仙 Jiaxian(2)	120.59	23.08	355	56	143.28
	35	01Q160	新豐 Xinfeng	120.65	22.88	166	55	139.97
	36	01Q250	泰武 Taiwu(1)	120.70	22.61	950	56	226.72
	37	01Q360	南和 Nanhe	120.64	22.43	140	46	144.12
	38	01Q910	阿禮 Ahli	120.76	22.73	1158	43	199.37
	39	01Q930	三地門 Sandimen	120.65	22.71	150	42	164.59
	40	01S210	知本 Zhiben(5)	121.00	22.69	100	31	115.23
	41	01S360	紹家 Shaojia	120.86	22.38	520	55	121.46
	42	01S430	霧鹿 Wulu	121.04	23.17	910	56	103.75
	43	01S440	新武 Xinwu(3)	121.13	23.13	420	39	111.61
	44	01S470	向陽 Xiangyang(2)	120.99	23.25	2400	38	113.11
	45	01T220	卓麓 zhuolu(4)	121.27	23.30	210	36	122.21
	46	01T230	立山 lishan	121.31	23.43	180	49	125.68
	47	01T560	西林 Xilin	121.43	23.82	200	37	142.45
	48	01T640	哇拉彙 Walabi	121.19	23.35	960	29	126.83
	49	01T660	馬太安 Mataian	121.37	23.67	1000	30	157.10
	50	01U080	南山 Nanshan	121.38	24.44	1050	46	92.11
	51	01U230	大濁水 Dazhuoshui	121.74	24.33	48	31	144.87
	52	01U470	武塔 Wuta	121.78	24.45	32	31	135.23
	53	01V050	藤枝 Tengzi(2)	120.76	23.07	1640	30	152.32
	54	01V070	天池 Tianchi	120.92	23.28	2230	32	130.30
	55	01V080	民族 Mingzhu	120.70	23.22	530	33	158.08
CWB	56	467420	永康 Yongkang*	120.22	23.04	8.1	30	119.57
	57	467440	高雄 Gaoxiong*	120.30	22.57	2.3	30	129.54
	58	467550	玉山 Yushan	120.95	23.49	3845	30	104.57
	59	467530	阿里山 Ahlishan	120.80	23.51	2413	30	187.25
	60	466990	花蓮 Hualian	121.60	23.98	16	30	127.03
	61	467080	宜蘭 Yilan	121.73	24.77	7.2	30	115.35
	62	467590	恆春 Hengchun	120.73	22.01	22.1	30	137.55
	63	467660	臺東 Taidong	121.13	22.75	9	30	121.67
	64	C1M510	樸子 Puzi*	120.23	23.47	8	19	112.18
	65	C1X070	北門 Beimeng*	120.10	23.27	14	19	103.13
	66	C1X060	下營 Xiaying*	120.27	23.24	5	19	120.97

Note: * Stations were used as the base stations for development of SDOIF.

Table of Contents
Table of Contents
Table of Contents
Table of Contents

(2) Hong Kong and Guangdong

Table Q3 4-hour Annual Maximum Rainfalls in Hong Kong and Guangdong (Sheet 1 of 2)

	No	ID	Long	Lat	Elevation	N-yr	Time Period of Available Data	4-hr Mean of Annual Maximum Rainfall
	1	H01	114.12	22.27	107	27	1984 - 2010	129.20
	2	H02	114.13	22.28	95	27	1984 - 2010	128.80
	3	H03	114.13	22.26	132	27	1984 - 2010	120.63
	4	H04	114.14	22.28	123	27	1984 - 2010	135.69
	5	H05	114.16	22.25	103	27	1984 - 2010	127.19
	6	H06	114.18	22.27	88	27	1984 - 2010	131.41
	7	H07	114.19	22.28	94	27	1984 - 2010	126.94
	8	H08	114.19	22.26	129	27	1984 - 2010	128.81
	9	H09	114.20	22.29	160	27	1984 - 2010	136.80
	10	H10	114.15	22.28	530	27	1984 - 2010	136.44
	11	H12	114.15	22.28	188	27	1984 - 2010	134.28
	12	H14	114.23	22.26	141	27	1984 - 2010	125.46
	13	H15	114.22	22.22	50	27	1984 - 2010	125.17
	14	H16	114.15	22.27	439	27	1984 - 2010	132.46
	15	H17	114.16	22.27	200	27	1984 - 2010	132.54
	16	H18	114.22	22.28	77	27	1984 - 2010	132.91
	17	H19	114.23	22.28	53	27	1984 - 2010	127.93
	18	H20	114.15	22.24	104	27	1984 - 2010	118.07
HK	19	H21	114.19	22.24	139	27	1984 - 2010	118.11
	20	K01	114.18	22.31	91	27	1984 - 2010	137.61
	21	K02	114.18	22.34	92	27	1984 - 2010	143.72
	22	K03	114.23	22.32	91	27	1984 - 2010	126.78
	23	K04	114.23	22.33	178	27	1984 - 2010	128.02
	24	K05	114.24	22.30	117	27	1984 - 2010	127.04
	25	K06	114.16	22.34	35	27	1984 - 2010	138.43
	26	K07	114.20	22.35	197	27	1984 - 2010	135.52
	27	K08	114.24	22.31	77	27	1984 - 2010	126.39
	28	N01	114.17	22.36	38	27	1984 - 2010	143.85
	29	N02	114.19	22.39	73	27	1984 - 2010	132.50
	30	N03	114.13	22.37	113	27	1984 - 2010	131.70
	31	N04	114.13	22.35	96	27	1984 - 2010	128.04
	32	N05	114.14	22.49	111	27	1984 - 2010	116.33
	33	N06	114.14	22.36	106	27	1984 - 2010	138.28
	34	N07	113.97	22.39	41	27	1984 - 2010	115.00
	35	N08	114.25	22.34	256	27	1984 - 2010	127.28
	36	N09	114.21	22.42	6	27	1984 - 2010	135.57
	37	N10	114.06	22.37	35	26	1984 - 2010	123.08

Table Q3 4-hour Annual Maximum Rainfalls in Hong Kong and Guangdong (Sheet 2 of 2)

	No	ID	Long	Lat	Elevation	N-yr	Time Period of Available Data	4-hr Mean of Annual Maximum Rainfall
HK	38	N11	114.09	22.34	40	26	1984 - 2010	128.71
	39	N12	114.02	22.45	79	27	1984 - 2010	115.46
	40	N13	114.34	22.38	87	27	1984 - 2010	138.04
	41	N14	114.12	22.41	944	27	1984 - 2010	156.91
	42	N15	114.27	22.38	41	26	1984 - 2010	128.56
	43	N16	114.27	22.32	114	26	1986 - 2010	124.42
	44	N17	113.94	22.28	17	19	1992 - 2010	167.34
	45	N18	114.00	22.27	69	19	1992 - 2010	155.16
	46	R01	114.17	22.30	32	24	1885 - 2010	125.24
	47	R11	113.91	22.26	478	24	1987 - 2010	147.15
	48	R12	114.01	22.29	106	24	1987 - 2010	124.21
	49	R13	114.12	22.22	32	24	1987 - 2010	108.65
	50	R14	114.26	22.21	45	24	1987 - 2010	121.85
	51	R17	114.11	22.29	90	24	1987 - 2010	111.48
	52	R18	114.29	22.31	122	24	1987 - 2010	107.54
	53	R19	114.21	22.29	7	18	1993 - 2010	125.61
	54	R21	113.92	22.38	28	24	1987 - 2010	118.17
	55	R22*	114.01	22.49	8	24	1987 - 2010	107.06
	56	R23	114.17	22.45	23	24	1987 - 2010	131.04
	57	R24	114.21	22.54	39	24	1987 - 2010	116.77
	58	R25	114.33	22.41	106	24	1987 - 2010	115.50
	59	R26	114.09	22.44	20	24	1987 - 2010	127.81
	60	R27	114.00	22.42	102	24	1987 - 2010	122.77
	61	R28	114.05	22.45	3	24	1987 - 2010	116.85
	62	R29	114.08	22.51	67	24	1987 - 2010	98.65
	63	R31	114.24	22.48	10	24	1987 - 2010	103.94
	64	R32	114.35	22.35	24	24	1987 - 2010	117.00
	65	R30*	114.30	22.54	23	21	1987 - 2008	105.79
SGD	1	Xili	113.95	22.59	35	36	1975 - 2010	- #
	2	Shiyan	113.92	22.68	38	37	1974 - 2010	- #
	3	Shenzhen*	114.10	22.55	27	29	1981 - 1989 1991 - 2010	111.87

Notes:
(1) * 2 Hong Kong stations (HK) have been joined with 1 South Guangdong (SGD) station as the base stations for development of SDOIF.
(2) # 4-hour annual maximum is not available for these stations. Since there is no raw hourly observation available in the Guangdong Hydrological Bureau (GD HB), it is impossible to restore the 4-hour annual maximum rainfall time series.

Table of Contents
Table of Contents
Table of Contents
Table of Contents

Q.3 Statistical PMP Estimate

Regionalized 4-hour statistical PMP estimates are:

(a) Employing HK data:	628 mm/4-hour	(regionalized)
(b) Employing N14 data only:	533 mm/4-hour	(N14 only - for reference and comparison)

It is suggested that the 4-hour statistical PMP falls between 533 mm and 628 mm. The details of computation are given in Appendix R.

Q.4 Storm Separation

Q.4.1 Development of SDOIF at Target Area

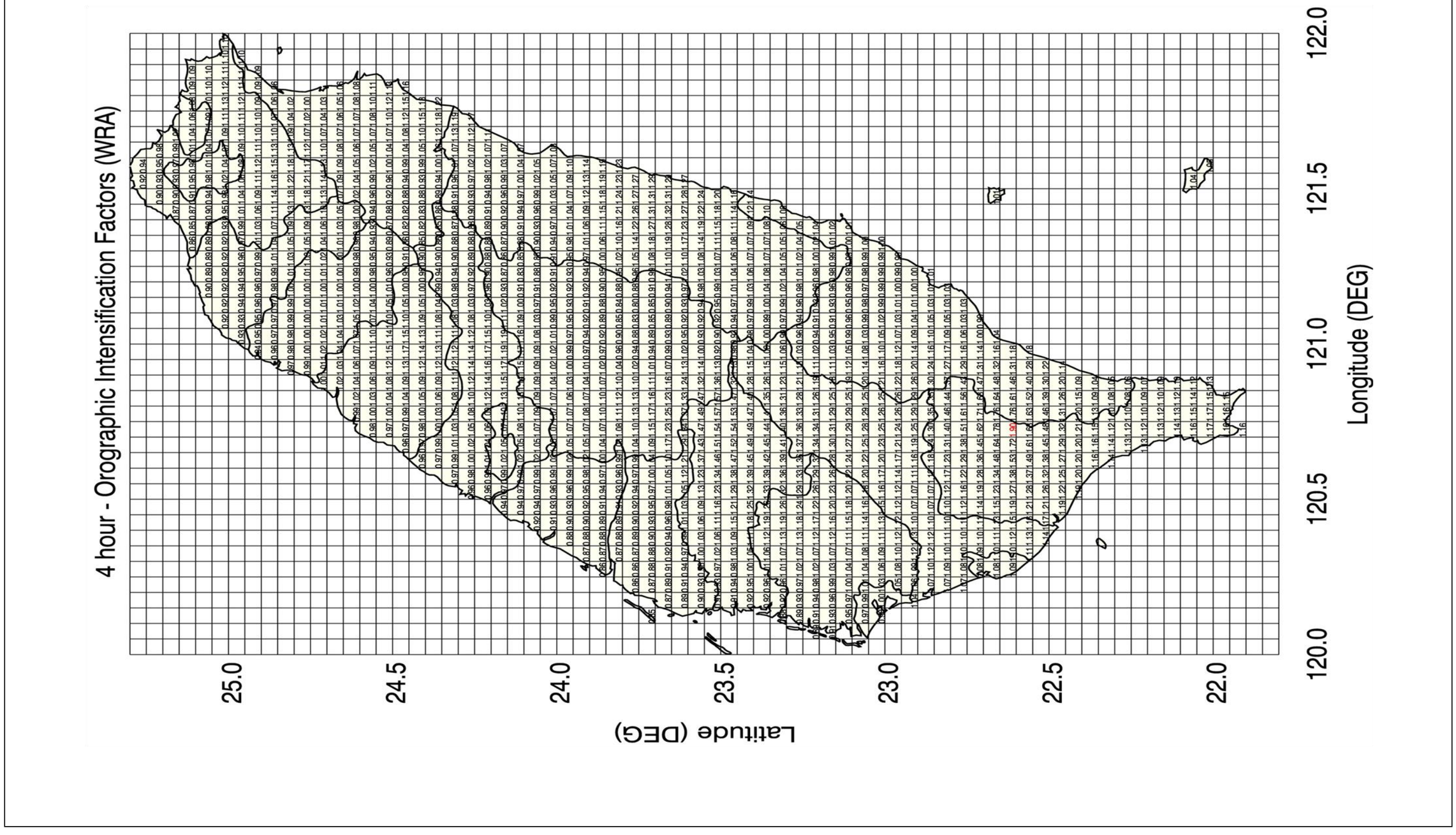

Figure Q1 4-hour SDOIF for Taiwan at a Resolution of 5 km x 5 km

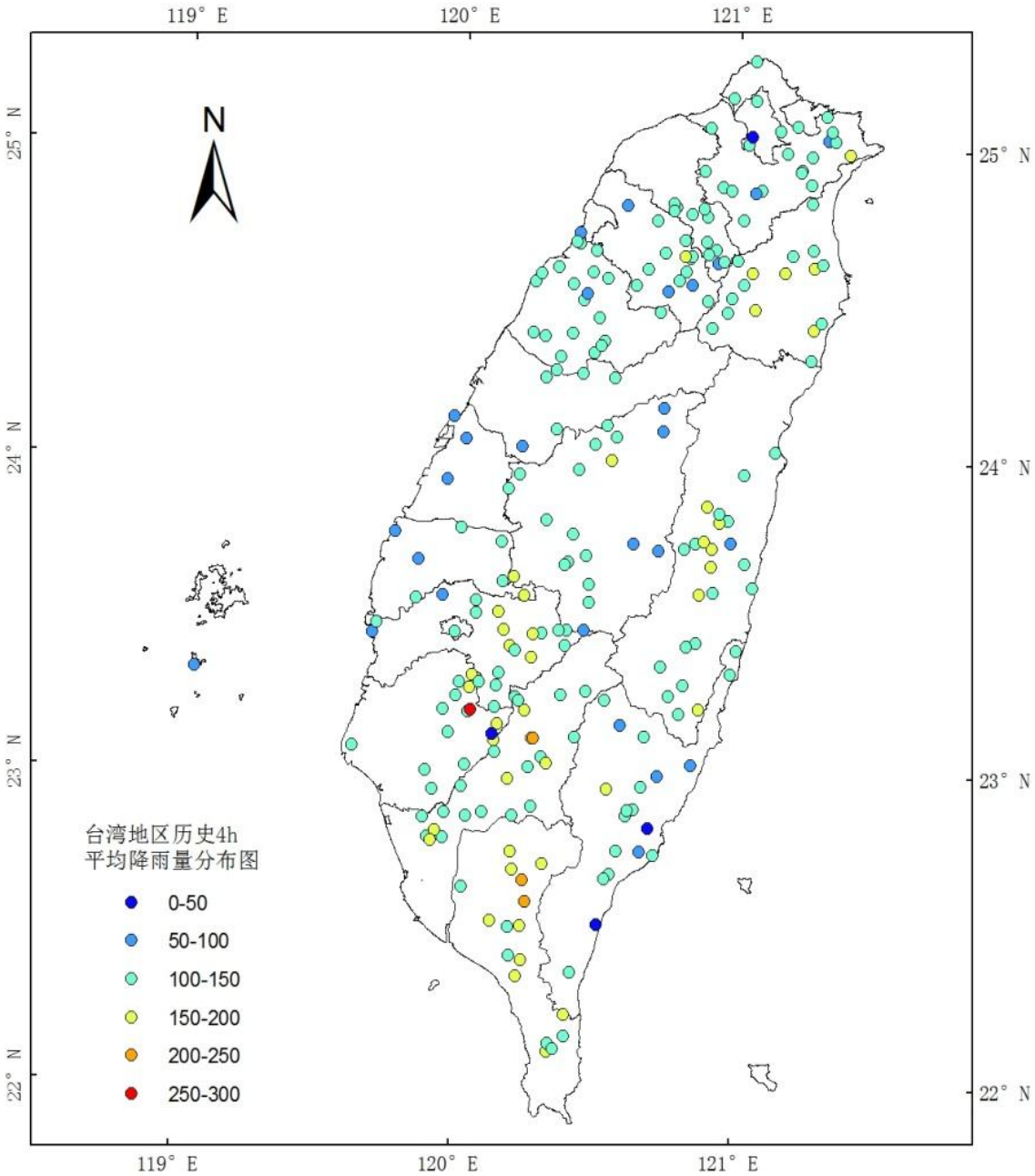

(Courtesy by Sinotech's data via AHMRI)

Figure Q2 4-hour Average Annual Maximum Rainfall in Taiwan

Q.4.2 Development of Convergence Rainfall Isohyets for the 4 Major Storms in Taiwan

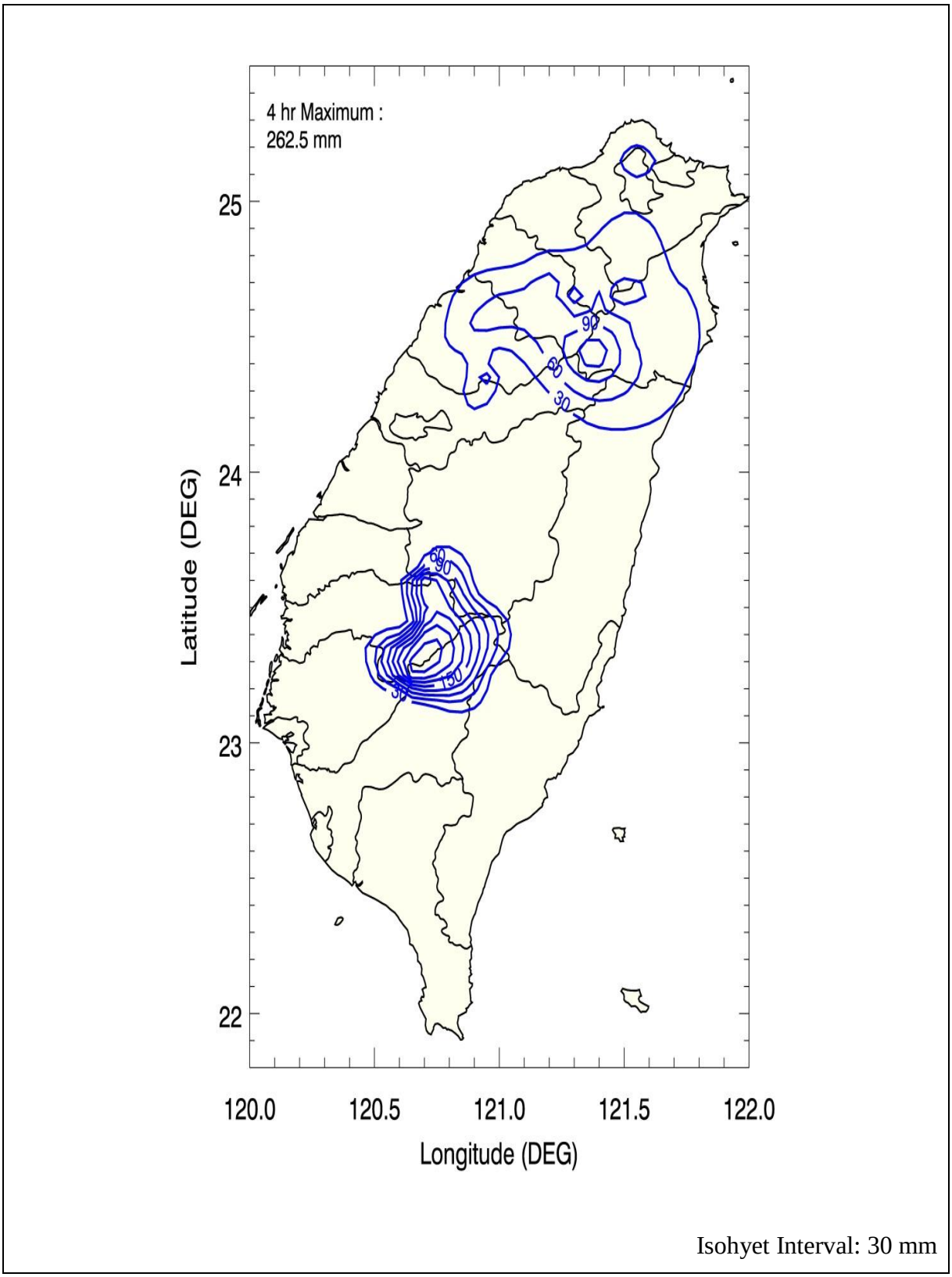

Figure Q3 Convergence Isohyets of Herb

Table of Contents
Table of Contents
Table of Contents
Table of Contents

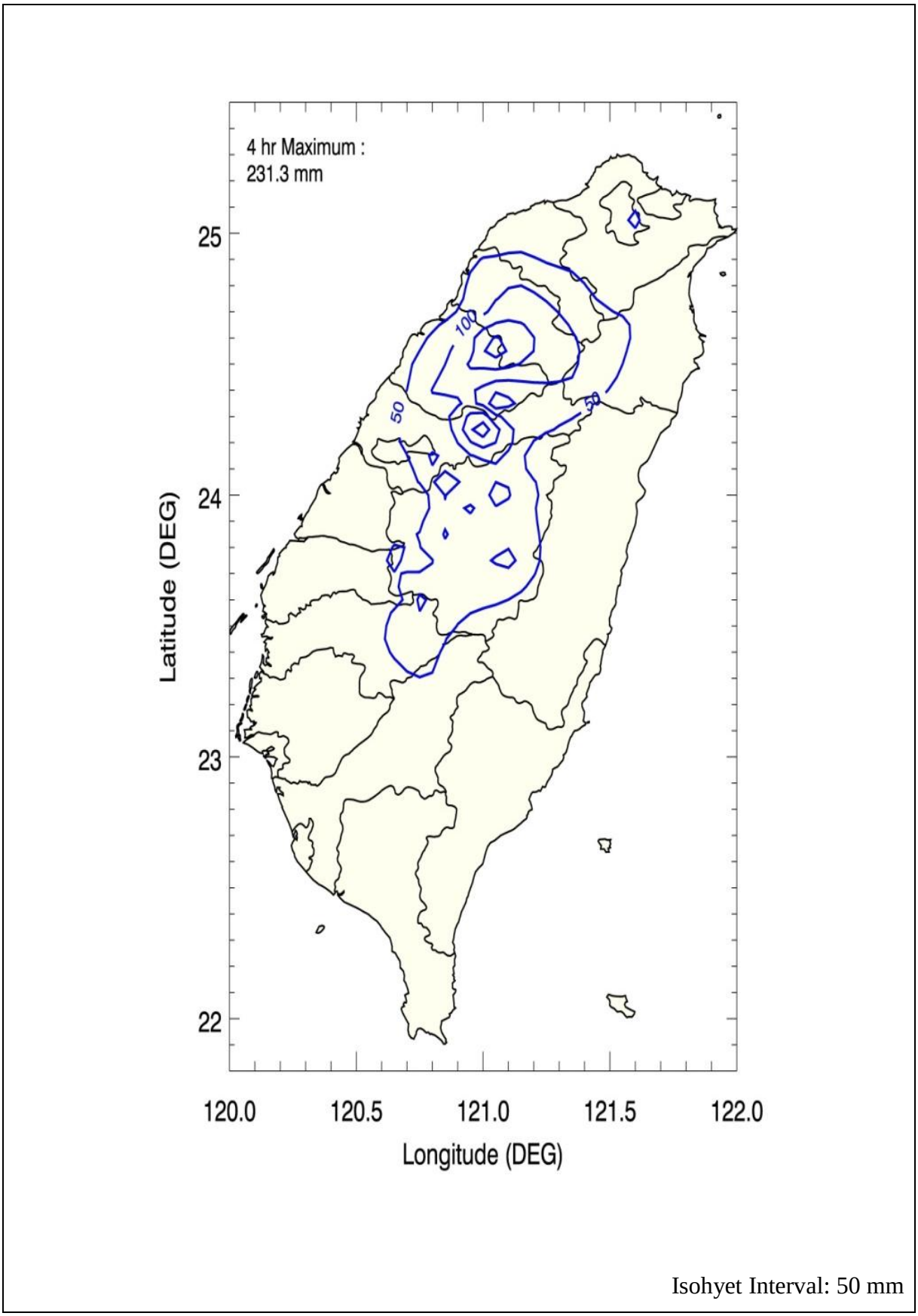

Figure Q4 Convergence Isohyets of Aere

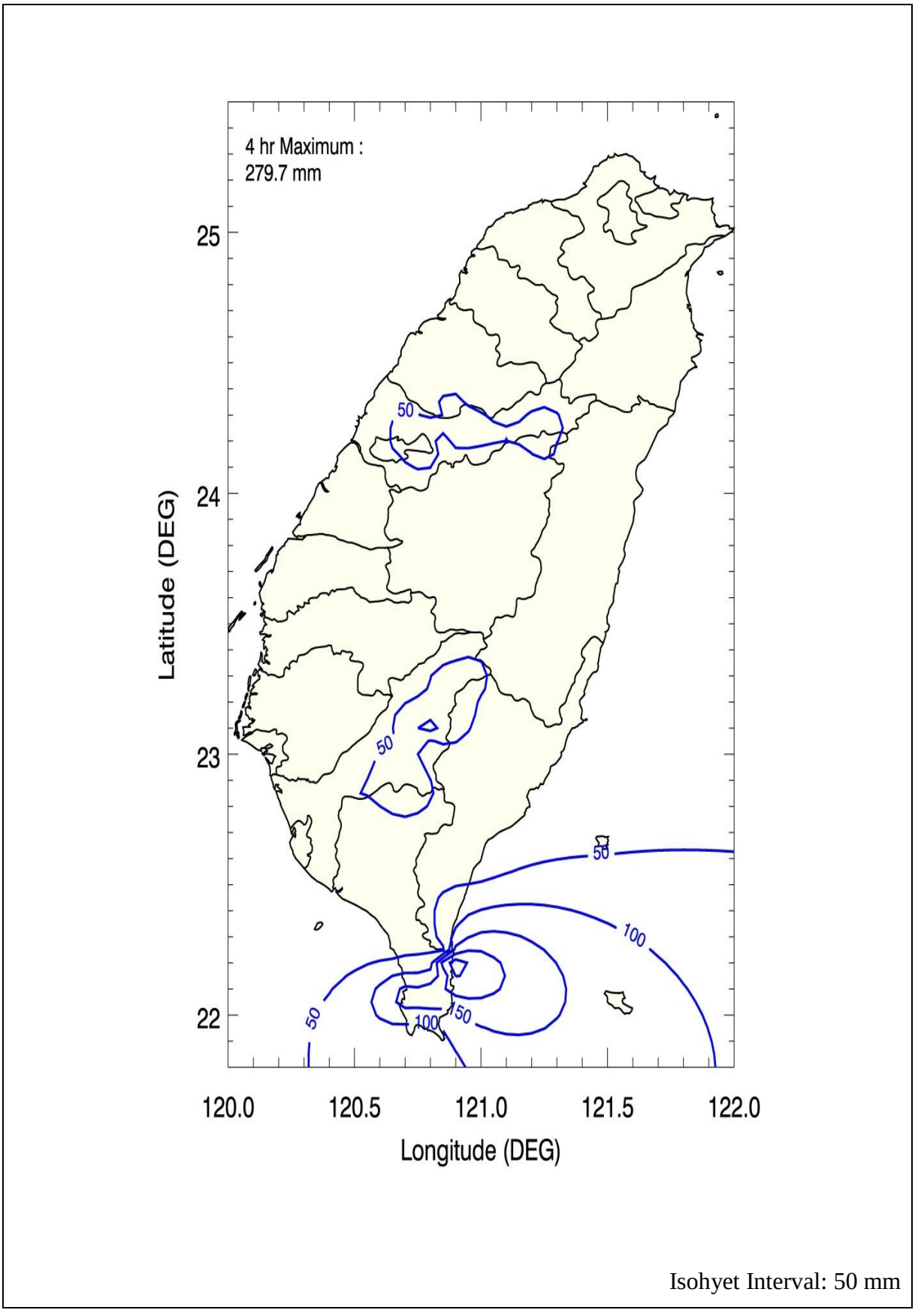

Figure Q5 Convergence Isohyets of Haitang

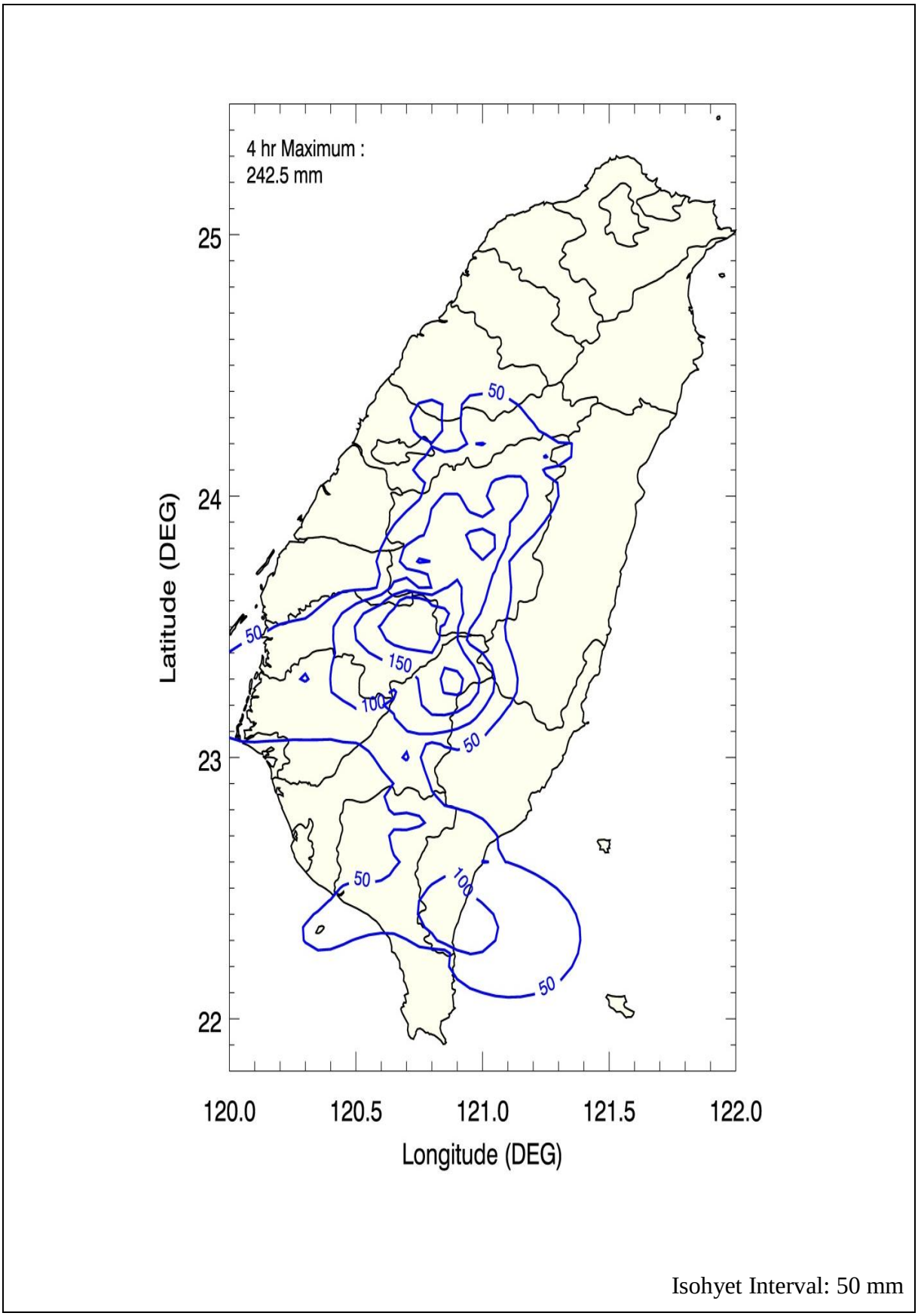

Figure Q6 Convergence Isohyets of Morakot

Q.4.3 Development of the Relation of Area Average Rainfall with Area Size in Taiwan

Table Q4 Relation of Area Average Rainfall with Area Size in Taiwan

4-hour Convergence Rainfall				
Isohyets (mm)	Area (km^2)			
	Herb	Aere	Haitang	Morakot
0 - 25	36074	32253	27151	25066
25 - 50	2925	4370	6319	7873
50 - 75	1150	1838	2716	3660
75 - 100	425	1724	1722	2045
100 - 125	259	665	1458	1162
125 - 150	173	292	1072	717
150 - 175	151	166	532	322
175 - 200	94	96	264	312
200 - 225	83	44	131	210
225 - 250	81	0	61	80
250 - 300	33		23	

Q.4.4 Construction of Generalized Convergence Component Pattern of Transposed Storm in the Target Area, Taiwan

The generalized convergence component of transposed storm consists of the values of isohyets and shape of the isohyets. The values are determined by the convergence component of Morakot storm except the centre value for 4-hour convergence component, for which Haitang is referred as comparable due to centre data unavailable for Morakot while the shape is a pattern generalized over the four outstanding storms, Morakot, Herb, Aere and Haitang.

The Morakot's 4-hour convergence patterns are used for storm transposition but the centre point value (279.7 mm) for 4-hour comes from the Haitang's convergence component. This is based on the review of the Depth-Area relation of the Morakot storm in comparison with the one of the Haitang that the isohyets of 225 - 250 mm correspond to 61 km^2 for Haitang and a larger of 80 km^2 for Morakot. Having been looking at the tendency over the Depth-Area after isohyets of 150 - 175 mm for both Morakot and Haitang, we have reason to assume that a higher or at least equal value of rainfall might occur at the centre of the Morakot when the area size of Morakot reduces to 61 km^2 or equivalent if there were rainfall data available there.

The results of storm separation for 4-hour rainfall are shown in Table Q5 and Figures Q7 and Q8.

Table Q5 Relation of Area Average 4-hour Generalized Convergence Rainfall with Area Size in Taiwan

Isohyets (mm)	Area (km^2)				Generalized Convergence Component
	Herb	Aere	Haitang	Morakot	
0 - 25	36074	32253	27151	25066	25066
25 - 50	2925	4370	6319	7873	7873
50 - 75	1150	1838	2716	3660	3660
75 - 100	425	1724	1722	2045	2045
100 - 125	259	665	1458	1162	1162
125 - 150	173	292	1072	717	717
150 - 175	151	166	532	322	322
175 - 200	94	96	264	312	312
200 - 225	83	44	131	210	210
225 - 250	81	0	61	80	80
250 - 300	33		23		23

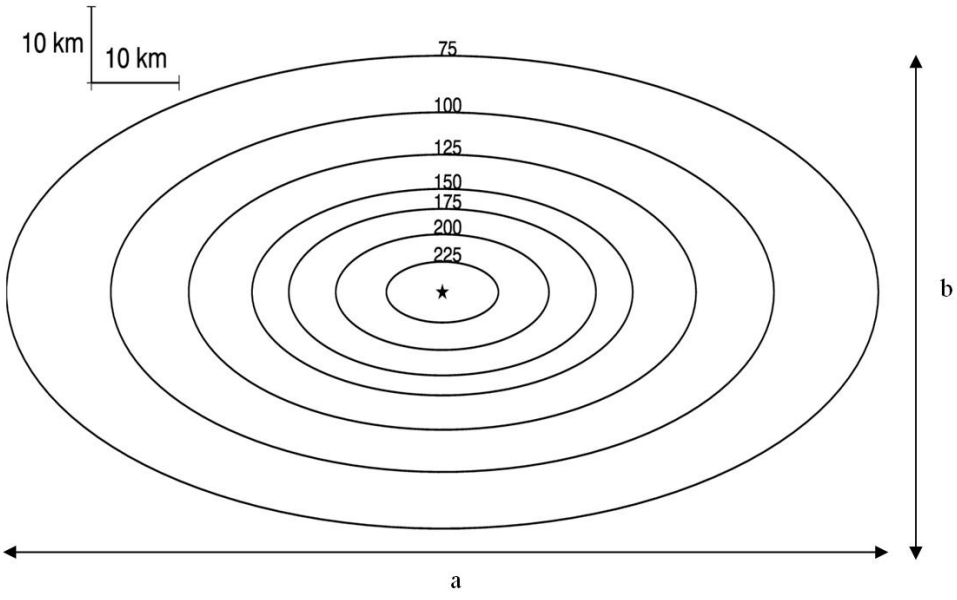

Note: a:b = 1.6:1.

Figure Q7 4-hr Generalized Convergence Pattern for Taiwan Storm

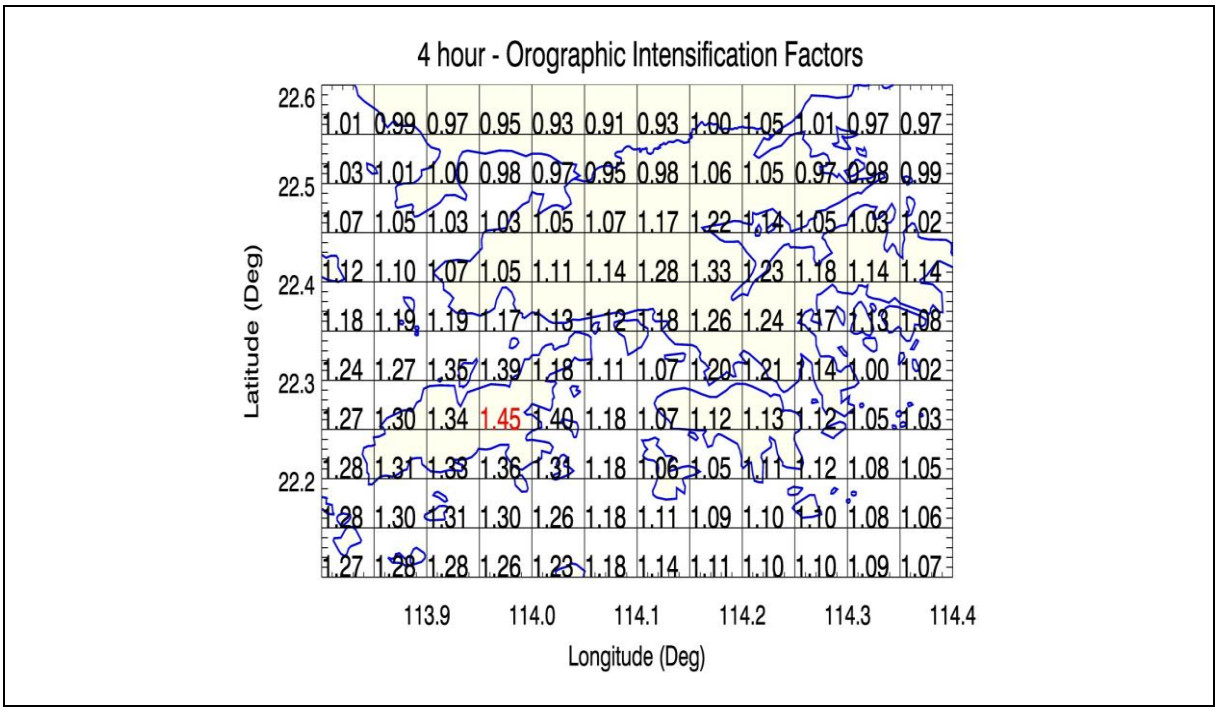

Figure Q8 4-hour SDOIF for Hong Kong at a Resolution of 5 km x 5 km

Q.5 Storm Transposition and Adjustment

A complete set of orientation of convergence pattern centred at Tai Mo Shan, Lantau and Hong Kong Island is given in Appendix S.

After the orientation adjustment of the convergence pattern has been applied to the gridded PMP fractions (OIF), embryonic PMP are obtained for the 8 selected orientation adjustment directions. Embryonic PMP in isohyets and grids are presented in Appendices T to V for the generalized convergence patterns centred at Tai Mo Shan, Lantau and HK Island respectively.

Q.6 Centre Point Value of the Embryonic PMP

The centre point value of the 4-hour PMP
= the highest grid value of the OIF map x the center value of the 4-hour generalized convergence component pattern

Peak Value at Lantau
= 1.45 x 280 = **406 mm**

Peak Value at Tai Mo Shan
= 1.33 x 280 = **372 mm**

(Note: The centre value of the generalized convergence component pattern comes from Haitang.)

Q.7 Table of the Depth-Area Relation for the Embryonic PMP

Four scenarios for orientation: (a) the East-West orientation specified as E-W or 0°; (b) the NE-SW or 45°; (c) the ENE-WSW or 22.5°; and (d) the NNE-SSW or 67.5° for the major ellipse axis of the convergence pattern are given in Table Q6, when they are superposed on Hong Kong (centred the highest OIF cell at Lantau). The orientation of 0° is the critical case. The dimensions of the superposition area are given below:

HK area:

	Lower Bound (°)	Upper Bound (°)	Range (°)
Longitude	113.8	114.4	0.6
Latitude	22.1	22.6	0.5

Notes: (1) 1° ~ 100 km.
(2) Area ~ 3000 km^2 (including the ocean area).

Table Q6 Relation of Depth-Area of the 4-hour Embryonic PMP for Hong Kong

Area (km^2)	Orientation of Major Storm Axis			
	E-W 0°	NE-SW 45°	ENE-WSW 22.5°	NNE-SSW 67.5°
	Depth (mm)	Depth (mm)	Depth (mm)	Depth (mm)
0	406	406	406	406
10	391	385	386	384
20	378	372	375	372
50	355	351	354	351
100	328	331	333	330
150	318	317	319	316
200	308	306	308	306
300	294	290	291	289
400	283	278	279	278
500	274	267	268	267
600	266	258	258	257
700	259	250	250	249
800	253	242	242	241
900	246	235	235	233
1000	240	228	229	227
1500	213	199	200	198
2000	189	177	178	176
3000	149	144	146	141

Note: The embryonic PMP with orientation adjustment of 90°, 112.5°, 135° and 157.5° are less critical and not shown here for clarity.

Q.8 Moisture Maximization for Transposed Storm

Then, the centre point value of the PMP based on transposition of the 4 Taiwan storms is as below:

4-hr: 406 mm x 1.304 = 529 mm

Isohyets in Appendices T to V are multiplied by the ratio of 1.304 and presented in Appendix W.

Q.9 Evaluation of PMP Estimates

The Depth-Area relation of the 4-hour PMP based on transposition of the 4 Taiwan storms is given in Table Q7.

Table Q7 Depth-Area Relationship of Moisture-maximized Transposed Storm Based on Typhoons Herb, Aere, Haitang & Morakot with Orientation Adjustment of 0°

Area (km^2)	PMP (4-hr)	Area (km^2)	PMP (4-hr)
0	529	500	357
10	510	600	347
20	493	700	338
50	463	800	330
100	428	900	321
150	415	1000	313
200	402	1500	278
300	383	2000	246
400	369	3000	194

A comparison between the above PMP (i.e. the moisture-maximized transposed storm) and the 2000 PMP (HKO, 2000) is shown in Figure Q9.

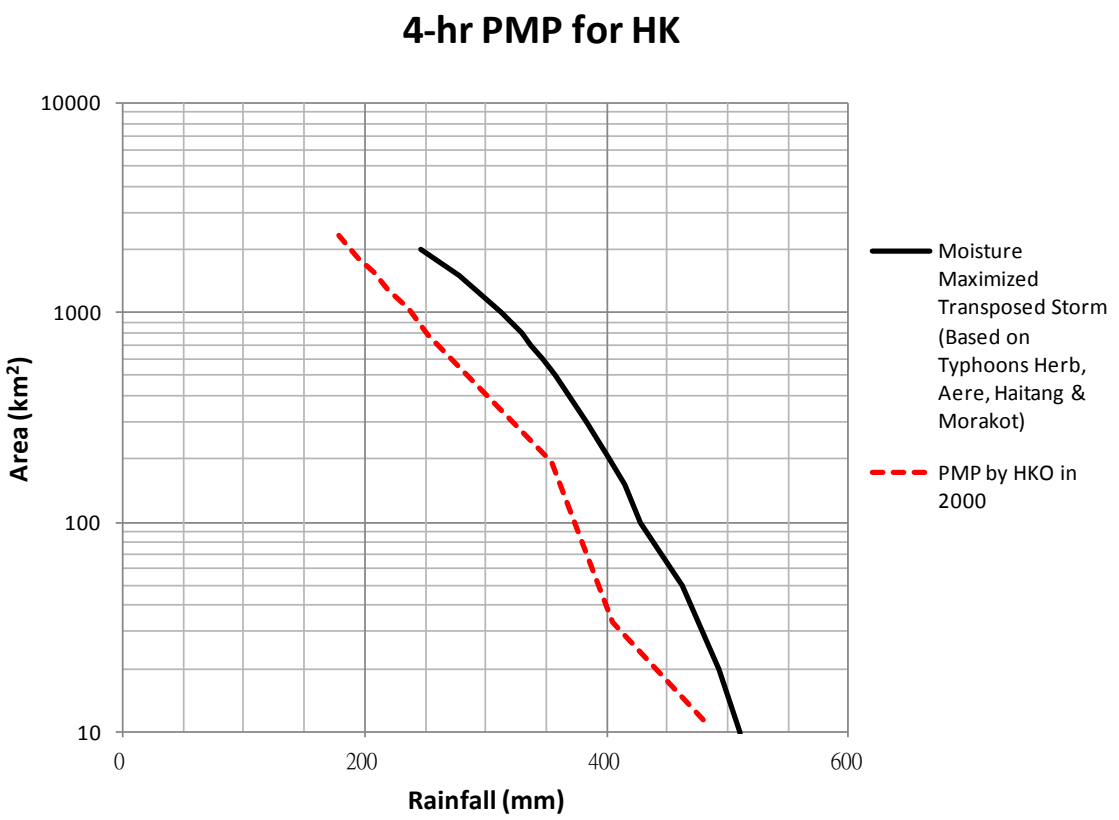

Figure Q9 DAD Curves of Moisture-maximized Transposed Storm Based on Typhoons Herb, Aere, Haitang & Morakot with Orientation Adjustment of 0° and 2000 PMP

Q.10 Reference

HKO (2000). *The 4-hour Probable Maximum Precipitation for Hong Kong, An Updating Study*. Hong Kong Observatory, 18 p.

Table of Contents
Table of Contents
Table of Contents

Appendix R

Calculation for 4-hour Statistical PMP

Hong Kong 4-hr

站号	資料年數(n)	Xm	$\bar{X}_{n-1}$	S_{n-1}	$\bar{X}_n$	S_n	$C_v=\frac{S_n}{\bar{X}_n}$	可能最大校正 $(1+\frac{3C_v}{\sqrt{n}})*\bar{X}_n$	$K_m=\frac{X_m-\bar{X}_{n-1}}{S_{n-1}}$	$\Phi_m=\frac{X_m-\bar{X}_n}{S_n}$	Φ_m^2+2	$n\geq(\Phi_m^2+2)$	required n, when $K_m-->\phi_m$	
N14	27	365	148.9038	53.0645	156.9074	66.6114	0.4245	195.3655	4.0723	3.1240	11.7592	√	68	
~~H15~~	~~27~~	~~348.5~~	~~116.5769~~	~~33.9593~~	~~125.1667~~	~~55.6870~~	~~0.4449~~	~~157.3176~~	~~6.5294~~	~~4.0105~~	~~18.0842~~	~~√~~	~~104~~	(Out)
H01	27	331	121.4423	42.4475	129.2037	57.9564	0.4486	162.6649	4.9369	3.4819	14.1234	√	81	
~~H21~~	~~27~~	~~319.5~~	~~110.3654~~	~~34.0504~~	~~118.1111~~	~~52.2947~~	~~0.4428~~	~~148.3035~~	~~6.1419~~	~~3.8510~~	~~16.8305~~	~~√~~	~~97~~	(Out)
H02	27	314.5	121.6538	40.6125	128.7963	54.4365	0.4227	160.2252	4.7484	3.4114	13.6375	√	78	
HK0	119	302.3	122.1160	45.3885	124.6563	48.0870	0.3858	138.0506	3.9698	3.6942	15.6472	√	90	
H04	27	297	129.4808	45.0081	135.6852	54.6551	0.4028	167.2403	3.7220	2.9515	10.7114	√	62	
H10	27	293.5	130.4038	44.2330	136.4444	53.5398	0.3924	167.3556	3.6872	2.9334	10.6051	√	61	
H16	27	293	126.2885	44.7346	132.4630	54.3468	0.4103	163.8401	3.7267	2.9539	10.7257	√	62	
N11	27	283.5	120.0385	33.3934	126.0926	45.4076	0.3601	152.3087	4.8950	3.4665	14.0169	√	81	
H17	27	273	127.1346	44.2702	132.5370	51.6962	0.3901	162.3839	3.2949	2.7171	9.3825	√		
H08	27	271.5	123.3269	44.3914	128.8148	52.0381	0.4040	158.8590	3.3379	2.7419	9.5182	√		
H03	27	271	114.8462	42.0692	120.6296	51.0378	0.4231	150.0963	3.7118	2.9463	10.6804	√		
K01	27	266.5	132.6538	48.2020	137.6111	53.8292	0.3912	168.6894	2.7768	2.3944	7.7332	√		
N05	27	266.5	110.5577	41.1855	116.3333	50.3157	0.4325	145.3831	3.7863	2.9845	10.9072	√		
H09	27	262.5	131.9615	37.4246	136.7963	44.4730	0.3251	162.4728	3.4880	2.8265	9.9892	√		
N04	27	262.5	122.8654	35.1558	128.0370	43.7097	0.3414	153.2728	3.9719	3.0763	11.4635	√		
K02	27	261	139.2115	47.5203	143.7222	52.1601	0.3629	173.8369	2.5629	2.2484	7.0554	√		
K06	27	260	133.7500	50.3844	138.4259	55.0571	0.3977	170.2131	2.5057	2.2081	6.8759	√		
N12	27	259	109.9423	39.4145	115.4630	48.1316	0.4169	143.2518	3.7818	2.9822	10.8934	√		
H07	27	258.5	121.8846	39.5460	126.9444	46.8507	0.3691	153.9937	3.4546	2.8080	9.8847	√		
H12	27	255	129.6346	42.3621	134.2778	48.0377	0.3577	162.0124	2.9594	2.5131	8.3155	√		
H06	27	252	126.7692	42.1272	131.4074	47.8256	0.3639	159.0195	2.9727	2.5215	8.3580	√		
N09	27	249.5	131.1923	33.8142	135.5741	40.2221	0.2967	158.7963	3.4988	2.8324	10.0226	√		
N01	27	247.5	139.8654	47.4617	143.8519	50.9417	0.3541	173.2630	2.2678	2.0346	6.1398	√		
N06	27	246	134.1346	45.5821	138.2778	49.6114	0.3588	166.9210	2.4541	2.1713	6.7146	√		
H18	27	243	128.6731	32.4617	132.9074	38.6953	0.2911	155.2482	3.5219	2.8451	10.0947	√		
N10	27	230.5	116.2308	41.8818	120.4630	46.5857	0.3867	147.3592	2.7284	2.3620	7.5792	√		
H05	27	229.5	123.2500	42.1922	127.1852	46.1501	0.3629	153.8299	2.5182	2.2170	6.9151	√		
N02	27	229.5	128.7692	38.4188	132.5000	42.3679	0.3198	156.9611	2.6219	2.2895	7.2417	√		
K08	27	229	122.4423	40.1020	126.3889	44.3492	0.3509	151.9939	2.6572	2.3137	7.3532	√		
N07	27	227	110.6923	43.9791	115.0000	48.5879	0.4225	143.0523	2.6446	2.3051	7.3135	√		
N13	27	227	134.6154	38.9706	138.0370	42.1474	0.3053	162.3708	2.3706	2.1108	6.4553	√		
H14	27	223.5	121.6923	39.1101	125.4630	43.0657	0.3433	150.3269	2.6031	2.2765	7.1822	√		
H19	27	222.5	124.2885	37.2956	127.9259	41.1668	0.3218	151.6936	2.6333	2.2973	7.2778	√		
N03	27	222.5	128.2115	45.3182	131.7037	48.0003	0.3645	159.4167	2.0806	1.8916	5.5781	√		
N15	27	218.5	122.9038	28.7632	126.4444	33.6744	0.2663	145.8864	3.3236	2.7337	9.4731	√		
K03	27	216	123.3462	37.6241	126.7778	40.9766	0.3232	150.4356	2.4626	2.1774	6.7410	√		
K07	27	215.5	132.4423	42.4307	135.5185	44.5716	0.3289	161.2519	1.9575	1.7945	5.2201	√		
K05	27	212.5	123.7500	41.8687	127.0370	44.4667	0.3500	152.7099	2.1197	1.9220	5.6939	√		
H20	27	203.5	114.7885	37.7950	118.0741	40.8043	0.3456	141.6325	2.3472	2.0935	6.3830	√		
N08	27	200	124.4808	30.9669	127.2778	33.6644	0.2645	146.7140	2.4387	2.1602	6.6665	√		
K04	27	194	125.4808	31.4647	128.0185	33.5535	0.2621	147.3906	2.1777	1.9665	5.8670	√		
Maximum							0.4486	195.3655	4.9369					
	$X_{pmp}=(1+K_m*CV_n)*\bar{x}_n$		828.005315											
			(4-h PMP)											
			(HK data)											
			533.116004											
			(4-h PMP)											
			(N14 only)											

Table of Contents
Table of Contents
Table of Contents

Appendix S

Complete Set of Orientation of Convergence Pattern on HK OIF (4-hour)

Contents

List of Figures

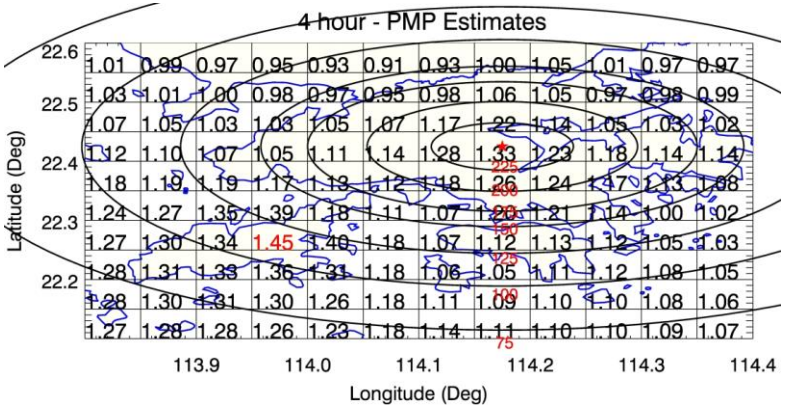

Centered at Tai Mo Shan

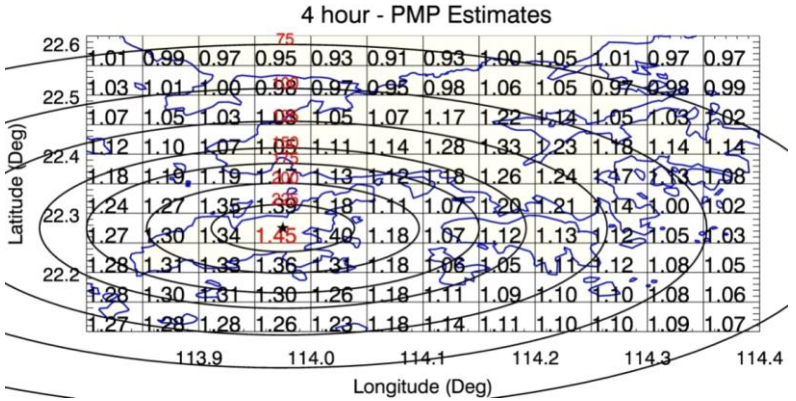

Centered at Lantau

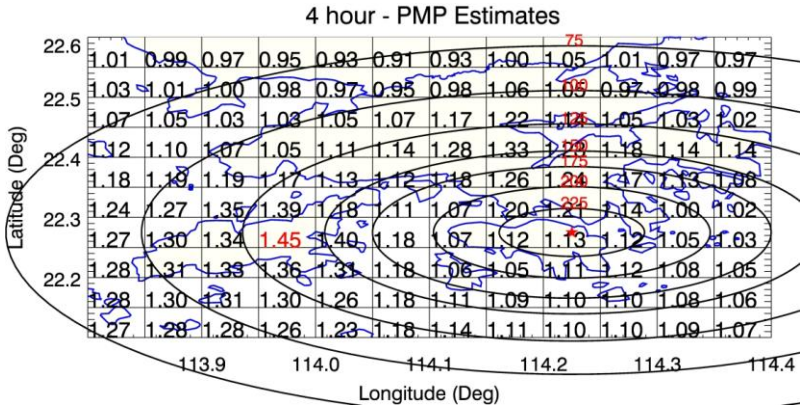

Centered at Hong Kong Island

Figure S1 E-W Orientation 0° - 4-hour (Embryonic PMP)

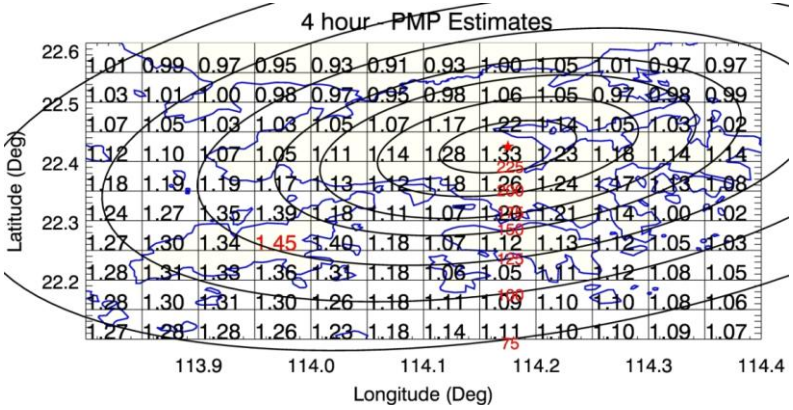

Centered at Tai Mo Shan

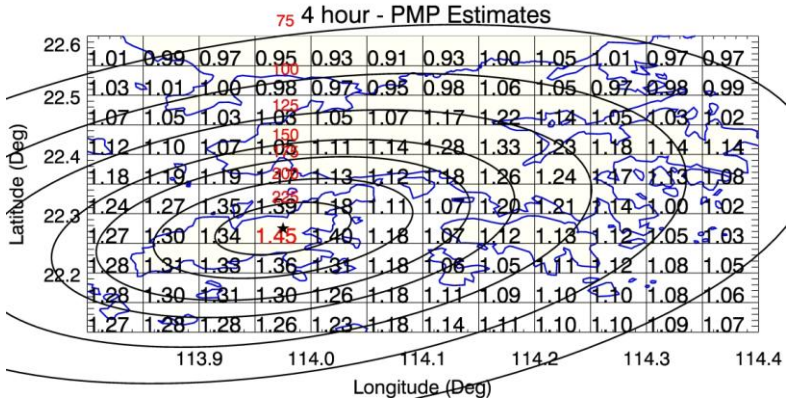

Centered at Lantau

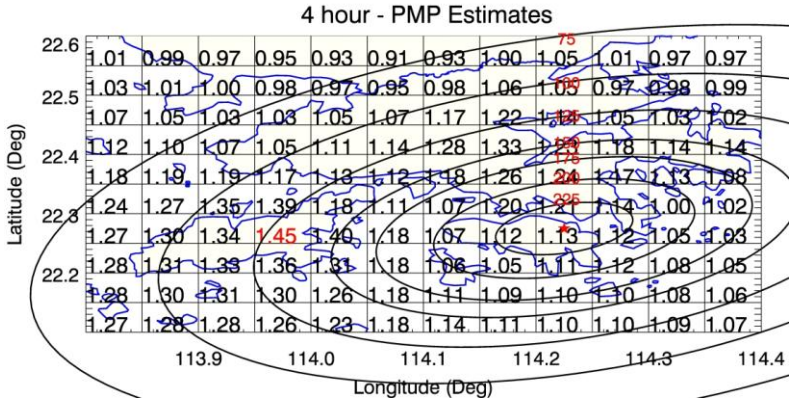

Centered at Hong Kong Island

Figure S2 ENE-WSW Orientation 22.5° - 4-hour (Embryonic PMP)

Table of Contents
Table of Contents
Table of Contents

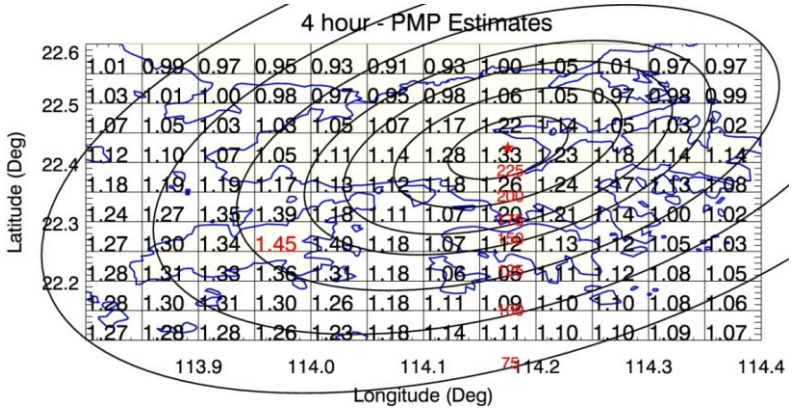

Centered at Tai Mo Shan

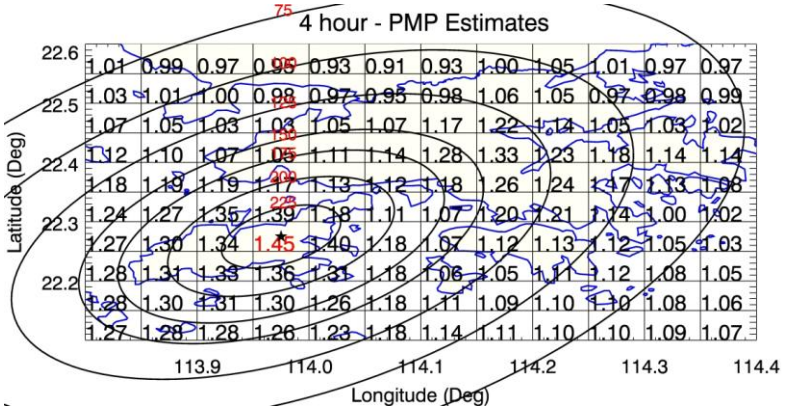

Centered at Lantau

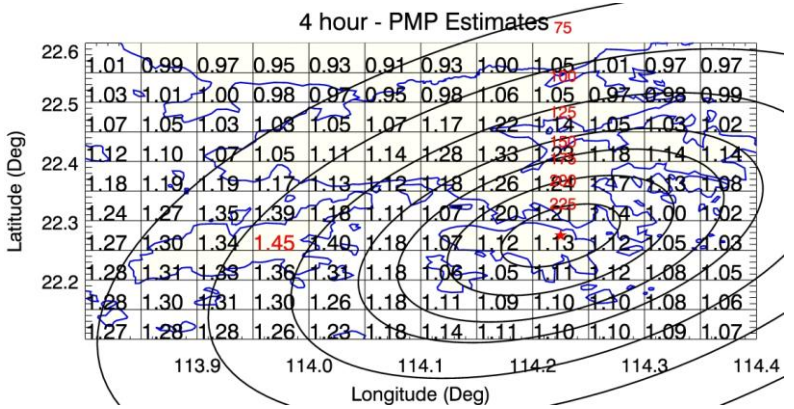

Centered at Hong Kong Island

Figure S3 NE-SW Orientation 45° - 4-hour (Embryonic PMP)

Table of Contents
Table of Contents
Table of Contents

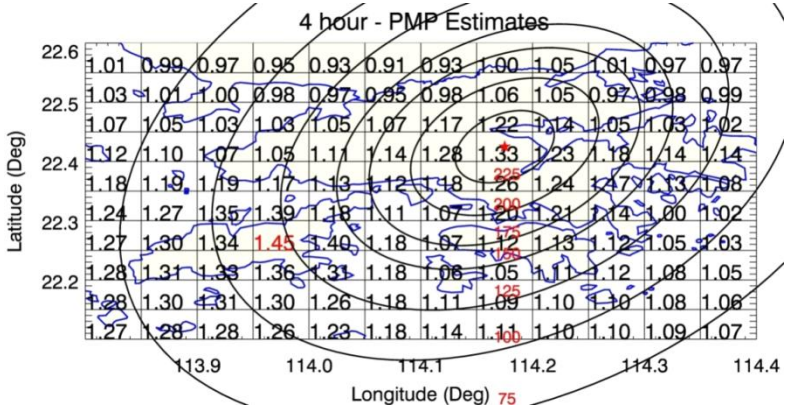

Centered at Tai Mo Shan

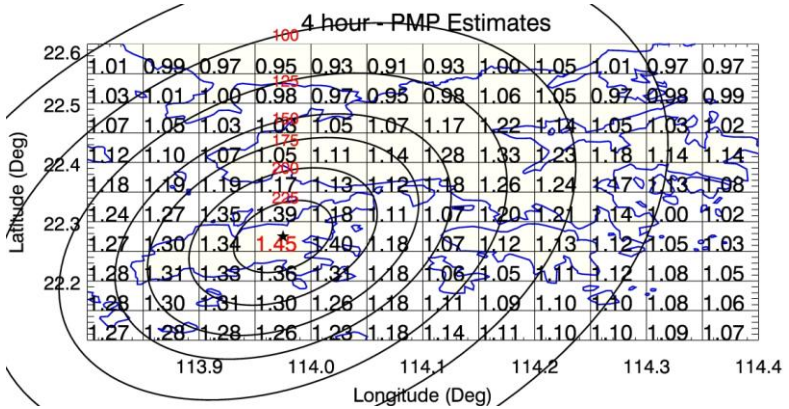

Centered at Lantau

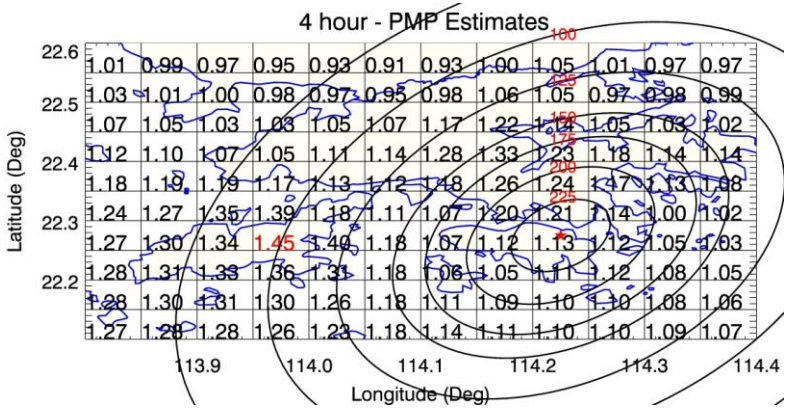

Centered at Hong Kong Island

Figure S4 NNE-SSW Orientation 67.5° - 4-hour (Embryonic PMP)

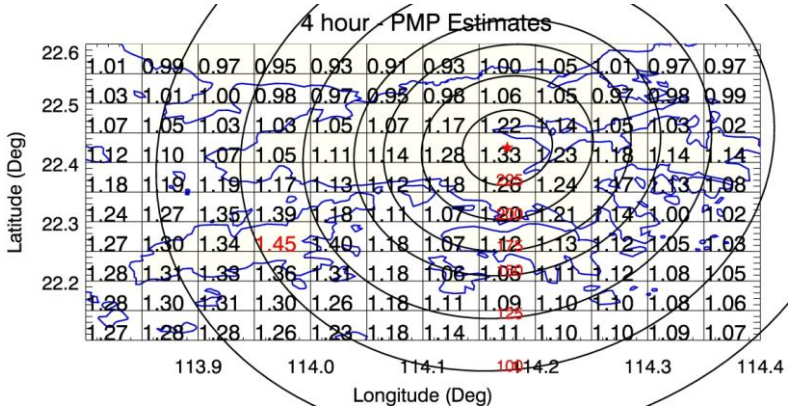

Centered at Tai Mo Shan

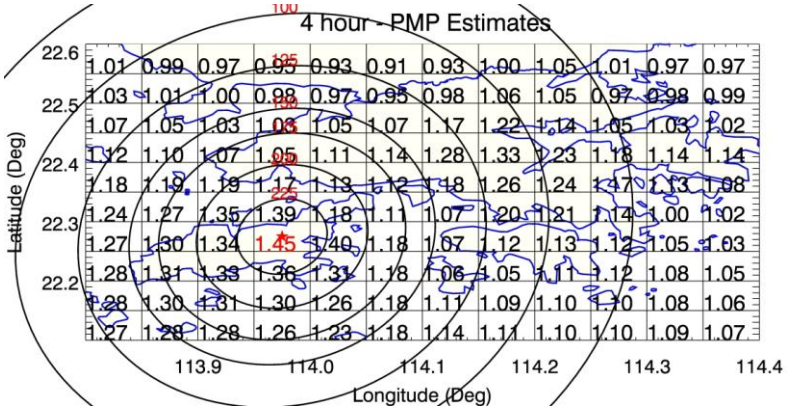

Centered at Lantau

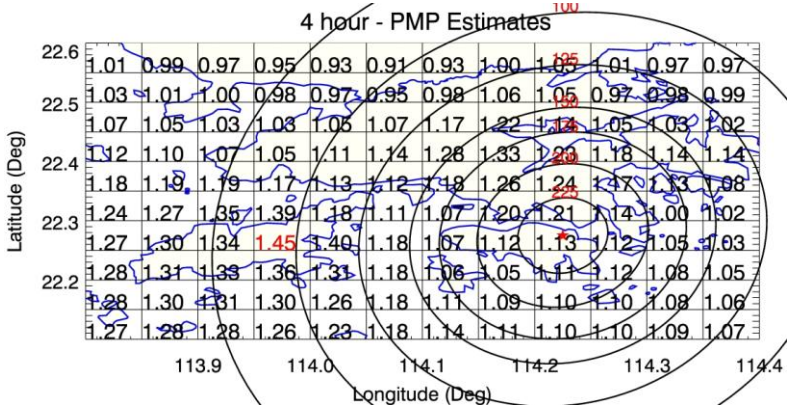

Centered at Hong Kong Island

Figure S5 N-S Orientation 85° - 4-hour (Embryonic PMP)

Table of Contents
Table of Contents
Table of Contents

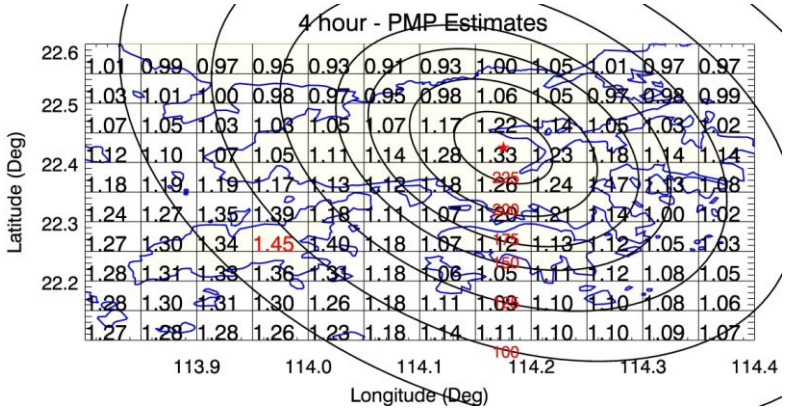

Centered at Tai Mo Shan

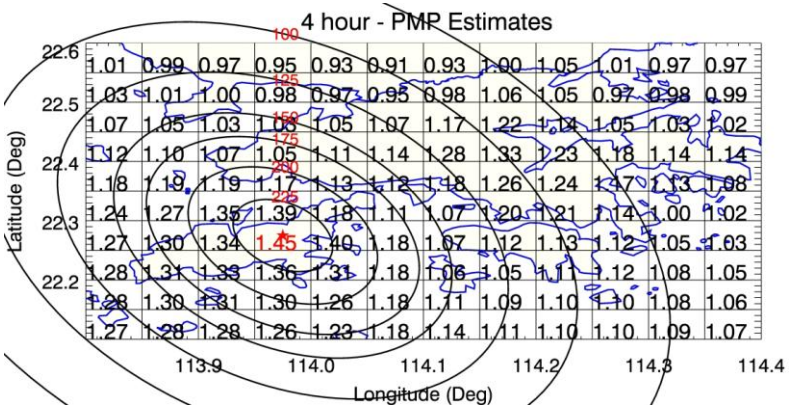

Centered at Lantau

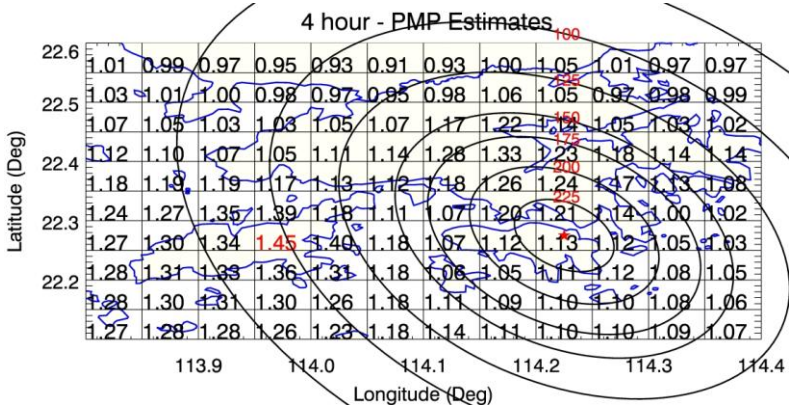

Centered at Hong Kong Island

Figure S6 NNW-SSE Orientation 112.5° - 4-hour (Embryonic PMP)

Table of Contents
Table of Contents
Table of Contents

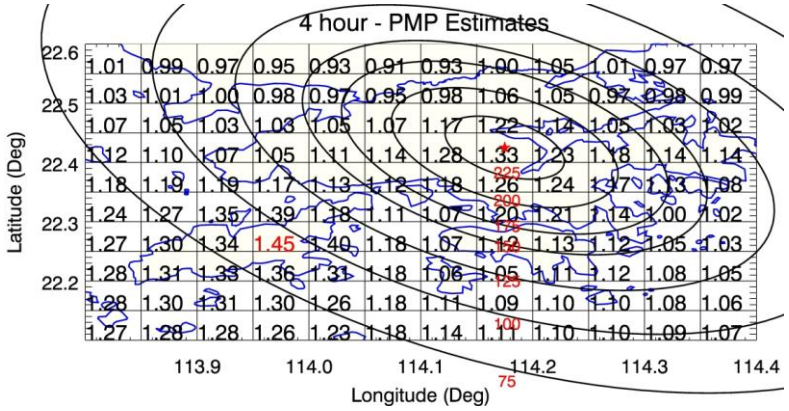

Centered at Tai Mo Shan

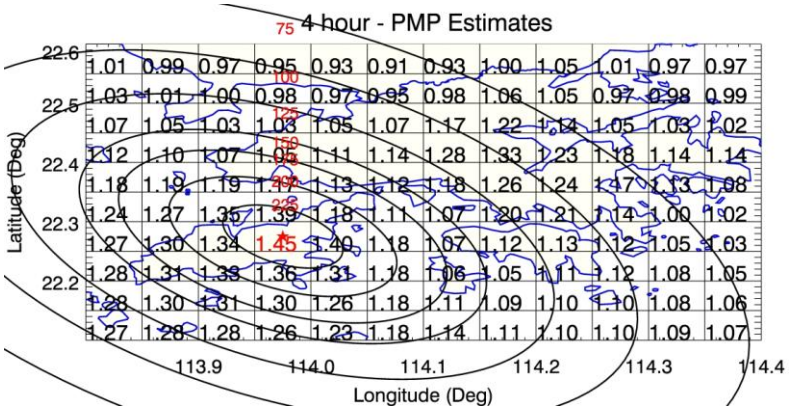

Centered at Lantau

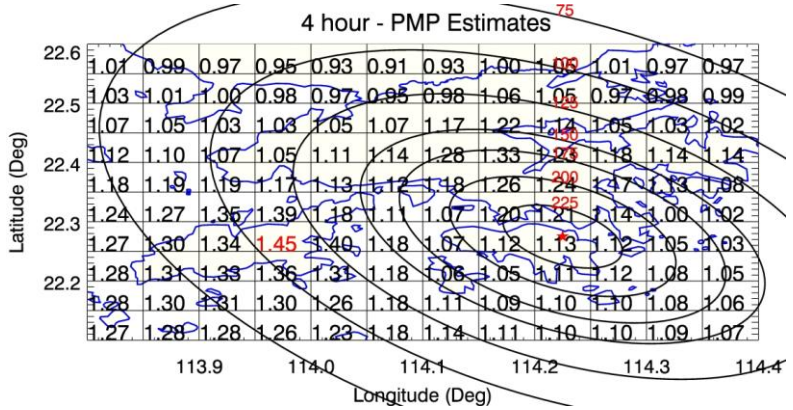

Centered at Hong Kong Island

Figure S7 NW-SE Orientation 135° - 4-hour (Embryonic PMP)

Table of Contents
Table of Contents
Table of Contents

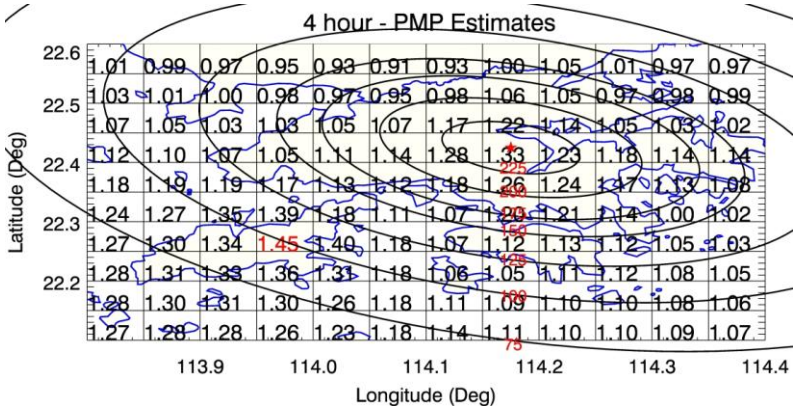

Centered at Tai Mo Shan

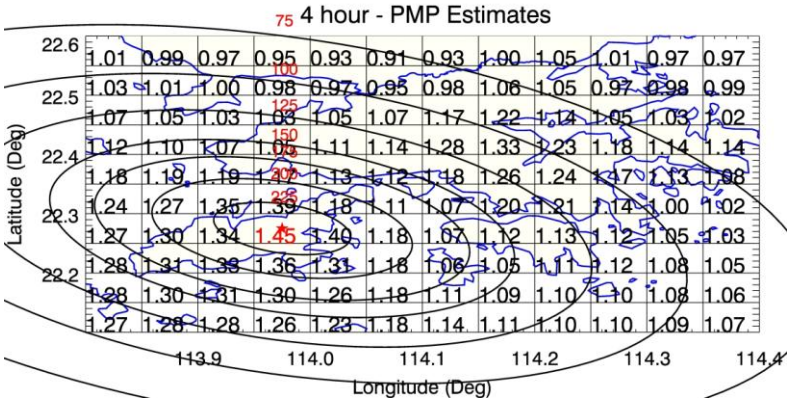

Centered at Lantau

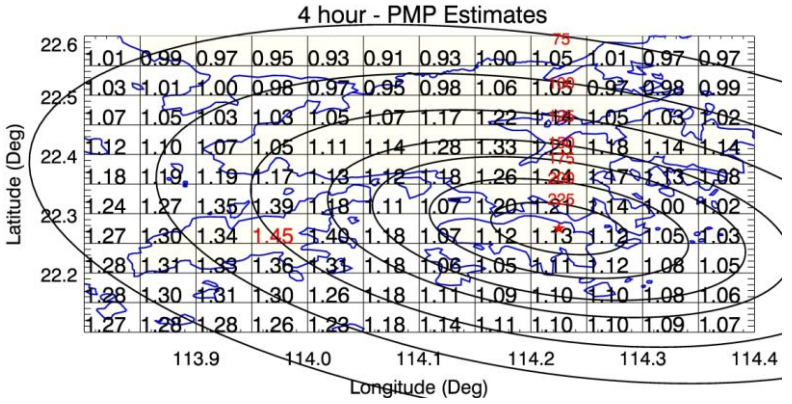

Centered at Hong Kong Island

Figure S8 WNW-ESE Orientation 157.5° - 4-hour (Embryonic PMP)

Table of Contents
Table of Contents
Table of Contents

Table of Contents
Table of Contents
Table of Contents

Appendix T

Embryonic PMP in Grids and Isohyets with the Generalized Convergence Pattern Centred at Tai Mo Shan for a Complete Set of Orientation Adjustments (4-hour)

Contents

List of Figures

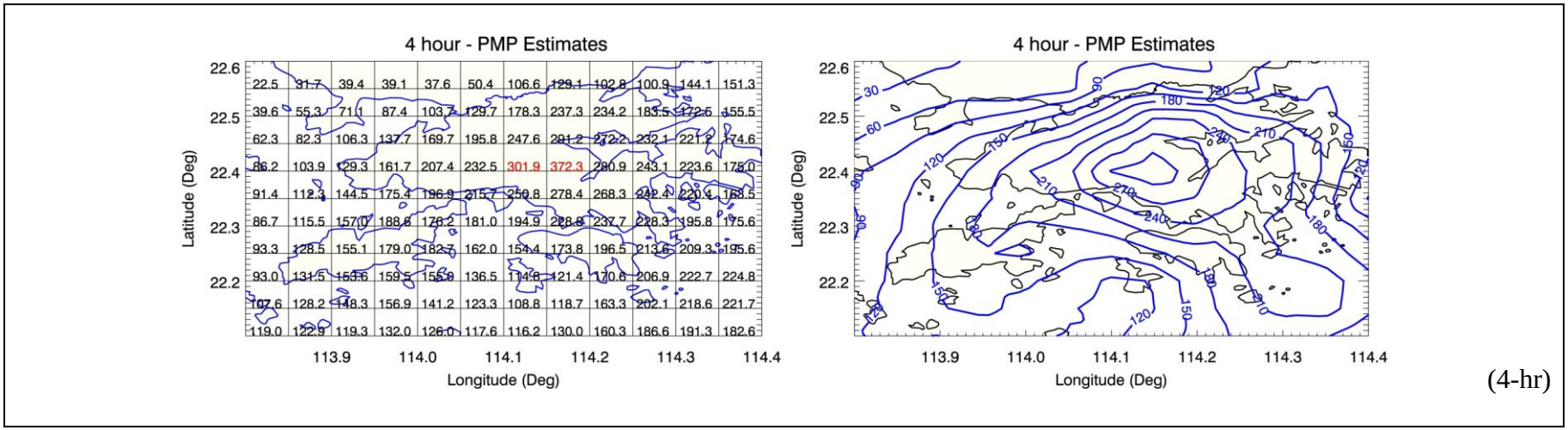

Figure T1 Embryonic PMP Centred at Tai Mo Shan, E-W Orientation - 0°

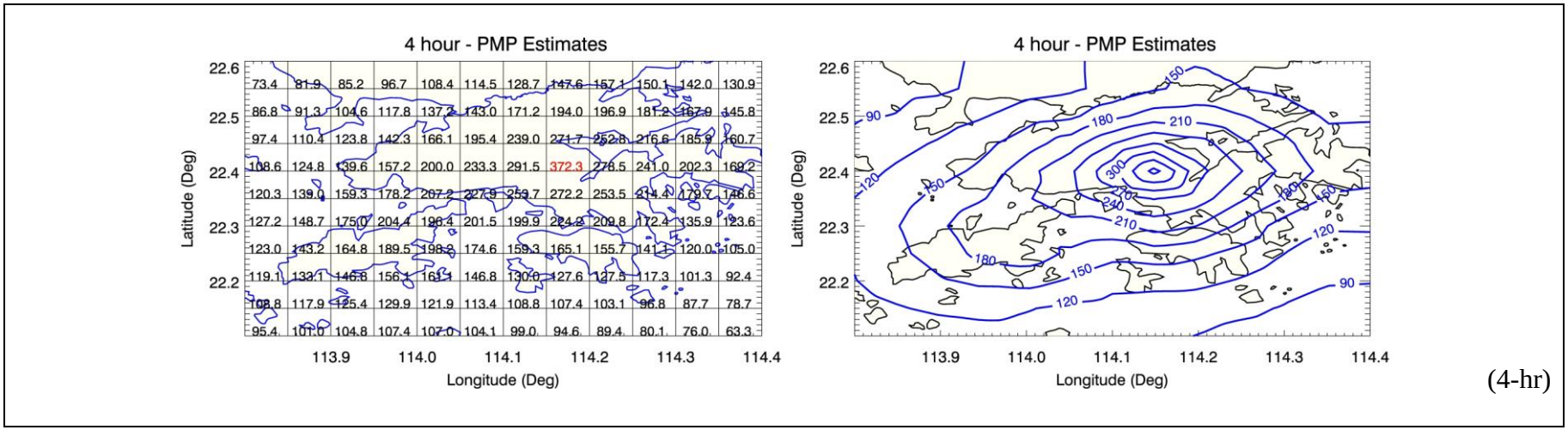

Figure T2 Embryonic PMP Centred at Tai Mo Shan, ENE-WSW Orientation - 22.5°

Table of Contents
Table of Contents
Table of Contents

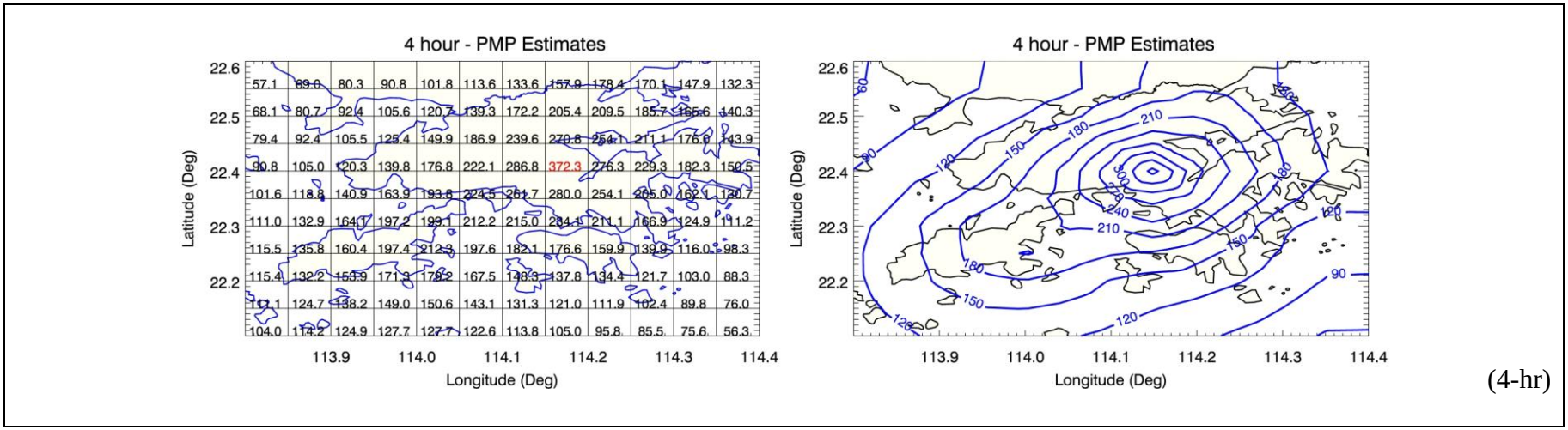

Figure T3 Embryonic PMP Centred at Tai Mo Shan, NE-SW Orientation - 45°

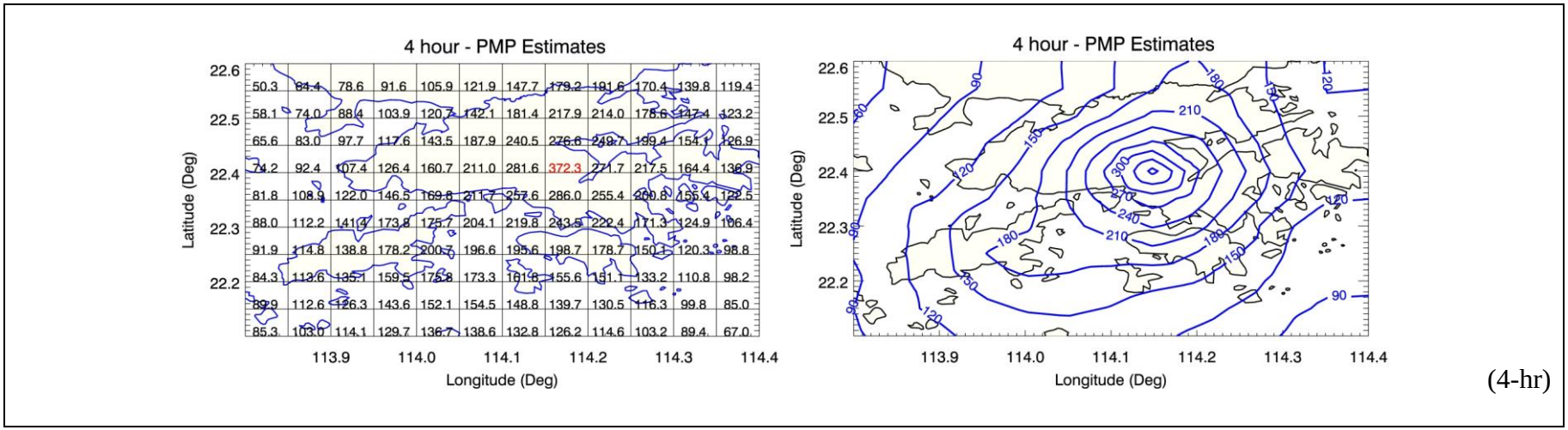

Figure T4 Embryonic PMP Centred at Tai Mo Shan, NNE-SSW Orientation - 67.5°

Table of Contents
Table of Contents
Table of Contents

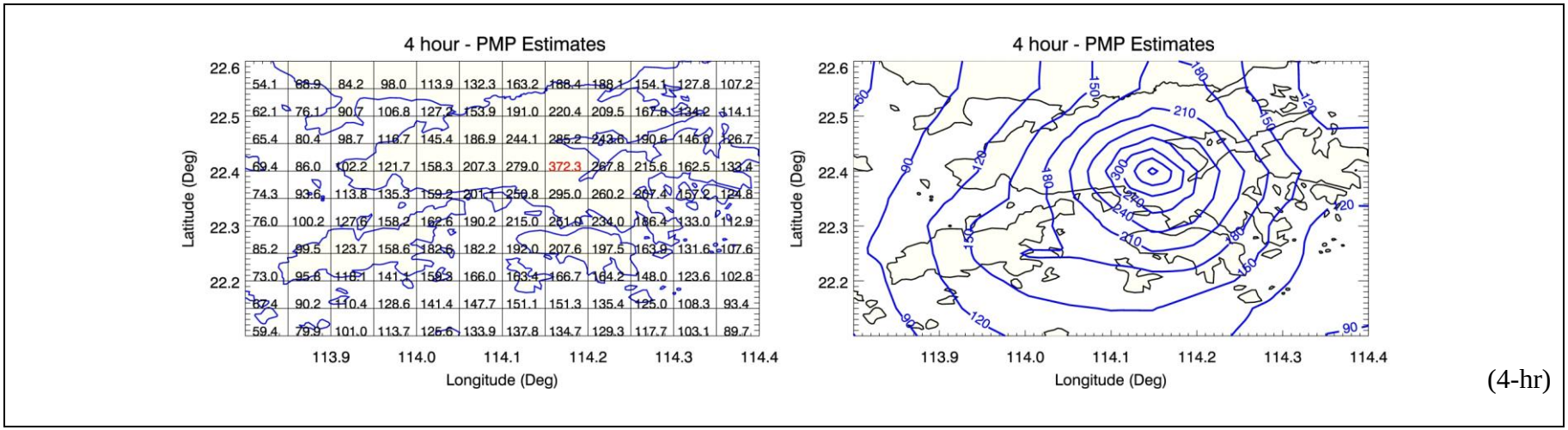

(4-hr)

Figure T5 Embryonic PMP Centred at Tai Mo Shan, N-S Orientation - 85°

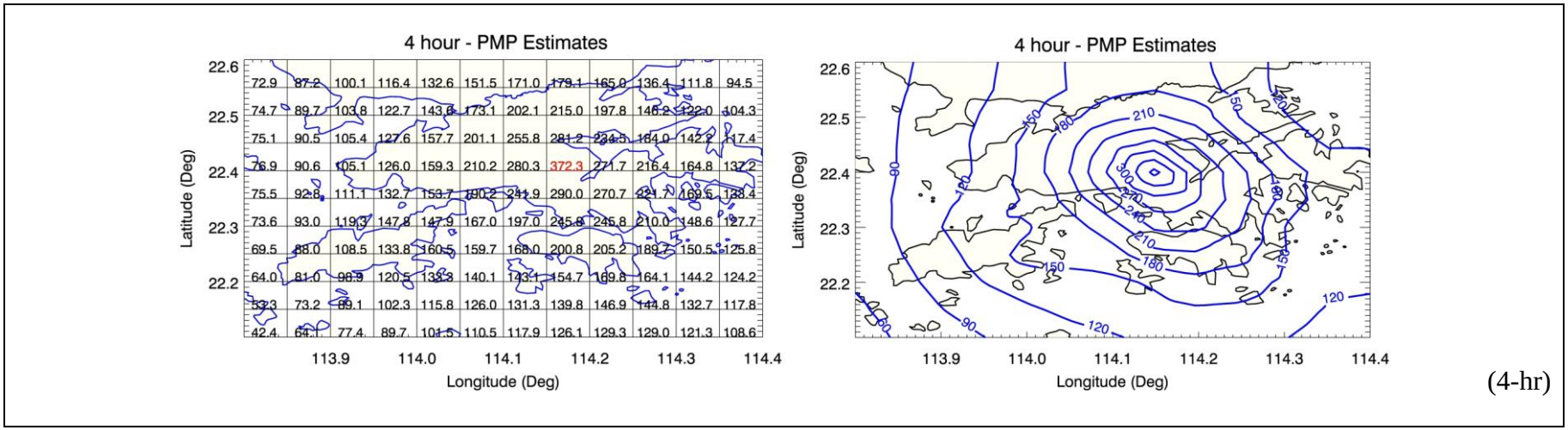

(4-hr)

Figure T6 Embryonic PMP Centred at Tai Mo Shan, NNW-SSE Orientation - 112.5°

Table of Contents
Table of Contents
Table of Contents

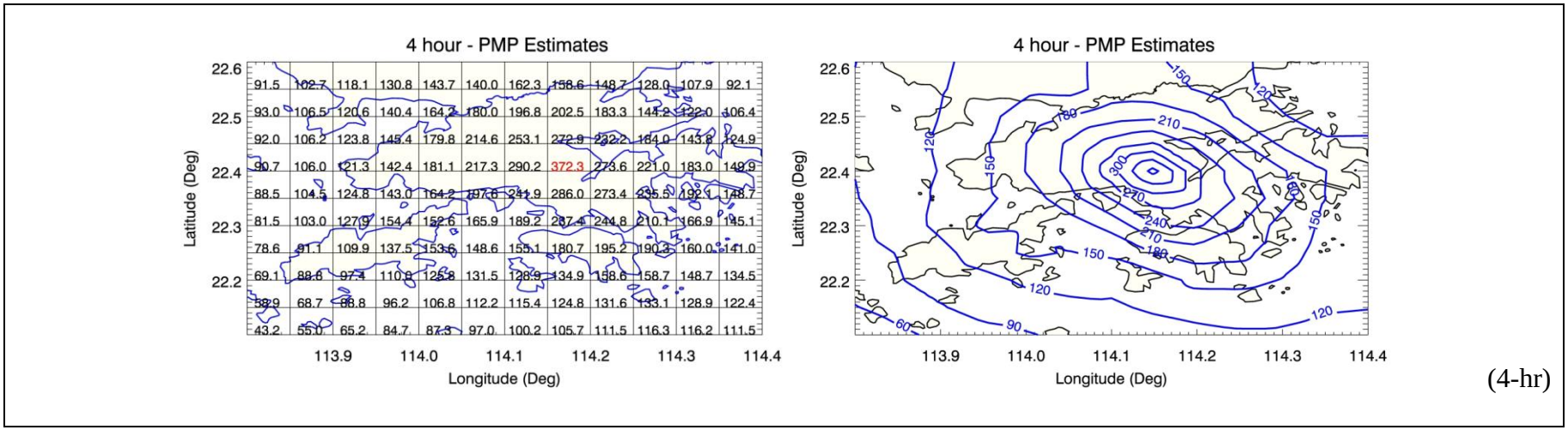

Figure T7 Embryonic PMP Centred at Tai Mo Shan, NW-SE Orientation - 135°

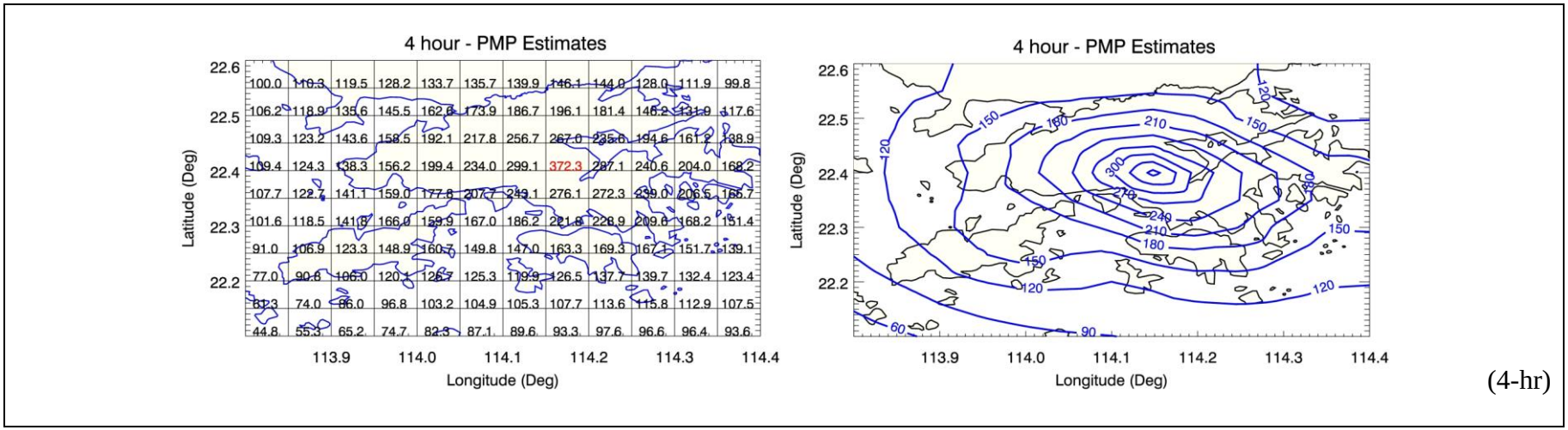

Figure T8 Embryonic PMP Centred at Tai Mo Shan, WNW-ESE Orientation - 157.5°

Table of Contents
Table of Contents
Table of Contents

Appendix U

Embryonic PMP in Grids and Isohyets with the Generalized Convergence Pattern Centred at Lantau for a Complete Set of Orientation Adjustments (4-hour)

Contents

List of Figures

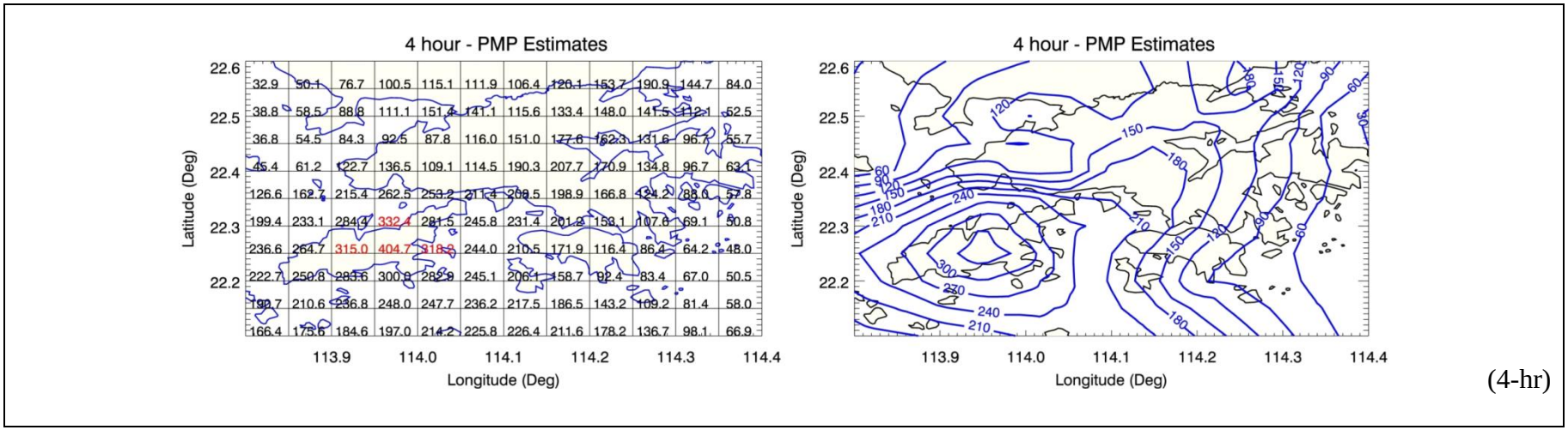

Figure U1 Embryonic PMP Centred at Lantau, E-W Orientation - 0°

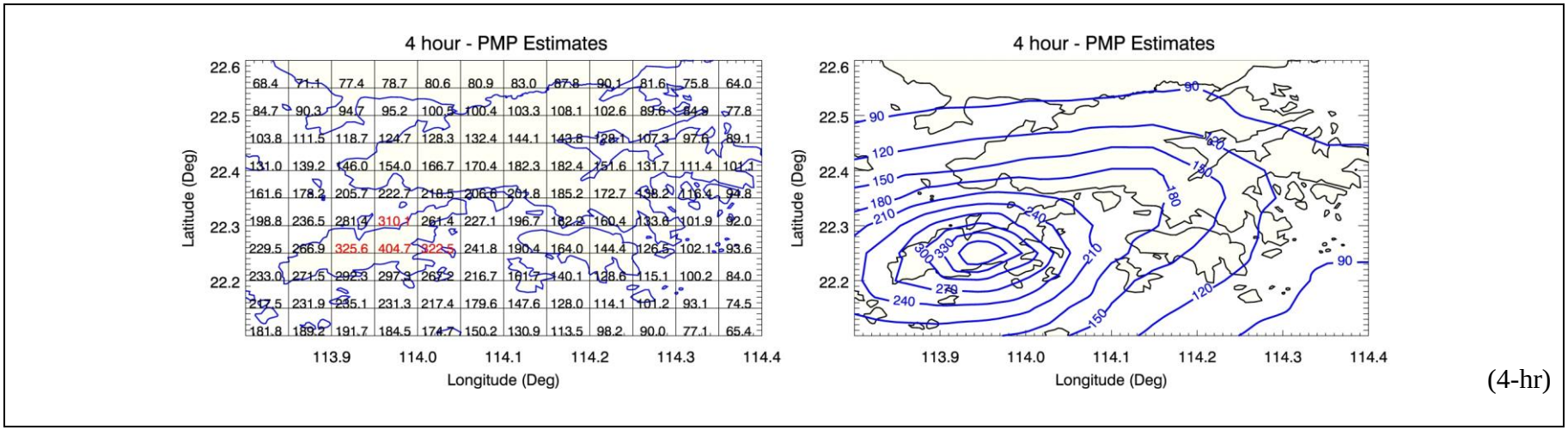

Figure U2 Embryonic PMP Centred at Lantau, ENE-WSW Orientation - 22.5°

Table of Contents
Table of Contents
Table of Contents

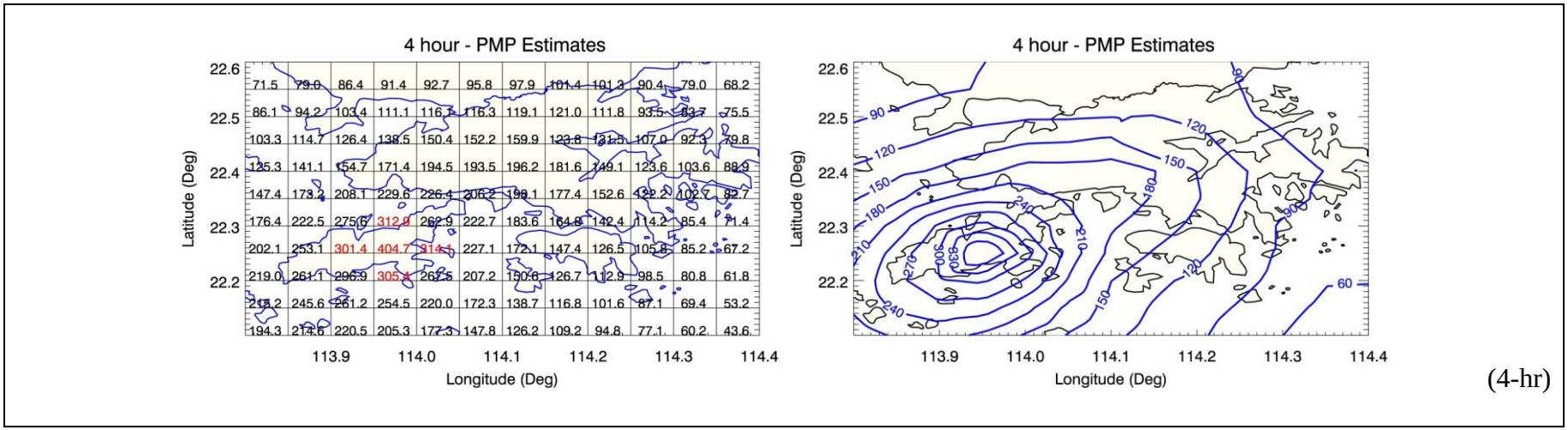

Figure U3 Embryonic PMP Centred at Lantau, NE-SW Orientation - 45°

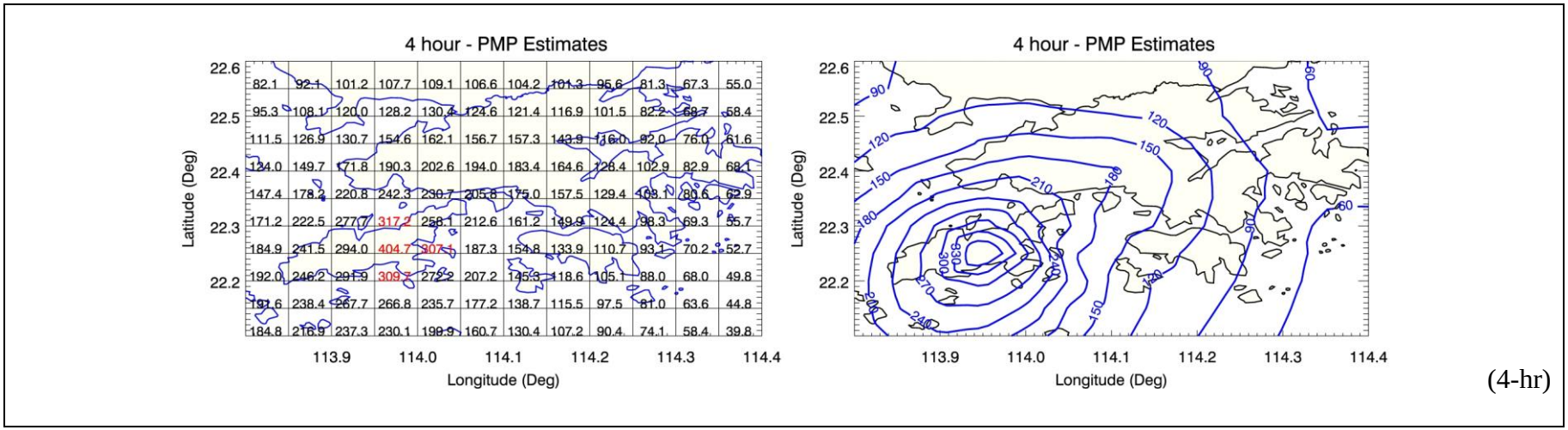

Figure U4 Embryonic PMP Centred at Lantau, NNE-SSW Orientation - 67.5°

Table of Contents
Table of Contents
Table of Contents

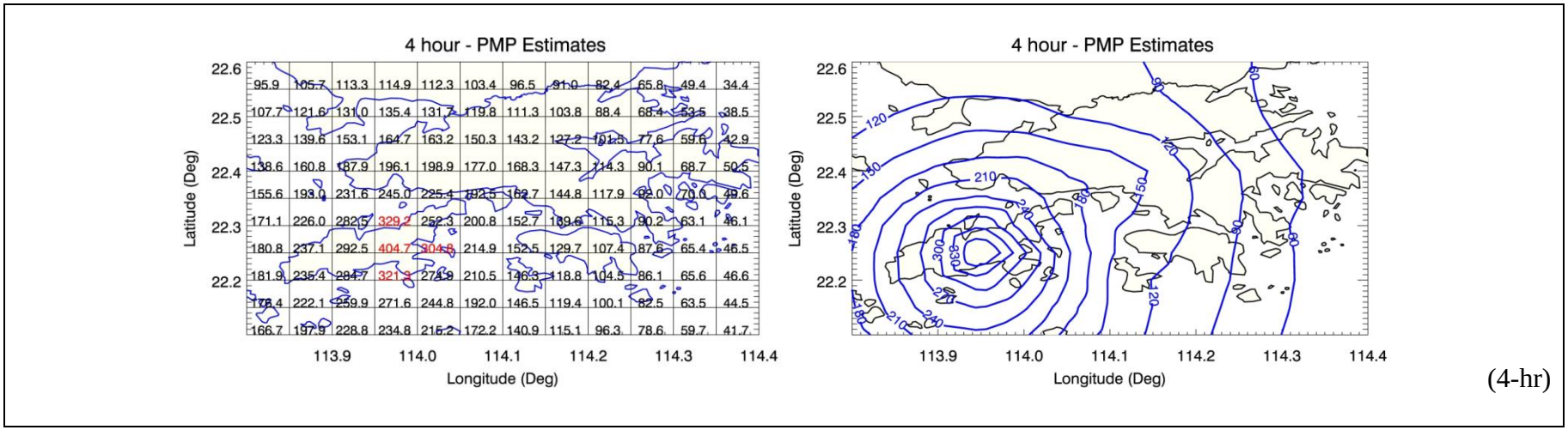

Figure U5 Embryonic PMP Centred at Lantau, N-S Orientation - 85°

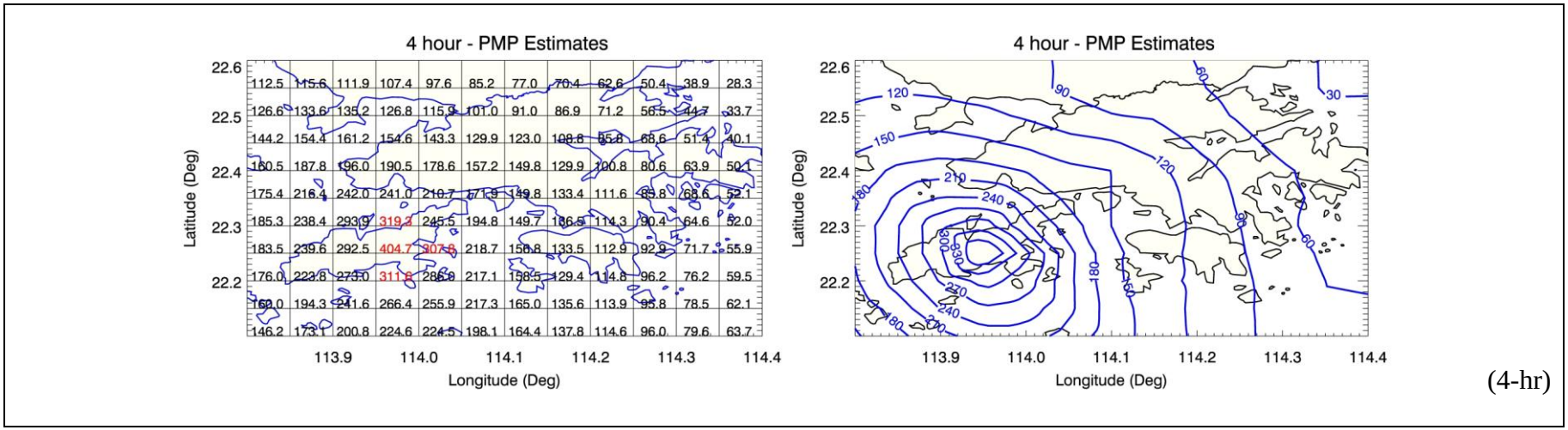

Figure U6 Embryonic PMP Centred at Lantau, NNW-SSE Orientation - 112.5°

Table of Contents
Table of Contents
Table of Contents

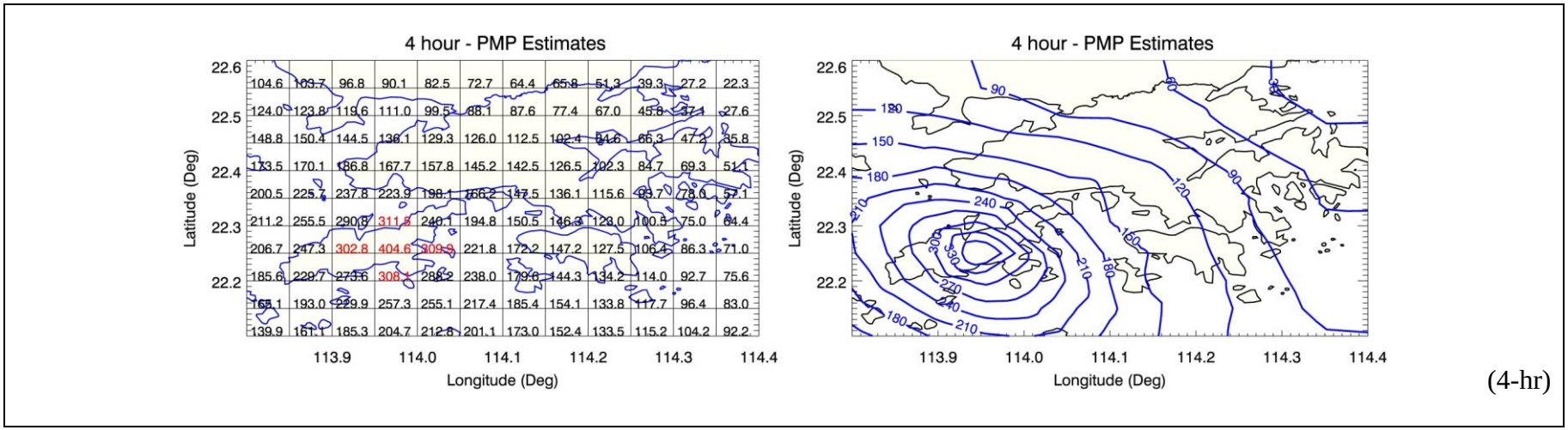

Figure U7 Embryonic PMP Centred at Lantau, NW-SE Orientation - 135°

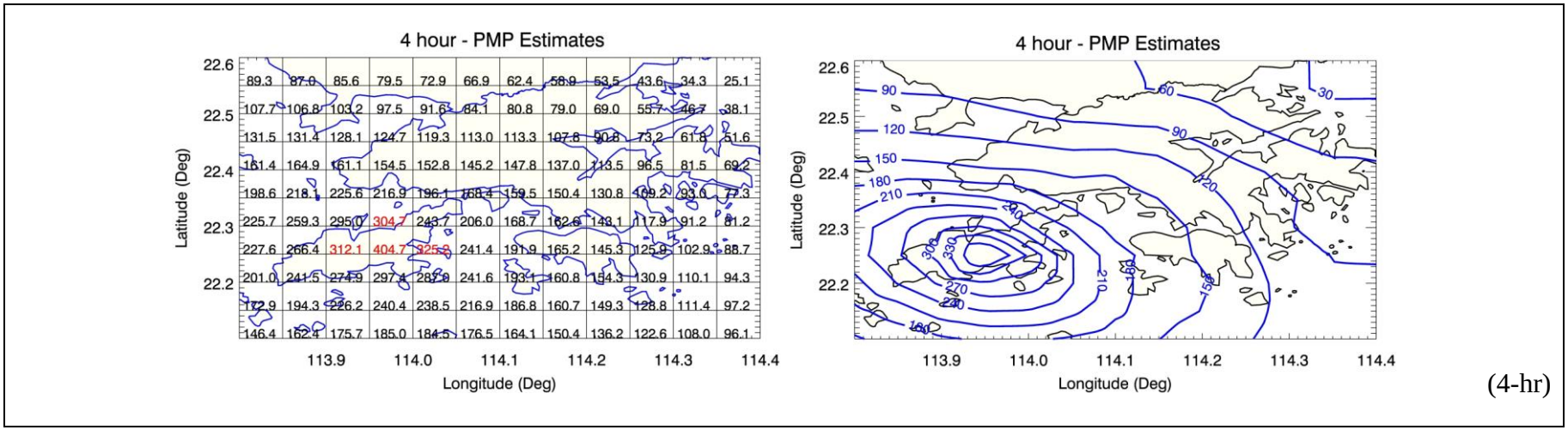

Figure U8 Embryonic PMP Centred at Lantau, WNW-ESE Orientation - 157.5°

Table of Contents
Table of Contents
Table of Contents

Table of Contents
Table of Contents
Table of Contents

Appendix V

Embryonic PMP in Grids and Isohyets with the Generalized Convergence Pattern Centred at Hong Kong Island for a Complete Set of Orientation Adjustments (4-hour)

Contents

List of Figures

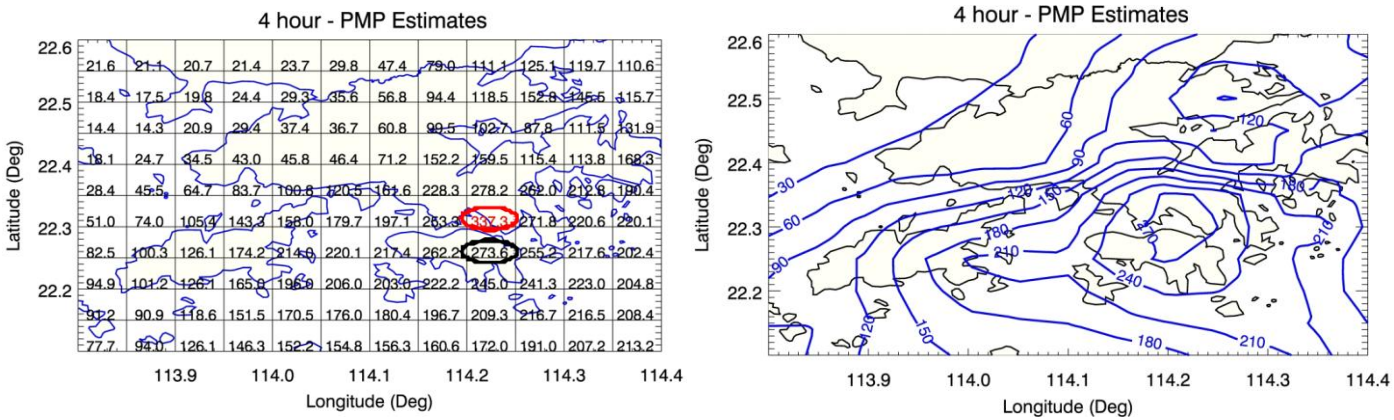

Figure V1 Embryonic PMP Centred at Hong Kong Island, E-W Orientation - 0°

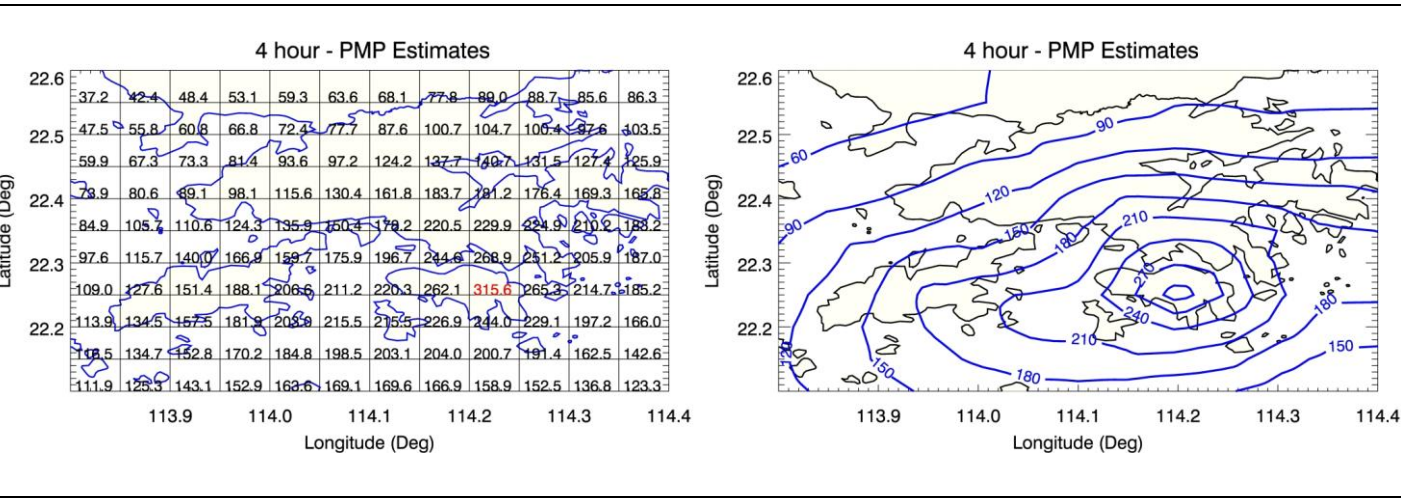

Figure V2 Embryonic PMP Centred at Hong Kong Island, ENE-WSW Orientation - 22.5°

Table of Contents
Table of Contents
Table of Contents

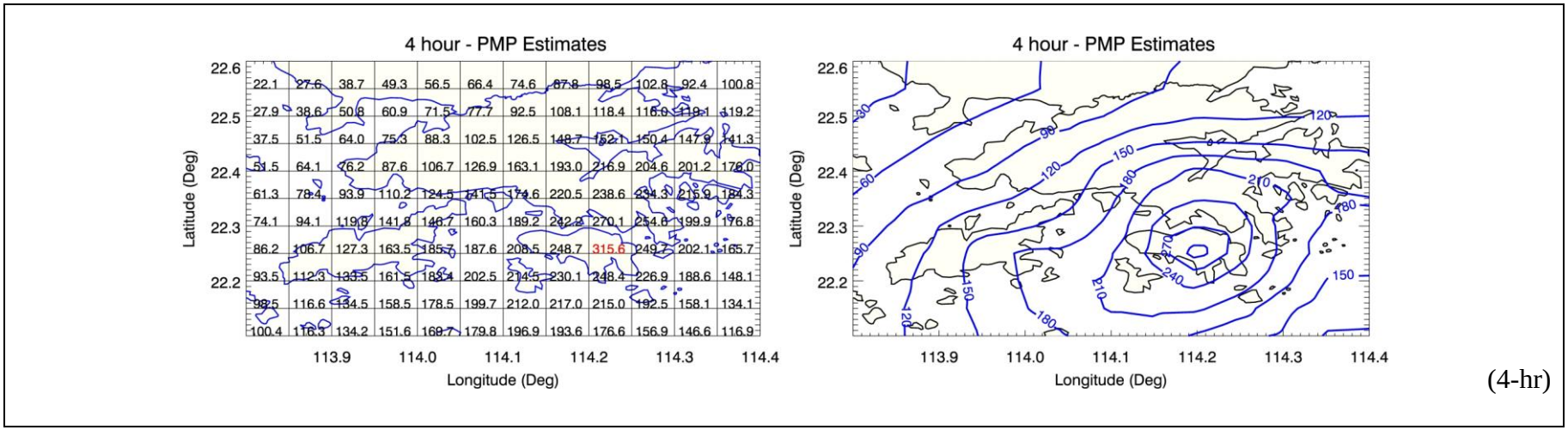

Figure V3 Embryonic PMP Centred at Hong Kong Island, NE-SW Orientation - 45°

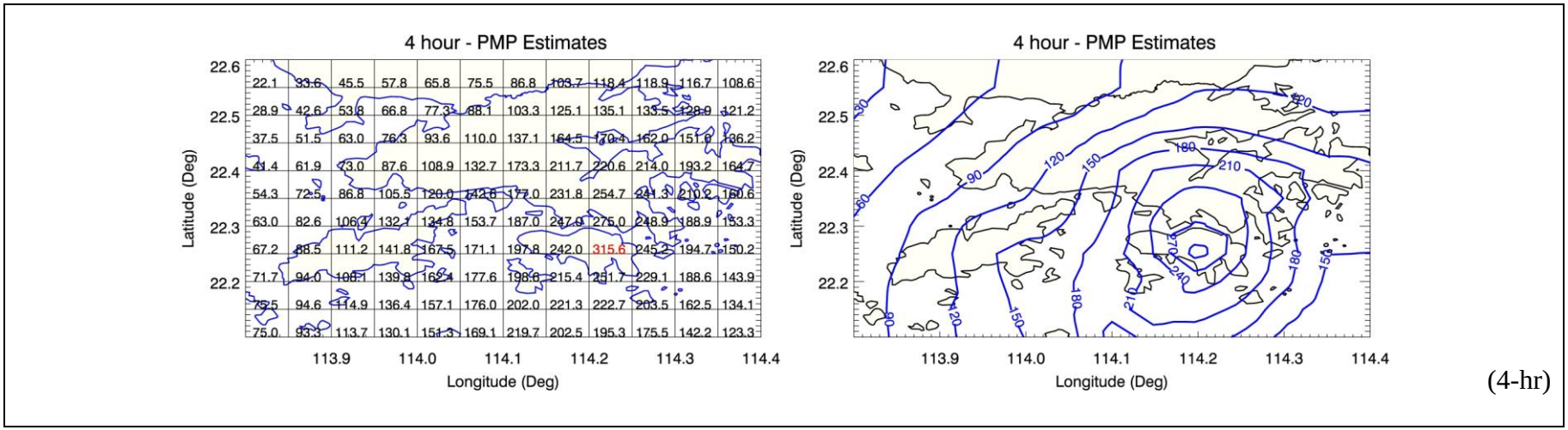

Figure V4 Embryonic PMP Centred at Hong Kong Island, NNE-SSW Orientation - 67.5°

Table of Contents
Table of Contents
Table of Contents

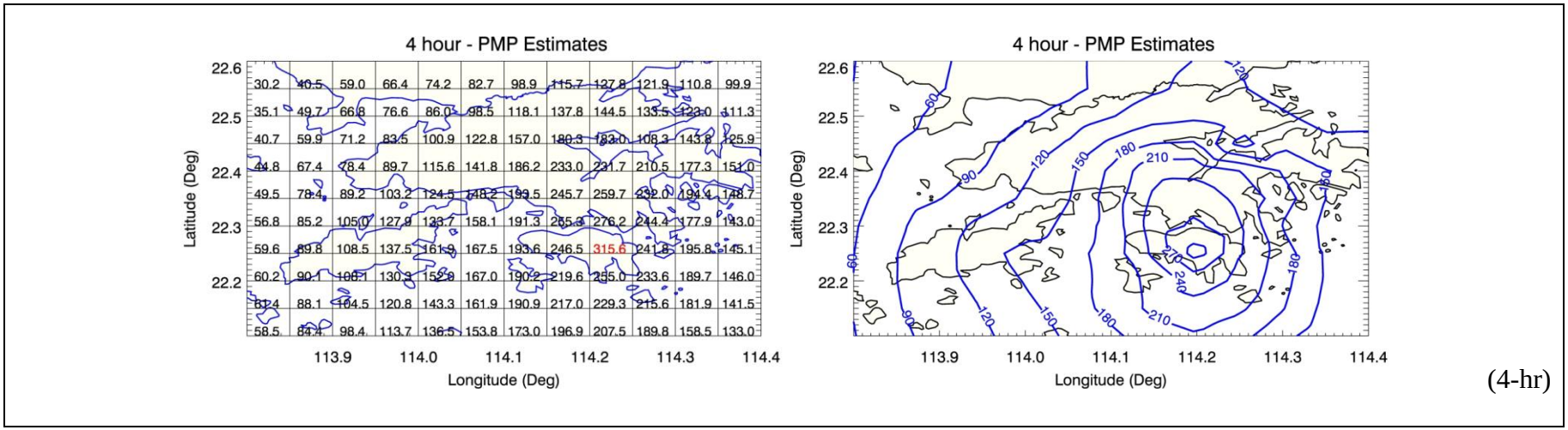

Figure V5 Embryonic PMP Centred at Hong Kong Island, N-S Orientation - 85°

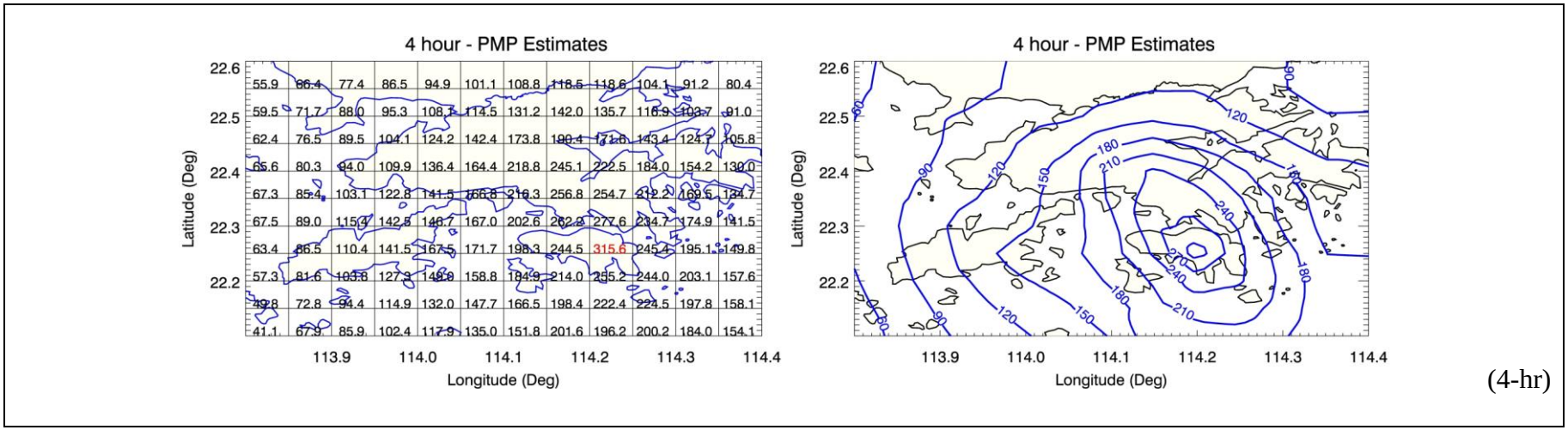

Figure V6 Embryonic PMP Centred at Hong Kong Island, NNW-SSE Orientation - 112.5°

Table of Contents
Table of Contents
Table of Contents

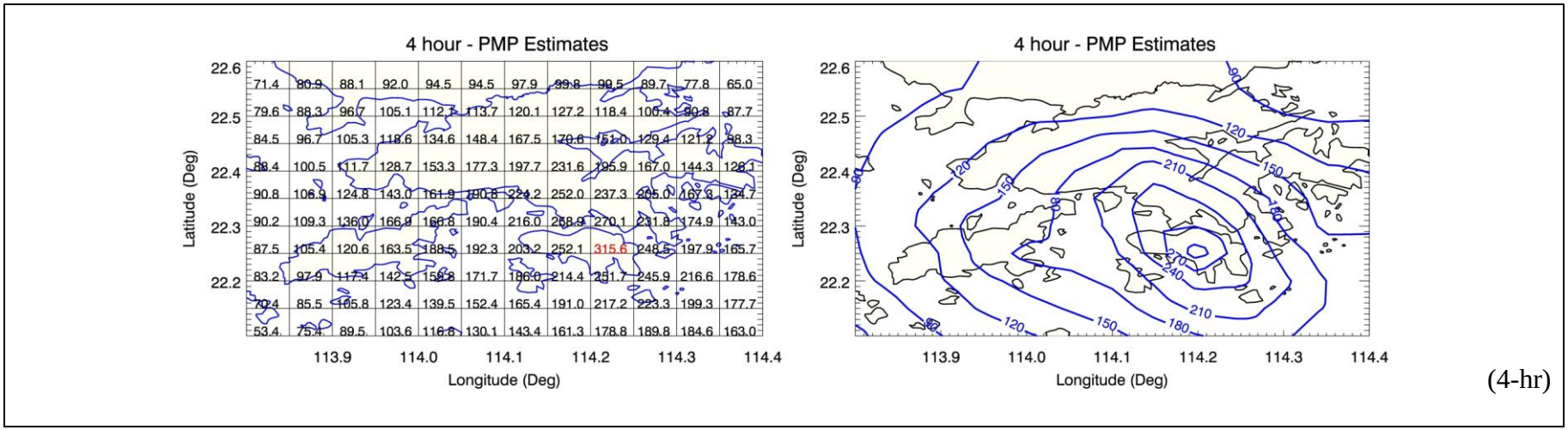

Figure V7 Embryonic PMP Centred at Hong Kong Island, NW-SE Orientation - 135°

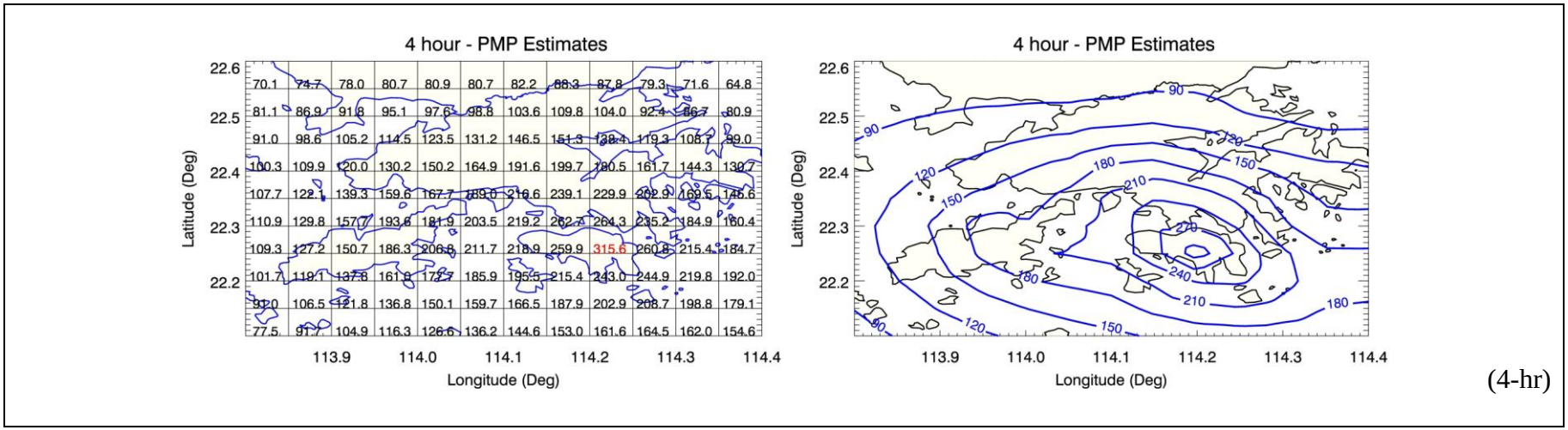

Figure V8 Embryonic PMP Centred at Hong Kong Island, WNW-ESE Orientation - 157.5°

Table of Contents
Table of Contents
Table of Contents

Appendix W

Isohyets from Storm Transposition with Moisture Maximization (4-hour)

Contents

W.1 Moisture-maximized 4-hour Isohyets for Storm Transposition Centred at Tai Mo Shan

E-W orientation - 0°

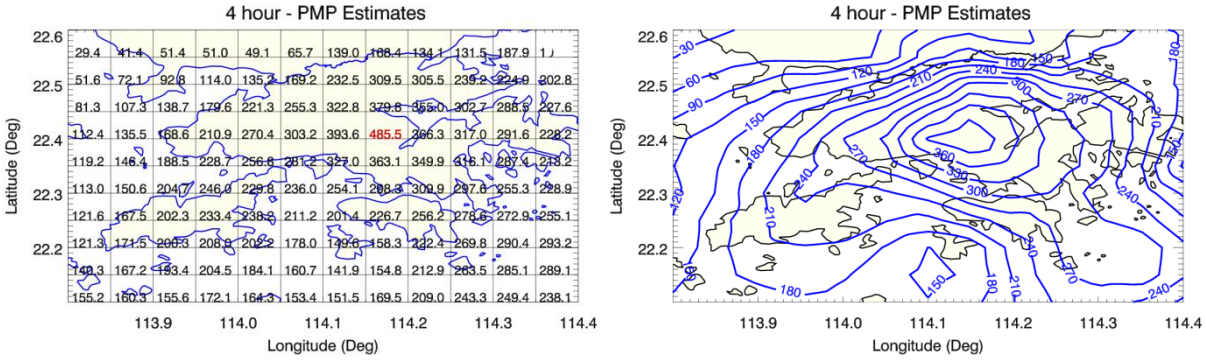

ENE-WSW orientation - 22.5°

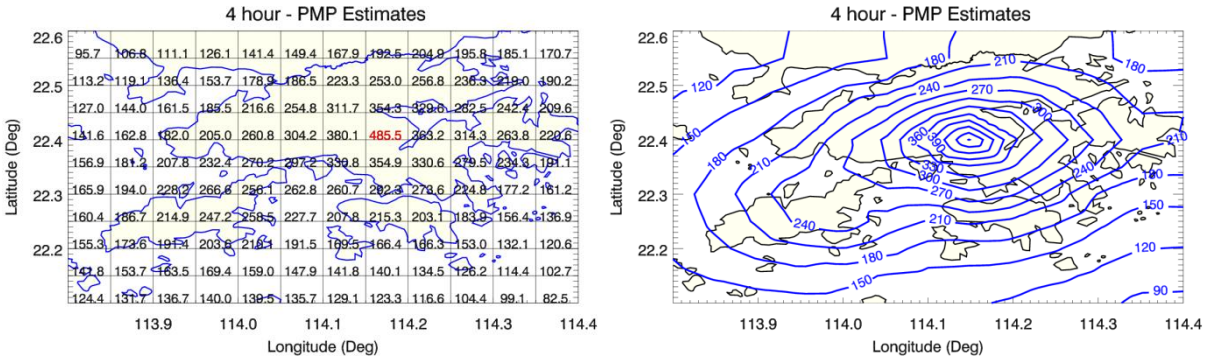

NE-SW orientation - 45°

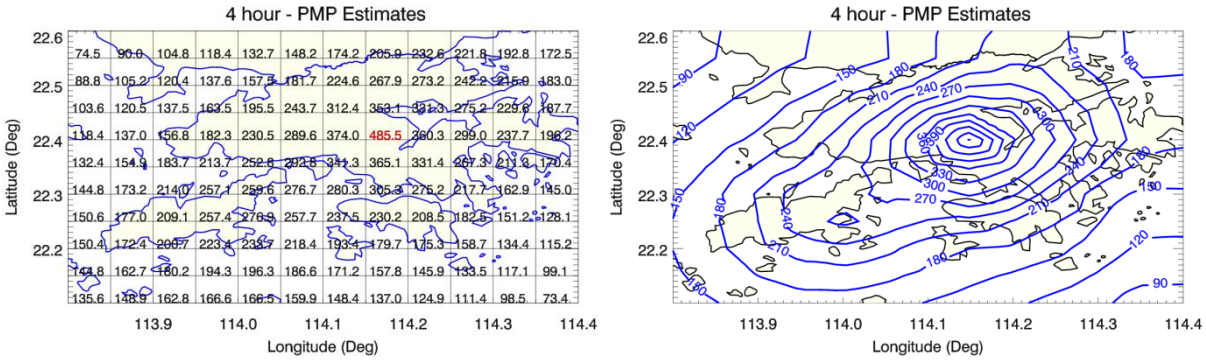

NNE-SSW orientation - 67.5°

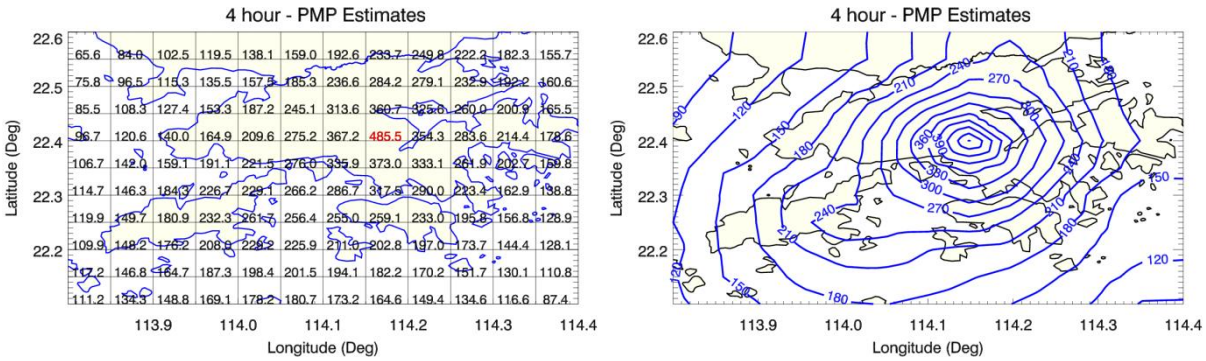

Table of Contents
Table of Contents
Table of Contents
Table of Contents

N-S orientation - 85°

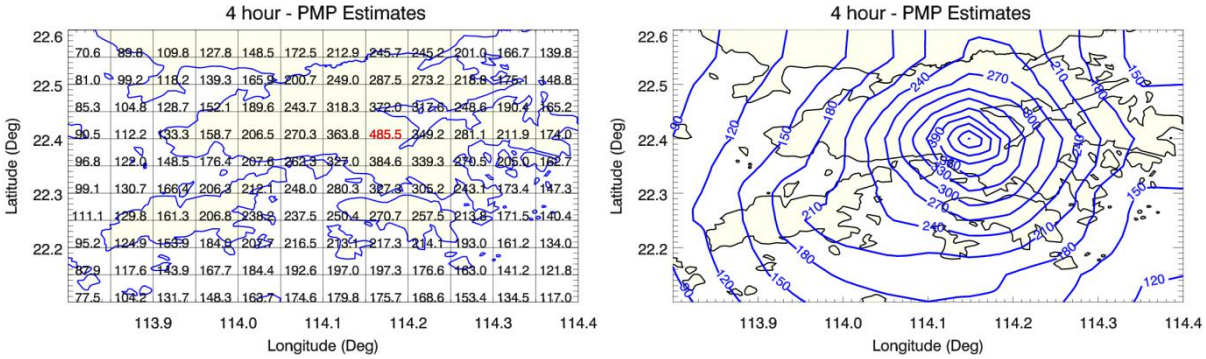

NNW-SSE orientation - 112.5°

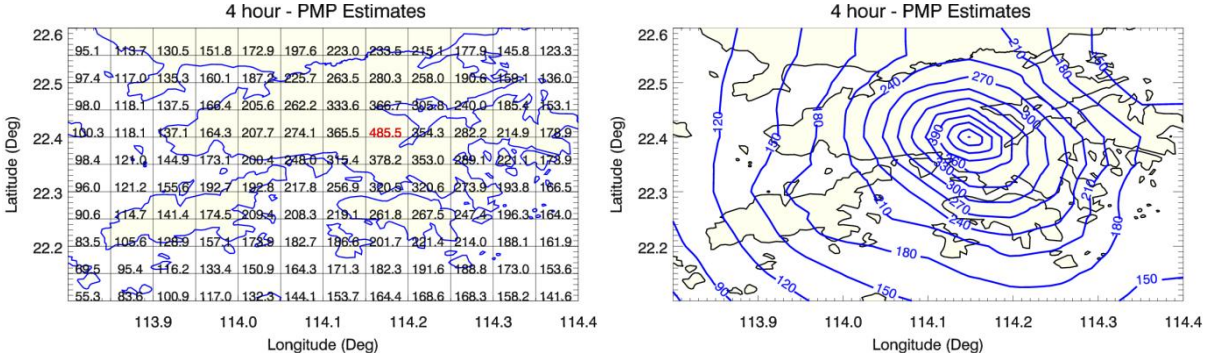

NW-SE orientation - 135°

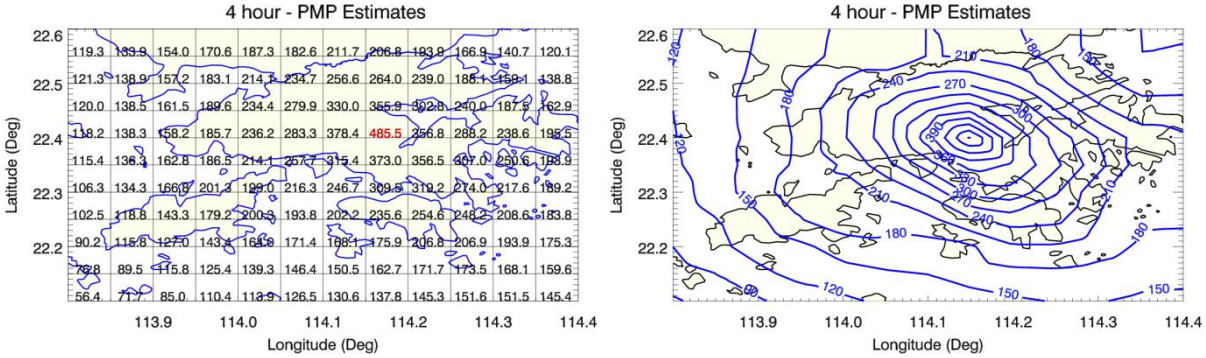

WNW-ESE orientation - 157.5°

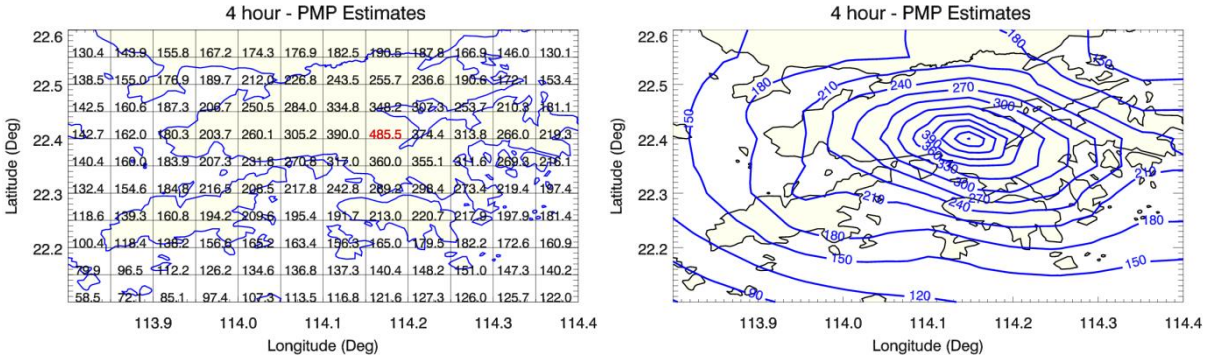

Table of Contents
Table of Contents
Table of Contents
Table of Contents

W.2 Moisture-maximized 4-hour Isohyets for Storm Transposition Centred at Lantau

E-W orientation - 0°

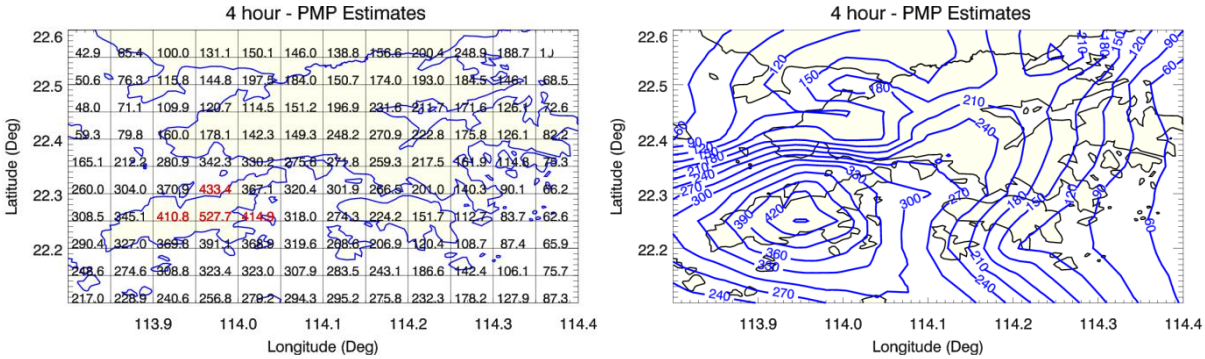

ENE-WSW orientation - 22.5°

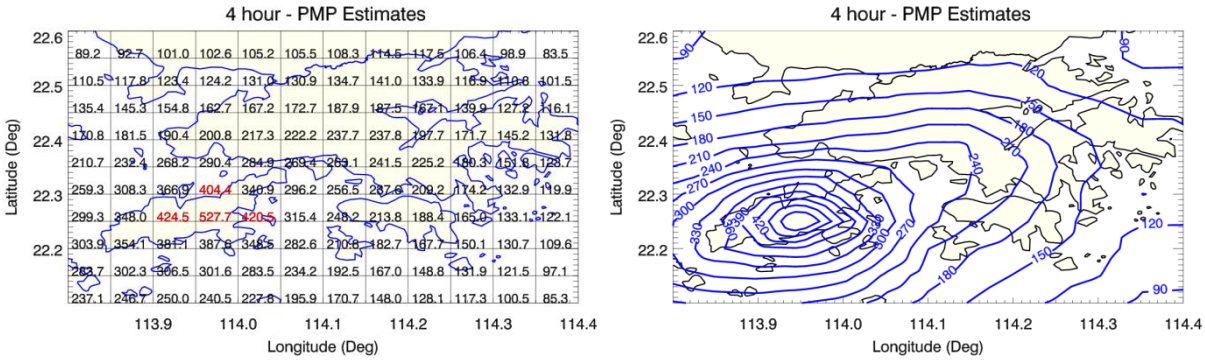

NE-SW orientation - 45°

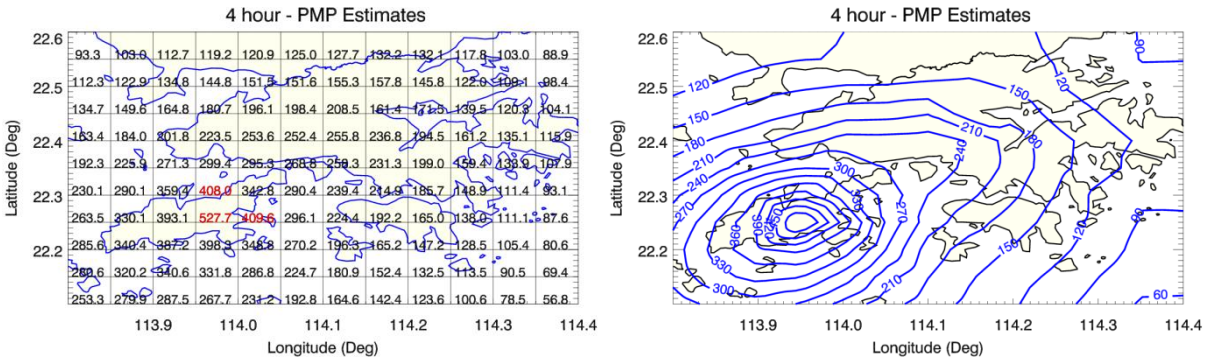

NNE-SSW orientation - 67.5°

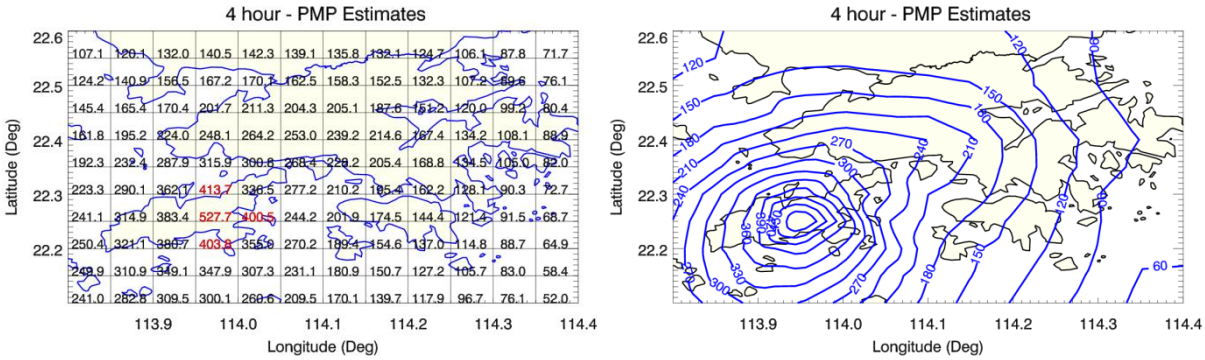

Table of Contents
Table of Contents
Table of Contents
Table of Contents

N-S orientation - 85°

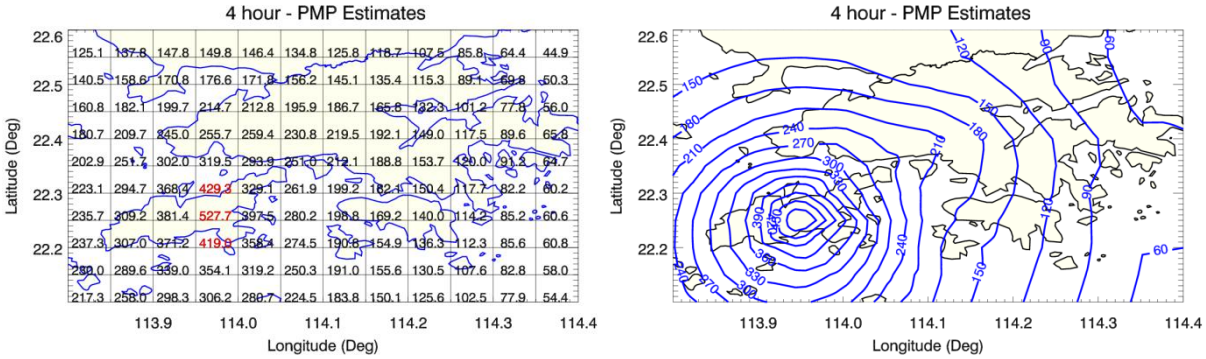

NNW-SSE orientation - 112.5°

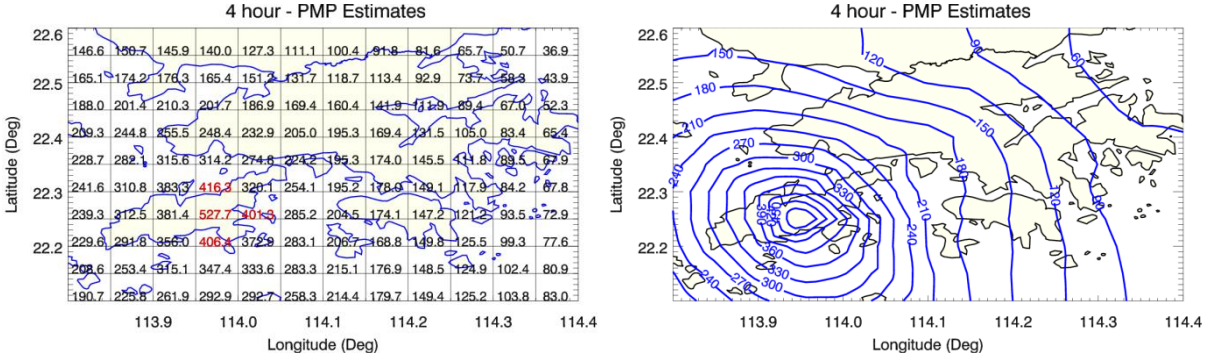

NW-SE orientation - 135°

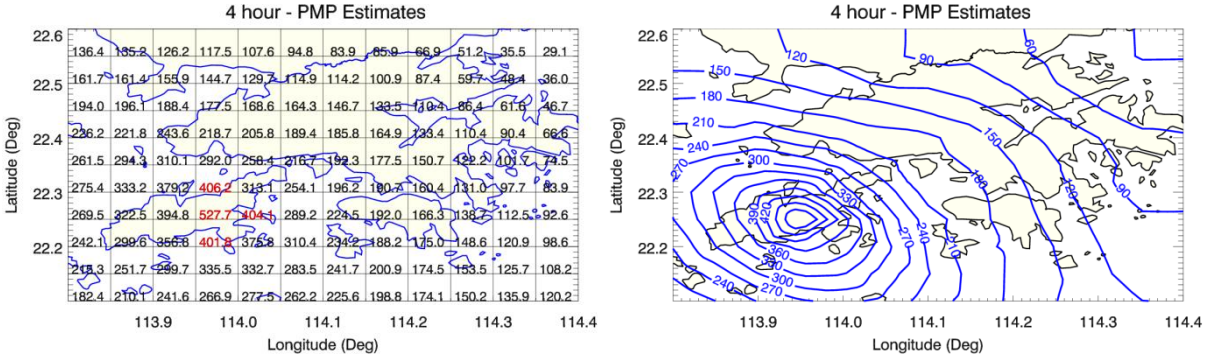

WNW-ESE orientation - 157.5°

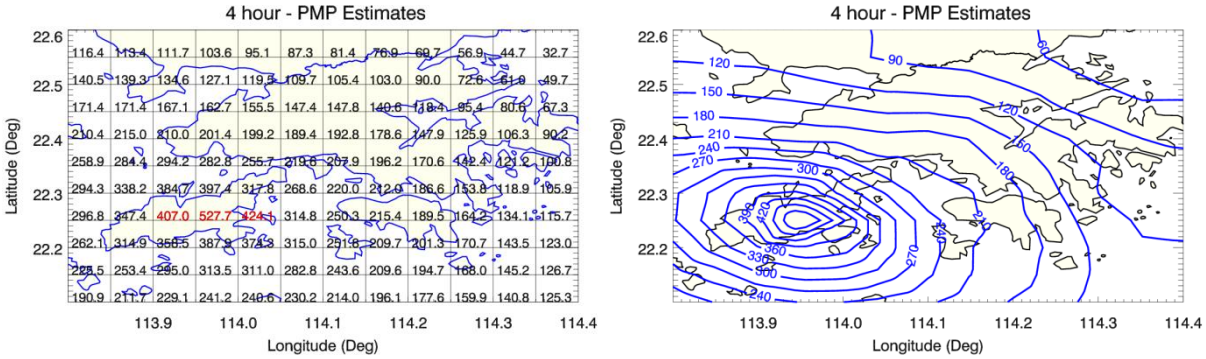

Table of Contents
Table of Contents
Table of Contents
Table of Contents

W.3 Moisture-maximized 4-hour Isohyets for Storm Transposition Centred at Hong Kong Island

E-W orientation - 0°

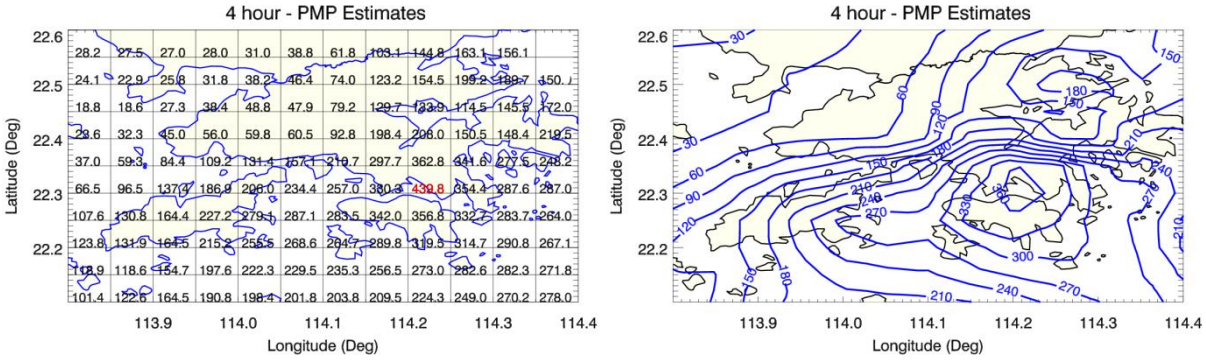

ENE-WSW orientation - 22.5°

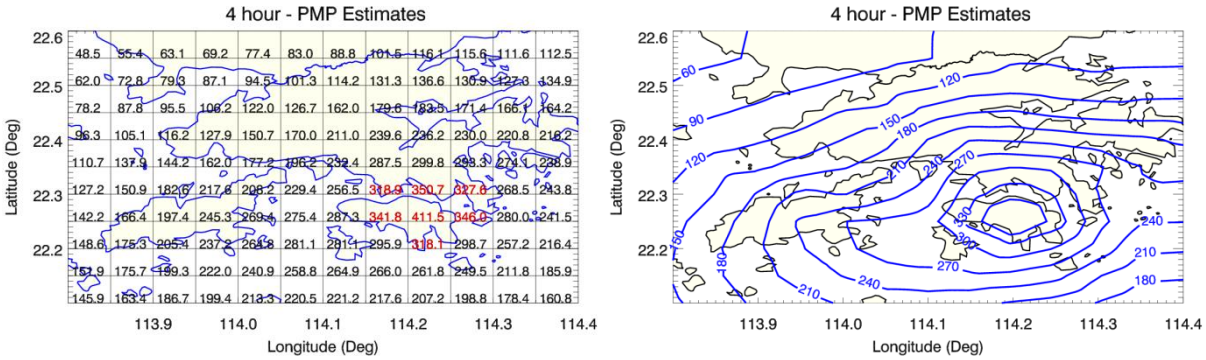

NE-SW orientation - 45°

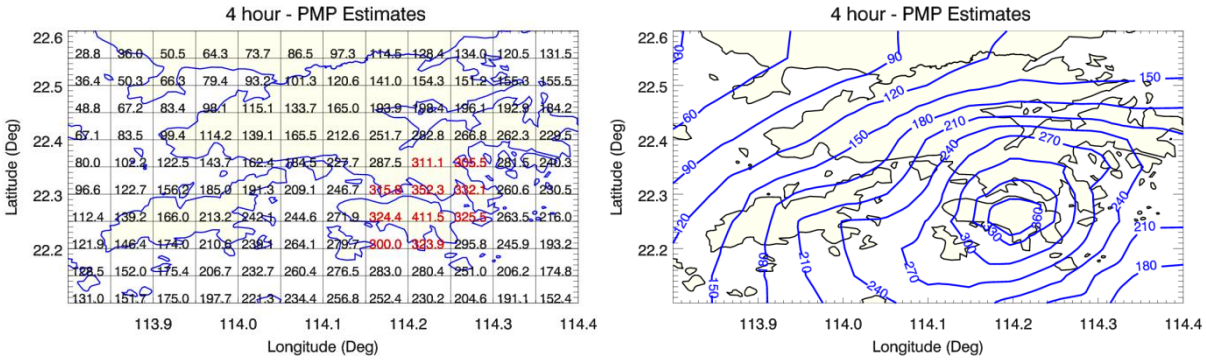

NNE-SSW orientation - 67.5°

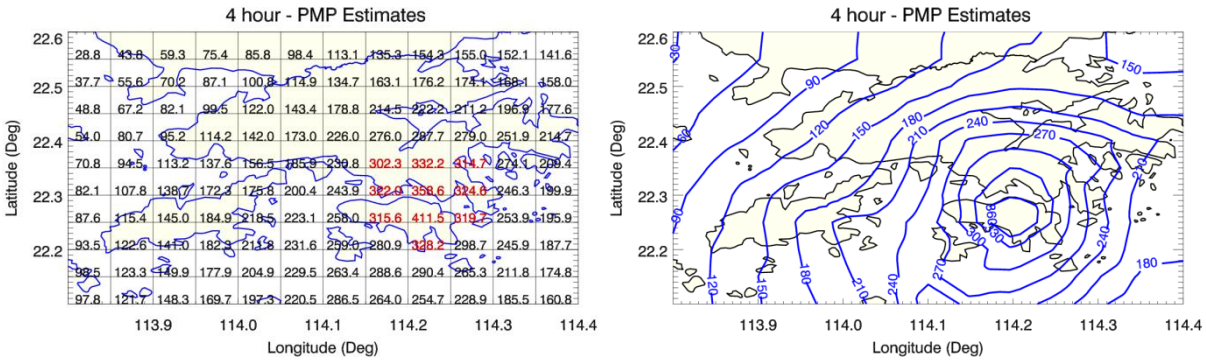

Table of Contents
Table of Contents
Table of Contents
Table of Contents

N-S orientation - 85°

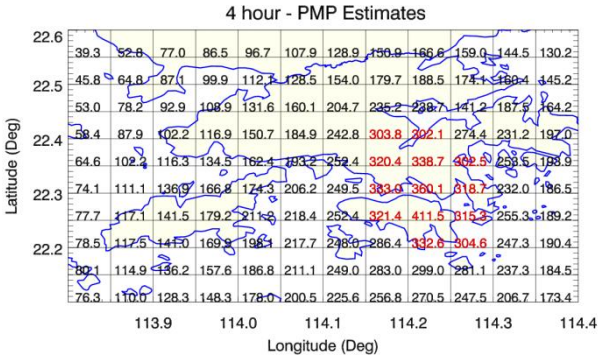

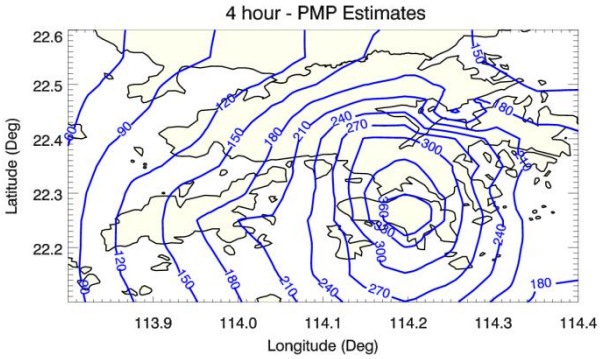

NNW-SSE orientation - 112.5°

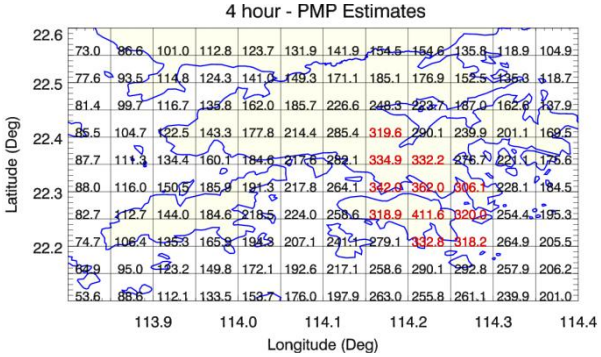

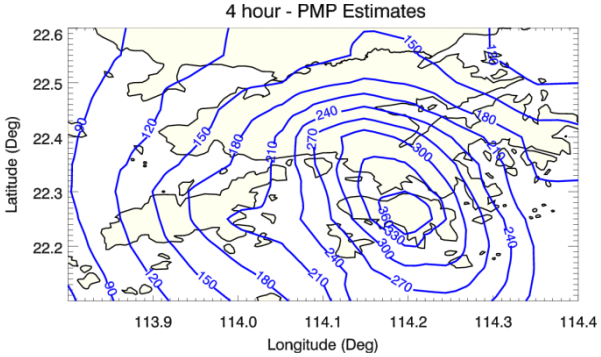

NW-SE orientation - 135°

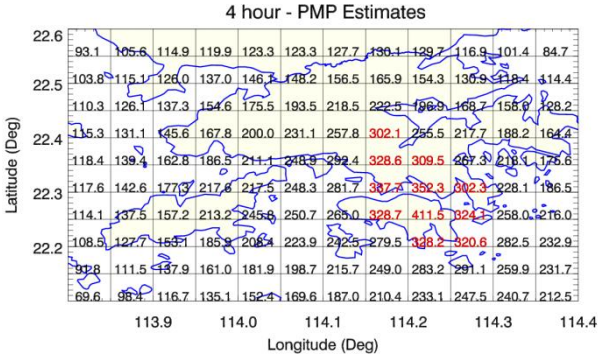

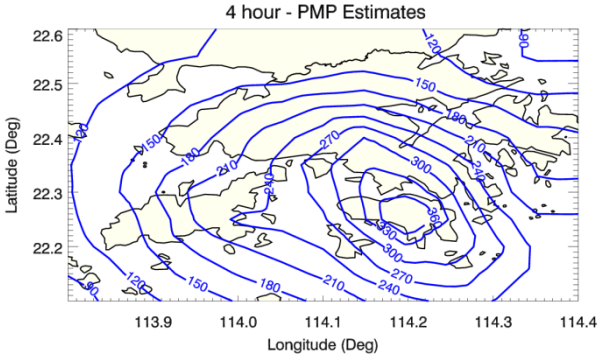

WNW-ESE orientation - 157.5°

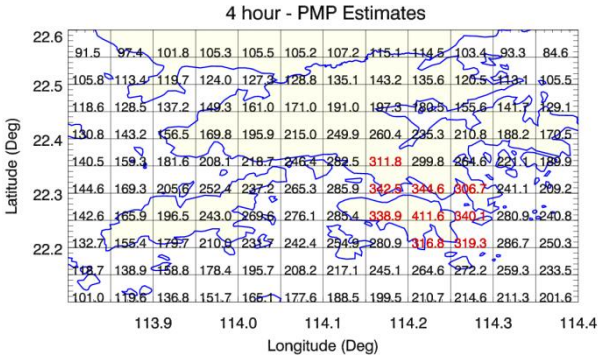

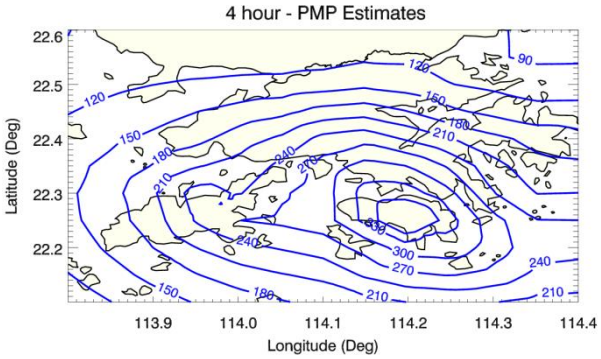

Table of Contents
Table of Contents
Table of Contents
Table of Contents

GEO PUBLICATIONS AND ORDERING INFORMATION
土力工程處刊物及訂購資料

A selected list of major GEO publications is given in the next page. An up-to-date full list of GEO publications can be found at the CEDD Website http://www.cedd.gov.hk on the Internet under "Publications". Abstracts for the documents can also be found at the same website. Technical Guidance Notes are published on the CEDD Website from time to time to provide updates to GEO publications prior to their next revision.

部份土力工程處的主要刊物目錄刊載於下頁。而詳盡及最新的土力工程處刊物目錄，則登載於土木工程拓展署的互聯網網頁 http://www.cedd.gov.hk 的"刊物"版面之內。刊物的摘要及更新刊物內容的工程技術指引，亦可在這個網址找到。

Copies of GEO publications (except geological maps and other publications which are free of charge) can be purchased either by:

Writing to
Publications Sales Unit,
Information Services Department,
Room 626, 6th Floor,
North Point Government Offices,
333 Java Road, North Point, Hong Kong.

or

- Calling the Publications Sales Section of Information Services Department (ISD) at (852) 2537 1910
- Visiting the online Government Bookstore at http:// www.bookstore.gov.hk
- Downloading the order form from the ISD website at http://www.isd.gov.hk and submitting the order online or by fax to (852) 2523 7195
- Placing order with ISD by e-mail at puborder@isd.gov.hk

讀者可採用以下方法購買土力工程處刊物(地質圖及免費刊物除外):

書面訂購
香港北角渣華道333號
北角政府合署6樓626室
政府新聞處
刊物銷售組

或

- 致電政府新聞處刊物銷售小組訂購 (電話：(852) 2537 1910)
- 進入網上「政府書店」選購，網址爲 http://www.bookstore.gov.hk
- 透過政府新聞處的網站 (http://www.isd.gov.hk) 於網上遞交訂購表格，或將表格傳真至刊物銷售小組 (傳真：(852) 2523 7195)
- 以電郵方式訂購 (電郵地址：puborder@isd.gov.hk)

1:100 000, 1:20 000 and 1:5 000 geological maps can be purchased from:

Map Publications Centre/HK,
Survey & Mapping Office, Lands Department,
23th Floor, North Point Government Offices,
333 Java Road, North Point, Hong Kong.
Tel: (852) 2231 3187
Fax: (852) 2116 0774

讀者可於下列地點購買1:100 000、1:20 000及1:5 000地質圖：

香港北角渣華道333號
北角政府合署23樓
地政總署測繪處
電話: (852) 2231 3187
傳真: (852) 2116 0774

Requests for copies of Geological Survey Sheet Reports and other publications which are free of charge should be directed to:

For Geological Survey Sheet Reports which are free of charge:
Chief Geotechnical Engineer/Planning,
(Attn: Hong Kong Geological Survey Section)
Geotechnical Engineering Office,
Civil Engineering and Development Department,
Civil Engineering and Development Building,
101 Princess Margaret Road,
Homantin, Kowloon, Hong Kong.
Tel: (852) 2762 5380
Fax: (852) 2714 0247
E-mail: jsewell@cedd.gov.hk

For other publications which are free of charge:
Chief Geotechnical Engineer/Standards and Testing,
Geotechnical Engineering Office,
Civil Engineering and Development Department,
Civil Engineering and Development Building,
101 Princess Margaret Road,
Homantin, Kowloon, Hong Kong.
Tel: (852) 2762 5346
Fax: (852) 2714 0275
E-mail: florenceko@cedd.gov.hk

如欲索取地質調查報告及其他免費刊物，請致函：

免費地質調查報告:
香港九龍何文田公主道101號
土木工程拓展署大樓
土木工程拓展署
土力工程處
規劃部總土力工程師
(請交:香港地質調查組)
電話: (852) 2762 5380
傳真: (852) 2714 0247
電子郵件: jsewell@cedd.gov.hk

其他免費刊物:
香港九龍何文田公主道101號
土木工程拓展署大樓
土木工程拓展署
土力工程處
標準及測試部總土力工程師
電話: (852) 2762 5346
傳真: (852) 2714 0275
電子郵件: florenceko@cedd.gov.hk

Table of Contents
Table of Contents
Table of Contents

MAJOR GEOTECHNICAL ENGINEERING OFFICE PUBLICATIONS
土力工程處之主要刊物

Table of Contents

GEOTECHNICAL MANUALS

Geotechnical Manual for Slopes, 2nd Edition (1984), 302 p. (English Version), (Reprinted, 2011).

斜坡岩土工程手冊(1998)，308頁(1984年英文版的中文譯本)。

Highway Slope Manual (2000), 114 p.

GEOGUIDES

Geoguide 1	Guide to Retaining Wall Design, 2nd Edition (1993), 258 p. (Reprinted, 2007).
Geoguide 2	Guide to Site Investigation (1987), 359 p. (Reprinted, 2000).
Geoguide 3	Guide to Rock and Soil Descriptions (1988), 186 p. (Reprinted, 2000).
Geoguide 4	Guide to Cavern Engineering (1992), 148 p. (Reprinted, 1998).
Geoguide 5	Guide to Slope Maintenance, 3rd Edition (2003), 132 p. (English Version).
岩土指南第五冊	斜坡維修指南，第三版(2003)，120頁(中文版)。
Geoguide 6	Guide to Reinforced Fill Structure and Slope Design (2002), 236 p.
Geoguide 7	Guide to Soil Nail Design and Construction (2008), 97 p.

Table of Contents

GEOSPECS

Geospec 1	Model Specification for Prestressed Ground Anchors, 2nd Edition (1989), 164 p. (Reprinted, 1997).
Geospec 3	Model Specification for Soil Testing (2001), 340 p.

GEO PUBLICATIONS

GCO Publication No. 1/90	Review of Design Methods for Excavations (1990), 187 p. (Reprinted, 2002).
GEO Publication No. 1/93	Review of Granular and Geotextile Filters (1993), 141 p.
GEO Publication No. 1/2006	Foundation Design and Construction (2006), 376 p.
GEO Publication No. 1/2007	Engineering Geological Practice in Hong Kong (2007), 278 p.
GEO Publication No. 1/2009	Prescriptive Measures for Man-Made Slopes and Retaining Walls (2009), 76 p.
GEO Publication No. 1/2011	Technical Guidelines on Landscape Treatment for Slopes (2011), 217 p.

Table of Contents

GEOLOGICAL PUBLICATIONS

The Quaternary Geology of Hong Kong, by J.A. Fyfe, R. Shaw, S.D.G. Campbell, K.W. Lai & P.A. Kirk (2000), 210 p. plus 6 maps.

The Pre-Quaternary Geology of Hong Kong, by R.J. Sewell, S.D.G. Campbell, C.J.N. Fletcher, K.W. Lai & P.A. Kirk (2000), 181 p. plus 4 maps.

TECHNICAL GUIDANCE NOTES

TGN 1	Technical Guidance Documents

Table of Contents